Mechanisms of Ca^{2+} entry and mechanical sensation in the vasculature

Bing Hou

Submitted in accordance with the requirements for the

Degree of Doctor of Philosophy

The University of Leeds

School of Biomedical Sciences

September 2014

Funded by CSC and the University of Leeds

Acknowledgements

I would like to express my sincerest gratitude to my supervisor Professor David Beech for all his support and guidance throughout my PhD. I came as a foreigner with English as my second language. However with his patience and help, I quickly found my feet and have learnt a great amount over the last 4 years. I am really grateful for his understanding and backing up during my PhD. I have really enjoyed my life at Leeds, and have been feeling proud to be a member in the Beech lab. I would also like to thank my co-supervisor Dr. Lin-Hua Jiang and my assessor Prof. Asipu Sivaprasadarao for all their assistance throughout my PhD.

I have learnt a lot from all of the Beech lab members who helped and supported during my PhD, for which I am really grateful. I would like to express my special thanks to Jing, who not only taught me many experimental techniques but also helped me a lot in my life. Also special thanks to Sarka Tumova for teaching me all about Western blotting and the proofreading of my thesis, and to Lynn and Amer for teaching me immunostaining and Ca^{2+} imaging. I would also like to thank all my good friends for their friendship and support.

I would like to thank China Scholarship Council, the University of Leeds, and the Beech lab for funding my PhD study.

Especially, I would like to thank my mum and dad for their love and support through my life. I would like to express a huge thank you to my wonderful wife Xin, who has been looking after our 1-year-old son, Chenbei, by herself. I want to thank her for her supports, encouragement and love throughout. Thanks are also to my lovely son, Chenbei, for bringing me so much happiness. Finally, a special thanks to my late grandfather. He was always so proud of me. I hope I am still making him proud.

Abstract

Both Ca^{2+} entry and shear stress sensation of vascular cells play important roles not only in vascular physiology, but also pathology. Therefore, understanding the mechanism of these processes could greatly help the therapeutic strategies to treat vascular diseases like atherosclerosis. The overall aim of this research was to develop a better understanding of molecular mechanisms of Ca^{2+} entry and shear stress sensation in the vasculature.

Transient Receptor Potential Canonical (TRPC) proteins assemble to form channels for calcium and sodium ion entry. TRPC5 readily forms functional homomers, whereas TRPC1 forms functional heteromers with TRPC5 but has weak or no channel function on its own. In this study, impact of cholesterol on these proteins was investigated, because it is an important membrane constituent and driver of cardiovascular and other diseases. I found that TRPC5-mediated calcium entry is suppressed by cholesterol due to internalization of TRPC5 via the caveolin-1-dependent retraction mechanism but that TRPC1 prevents the internalization by heteromerising with TRPC5 and causing segregation to a membrane raft rich in GM1 ganglioside and dissociated from caveolin-1. Endogenous TRPC5 containing channels of vascular smooth muscle cells are stimulated by exogenous GM1 gangliosides and resistant to inhibition by cholesterol. The data suggest that a previously unrecognized purpose of incorporating a subunit in a heteromer is to segregate the protein complex to a membrane raft that is protected against cholesterol-evoked internalization.

Force sensors used by endothelial cells to detect fluid shear stress are pivotal in vascular physiology and disease but there is lack of clarity about their identity. Here I show that a recently-discovered calcium-permeable channel formed by Piezo1 is important in sensing physiological shear stress and in driving a key downstream functional event. Calcium influx evoked by physiological shear stress depended on endogenous Piezo1. Exogenous Piezo1 confers sensitivity to shear stress on otherwise resistant cells. Real-time subcellular tracking

studies showed accumulation of Piezo1 at the endothelial cell leading edge. Depletion of endogenous Piezo1 prevented endothelial cell alignment to shear stress. Calpain activation and focal adhesion is the mechanism of Piezo1-dependent alignment of endothelial cells to shear stress. Piezo1 also crosstalks with CD31, which is a component of a known shear stress sensory complex. The data suggest that Piezo1 has the dual function of sensing physiological shear stress and driving downstream endothelial cell alignment through calcium ion entry and a calpain-focal adhesion mechanism. Alignment of endothelial cells has major roles in physiology and various disease processes which include protection against atherosclerosis.

In summary, this research has generated new knowledge and hypotheses about molecular mechanism of Ca^{2+} entry and mechanical sensation of vascular cells under physiological and pathological conditions, which may help generate new strategies to treat cardiovascular diseases such as atherosclerosis.

Table of Contents

List of Figures

List of Tables

List of Abbreviations

αCD	α cyclodextrin
µl; ml	microlitre; millilitre
µm; mm; cm	micrometre; millimetre; centimetre
µM; mM	micromolar; millimolar
ATP	Adenosine triphosphate
bp	Base pair
Ca^{2+}	Calcium ion
CD31(PECAM-1)	Platelet endothelial cell adhesion molecule
ChTxB	Cholera toxin subunit B
DAG	Diacylglycerol
DAPI	4',6-diamidino-2-phenylindole
DNA	Deoxyribonucleic acid
DNAse	Deoxyribonuclease
DMSO	Dimethyl sulphoxide
EC	Endothelial cell
EGM	Enodothelial growth medium
EDTA	Ethylene diaminetetraacetic acid
eNOS	Endothelial nitric oxide synthase
FA	Focal adhesion
FAK	Focal adhesion kinase
Fura-2 AM	Fura-2-acetoxymethyl ester
FITC	Flurosceine isothiocyanate
Gd^{3+}	Gadolinium
GFP	Green fluorescent protein
GM1	GM1 ganglioside

GsMTx4	Grammostola spatulata, mechanotoxin 4
GPCR	G protein coupled receptor
G protein	Guanosine nucleotide-binding protein
HA	Hemagglutinin
HEPES	Hydroxyethyl piperazineethanesulfoic acid
HEK	Human embryonic kidney cells
HUVEC	Human umbilical vein endothelial cell
IF	Immunofluorescence
IP$_3$	Inositol 1,4,5-trisphosphate
IP$_3$R	Inositol 1,4,5-trisphosphate receptor
L-NAME	L-NG-Nitroarginine Methyl Ester
L-NMMA	L-NG-Monomethyl-L-arginine
LEC	Liver endothelial cell
LGC	Ligand-gated channels
mβCD	Methyl-β-cyclodextrin
MAPK	Mitogen-activated protein kinases
MCU	Mitochondrial Ca^{2+} uniporter
mRNA	Messenger RNA
MSC	Mechanosensitive channels
NCX	Na^+/Ca^{2+} exchanger
NO	Nitric oxide
P2X4	P2X purinoceptor 4
PBS	Phosphate buffered saline
PC	Polycystin
PCR	Polymerase chain reaction
PECAM-1 (CD31)	Platelet endothelial cell adhesion molecule
PGPC	3,1-Palmitoyl-2-glutaryl phosphatidylcholine

PLC	Phospholipase C
PMCA	Plasma membrane Ca^{2+} ATPase
RNA	Ribonucleic acid
ROC	Receptor-operated channel
rpm	Revolutions per minute
R_yR	Ryanodine receptor
SAC	Stretch-activated channels
SBS	Standard bath solution
SDS	Sodium dodecyl sulfate
SR	Sarcoplasmic endoplasmic reticulum
src	Proto-oncogene, non-receptor tyrosine kinase
SERCA	Sarcoplasmic endoplasmic reticulum Ca^{2+}ATPase
SOC	Store-operated channel
TPC	Two-pore channels
TRP	Transient receptor potential
TRPC	Classical transient receptor potential
TRPP	Polycystic transient receptor potential
TRPV	Vanilloid transient receptor potential
VEGF	Vascular endothelial growth factors
VGCC	Voltage-gated calcium channel
VSMC	Vascular smooth musclecCell
VCAM-1	Vascular cell adhesion molecule-1
WB	Western blotting

Publications and Communications

Publications

Jing Li[†], **Bing Hou**[†], Sarka Tumova, Katsuhiko Muraki, Alexander Bruns, Melanie J. Ludlow, Alicia Sedo, Adam J. Hyman, Lynn McKeown, Richard S. Young, Nadira Y. Yuldasheva, Yasser Majeed, Lesley A. Wilson, Baptiste Rode, Marc A. Bailey, Hyejeong R. Kim, Zhaojun Fu, Deborah A. L. Carter, Jan Bilton, Helen Imrie, Paul Ajuh, T. Neil Dear, Richard M. Cubbon, Mark T. Kearney, Raj K. Prasad, Paul C. Evans, Justin F. X. Ainscough, David J. Beech: ***Piezo1 integration of vascular architecture with physiological force.*** Nature 08/2014; advance online publication († equal contributors).

Mohamed S Amer, Lynn McKeown, Sarka Tumova, Ruifeng Liu, Victoria Al Seymour, Lesley A Wilson, Jacqueline Naylor, Katriona Reenhalgh, **Bing Hou**, Yasser Majeed, Paul Turner, Alicia Sedo, David J O'Regan, Jing Li, Robin S Bon, Karen E Porter, David J Beech: **Inhibition of endothelial cell Ca(2+) entry and Transient Receptor Potential channels by Sigma-1 receptor ligands.** British Journal of Pharmacology 11/2012.

Jing Li, Richard M Cubbon, Lesley A Wilson, Mohamed S Amer, Lynn McKeown, **Bing Hou**, Yasser Majeed, Sarka Tumova, Victoria A L Seymour, Hilary Taylor, Martin Stacey, David O'Regan, Richard Foster, Karen E Porter, Mark T Kearney, David J Beech: ***Orai1 and CRAC channel dependence of VEGF-activated Ca2+ entry and endothelial tube formation.*** Circulation Research 03/2011; 108(10):1190-8.

Jacqueline Naylor, Jing Li, Carol J Milligan, Fanning Zeng, Piruthivi Sukumar, **Bing Hou**, Alicia Sedo, Nadira Yuldasheva, Yasser Majeed, Dhananjay Beri, Shan Jiang, Victoria A L Seymour, Lynn McKeown, Bhaskar Kumar, Christian Harteneck, David O'Regan, Stephen B Wheatcroft, Mark T Kearney, Clare Jones, Karen E Porter, David J Beech: ***Pregnenolone sulphate- and cholesterol-regulated TRPM3 channels coupled to vascular smooth muscle secretion and contraction.*** Circulation Research 04/2010; 106(9):1507-15.

Manuscripts submitted or in preparation

Bing Hou[†], Sarka Tumova[†], Mohamed S Amer[†], Lynn McKeown, Nicholas K Moss, Alicia Sedo,Yahya M Bahnasi1, Rucha Karnik, Piruthivi Sukumar1, Jing Li, Marc A Bailey, David O'Regan, Katsuhiko Muraki, Karen E Porter, Asipu Sivaprasadarao, David J Beech: **TRPC1 segregates TRPC5 to protect calcium entry against cholesterol-evoked internalization**. Science Signalling, under revision.

Bing Hou, Adam Hyman, Sarka Tumova, David J Beech: **Piezo1 crosstalks with CD31 in shear stress sensation.** In preparation.

Communications

An ion channel component for shear-stress sensing in vascular endothelial cells: Piezo1 (Presentation). Postgraduate Symposium, University of Leeds. 2014 and Endothelial Retreat, Lake District. 2013.

TRPC1 redistributes TRPC5 in the surface membrane and prevents its cholesterol- and caveolin-1- dependent retraction (Poster Presentation). 4th International Ion Channel Conference, Shijiazhuang, China. 2013 and Postgraduate Symposium, University of Leeds. 2011

Vascular endothelial growth factor (VEGF) drives calcium entry and angiogenesis through surface delivery of Orai3 (Presentation). Ion Channel Retreat, Lake District, 2012.

Chapter 1. Introduction

1.1. Cardiovascular system

The cardiovascular system is an organ system comprised of heart, blood, and blood vessels, which permits blood to circulate through the body and supply oxygen and nutrients for the survival of all cells. There are three major types of the blood vessels including arteries, which carry blood out of the heart; capillaries, which allow exchange of oxygen, carbon dioxide, nutrition, and metabolic waste products between blood and tissues; and veins, which carry the deoxygenated blood back towards the heart. Capillaries link to arteries and veins through small vessels called arterioles and venules respectively.

The walls of arteries and veins contain three major layers (from inner to outer): tunica intima, tunica media and tunica adventitia. Tunica intima is comprised of endothelium, a single layer of endothelial cells, which is surrounded by connective tissue interlaced with elastic tissue called internal elastic lamina. Tunica intima is in direct contact with the blood flow and shear stress generated by the blood flow, which ranges from 1 to 70 $dyn.cm^{-2}$ in different types of blood vessels (Chiu and Chien, 2011). In arteries, the thickest layer is tunica media, which is predominately composed of smooth muscle cells and elastic tissue. On the other hand, in veins, tunica media mainly consists of a thick layer of connective tissue with elastic fibres, controlling the vessel calibre. External elastic lamina separates it from tunica adventitia. Tunica adventitia, also known as tunica externa, the thickest layer in a vein, is the outermost layer of a vessel. It is mainly made of connective tissue, and contains nerves in large blood vessels. The vasa vasorum, a network of small vessels supplying the walls of large blood vessels, is also localized in this layer. On the other hand, capillaries are composed of a single thin layer of endothelium surrounded by a basal lamina.

The heart is the active organ that generates the blood flow, but blood vessels can regulate the blood flow to downstream organs by changing their inner diameter. The changes are regulated by vasoconstriction (narrowing of blood vessels) and vasodilation. Contraction of vascular smooth muscle cells (VSMCs) is responsible for vasoconstriction, which can be induced by a variety of endogenous vasoconstrictors (pressors), including ATP, angiotensin II, endothelin, etc (Navar et al., 1996). Many of these pressors are functional by regulating the intracellular Ca^{2+} level in VSMCs (Loukotova et al., 1998, Navar et al., 1996). On the other hand, nitric oxide (NO) is the most prominent vasodilator, which can be released by endothelial cells in response to shear stress (Navar et al., 1996).

1.2. Cardiovascular disease: Atherosclerosis

Cardiovascular disease (CVD) is a term referring to all diseases of the heart and blood vessels, including coronary heart disease, heart failure, congenital heart disease and stroke. CVDs are the leading cause of deaths globally. According to the estimation of World Health Organization (WHO), CVDs killed 17.3 million people in 2008, accounting for 30% of all global deaths. The death number is estimated to increase to 23.6 million in 2030 (Mathers and Loncar, 2006). The British Heart Foundation (BHF) reported that almost 160,000 people in the UK died from CVDs in 2011.

Atherosclerosis is a progressive disease which gives rise to coronary heart disease and other circulatory diseases. It is characterized by the deposition of lipids and fibres in the large arteries, causing slowly progressing lesion formation and narrowing of the vessels. The underlying pathology is considered as a chronic inflammatory process within the arterial wall predominantly at sites exposed to disturbed blood flow, such as branch points (Lusis, 2000, Tamminen, 1999). Studies over the last 50 years revealed a number of risk factors for atherosclerosis, genetic or environmental, including elevation of the low density lipoprotein (LDL), elevated blood pressure, elevated levels of homocysteine,

family history, diabetes and obesity, systematic inflammation, metabolic syndrome, high fat diet, lack of exercise, smoking, and infectious agents (Lusis, 2000). High level of LDL, which transports cholesterol in the blood is one of the most important risk factors for atherosclerosis (Ross, 1999).

1.2.1. Pathogenesis of atherosclerosis

Pathogenesis of the atherosclerotic lesion is considered to be initiated by endothelial dysfunction and structural alterations including the loss of confluent luminal elastin layer and the exposure of proteoglycans, which leads to the intracellular accumulation of LDL in endothelial cells (Kwon et al., 2008, Weber and Noels, 2011). Endothelial dysfunction is characterised by the changes of the activities of the endothelium toward decreased vasodilation, a proinflammatory condition, and prothrombic state, which can result from multiple factors including hypercholesterolemia and smoking tobacco (Endemann and Schiffrin, 2004, Munzel et al., 2008). The underlying mechanism of reduced vasodilation includes reduction of the vasodilator NO production and subsequent increase in the vasoconstrictors like endothelin-1 (ET-1) (Ross, 1999). Low NO bioavailability can increase the expression of vascular cell adhesion molecule-1 (VCAM-1), which binds to monocytes and T lymphocytes, initiating invasion of inflammatory cells into the vessel wall in atherogenesis (Khan et al., 1996, Libby et al., 2010). Disturbed or low shear stress may promote endothelial dysfunction, thereby contributing to atherogenesis (Firasat et al., 2014).

The binding of apolipoprotein B100 (ApoB100), the apolipoproteins of LDL, with extracellular matrix proteoglycans leads to the accumulation of LDL in the intima (Hansson and Hermansson, 2011). LDL is then modified by reactive oxygen species or enzymes, predominantly turning into oxidised LDL (oxLDL), which also promotes the expression of adhesion molecules including VCAM-1 and intracellular adhesion molecule-1 (ICAM-1). Adhesion molecules, together with endothelia and platelet-derived chemokines, trigger the intimal invasion of

monocytes and T cells (Blankenberg et al., 2003, Weber and Noels, 2011, Zernecke and Weber, 2010). Monocytes differentiate into macrophages after entering the intima. Macrophages recognise and internalise modified LDL by macrophage scavenger receptors including SR-A, CD36 and CD68, forming foam cells. Several cytokines like tumour necrosis factor-α (TNF-α) and interferon-γ (IFN-γ) induce the expression of scavenger receptors (Bobryshev, 2006, Lusis, 2000, Moore and Tabas, 2011, De Villiers and Smart, 1999). A recent study indicated that macrophages might be derived not only from monocytes, but also from vascular smooth muscle cells (VSMCs) (Allahverdian et al., 2014). Foam cells together with T cells form the early 'fatty-streak' atherosclerotic lesions.

Prolonged endoplasmic reticulum (ER) stress and other stimuli induce apoptosis of foam cells. Dead cells leave behind accumulating extracellular lipids and cell debris, leading to secondary cellular necrosis, and finally to the formation of a lipid-rich necrotic core of the fibrous plaques (Weber and Noels, 2011, Moore and Tabas, 2011). Many risk factors such as elevated levels of homocysteine and angiotensin II trigger proliferation or migration of VSMCs to the intima. The intimal VSMCs secrete collagen-rich extracellular matrix and give rise to a fibrous cap, which is composed VSMCs and the matrix, surrounding the atherosclerotic plaque. T cell and macrophage-expressing cytokines such as IFN-γ contribute to inflammation, VSMC growth and matrix accumulation (Lusis, 2000, Moore and Tabas, 2011, Ross, 1999, Rudijanto, 2007).

With the gradual progression of the lesion, smooth muscle cells undergo apoptosis. Meanwhile, elevated activity and level of proteases, such as metalloproteinases (MMPs), collagenases, elastases, and stromelysins expressed in activated macrophages, degrade extracellular matrix. These processes make the fibrous cap fragile and susceptible to rupture, further implicating the immune response in the atherogenesis (Moore and Tabas, 2011, Newby, 2007, Rudijanto, 2007, Shipley et al., 1996). Rupture is commonly seen at the edges of the lesion. Exposed thrombogenic material in these

atherosclerotic lesions causes platelet aggregation and thrombus formation, which is the main cause of coronary artery thrombosis (Moore and Tabas, 2011). Plaque rupture and thrombosis is reported to be responsible for half of the cases of acute coronary syndromes and myocardial infarction. It is also estimated 76% of global fatal heart attacks are due to the plaque rupture. Growing plaques, which do not rupture, may cause gradual occlusion of the vascular wall, and subsequently cause chronic ischemia (Falk, 2000 & 2006).

The most effective and direct treatment of atherosclerosis is to reduce lipids in the blood, and subsequently to lower apoB-LP retention through lifestyle changes or drugs (Steinberg et al., 2008). The most commonly used drugs to reduce blood lipid are statins, which not only inhibit cholesterol synthesis but also have anti-inflammatory effect (Nissen, 2005, Ray and Cannon 2005). There are also other therapies with different mechanisms, such as aspirin, which suppresses platelet aggregation (Wallentin et al., 2009), and β-blockers, which are antihypertensive (Sipahi et al., 2007). New therapeutic strategies are emerging from mice studies. For example, in mice, prevention of monocyte invasion into lesions by antibodies, or gene-targeted neutralization of adhesion molecules, chemokines and their receptors has been shown to lessen atherosclerosis (Mestas and Ley, 2008). In severe cases of acute coronary thrombosis, however, surgical interference may be required to overcome the artery occlusion by using bypass graft or balloon angioplasty.

In summary, the pathogenesis of atherosclerosis starts from risk factors-induced endothelial dysfunction, which causes decreased vasodilation, lipid accumulation, vascular inflammation, and foam cell formation. Foam cells together with T cells form the early 'fatty-streak' atherosclerotic lesions. Migration of VSMCs to the intima thickens the lesion, and causes formation of a fibrous cap, which can become fragile due to the apoptosis of VSMCs and elevated activity and level of proteases and leads to the final stage of atherosclerosis, plaque rupture and thrombosis.

1.2.2. Ca^{2+} in atherosclerosis

Calcium (Ca^{2+}) is an important intracellular second messenger in almost all eukaryotic cells. Moreover, Ca^{2+} signalling plays key roles in pathogenesis of atherosclerosis. For example, in endothelial cells, Ca^{2+} reversibly binds the protein calmodulin to form a Ca^{2+}/calmodulin complex, which can activate endothelial NO synthase (eNOS), inducing NO production (Lin et al., 2000). As described above, NO is important to keep normal endothelial function and it also inhibits VSMC proliferation and platelets aggregation, therefore it is an important atheroprotective factor (Shaul, 2003). ER stress-induced and Ca^{2+}/calmodulin-dependent apoptosis of macrophages, smooth muscle cells, and endothelial cells also play important roles in atherosclerotic plaque formation (Scull and Tabas, 2011). Ca^{2+} is also known to regulate phosphoinositide 3-kinase (PI3K) signalling, which is involved in the pathogenesis of atherosclerosis (Morello et al., 2009). Ca^{2+} is also important for VSMC migration, which is involved in fibrous plaque formation as described above (Gerthoffer 2007). The importance of Ca^{2+} signalling and the regulation of Ca^{2+} homeostasis are highlighted in the next part of this introduction.

1.2.3. Shear stress in atherosclerosis

Shear stress caused by blood flow, a frictional force applied on endothelial cells, plays a key role in regulating endothelial cell function. While laminar shear stress exerted by laminar blood flow induces production of NO, and is thus atheroprotective, disturbed or low shear stress may promote endothelial dysfunction, induce expression of inflammatory proteins, and create an atheroprone environment (Firasat et al., 2014, Heo et al., 2014). Shear stress sensing and mechanotransduction in endothelial cells are also described below.

1.3. Ca^{2+} signalling in the vascular system

Ca^{2+} is well established as a major intracellular signal, as it regulates a variety of cellular processes such as cell proliferation, migration, and cell apoptosis. Ca^{2+} signal also plays key roles in regulation of gene transcription, cell differentiation, migration, neurotransmitter release. In vascular system, Ca^{2+} is required for many vital functions such as vasoconstriction and dilation, vascular endothelium permeability and angiogenesis (Berridge et al., 2003, Jernigan and Resta, 2014, Khazaei et al., 2008).

Because continuous elevation of intracellular (cytoplasmic) concentration of Ca^{2+} ([Ca^{2+}]$_i$) is considered toxic and can induce cell death, [Ca^{2+}]$_i$ is tightly maintained at about 100 nM, which is 20,000-fold lower than extracellular Ca^{2+} concentration (Clapham, 2007). This concentration gradient requires a balance between the 'on' reactions that allow Ca^{2+} influx into the cytoplasm and 'off' reaction that removes Ca^{2+} from the cytoplasm, by chelation, compartmentalisation and extrusion.

Ca^{2+} is not only present in the cytoplasm, but is also contained in intracellular stores such as endoplasmic reticulum (ER), mitochondria, Golgi, and lysosomes. ER and mitochondria are well-established cellular compartments for Ca^{2+} storage and release, and thus important for maintaining Ca^{2+} homeostasis (Berridge, 2002, Dickson et al., 2012, Tran et al., 2000). ER is now considered as a multifunctional signalling organelle and the major intracellular Ca^{2+} store. In endothelial cells, up to 75% of the total intracellular Ca^{2+} is localised in ER. ER Ca^{2+} concentration is normally 100-500 μM, but can reach up to 3 mM (Berridge, 2002, Tran et al., 2000). Mitochondria are intimately connected with ER, and help to regulate the Ca^{2+} signal. Mitochondria are important for taking up Ca^{2+} released from ER, while a large amount of Ca^{2+} moving from ER to the mitochondria induce a number of stress signals (Berridge, 2002).

A variety of receptors, Ca^{2+}-permeable ion channels, pumps and exchangers located in both the intracellular and plasma membrane are important for the accurate regulation of Ca^{2+} homeostasis. The mechanism by which a cell controls Ca^{2+} homeostasis is summarised schematically in Figure 1.1. The details are discussed in the next sections.
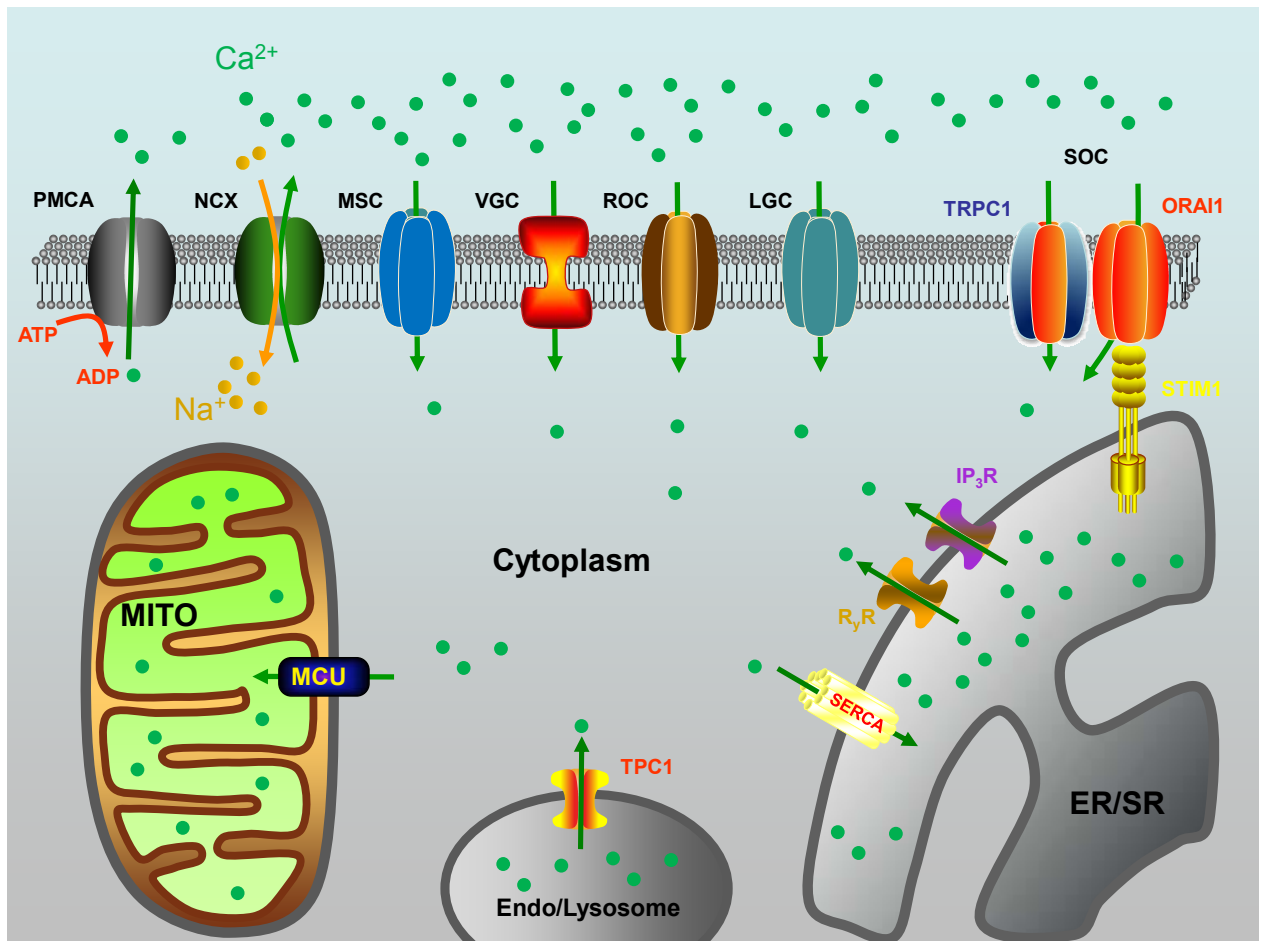
Figure 1.1. Schematic of Ca^{2+} handling in a vascular cell. Intracellular Ca^{2+} stores: ER/SR, endo/sarcoplasmic reticulum, MITO, mitochondria. Ca^{2+} entry mechanism: VGCC, votage-gated Ca^{2+} channel, is activated in response to membrane depolarisation. ROC, receptor-operated Ca^{2+} channel, mediate Ca^{2+} entry in response to agonists binding to corresponding G-protein coupled receptors. SOC, store-operated Ca^{2+} channel, opens in response to depletion of the intracellular Ca^{2+} stores. Upon store depletion, STIM1 (stromal interaction molecules1) oligomerize and traffic to ER-plasma membrane junction areas and couple Orai1, allowing aggregation and activation of Orai1, inducing Ca^{2+} influx. TRPC1, transient receptor potential canonical 1, is also considered as a SOC. LGC, ligand-gated Ca^{2+} channel, can be activated by direct agonist binding to the channel. MSC, mechanosensitive Ca^{2+} channel, is activated in response to a wide range of external mechanical stress stimuli. Intracellular Ca^{2+} release and uptake mechanisms: Ca^{2+} release from ER is mainly mediated by two channels, the inositol 1,4,5-trisphosphate receptor (IP3R) and ryanodine receptor (R$_y$R). The uptake of Ca^{2+} by ER is mediated by Sarco/endoplasmic reticulum calcium ATPase (SERCA) pump. Two pore channel 1 (TPC1), is required for NAADP-induced Ca^{2+} release from endosomes and lysosomes. The mitochondrial Ca^{2+} uniporter (MCU) is considered to be responsible for mitochondrial Ca^{2+} uptake. Ca^{2+} extrusion mechanism: plasma membrane Ca^{2+}-ATPase (PMCA) and Na$^+$/Ca^{2+} exchanger (NCX) are responsible for the processes. Modified from Harraz and Altier (2014).

1.3.1. Ca^{2+} entry mechanism

The lipid bilayer is impermeable to charged ions like Ca^{2+}. Instead the entry of Ca^{2+} or other ions is through specific pore-forming membrane channel proteins termed ion channels. Ca^{2+} channels can be classified to two main types according to the gating mechanism: voltage-gated Ca^{2+} channels and non-voltage-gated Ca^{2+} channels. Voltage-gated Ca^{2+} channels (VGCCs) open and close in response to changing in membrane potential, while non-voltage gated Ca^{2+} channels cannot be activated by membrane depolarization. However, in some cases, once activated, non-voltage gated Ca^{2+} channel activity contributes to changes of membrane potential, and can be modulated by membrane potential (Gee et al., 2010). Non-voltage gated channels can be classified to several classes, including receptor-operated channels (ROCs), store-operated channels (SOCs), ligand-gated channels (LGCs) and mechanosensitive channels (MSCs).

Voltage-gated Ca^{2+} channels (VGCC)

Voltage gated Ca^{2+} channels are broadly expressed in excitable cells like neurons and muscular cells, involved in excitation and contraction. VGCCs have a high selectivity for Ca^{2+} and are activated by cell membrane depolarisation. VGCCs were initially classified to 5 sub-families according to their physiological roles and/or inhibition by specific toxins, including L- , N-, P/Q, R- and T-type VGCC. VGCCs were then re-classified to 3 major subfamilies, Ca$_V$1, Ca$_V$2, Ca$_V$3, according to the gene encoding pore-forming α$_1$ subunits (Ertel et al., 2000). Ca$_V$1, which mediates L-type Ca^{2+} current, is responsible for regulation of gene expression, vascular contraction, hormone secretion, and integration of synaptic signal. Ca$_V$2 mediates P/Q-, N- and R-type current and initiates synaptic transmission at fast synapses. Ca$_V$3 mediates T-type Ca^{2+} current, and can be activated by more negative membrane potentials compared with other subfamilies. It controls action potentials in rhythmically firing cells including cardiac myocytes and thalamic neurons (Catterall, 2011). In VSMC, L-

and T-type VGCCs are involved in contractility and cell proliferation (Muramatsu et al., 1997, Rodman et al., 2005). VGCC in VSMCs has also been implicated in conditions like hypoxia and CVDs, such as hypertension and coronary ischemia (Hansen et al., 2011, Hou et al., 2002, Shirahata and Fitzgerald, 1991). L-type VGCCs are considered to be the major target for the pharmacological Ca^{2+} channel antagonists like dihydropyridines, which are used to treat CVDs (Jernigan and Resta, 2014, Lundy et al., 2009, Tijssen and hugenholtz, 1996). Endothelial cells are generally considered as non-excitable and lacking VGCC. However, several reports have shown VGCC expression in microvascular ECs, but not macrovascular ECs, suggesting a specific role of VGCCs in microvascular ECs (Bossu et al., 1992a, Bossu et al., 1992b, Zhou and Wu, 2006). It is suggested that T-type Ca^{2+} channels are responsible for P-selectin surface expression and von Willebrand factor secretion in pulmonary microvascular endothelium (Zhou et al., 2007&2010).

Receptor-operated channels (ROCs) and Store-operated Channels (SOCs)

Receptor-operated channels are membrane-spanning non-selective cation channels, which mediate Ca^{2+} entry in response to agonist binding to its corresponding G-protein coupled receptor (GPCR). Activation of GPCRs by agonists such as histamine, angiotensin II, endothelin-1 binding triggers the synthesis of Inositol trisphosphate (IP3) and diacylglycerol (DAG) via phospholipase C (PLC) activation. Several transient receptor potential canonical (TRPC) channels are known to be activated by GPCR agonists or downstream signalling molecules. TRPC3, TRPC6 and TRPC7 can be activated by DAG (Eder and Groschner, 2008), and TRPC5 is commonly stimulated by agonists binding to corresponding GPCRs (Jiang et al., 2011).

Store-operated Ca^{2+} entry (SOCE) confers plasma membrane Ca^{2+} entry via store-operated channels (SOC) in response to depletion of the intracellular Ca^{2+} stores. SOCE is considered to be a major Ca^{2+} entry mechanism in non-excitable cells (Parekh and Putney, 2005). IP3 induces depletion of Ca^{2+} from the ER store, which also causes Ca^{2+} influx through SOC. Both SOCE and

ROCE (receptor-operated Ca^{2+} entry) are dynamic and highly regulated processes likely to be mediated by macromolecular complexes. Therefore, the molecular components of ROC and SOC remain controversial and may be different in different cell types (Jernigan and Resta, 2014). However, recent studies revealed the importance of two components of SOCE, stromal interaction molecules1 (STIM1) and Orai1. STIM1 locates in ER membrane, while Orai1 is a plasma membrane protein (Feske et al., 2006, Liou et al., 2005, Roos et al., 2005, Vig et al., 2006, Zhang et al., 2005). Upon store depletion, STIM1 molecules oligomerize and traffic to the ER-plasma membrane junction areas and couple to Orai1, allowing aggregation and activation of Orai1, thus inducing Ca^{2+} influx (Lewis 2011). Furthermore, several reports also suggest TRPC1 contributes to SOCE (Li et al., 2008, Liu et al., 2003). STIM has been implicated in activating TRPC channels, TRPC1-6 (not TRPC7), suggesting SOCs and ROCs may be closely related (Cahalan, 2009, McFadzean and Gibson, 2002). It is also suggested TRPC channels may contribute to SOCE or ROCE in the same cell type depending on their expression levels (Vazquez et al., 2003).

SOCE is important in VSMC proliferation and migration (Li et al., 2008), and regulates tube formation from endothelial cells (Li et al., 2011). In endothelial progenitor cells isolated from patients with primary myelofibrosis, an enhanced SOCE was observed, correlated with an increased expression of STIM, Orai and TRPC1 (Dragoni et al., 2014). SOCE and ROCE have also been implicated in cardiovascular disease. Chronic hypoxia elevates SOCE and ROCE in pulmonary arterial smooth muscle cells, which correlates with an increase of TRPC1 and TRPC6 (Lin et al., 2004). They also contribute to vasoconstriction of small pulmonary arteries isolated from animals with pulmonary hypertension (Jernigan et al., 2012).

Ligand-gated channels (LGCs)

Ligand-gated Ca^{2+} channels (LGCs) can be activated by an agonist binding to the channel itself, and trigger non-selective Ca^{2+} entry. P2X receptors are

classic examples of LGCs, which mediate Ca^{2+} entry in response to adenosine 5-triphosphate (ATP) stimulation. They belong to a larger family of receptors termed purinergic receptors. P2X receptors consist of 7 subfamilies ($P2X_1$-$P2X_7$), and are widely distributed throughout human body including central nervous system, endothelium, smooth muscle, and bone (Fountain, 2013). P2X receptors are implicated in regulating the physiology of blood vessels. P2X1 expressing in VSMCs has a vasoconstrictive function. In endothelial cells, both P2X1 and P2X4 can be activated by ATP released in response to blood shear stress, causing vasodilation (Burnstock and Ralevic, 2014, Harrington et al 2007).

Mechanosensitive channels (MSCs)

Mechanosensitive Ca^{2+} channels (MSCs) (also termed stretch activated Ca^{2+} channels (SACs) are membrane proteins mediating non-selective Ca^{2+} entry that are activated in response to a wide range of external mechanical stress stimuli, such as pressure or shear stress acting at the plasma membrane. MSCs were first identified in chick skeletal muscle (Guharay and Sachs, 1984), and were later found to be widely expressed in a range of cell types including neuron, endothelial cells, myocytes, fibroblasts and cells in renal tract (Kalapesi et al., 2005). The underlying molecular mechanisms of MSCs sensing mechanostimuli are not fully understood. It was suggested mechanosensitivity of ion channels requires protein-lipid interactions (Yoshimura and Sokabe, 2010). GsMTx4, a spider toxin, specifically inhibits MSC channels by disturbing the lipid-channel boundary (Suchyna et al., 2000). There is also evidence that PLC is involved in the downstream signalling pathway of MSC (Spassova et al., 2006).

Several TRP channels have been reported to be mechanosensitive, including TRPV2, TRPV4, TRPM4, TRPC1, TRPC5, TRPC6, and TRPP1 and 2 complex (PC1 and PC2), which can be activated by mechanically or osmotically induced membrane stretch (Beech et al., 2004, Earley et al., 2004, Gomis et al., 2008, Maroto et al., 2005, Nauli et al., 2003, Muraki et al., 2003, Spassova et al., 2006,

Yao and Garland, 2005). However, the mechanical gating of TRP channels remains controversial (Gomis et al., 2008). A recent study by Coste et al. (2010) showed Piezo1 and Piezo2 proteins are linked to mechanically-activated (MA) cation channel activities. In sensory neurons or when over-expressed in the HEK293 cell-line, Piezo1 generated Ca^{2+}-permeable non-selective cationic channels that were activated rapidly and transiently by mechanical impact. Furthermore, it was able to reconstitute an ion channel when purified and incorporated in artificial lipid bilayers, suggesting Piezo protein is a MSC (Coste et al., 2012).

TRPV4 expressed in VSMCs is reported to be involved in basal pulmonary arterial tone. Its expression is up-regulated following chronic hypoxia, and mechanosensitive TRPV4 is important for a feed-forward mechanism, which facilitates Ca^{2+} entry in response to an increase in intraluminal pressure and induces pulmonary hypertension (Yang et al., 2012).

Shear stress caused by blood flow is a common stimulus acting on vascular endothelial cells. Several ion channels have been reported to be involved in the shear stress response, such as TRPV4 and P2X4 (Gao et al., 2003, Kohler et al., 2006, Yamamoto et al., 2000). Shear stress sensing of endothelial cells is discussed in detail in the next part of this introduction, and a novel Piezo1-mediated shear stress response will be described in Chapter 4 and Chapter 5 of this thesis.

1.3.2. Intracellular Ca^{2+} release and uptake mechanisms

Ca^{2+} release from ER is mainly mediated by two channels, the inositol 1,4,5-trisphosphate receptor (IP_3R) and ryanodine receptor (R_yR) (Berridge, 2002). The second messenger IP_3 generated by PLC activation stimulates IP_3R and triggers Ca^{2+} release from ER store. R_yR is a structural analogue of IP_3R. It is activated by caffeine and mediates Ca^{2+} release pharmacologically. Physiologically, R_yR is stimulated by Ca^{2+} influx, and therefore termed Ca^{2+}-

induced Ca^{2+} release (CICR) channel (Fellner and Arendshorst, 2000, Hamilton and Serysheva, 2008). Nicotinic acid adenine dinucleotide phosphate (NAADP) is an intracellular Ca^{2+}-mobilizing agent, which induces Ca^{2+} release from intracellular acidic Ca^{2+} stores, such as endosomes and lysosome (Patel and Docampo, 2010). It is suggested that a member of the two pore channels (TPCs), TPC1, is required for NAADP-induced Ca^{2+} release (Brailoiu et al., 2009).

The uptake of Ca^{2+} by ER is mediated by sarco/endoplasmic reticulum calcium ATPase (SERCA) pump, which can transfer cytoplasmic Ca^{2+} into SR/ER against its concentration gradient. Pharmacologically, SERCA can be blocked by thapsigargin (Sagara and Inesi 1991). Beside ER, mitochondria can also take up Ca^{2+} released from ER via mitochondrial Ca^{2+} uniporter (MCU), a highly selective calcium channel in the organelle's inner membrane. Essential MCU regulator (EMRE) has been recently shown to be an essential component of the MCU (Sancak et al., 2013).It has also been reported that Ca^{2+} could transfer between ER and mitochondria at ER-mitochondria contact sites without going into the cytosol (Rizzuto et al., 2009).

1.3.3. Ca^{2+} extrusion mechanism

Extrusion of the cytosolic Ca^{2+} to the extracellular space plays an important role in regulating Ca^{2+} homeostasis. Plasma membrane Ca^{2+}-ATPase (PMCA) and Na^+/Ca^{2+} exchanger (NCX) are responsible for the process (Berridge et al., 2003). The PMCA is localised on the plasma membrane. It has low transport capacity but high affinity for Ca^{2+}, which means PMCA is able to respond to small changes in cytoplasmic Ca^{2+} concentration over long duration, and maintain the resting Ca^{2+} level at ~100nM (Clapham, 2007). One Ca^{2+} is removed by PMCA from cytoplasm for each ATP hydrolysed (Moccia et al., 2012). Four isoforms of PMCA encoded by four genes have been identified. PMCA1 is the predominant isoform in ECs, while VSMC express PMCA4 and PMCA1 (Abramowitz et al., 2000, Szewczyk et al., 2007).

NCXs are also localised on the plasma membrane. NCX has higher transport capacity but lower affinity for Ca^{2+} compared to PMCA, which enables rapid regulation in Ca^{2+} concentration (Clapham, 2007). Three isoforms of the NCX family have been identified (NCX1-3), of which NCX1 is most broadly expressed. Both EC and VSMC express NCX1 (Szewczyk et al., 2007).

1.3.4. TRP Channels

The mammalian TRP (Transient Receptor Potential) family of ion channels contains 6 subfamilies: TRPC (canonical), TRPM (melastatin), TRPV (vanilloid), TRPA (ankyrin), TRPP (polycystin), TRPML (mucolipin). TRP channels are tetramers of TRP protein subunits, which could be homo- or heteromultimeric. All the TRP proteins share a common structure with 6 transmembrane (TM) segments, including a pore-forming region between TM5 and TM6, intracellular C- and N- termini. The N-termini of TRPC channels and the C-termini of TRPM and TRPA channels contain coiled-coil domains, which function to connect different subunits of oligomeric complexes. The N-termini of TRPC, TRPV and TRPA channels contain ankyrin binding repeats. TRPC, TRPV and TRPM subfamilies have a TRP domain after the ion channel domain, which includes three variations of the Glu-Trp-Lys- Phe-Ala-Arg (EWKFAR) TRP box (Clapham, 2003, Montell et al., 2002, Birnbaumer, 2009).

The TRP channels are generally considered to be non-selective channels permeable to monovalent and divalent cations. Most TRP channels have some Ca^{2+} permeability while TRPM4 and TRPM5 are impermeable to Ca^{2+} , and TRPV5 and TRPV6 are highly selective to Ca^{2+} (Owsianik et al., 2006). TRP channels can be activated by external ligands, G protein–coupled receptors (GPCR), metabolites, or physical stimuli. Once activated, the influx of cations through TRP channels causes depolarisation of the membrane potential (Birnbaumer, 2009).

TRP channels appear to be expressed in every mammalian tissue. Many TRPs are expressed at the dendritic ends of sensory neurons, conferring a role in sensory signal transduction. For example, TRPV1 is a cellular sensor for heat and TRPM8 is a sensor for cold, TRPV4 is sensor for hypo-osmolality, and TRPA1 may mediate mechano-transduction (Pedersen et al., 2005).

The TRPC subfamily of TRP contains the closest mammalian homologues of the *Drosophila* TRP, the first described TRP channel (Montell and Rubin, 1989). It has seven members (TRPC1-7), of which TRPC1 was the first to be identified (Wes et al., 1995). The difference between TRPC channels and other TRP families of ion channels is that in addition to mediating agonist-induced cation influx, TRPC channels are also commonly, although controversially, proposed to participate in store operated Ca^{2+} entry (SOCE). TRPC channels have been implicated in a wide range of processes in vascular physiology and disease, including vessel dilation, vessel constriction, angiogenesis, and atherogenisis (Beech, 2013).

TRPC1

TRPC1 is widely expressed in many human cells and tissues including VSMCs, ECs, neurons, liver, platelets and salivary glands (Beech, 2005b). A feature of TRPC1 is that it can form a heterotetrameric complex with other TRPCs including TRPC4 and TRPC5, and possibly TRPC3 (Hofmann et al., 2002, Strubing et al., 2001, Strubing et al., 2003). TRPC1-TRPC5 heteromer is especially well established (Al-Shawaf et al., 2010, Beech, 2005a, Bezzerides et al., 2004, Hofmann et al., 2002, Shi et al., 2012, Strubing et al., 2001, Strubing et al., 2003, Sukumar et al., 2012, Xu et al., 2006, Xu et al., 2008). The specific functions and mechanisms of these heteromultimeric channels are not fully understood. However, compared to TRPC5 homomeric channels, heteromers containing TRPC1 show decreased unitary conductance and lower Ca^{2+} permeability, leading to smaller whole-cell currents and less Ca^{2+} entry (Beech, 2005a, Xu et al., 2008). TRPC1 has been reported to be activated by store depletion (Ahmmed et al., 2004, Beech, 2005a), and plasma membrane recruitment of TRPC1 has been reported to be regulated by local Ca^{2+} entry via Orai1, while knock-down of TRPC1 significantly inhibits SOCE (Cheng et al.,2011).

TRPC1 expression is up-regulated under physical and metabolic injury condition in vivo (Kumar *et al.,* 2006, Edwards *et al.,* 2010). It has positive

effects on VSMCs proliferation, migration and hypertrophy (Sweeney *et al.*, 2002, Takahashi et al., 2007, Li et al., 2008). Such effects and the associated Ca^{2+} influx raise a paradox because TRPC1 fails to form functional ion channels on its own and actually suppresses the conductance of channels formed by other TRPCs (Beech, 2005a, Strubing *et al.*, 2001). So the mechanism by which upregulated TRPC1 plays a positive role in Ca^{2+} entry and vascular remodeling remains unclear.

TRPC5

TRPC5 is also reported to be expressed in various tissues including, but not limited to, vascular smooth muscle cells (Beech et al., 2004, Xu et al., 2006), endothelial cells (Yoshida et al., 2006, Chaudhuri et al., 2008) and neurons (Greka et al., 2003). It can form heteromultimers with TRPC1 and is also implicated in vascular cell migration (Xu *et al.*, 2006).

TRPC5 can be activated by agonists binding to G-protein coupled receptors (GPCR) like ATP, sphingosine-1-phosphate (S1P), or histamine (Beech, 2009, Zeng et al., 2004). PLC is implicated in TRPC5 activation because PLC inhibitor, U73122, down-regulates TRPC5 activity (Kanki et al., 2001, Schaefer et al., 2000). It has been reported that phosphatidylinositol 4-phosphate and phosphatidylinositol 4,5- bisphosphate (PIP2) negatively modulate TRPC5 channels (Trebak et al., 2009), while PLC leads to the PIP2 hydrolysis and formation of IP3 and DAG, which can subsequently activate plasma membrane calcium-permeable channels like TRPC channels (Jiang et al., 2011, Putney, 1986, Berridge, 1995, Parekh and Putney, 2005).

TRPC5 is transported rapidly from intracellular vesicles to plasma membrane in response to epidermal growth factor stimuli. This process, which Bezzerides et

al. (2004) termed 'rapid vesicular insertion of TRP', increases plasma membrane TRPC5 channels and functional TRPC5 current. The process requires phosphatidylinositide 3-kinase, the Rho GTPase Rac1 and phosphatidylinositol 4-phosphate 5-kinase, but is inhibited by co-expression of TRPC1 (Bezzerides et al., 2004).

A unique feature of TRPC4 and TRPC5 is that they can be directly activated by lanthanides like Gd^{3+} and La^{3+} by an action at extracellular site (Jung et al., 2003, Zeng et al., 2004). It has also been reported recently that TRPC5 can be directly activated by lead ion (Pb^{2+}), suggesting TRPC5 has a potential role in sensing metal ion toxicity (Sukumar and Beech, 2010). Ca^{2+} entry through TRPC5-containing channels are also evoked by 1-palmitoyl-2-glutaroyl-phosphatidylcholine (PGPC), which is an oxidized phospholipid (Al-Shawaf et al., 2010). Also, cross-linking of GM1, one of the gangliosides, with multivalent ligands induces TRPC5-dependent Ca^{2+} influx (Wu et al., 2007).

Cholesterol regulation of TRPC channels

Cholesterol is a key constituent of membranes and an important driver of cardiovascular and other common diseases, such as atherosclerosis. Most major families of ion channels have been shown to be regulated by changing levels of membrane cholesterol, although the impacts of cholesterol on different types of ion channels are really heterogeneous. Several hypotheses of the mechanisms underlying the regulation have been proposed. In these hypotheses, cholesterol may regulate the ion channels by direct interaction or indirectly through other signalling molecules, or by changing the physical properties of the membrane bilayer (Levitan et al., 2010).

Several members in the TRP family of ion channels have been shown to be regulated by cholesterol, including TRPC1, TRPC3 and TRPC6. TRPC1 has been reported to be localized in caveolae and associate with signaling proteins (Beech, 2005a, Beech, 2012). Methyl β-cyclodextrin (mβCD) is a 7-D-

glycopyranose cyclic oligosaccharide. The size of the hydrophobic cavity of mβCD makes it highly effective to include and extract cholesterol from cell plasma membrane and, consequently, it is the most commonly used compound to deplete cellular cholesterol. On the other hand, incubation with mβCD/cholesterol complex (water-soluble cholesterol can increase the cholesterol level in the cell membrane (Zidovetzki and Levitan, 2007). In mβCD-treated caudal arteries, Ca^{2+} influx was significantly reduced, and co-localization of TRPC1 with caveolin-1 was also reduced, as seen by immunofluorescent staining. (Bergdahl et al., 2003). Furthermore, the co-localization of TRPC1 and caveolin-1 was reduced after cholesterol depletion in human platelets (Brownlow, 2004). Cholesterol enrichment, however, resulted in a redistribution of the channels to raft fractions (Kannan et al., 2007).

Cholesterol loading has been shown to enhance TRPC3 channel function (Graziani et al., 2006). Cholesterol-loading activated a non-selective cation conductance and a Ca^{2+} entry pathway in TRPC3-overexpressing cells but not in wild-type HEK293. The current-voltage relationship was similar to that of PLC-dependent TRPC3 channels. Also cholesterol loading was found to increase surface expression of TRPC3 like PLC stimulation (Graziani et al., 2006).

Cholesterol is the precursor for steroid hormones such as the neuroactive steroids. TRPC5 is inhibited by specific types of neuroactive steroid via a rapid, non-genomic mechanism (Beech, 2012, Majeed et al., 2011).

TRPC6 distributes both into insoluble and soluble platelet fractions. The distribution of the channels was not affected by cholesterol depletion (Brownlow, 2005). However, the regulation of TRPC6 by podocin required cholesterol binding (Huber et al., 2006). Podocin is a protein involved in the function of the filtration barrier in the mammalian kidney, and binds cholesterol. It interacts with TRPC6, and mediates TRPC6 activation. The podocin-dependent activation of TRPC6 is suppressed by cholesterol depletion (Huber et al., 2006). Although

some members in TRPC family have been shown to be regulated by cholesterol, the impact of cholesterol on other TRPC channels remains unclear.

1.4. Shear-stress sensing of vascular endothelial cells

Vascular endothelial cells are subjected to shear stress when blood flows through the endothelium. The intensity of shear stress (τ) can be calculated using the formula: $τ = 4μQ/πr^3$ (μ: blood viscosity, Q: the blood flow rate, π: circumference ratio, and r: the radius of the blood vessel) (Ando and Yamamoto, 2013). Human physiological shear stress ranges from 1 to 70 $dyn.cm^{-2}$ in different types of blood vessels (Chiu and Chien, 2011). Blood flow is laminar in the straight segments of blood vessels, which induces ECs to produce atheroprotective factors like NO and vascular endothelial growth factor (VEGF) (Firasat et al., 2014, dela Paz et al., 2012). However, in curved part or at branch points, the blood flow becomes turbulent, which can promote endothelial dysfunction, induce expression of inflammatory proteins, and create an atheroprone environment (Firasat et al., 2014, Heo et al., 2014). Shear stress acting on endothelial cells is converted into biochemical signals which trigger changes in transcriptional factor activation, gene expression and cell function. Determination of the mechanisms by which ECs sense physical forces remains one of the major challenges of biology research. Multiple molecules are implicated, including extracellular matrix proteins, adhesion molecules (e.g. CD31/PECAM-1), membrane proteins (integrins, ion channels, receptors, caveolins etc) and organelles like primary cilia.

The shear stress-sensing mechanism of an endothelial cell is summarised schematically in Figure 1.2. The detailed mechanisms are discussed in the next sections.
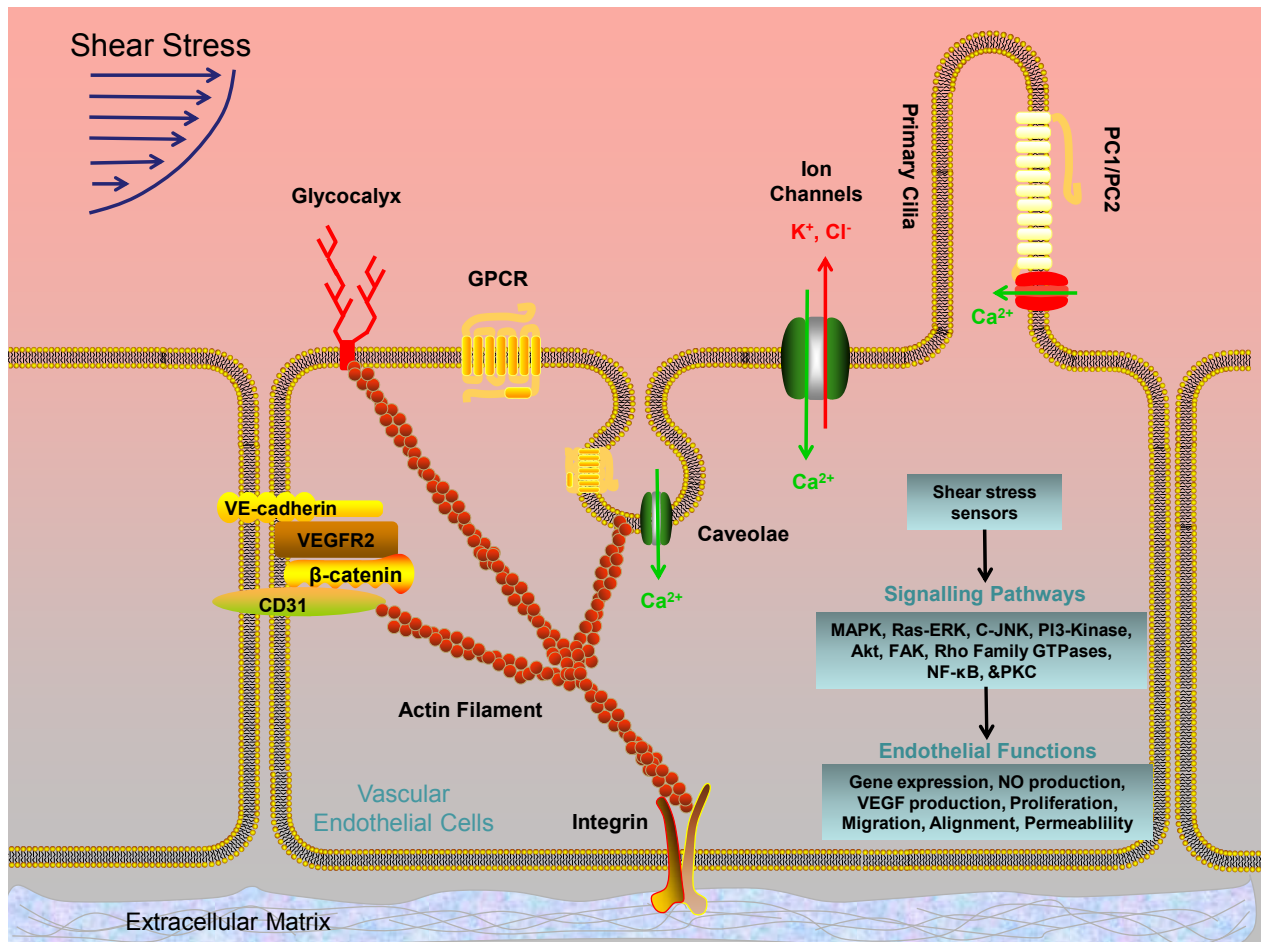
Figure 1.2. Candidates for shear stress sensors and downstream signalling pathways in endothelial cells. Multiple ion channels have been shown to be shear stress sensitive. They mediate Ca^{2+} influx and outflow of K^+ or Cl^- in response to flow. PC1 and PC2, polycystin-1and polycystin-2, form a shear stress sensitive Ca^{2+} permeable channel localised in the plasma membrane of primary cilia. CD31, vascular endothelial cell cadherin (VE-cadherin), and vascular endothelial growth factor receptor2 (VEGFR2) form a mechanosensory complex at cell-cell junctions. CD31 directly transmits mechanical force, VE-Cadherin works as an adaptor, and VEGFR2 activates phosphatidylinositol-3-OH kinase (PI3K). Integrin are transmembrane receptors composed of α and β subunits. They interact with extracellular matrix (ECM), and can be activated in response to shear stress, mediating endothelial cell alignment in the direction of flow. Caveolae are considered as small, distinct flask-shaped invaginations of plasma membrane, which plays an important role in mechanosignal transduction by forming a platform on which a variety of receptors, ion channels, and signalling factors accumulate. GTP binding protein-coupled receptors (GPCRs) have also been reported to be involved in shear stress sensing as a primary mechanotransducers. Glycocalyx is an extension of the cell surface connected with cytoskeleton. Actin Filament, component of the cytoskeleton, provides a tension within the cytoskeleton. Shear stress redistributes the tension force within the cytoskeleton and the lipid bilayer, which is then translated into chemical signals by these sensors. These sensors may act independently or as a network in response to different shear stresses and under different conditions. Following the shear stress sensation by these sensors, varieties of downstream signalling pathways are activated, such as MAPK (mitogen-activated protein kinase), Ras-ERK (extracellular signal-regulated kinase), c-JNK(c-Jun N-terminal kinases), Akt, FAK (focal adhesion kinase), NF-κB (nuclear factor-κB), and PKC (protein kinase C). The schema is modified from Ando and Yamamoto (2013). The signalling pathway is modified from Johnson et al. (2011).

1.4.1. Ion Channels in shear stress sensing

TRP channels

TRPV4 has been reported to be activated by cell swelling-induced membrane stretch (Strotmann et al., 2000). It can also respond to heat (>27°C) (Guler et al 2002), low pH (Suzuki et al., 2003), 4α-phorbol 12, 13-didecanoate (4αPDD), arachidonic acid (AA) (Watanabe et al., 2003), and shear stress (Kohler et al., 2006). An important feature of shear stress is that it evokes elevation of intracellular Ca^{2+} levels of EC. At 37°C, but not at room temperature, TRPV4 is able to reconstitute shear stress evoked Ca^{2+} oscillations in HEK293 cells, a cell type that does not normally exhibit shear stress sensing (Gao et al., 2003). It is also reported that TRPV4 is activated in response to shear stress in native collecting duct cells. Furthermore, shear stress-induced, NO-dependent vasodilation is decreased in carotid arteries from TRPV4 knockout mice (Hartmannsgruber et al., 2007).

TRPP1 and TRPP2, also known as polycystin-1 (PC1) and polycystin-2 (PC2), are encoded by *PKD1* and *PKD2* genes respectively. The mutations of PC1 or PC2 commonly cause polycystic kidney disease, which is characterized by the presence and progressive development of multiple cysts in both kidneys (Ong and Harris, 2005). PC1 activates a G-protein signalling pathway, while PC2 forms a nonselective Ca^{2+}-permeable channel (Delmas et al., 2002, Gonzalez-Perrett et al., 2001). PC1 and PC2 form a complex localised in the plasma membrane of primary cilia of kidney epithelium, which has been shown to induce Ca^{2+} influx in response to shear stress (Nauli et al., 2003, Newby et al., 2002). A later study provides evidence that PC1 and its proper localization in primary cilium is necessary for shear stress-evoked Ca^{2+} signalling and NO production (Nauli et al., 2008). Furthermore, in MDCK (Madin-Darby canine kidney) cells, PC1 is suggested to be a cell adhesion molecule and its interactions regulate the recruitment of E-cadherin (Streets et al., 2009), a molecule that contributes to shear stress sensing (le Duc et al., 2010). PC2

and its localization in cilia have also been shown to be responsible for shear stress sensing in mouse endothelial cells (AbouAlaiw, 2009). Consistent with these finding, endothelial cells isolated from patients with autosomal dominant polycystic kidney disease (ADPKD), which lack PC2, are unable to sense fluid flow (AbouAlaiw, 2009).

TRPC3 and TRPM7 have also been reported to be involved in endothelial responses to shear stress (Liu et al., 2006, Oancea et al., 2006). TRPC3 is involved in flow-induced vasodilation in rat small mesenteric arteries (Liu et al., 2006). Flow causes functional TRPM7 channels to accumulate at the plasma membrane, and consequently increase TRPM7-dependent current (Oancea et al., 2006).

P2X4 Purinoceptors

As described above, the P2X4 receptor is a ligand-gated Ca^{2+} channel activated by ATP. It is suggested that P2X4 is the major contributor to shear stress-evoked Ca^{2+} influx. Knock-down of P2X4 in human umbilical vein endothelial cells (HUVECs) abolishes the flow-induced Ca^{2+} response. HEK293 cells over-expressing P2X4 exhibit shear stress-dependent Ca^{2+} influx (Yamamoto et al., 2000). Furthermore, endothelial cells isolated from P2X4-deficient mice do not have normal response to shear stress. The shear stress-evoked Ca^{2+} influx and NO production are almost abolished in these cells. Flow induced vasodilation is also suppressed in P2X4-deficient mice (Yamamoto et al., 2006).

K^+ Channels and Cl^- Channels

Beside Ca^{2+} channels, K^+ channels and Cl^- channels are also implicated in shear stress sensing. It has been shown that flow evokes a K^+ selective current, which varies in magnitude and duration as a function of shear stress (Olesen et al., 1988). The shear stress-induced K^+ current leads to the hyperpolarization of

EC membranes, which was confirmed by a voltage-sensitive dye (Nakache and Gaub 1988). It has been reported that blockade of K^+ channels impaired shear stress-mediated NO production (Uematsu et al., 1995). Cl^- channels contribute to the membrane depolarization of endothelial cells following the shear stress-evoked membrane hyperpolarization (Barakat et al., 1999).

1.4.2. CD31/VE-cadherin/VEGFR2 mechanosensory complex

Endothelial cell functions are dependent on assembly of various adhesion complexes. Platelet endothelial cell adhesion molecule-1 (PECAM-1) or CD31 is concentrated at cell-cell junctions and exhibits homophilic binding between neighbouring endothelial cells. It is important for leucocyte transmigration through vascular endothelium, cell adhesion and angiogenesis (DeLisser et al., 1997). Vascular endothelial cell cadherin (VE-cadherin) which is specifically expressed in ECs, is the major adhesive protein at adherence junctions. It is connected with cytoskeleton through β-catenin, an anchoring molecule. VE-cadherin is required for vascular endothelial growth factor (VEGF) -dependent cell survival, vessel remodeling and maturation of the vascular network (Carmeliet et al., 1999). VEGF is an important signaling protein involved in both the formation of the circulation system and angiogenesis. It activates its receptors (VEGFR), especially VEGFR2 in endothelial cells (Carmeliet et al., 1999).

Application of fluid shear stress to endothelial cells induces rapid tyrosine phosphorylation of CD31, which reached a plateau within 2 minutes (Osawa et al., 2002). The response cannot be mimicked by elevating intracellular Ca^{2+} or treating the cells with growth factors, suggesting CD31 may be a shear stress sensor (Osawa et al., 2002). Furthermore, fluid flow can activate extracellular signal-regulated kinases (ERK) and such activation is dependent on CD31 tyrosine phosphorylation (Osawa et al 2002). Shear stress has been reported to cause re-distribution of VE-Cadherin to form a dash-like structure at cell-cell junctions (Noria et al., 1999). VEGFR2 has been reported to be activated by the

onset of flow independently of VEGF. It forms clusters in the plasma membrane and binds to the adaptor protein Shc, recruits PI3K, and consequently activates Akt and eNOS (Chen et al., 1999).

It has been reported that CD31, VE-cadherin and VEGFR2 comprise a shear-stress sensory complex in endothelial cells (Tzima et al., 2005). In this model, CD31 directly transmits mechanical force, VE-Cadherin works as an adaptor; and VEGFR2 activates phosphatidylinositol-3-OH kinase (Tzima et al., 2005). In vitro, disruption of this complex abolishes endothelial alignment to shear stress, which is an important downstream function of laminar shear stress. The complex is sufficient to confer responsiveness to flow in heterologous cells. Consistent with the in vitro data, NF-kB and downstream inflammatory genes were not activated in regions of disturbed flow in CD31-knockout mice. These findings suggest the complex may be involved in the EC response to both laminar and disturbed shear stress.

There is a conceptual model for the mechanosensory complex, in which shear stress directly affects CD31, resulting in activation of a src family kinase, probably Fyn (Chiu et al., 2008). VEGFR2 is then brought into this complex in the presence of VE-Cadherin, and is activated by Fyn in a ligand-independent manner (Conway and Schwartz, 2012), and subsequently mediates downstream pathways including activation of phosphatidylinositol-3-OH kinase, activation of integrin, and production of nitric oxide (Tzima et al., 2005).

1.4.3. Integrins

Downstream of the mechanosensory complex is suggested to be the activation of integrins (Tzima et al., 2005). Integrins are a family of transmembrane receptors, composed of α and β subunits. They interact with extracellular matrix (ECM), participating to intracellular transmission of mechanical signals, regulating cell shape, cells attachment and cell mobility. Integrin can be activated in response to shear stress, and mediates endothelial cell alignment in

the direction of flow (Tzima et al., 2001). Furthermore, flow-induced vasodilation is abolished by antibodies targeting β3 subunits of integrin or inhibitory peptides in isolated coronary arteries (Muller et al., 1997). The cytoplasmic domain of integrin has been functionally linked to focal adhesion kinase (FAK) (Guan, 1997), which is an important regulator of signaling pathways initiated by mechanical forces (Ngai and Yao, 2010). FAK has been reported to be activated by shear stress in endothelial cells (Li et al., 1997), suggesting it might be the downstream mechanism of integrins.

1.4.4. Caveolae

Lipid rafts are plasma membrane microdomains rich in organized sphingolipids and cholesterol. One of the most investigated lipid rafts are the caveolae. Caveolae are considered as small (approximately 50-100 nm), distinct flask-shaped invaginations of plasma membrane, which are abundant in ECs. Caveolae are rich in caveolins, cholesterol, and sphingolipids. They play an important role in signal transduction by forming a platform on which a variety of receptors, ion channels, and signaling factors accumulate (Simon and Toomre, 2000). Disruption of caveolae using mβCD, which depletes membrane cholesterol, abolishes flow-induced activation of ERK in bovine arotic ECs (Park et al., 1998). Disassembly of caveolae with cholesterol-binding agent also inhibits a shear stress-activated Ras-Raf-mitogen-activated protein kinase pathway (Rizzo et al., 1998). Furthermore, caveolin-1 knockout mice have impaired arterial remodeling in response to chronic changes in blood flow, and less flow-induced vasodilation (Yu et al., 2006).

1.4.5. G proteins and GPCRs

GPCRs have also been reported to participate in shear stress sensing as primary mechanotransducers (Gudi et al., 1996, Chachisvilis et al., 2006). G proteins can be activated within 1s after onset of flow, and this activation is

observed on EC membrane vesicles independently of the cytoskeletal and cytosolic components (Gudi et al., 1996). Blockade of G proteins can inhibit shear stress-mediated activation of Ras-GTPase and ERK1/2 (Gudi et al., 2003, Jo et al., 1997). Furthermore, Gudi et al. (1998) investigated the activation of purified G proteins reconstituted into phospholipid vesicles, and found shear stress still increased the activity of G proteins in the liposomes. The increase could be attenuated by addition of cholesterol, which makes lipid bilayer more rigid. The findings suggest phospholipid bilayer mediates the shear stress-induced activation of G proteins in the absence of their protein receptors.

1.4.6. The Glycocalyx

The inner surface of the vascular endothelium is lined with a layer of highly charged, glycoprotein-rich, and membrane-bound glycocalyx. It is an extension of the cell surface connected with cytoskeleton. Removal of heparan sulphate, the major glycosaminoglycan of the glycocalyx, significantly inhibits flow-induced NO production in bovine aortic endothelial cells (Florian et al., 2003). It is also reported that ECs do not align in the direction of flow after removal of the glycocalyx by using the specific enzyme heparinase III (Yao et al., 2007). Yao et al. (2007) also reported that shear stress caused modulation and redistribution of glycocalyx. Heparan sulphate formed a peripheral pattern with most molecules detected at the cell-cell junctions, serving as a cell-adaptive mechanism by reducing the shear gradients acting on the cell surface.

1.4.7. The Cytoskeleton

The glycocalyx, as well as many other endothelial proteins and structures that are linked to the sensing of shear stress, interacts with the cytoskeleton. Many of these proteins and structures are not exposed to shear stress directly, suggesting there may be a structure connecting them together and transducing shear stress (Ngai and Yao, 2010). Flow causes rapid structural changes of the

cytoskeleton which binds to many shear stress receptors (Barbee et al., 1994, Helmke and Davies, 2002). Therefore, the endothelial cytoskeleton is considered as a candidate for this function (Ngai and Yao, 2010). The endothelial cytoskeleton is formed by a complex network of microtubules, intermediate filaments and actin fibers across the cell, providing a tension within the cytoskeleton. Shear stress redistributes the force, which is translated into chemical signal at the end of a filament or actin fibers. Disruption of the actin cytoskeleton abolishes flow-induced activation of NFκB and upregulation of ICAM-1 (Imberti et al., 2000, Ngai and Yao, 2010). It has been suggested that intermediate filament vimentin plays a key role in shear stress transduction. Knock-down of the gene that encodes vimentin significantly decreases flow-evoked vasodilation (Henrion et al., 1997). Nevertheless, there is one study (Knudsen and Frangos, 1997) suggesting flow induced NO production does not require cytoskeleton re-arrangement.

As discussed above, both Ca^{2+} handling and shear stress response of vascular cells play important roles not only in vascular physiology, but also pathology. Therefore, understanding the mechanism of these processes could greatly help the therapeutic strategies to treat vascular diseases like atherosclerosis.

1.5. Aims of the study

The overall aim of this work was to develop better understanding of the molecular components, regulation, and significance of Ca^{2+} entry mechanisms in the primary cell types of the vascular wall: smooth muscle cells and endothelial cells. The focus of attention was on the relationships of Ca^{2+} entry mechanisms to two factors, both of which play major roles in the cardiovascular system in health and disease: these factors are cholesterol and mechanical force, both of which impact on the plasma membrane and the proteins within it.

First it was hypothesized that cholesterol might have an important relationship with TRPC channels because these channels were previously suggested to be particularly sensitive to the lipid composition of the membrane. The objectives of study were: 1) to determine the effects of cholesterol loading and depletion on TRPC5 channels over-expressed in HEK 293 cells; 2) to determine the mechanisms of the effects of cholesterol; 3) to determine if TRPC heteromultimerisation affects the action of cholesterol; 4) to determine the relevance of the mechanisms to endogenous channels of vascular smooth muscle cells obtained from patients undergoing coronary artery bypass operations.

Second it was hypothesized that in vasculature, mechanical force such as shear stress might act through mechanosensitive channels formed from Piezo1 proteins. The objectives of the study were: 1) to determine if Piezo1 is important for Ca^{2+} signals evoked by the mechanical force of shear stress applied to endothelial cells; 2) to determine downstream functional consequences of activating Piezo1 channels by shear stress; 3) to determine downstream signalling pathways linking Piezo1 to functional endpoints; 4) to determine relationships of Piezo1 to previously suggested shear stress-sensing mechanisms.

Chapter 2. Materials and Methods

2.1. Cells

Human umbilical vein endothelial cells (HUVECs) were obtained from Lonza. GripTite^{TM} HEK293 MSR cells (MSR) are a genetically engineered cell line derived from the HEK293. They have over-expressed Macrophage scavenging receptor and are more adherent than HEK293, which makes the cells suitable for transfection and immunostaining. MSR were provided by Prof. Asipu Sivaprasadarao. Proliferating vascular smooth muscle cells (VSMC) were provided by Dr. Karen E Porter. VSMCs were isolated from patients with coronary artery disease. VSMCs passaged 3-5 times were used for experiments. The work was carried under approval granted by Leeds Research ethics Committee (Ref CA01/040). Human TRPC5 was over-expressed in HEK293 cells (TRPC5-HEK) using cDNA encoding TRPC5 channels under the control of a tetracycline-regulated expression system. The addition of 1µg/ml tetracycline (Tet+) induced expression of TRPC5 channels, while Tet- cells were used as control (Zeng, 2004). Mouse embryonic endothelial cells were isolated from E9.5 wildtype or Piezo1 gene-disrupted mouse embryos by Dr.Jing Li (Li et al., 2014). Cells were isolated using Hank's solution containing collagenase (1.5 mg/ml) and DNase (25 µg/ml). All animal use was authorized by both the University of Leeds Animal Ethics Committee and by The Home Office, UK. Project licenses used in this study were 40/3557 and 40/2946. Embryonic endothelial cells were used for experiments 1 day after isolation. Human liver endothelial cells (LECs) were isolated in patients undergoing liver resection for colorectal metastases by Dr. Richard Young at St James's University Hospital, Leeds Teaching Hospitals NHSTrust. Cells were isolated using anti-CD31-conjugated paramagnetic microbeads (Li et al., 2014). The work was carried out under approval granted by the local ethics committee (Ref 10/H1306/82) and the study was adopted into the United Kingdom Clinical Research Network portfolio (ID 9442). LECs passaged 1-3 times were used for experiments.

2.2. Ionic solutions

Dulbecco's Phosphate-Buffered Saline (DPBS) from Gibco contained 1,000 mg/L D-glucose and 36 mg/L sodium pyruvate, 36mg/L calcium, and 36 mg/L magnesium. Standard bath solution (SBS) contained: NaCl 135 mM, KCl 5 mM, $MgCl_2$ 1.2 mM, $CaCl_2$ 1.5 mM, D-glucose 8 mM and HEPES 10 mM. pH was titrated to 7.4 using 4M NaOH and the osmolality was ~290 mOsm/kg. Ca^{2+} - free SBS contained the same components as normal SBS except containing 0.4mM EGTA and containing no $CaCl_2$. Normal Krebs-Henseleit solution (Krebs) contained NaCl 125 mM, KCl 3.8 mM, $NaHCO_3$ 25 mM, $MgSO_4$ 1.5 mM, KH_2PO_4 1.2 mM, D-Glucose 8 mM, $CaCl_2$ 1.2 mM, EDTA 0.02 mM. pH was titrated to 7.4 using 4M NaOH. Krebs was filter sterilized before experiments. Extremly-low-Ca^{2+} Krebs (0 Ca^{2+} Kreb) had the same components as normal Krebs except containing no $CaCl_2$.

2.3. Reagents and chemicals

All general salts and solutions were purchased from Sigma. Other reagents and chemicals are summarized in Table 2.1.

Name	Company	Solvents	Working concentration	Description
PGPC	Cayman (Europe)	Ethanol	3 µM	TRPC5-containing channel activator
GM1 gangliosides	Avanti Polar Lipids	Water	25 µM	Total ganglioside extract
GsMTx4	PEPTIDE INSTITUTE	Water	2.5 µM	Spider toxin, Piezo1 blocker
PD145305	Santa Cruz Biotechnology	DMSO	20 µM	Negative control for PD151746
PD151746	Santa Cruz Biotechnology	DMSO	20 µM	Calpain inhibitor
PD150606	EMD Millipore	DMSO	3 µM	Calpain inhibitor
CK59	EMD Millipore	DMSO	25 µM	CaMK II inhibitor
CN585	EMD Millipore	DMSO	6 µM	Calcineurin inhibitor VII
PP2	EMD Millipore	DMSO	1 µM	Src-family kinases inhibitor
UO126	EMD Millipore	DMSO	1 µM	MEK inhibitor
SB203580	EMD Millipore	DMSO	10 µM	p38 MAPK inhibitor
L-NAME	Sigma-Aldrich	Water	100 µM	NOS inhibitor
L-NMMA	Sigma-Aldrich	Water	300 µM	NOS inhibitor

Table 2.1. List of reagents and chemicals. Full name of the chemicals are shown in the following chapters.

2.4. Cell culture

MSR cells were cultured in Dulbecco's Modified Eagle's Medium (DMEM) -F12 + Glutamax-1 (GIBCO) supplemented with 10% fetal bovine serum serum (FBS) and 100 U/ml penicillin ,100 µg/ml streptomycin (Sigma), and selection antibiotics (600 µg/ml G418, Sigma), in T-75 flasks at 37 °C in a 5% CO_2 incubator. HEK293 cells over-expressing human TRPC5 channels (TRPC5-HEK) were cultured in the same medium as MSR cells and selected using 5 µg/ml blasticidin, 400 µg/mL zeocin (Invitrogen). Cells were detached and passaged at the confluence of 70-80% using 0.05% Trypsin-EDTA (GIBCO). To induce expression of TRPC5 in TRPC5-HEK, 1 µg/ml tetracycline was added to the culture medium 24 hours prior to experiments.

HUVECs and LECs were cultured in EGM-2 growth medium (Lonza) supplemented with 2% fetal calf serum (FCS), 10 ng/ml VEGF, 5 ng/ml human basic fibroblast growth factor, 1 µg/ml hydrocortisone, 50 ng/ml gentamicin, 50ng/mL amphotericin B, and 10 µg/ml heparin at 37°C in a humidified atmosphere containing 5% CO_2. Cells were detached and passaged at the confluence of 70-80% using Detachin (Genlantis). Mouse embryonic endothelial cells were cultured in EGM-2 growth medium (Lonza) supplemented with 5% fetal calf serum (FCS), 10 ng/ml VEGF, 5 ng/ml human basic fibroblast growth factor, 1 µg/ml hydrocortisone, 50 ng/ml gentamicin, 50 ng/ml amphotericin B, and 10 µg/ml heparin at 37°C in a humidified atmosphere containing 5% CO_2.

VSMCs were grown in DMEM + GLUTAMAX (GIBCO), supplemented with 10% FBS, 100 units/ml penicillin/streptomycin (Sigma) at 37°C in a 5% CO_2 incubator. Cells were passaged at the confluence of 70-80% using 0.05% Trypsin-EDTA (GIBCO).

2.5. Cell transfection

2.5.1. Lipofectamine^{TM} 2000

MSRs, HEK-TRPC5s, HUVECs and LECs were transfected at 80-90% confluence with 20 nM short interference RNA (siRNA) using Lipofectamine^{TM} 2000 (Invitrogen) in Opti-MEM (GIBCO) as per the manufacturer's instructions. Briefly, cells were grown on 6-well plate to 80-90% confluence. Culture medium was removed and 1 ml Opti-MEM added before transfection. 0.5 µl siRNA (50 µM stock) and 3 µl Lipofectamine^{TM} 2000 were added to 100 µl Opti-MEM respectively and mixed. The mixture was incubated at room temperature for 20 minutes before being added to the cells. 4 hours after transfection, Opti-MEM was removed and fresh cell culture medium added. Experiments were performed 48-72 hours after transfection. siRNA sequences are listed in Table 2.2. Lipofectamine^{TM} 2000 was also used for transfecting cDNA to MSRs and HEK-TRPC5. Cells were transfected with 0.5 µg/ml cDNA using the same protocol as transfecting siRNA.

2.5.2. FuGene HD transfection reagent

HUVECs were transfected at 80-90% confluence with 0.5 µg/ml cDNA using FuGene HD transfection reagent (Roche) according to the manufacturer's instructions. In brief, 3 µl FuGene and 1 µl cDNA were added to 100 µl Opti-MEM, mixed, and incubated at room temperature for 20 minutes. The mixture was then added onto the cells in 2 ml normal culture medium. Experiments were performed 48-72 hours after transfection.

2.5.3. Nucleofector^{TM}

VSMC were transfected using Amaxa^{TM} Basic Nucleofector^{TM} Kit for Smooth Muscle Cells (Lonza) as the manufacturer's instructions. Cells at 90% confluence on T-75 flask were transfected with 2µg DNA or 100 µmol siRNA. Briefly, Cells were detached using 2ml 0.05%Trypsin-EDTA and centrifuged in a 10 ml Falcon tube at 100 g/min for 5 minutes. The supernatant was removed and discarded before 100µl Nucleofector^{TM} transfect solution was added to the cells and mixed. The mixture was transferred to an Eppendorf tube and mixed with 2 µg DNA or 100 µmol siRNA before being transferred again to a Lonza electroporation cuvette. Nucleofector^{TM} program U-025 was used to transfect the cells in the cuvette. Cells were then transferred to 2 ml pre-warmed medium and mixed before seeded onto cover slips or a 96-well plate. Experiments were performed 48-72 hours after transfection.

2.5.4. DNA constructs

TRPC1-Flag was human TRPC1 with a Flag epitope tag at the N terminus cloned into pcDNA3.1 and was a gift from Craig Montell from University of California. TRPC5-GFP was human TRPC5 in a construct with enhanced green fluorescent protein (EGFP) achieved through cloning into pEGFP-N1 (Xu et al., 2008). TRPC5-[HA]-GFP was human TRPC5 with a hemagglutinin (HA) epitope tag in the second extracellular loop (Naylor et al., 2011) cloned into pEGFP-N1. Human caveolin-1 (Cav1) was in pCMV-Sport6. Cav1-GFP included a C-terminal EGFP and was a gift from Nikita Gamper from University of Leeds. Human Piezo1 IRES GFP (a gift from John Wood from University College London) was used as a PCR template to create Piezo1–GFP (by Dr. L McKeown from University of Leeds, Li et al., 2014). IRES tag was deleted and a linker of four glycine residues was inserted. Human PECAM1 (CD31) was in pCMV6-XL5, and was purchased from Origene (TrueClone).

2.5.5. Short interfering (si) RNAs

Short interfering RNAs were used to knock-down the expression level of specific endogenous proteins. siRNA sequences were listed in Table 2.2.

2.6. Membrane cholesterol depletion and loading

Cell membrane cholesterol was depleted using 2.78 mM Methyl-beta-Cyclodextrin (mβCD, Sigma), at 37 °C for 1 hour. α-Cyclodextrin (αCD, Sigma) was used as negative control. Cholesterol was loaded into cells by incubating with 0.5 mM water-soluble cholesterol (0.5 mM cholesterol/2.78 mM mβCD complex, Sigma) for 1 hour at 37 °C.

Gene	Sequence (5'-3') sense	Company
Scrambled siRNA*		Ambion
Caveolin-1	CCUUCACUGUGACGAAAUAtt	Ambion
TRPC1	GCCCGGAAUUCUCGUGAAUtt	Ambion
Piezo1	GCCUCGUGGUCUACAAGAUtt	Ambion
eNOS	GAACAGCACAAGAGUUAUAtt	Ambion
VEGFR2	GGGCAUGUACUGACGAUUA CUACAUUGUUCUUCCGAUA GGAAAUCUCUUGCAAGCUA GCGAUGGCCUCUUCUGUAA	Dharmacon
CD31	CAAAUGUCCUGCGGUAUU CCACUGAAGACGUCGAAUA GCAACACAGUCCAGAUAGU UGAAGAGCACAGAGAGUUA	Dharmacon

Table 2.2. List of siRNA sequences. * The scrambled control siRNA (sc.si) was Silencer Negative Control #1, which is a 19-bp scrambled sequence with no significant homology to human gene sequences. siRNAs targeting VEGFR2 and CD31 are Dharmacon ON-TARGET plus SMARTpool siRNAs, with a mixture of 4 siRNA as a single reagent.

2.7. Intracellular Ca^{2+} measurement

2.7.1. Fura-2 acetoxymethyl easter (Fura-2 AM)

Fura-2 AM (Invitrogen) is one of the most commonly used Ca^{2+} indicator dyes, which has high Ca^{2+} binding affinity. The acetoxymethyl ester (AM) form of Fura-2 is membrane permeable. Once inside the cell, AM is cleaved by nonspecific esterases, generating a charged and Ca^{2+} sensitive form of Fura-2. Fura-2 AM is excited at 340 and 380 nm wavelengths, with emission at 510nm. Once bound to Ca^{2+}, the emission intensity at 510 nm increases at excitation wavelength 340 nm, while it decreases at 380 nm. Therefore, increase in the intracellular Ca^{2+} concentration ([Ca^{2+}]$_i$) induces an overall elevation of 340/380 ratio. The ratiometric property of the dye minimises experiment errors caused by uneven dye concentration, leakage of dye from cell, and photobleaching (Grynkiewicz et al., 1985). Pluronic acid is a non-ionic surfactant which increases the aqueous solubility of Fura-2. Cells are loaded with Fura-2 mixed with pluronic acid before Ca^{2+} measurement is performed.

2.7.2. Ca^{2+} measurement using FlexStation II^{384}

Changes in [Ca^{2+}]$_i$ induced by chemicals were measured using FlexStation II^{384}(Molecular Devices). FlexStation II^{384} is a bench-top fluorescence plate reader with high throughput. It has three drawers for tips, a compound plate (96-well plate) and a cell plate (96-well plate). Drugs from the compound plate can be delivered automatically to the cell plate at designated time points. FlexStation II^{384} is programed to read cell plate column by column using software Softmax Pro 4.7.1. Software Softmax Pro 4.7.1 is also used for experimental setup and data collection.

In brief, 24 hours before experiments, VSMCs were seeded on 96-well clear non-coated plates (Nunc, Denmark) and HEK-TRPC5 cells on poly-D-lysine

black-walled, clear-bottomed plates (Corning, USA) at a confluence of 80-90%. The cells were incubated with SBS, 0.5 mM Cholesterol or 2.78 mM mBCD in presence of fura-2 AM (1 µM) and 0.01% pluronic acid at 37 °C for 1 hour followed by a 0.5 h wash at room temperature. Measurements were made at room temperature using FlexStation II[384]. The change (Δ) in intracellular Ca^{2+} concentration was indicated as the ratio of fura-2 emission intensities for 340 nm and 380 nm excitation (F ratio). Wells within columns of the 96-well plate were loaded alternately for test and control conditions. Recordings were made in 200µl SBS before and after supplementation with 50 µl compound solution (100 µM Gd^{3+}, 3 µM PGPC, or 25 µM GM1 gangliosides).

2.7.2. Ca^{2+} measurement using fluorescent microscope

Shear stress-evoked Ca^{2+} signals were measured using Zeiss Axiovert fluorescent microscope. While FlexStation II[384] reads the fluorescence from an area containing multiple cells, the fluorescent microscope allows single-cell Ca^{2+} measurements. Excitation light is from a xenon lamp, and the wavelength is selected by a monochromator (Till photonics, Germany). Emitted light is collected through an emission filter and images captured by an Orca-ER digital camera (Hamamatsu, Japan).

HUVECs and LECs were seeded on Ibidi µ-Slide VI[0.4] (Ibidi treated) 4 hours before the experiments, while mouse embryonic endothelial cells and HEK-MSRs were seeded 24 hours prior to the experiments. Cells were loaded with Fura-2 AM with the same protocol as that for FlexStation II[384] experiments except 2 ng.ml^{-1} VEGF was included in SBS during the entire experiment. Open Lab software (Improvision) was used to collect data.

2.8. Western blotting

2.8.1. Normal western blotting

Western blotting was performed according to the general western blotting protocol (http://www.abcam.com/index.html?pageconfig= resource&rid=13045). Briefly, Cells were transfected and harvested in lysis buffer containing 10 mM Tris, pH 7.5, 150 mM NaCl, 0.5 mM EDTA, 0.5% NP-40 and MiniComplete protease inhibitors (Roche). Cell lysate was incubated with Laemmli protein sample buffer (Bio-rad) at 95 °C for 5 minute before equal amount of protein (20 μg/well) was loaded into the wells of the 8% SDS-PAGE gels and resolved at a voltage of 170V. Samples were then transferred to PVDF membranes using a semi-dry transfer method at a constant current at 0.05A for 80 min. PVDF was blocked by TBS-Tween buffer (0.1% Tween-20, 20 mM Tris, 150 mM NaCl at pH 7.4) containing 5% non-fat dry milk at room temperature for 1 hour. Membranes were incubated overnight at 4 °C with primary antibody followed by secondary anti-mouse (or anti-rabbit) antibody conjugated to HRP (1:10000, Santa Cruz) incubation for 1 hour at room temperature. All antibodies are listed in Table 2.3. Chemiluminescent substrate SuperSignal Femto (Thermo Scientific) was used for detection followed by brief exposure to Kodak X-ray film (Sigma). The protocol for western blotting is summarised in Figure 2.1.
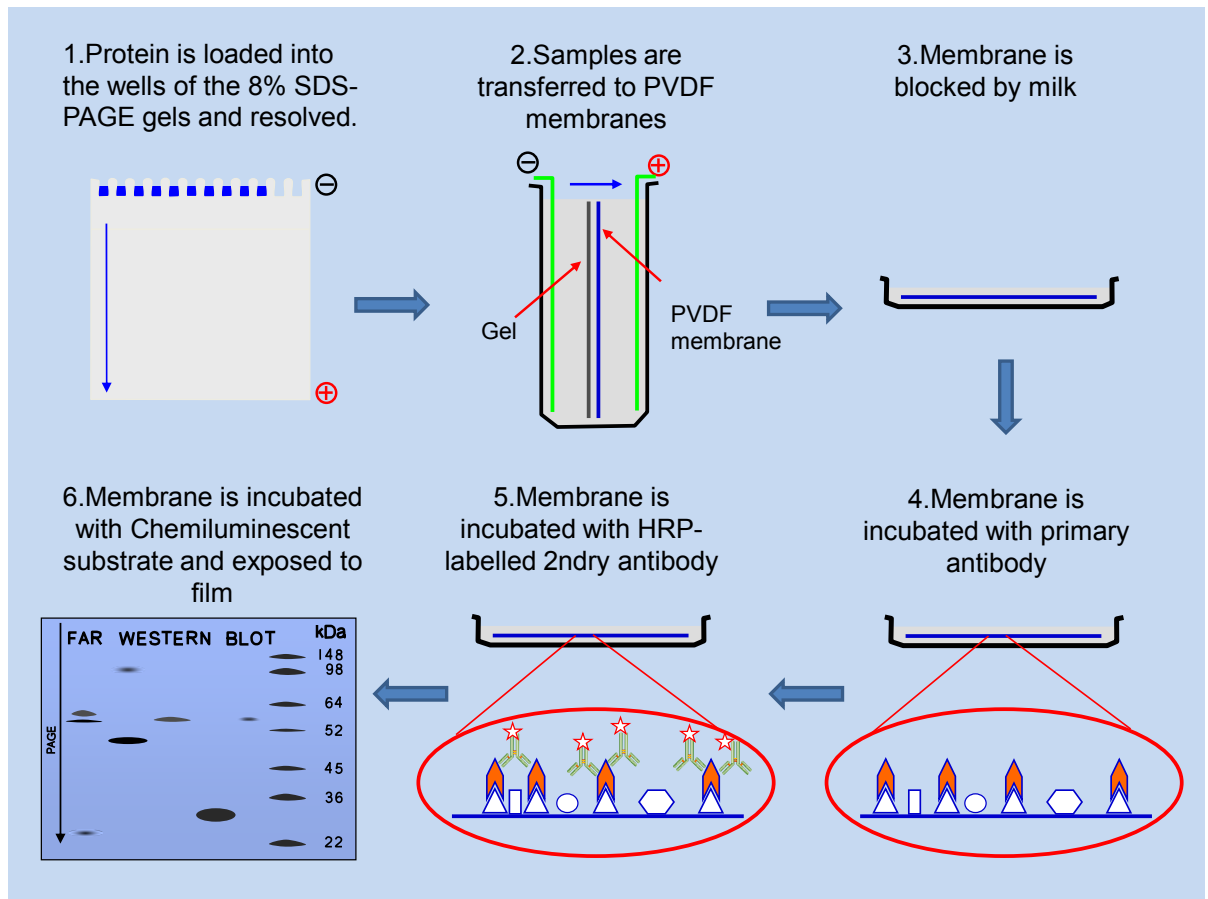
Figure.2.1. General protocol for western blotting. Modified from http://www.scienceslides.com/Ksl/western-blotting#

Name	Dilution (IF)	Dilution (WB)	Dillution (Block)	Company	Formart and Targets
T5C3	1 : 250	N/A	N/A	custom made*	rabbit polyclonal, C-terminal of TRPC5
T5E3	1 : 50	N/A	1 :100	custom made*	rabbit polyclonal, 3rd extracellular loop of TRPC5
T1E3	N/A	N/A	1 : 500	custom made*	rabbit polyclonal, 3th extracellular loop of TRPC1
anti-GFP	N/A	1 : 8000	N/A	AbCam	mouse monoclonal, GFP
anti-HA	1 : 500	N/A	N/A	Covance	mouse monoclonal, HA tag
anti-Flag	1 : 1000	N/A	N/A	Sigma	mouse monoclonal, Flag tag
anti-Halo	1 : 500	1 : 1000	N/A	Promega	mouse monoclonal, Halo tag
anti-caveolin1	N/A	1 : 1000	N/A	BD Biosciences	mouse monoclonal, human caveolin 1
anti-Piezo1	N/A	1 : 1000	N/A	Proteintech	rabbit polyclonal, human Piezo1
anti-CD31	1 : 500	1 : 1000	N/A	Dako	mouse monoclonal, human CD31
anti-Paxillin	1 : 500	N/A	N/A	BD Biosciences	mouse monoclonal, human Paxillin 1
anti-β-actin	N/A	1 : 10000	N/A	Santa Cruz	mouse monoclonal, β-actin of human,mice, rabbit
anti-VEGFR2	N/A	1 : 1000	N/A	R&D systems	goat polyclonal, human VEGFR2

Table 2.3. List of antibodies. IF, immunofluorescence, WB, western blotting. * , all custom made antibodies have been described previously (Xu et al., 2006, Sukumar et al., 2012, Xu et al., 2005). For T5E3 and T1E3 antibody blocking experiments, neutralized antibodies (antibodies pre-incubated with an excess of peptide that corresponds to the epitope recognized by the antibody) were used as controls.

2.8.2. Density gradient centrifugation

Density gradient centrifugation is a technique used to separate molecules according to their buoyant density. OptiPrep™ is a solution of 60% iodixanol in water with a density of 1.32 g/ml. It is used to establish a density gradient. After centrifugation, tested molecules concentrate where the molecule density matches that of the surrounding OptiPrep™ (Fig. 2.2). The density gradient centrifugation was performed by Dr. Sarka Tumova.

The method was adapted from a previously described protocol (Yao et al., 2009). In brief, MSR cells on 10-cm plates were transfected with TRPC5-GFP alone or together with TRPC1-Flag and incubated with cholesterol for 1 hour. Cells were then harvest using 0.5 ml cold 0.5 % TritonX-100 solution containing 20 mM Hepes, 150 mM NaCl, 5 mM EDTA, pH 7.4 (THNE buffer) with protease inhibitors (Complete, Roche). Biochemically, lipid rafts are resistant to solubilization by cold Triton X-100 (Yao et al., 2009). To homogenize the cell lysate, it is passed through a 23G needle 10 times. Homogenate was mixed with 1ml 60 % OptiPrep (Sigma) to 40 % final density, transferred to a 5-ml Ultra-clear centrifugation tube (Beckman) and over-laid with 1.75 ml 30 % Optiprep in THNE buffer, 1.5 ml 20 % OptiPrep in THNE buffer and 0.5 ml THNE buffer on top. Homogenates were centrifuged for 4 hours at 41000 rpm in a SW55Ti rotor (Beckman) at 4 °C to separate domains according to buoyancy. Fractions of 0.5 ml were collected from the top of the gradient. Proteins in the fractions were detected by normal western blotting (Fig. 2.2).
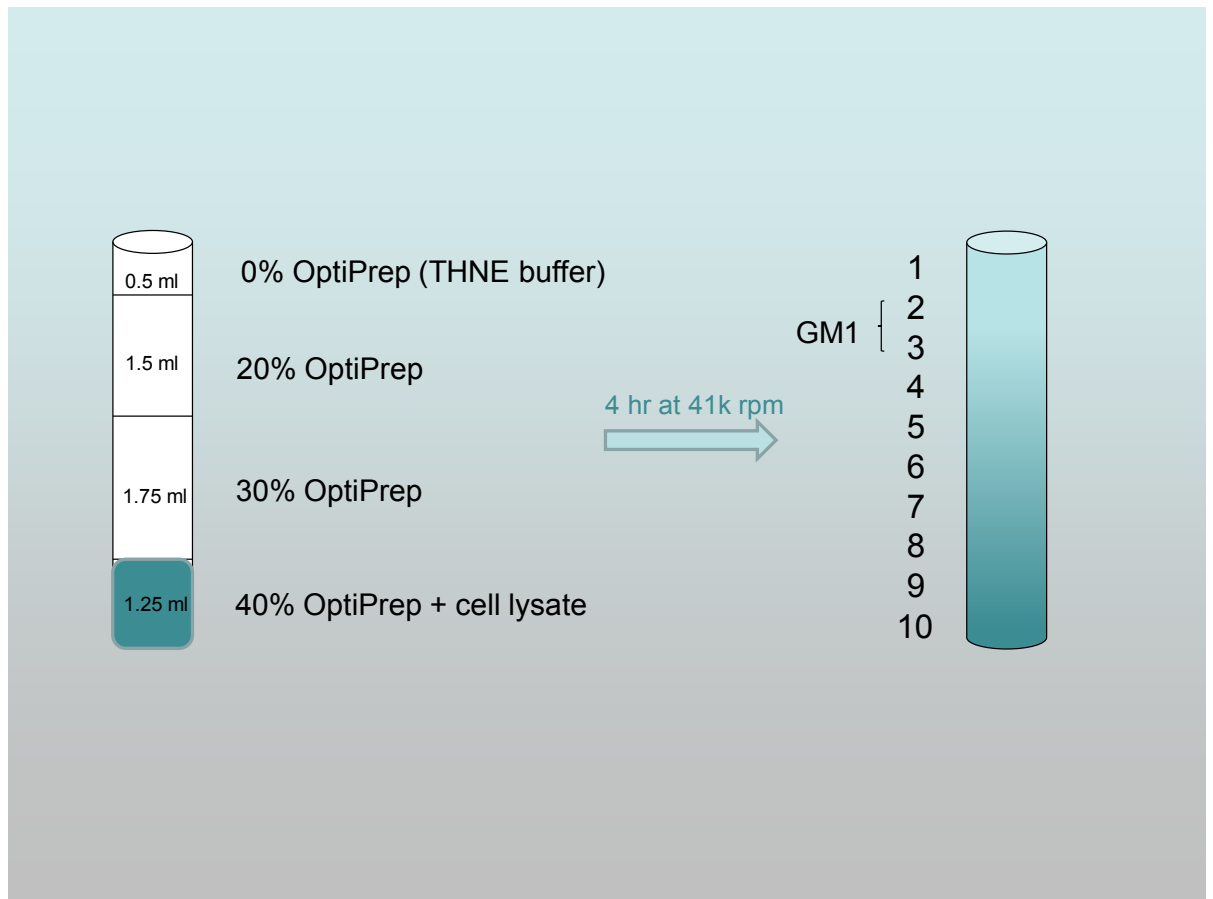
Figure.2.2. General principle for density gradient centrifugation using OptiPrep^TM. OptiPrep™ is a solution of 60% iodixanol in water with a density of 1.32 g/ml. It is used to establish a density gradient. After centrifugation, tested molecules concentrate where the molecule density matches that of the surrounding OptiPrep™. GM1 gangliosides is normally present in fraction 2 and fraction 3 (Yao et al., 2009).

2.8.3. Halo-Tag pull-down assay

To investigate the Piezo1 interaction with other proteins, Halo-tagged piezo1 was pulled-down using HaloTag® Mammalian Pull-Down Systems (Promega) as per the manufacturer's instructions. Briefly, MSR cells on a 6-well plate were transfected with Halo-Piezo1 together with human CD31. Cells were collected using cold PBS and spun down for 5 min at 500 x g at 4 °C to collect the cell pellet. The pellet was frozen at -80 °C for at least 30 minutes. The pellet was then re-suspended using lysis buffer with 4 µl 50x protease inhibitors from the HaloTag® kit, and homogenized by passing through a 23G needle 10 times. The homogenate was centrifuged at 14,000 x g for 5 minutes. The supernatant was rotated with Halo-resin for 45 minutes at room temperature so that protein complexes containing Halo-tag bound to the resin. Proteins were then elute with 4x laemmli protein sample buffer (Bio-rad) and detected by normal western blotting. The experiments using this method were performed by Dr. Sarka Tumova.

2.8.4. GFP-Trap pull-down assay

To investigate the TRPC5 interaction with caveolin-1, GFP-tagged TRPC5 was pulled-down using GFP-Trap agarose beads (ChromoTek, Germany) according to manufacturer's instructions. Briefly, MSR cells transfected with TRPC5-GFP and caveolin-1 with or without TRPC1-Flag were incubated in 0.5 mM cholesterol for 1 hr and lysed in 0.5 % NP-40, 10 mM Tris, 150 mM NaCl, 0.5 mM EDTA, pH 7.4 with complete protease inhibitors (Roche). The lysate was incubated on ice for 5 minutes and then spun for 5 minutes at 14000xg. The lysate was diluted 5 times with 10 mM Tris, 150 mM NaCl, 0.5 mM EDTA buffer (pH 7.4) containing protease inhibitors and rotated for 1 hour at 4 °C with 15 µl GFP-Trap agarose beads (ChromoTek, Germany). Beads were washed with the dilution buffer followed by 50 mM Tris pH 6.8 and the protein complexes were eluted by boiling in laemmli protein sample buffer (Bio-rad) and detected

by normal western blotting. The experiments using this method were performed by Dr. Sarka Tumova.

2.9. Immunofluorescence

2.9.1. Immunostaining and DeltaVision deconvolution system

Immunofluorescence is a technique used to visualize fluorescent proteins or other cell components. Specific binding of fluorescent dye-conjugated antibodies to their antigen within a cell allows visualization of the distribution of the target molecule. Briefly, cells were seeded on cover slips (Thermo Scientific, thickness 0.15 mm) in 24-well plates 24 hours before experiments at 80 % confluence. For HEK-TRPC5 cell, coverslips were coated with poly-D-lysine (Sigma) to enhance cell binding to the coverslips. Cells were washed with DPBS, fixed with 2% paraformaldehyde (PFA) for 5 minutes and washed again with DPBS. For permeabilization, 0.1 % TritonX-100 in DPBS was used. Permeabilized cells were blocked using 10% donkey serum (Gibco) in DPBS for 1 hour, following incubation with primary antibody for 1 hour at room temperature. All antibodies are listed in Table 2.3. Cells were incubated with fluorescent dye-conjugated secondary antibodies (1:300; Jackson ImmunoResearch Laboratories, Inc) for 30 minutes at room temperature before being mounted on slides with Prolong Gold Antifade Reagent (Invitrogen). Cell nuclei were labeled with DAPI (4',6-diamidino-2-phenylindole). For GM1 staining, permeabilized cells were incubated with 1:500 Alexa 594-conjugated cholera toxin subunit B (Invitrogen) for 20 minutes. For f-actin staining, cells were incubated with Rhodamine Phalloidin (1:250, Cytoskeleton Inc.) for 30 min at room temperature.

Antigens were visualized using a DeltaVision deconvolution system (Applied Precision Instruments, Seattle, WA). The DeltaVision deconvolution system is an inverted fluorescence microscope (Olympus IX-70) equipped with a x100

UPLAN objective (NA 1.35). Images were collected at room temperature using a Roper CoolSNAP HQ CCD camera with SoftWoRx acquisition and analysis software. With the software-based deconvolution, all out of focus light is redirected to become in focus for sharp images. Intensity of the fluorescence is quantified using ImageJ software.

2.9.2. Live cell imaging

The DeltaVision deconvolution system was also used for live-cell imaging. Cells transfected with GFP tagged TRPC5 or Piezo1 were seeded onto a live-cell imaging dish (Thermo Scientific™ Nunc) and Ibidi μ-Slide VI$^{0.4}$ (Ibidi treated) respectively 4 hours before performing the experiments. Cells with overexpressed TRPC5-GFP were seeded at 50 % confluence, while cells expressing Piezo1-GFP were seeded at 90% confluence.

TRPC5-GFP was observed at the excitation wavelength of 488 nm. For TRPC5-GFP tracking in live MSR cells, images were acquired every 15 s for 20 min after 0.5mM cholesterol was applied. For tracking Piezo1-GFP in live HUVECs, cells were imaged every 15 s for 10 min before shear stress of 15 dyn.cm^{-2} was applied and imaging continued for another 50 min. The intensity of GFP fluorescence was quantified in multiple squares (5 or 9 μm^2 depending on the shape of the cell edge) using ImageJ software for each region of the cell (as shown in Fig.4.13). The number of squares for each region was 3-5 and the mean intensity for all squares in each region was used.

2.10. Shear Stress

Shear stress was achieved in microfluidic chambers, Ibidi μ-Slide VI$^{0.4}$ (http://ibidi.com/) or on an orbital shaker that generated circulating flow of medium in wells of a 6-well plate, producing tangential shear stress (Warboys et al., 2014).

For generating shear stress in microfluidic chambers, an Ibidi pump system was used. The Ibidi Pump System has two main components: The Ibidi Pump (software controlled air pump) and the Fluidic Unit (holder for cell media perfusion set, μ-Slide, and electrically controlled valve set). The PumpControl software controls the air pressure, and consequently the shear stress acting on the cells in the chambers. In order to save medium, liquid was pumped back and forth between the two media reservoirs (Fig.2.3). For Ca^{2+} imaging experiments, HUVECs and LECs were seeded on Ibidi μ-Slide $VI^{0.4}$ 4 hours before the experiments, while mouse embryonic endothelial cells and HEK-MSRs were seeded 24 hours prior to the experiments (at 90 % confluence). To better characterize the full range of the responses, incrementing shear stresses were applied (5, 10, 15, 20 and 25 dyn/cm^2 for HUVECs and LECs, 5, 10, 15, 20 dyn/cm^2 for MSRs, 15 and 25 dyn/cm^2 for mouse embryonic endothelial cells). For endothelial cell alignment experiment, HUVECs were seeded on Ibidi μ-Slide $VI^{0.4}$ 4 hours before shear stress of 15 $dyn.cm^{-2}$ was applied and lasted for 24 hours, while mouse embryonic endothelial cells were seeded on the slide right after the isolation, and 24 hours before the experiments. Mouse embryonic endothelial cells were then cultured under 15 $dyn.cm^{-2}$ shear stress for 72 hours to achieve alignment.

For generating shear stress using an orbital shaker, HUVECs were plated on a 6-well plate at 70 % confluence 4 hours before being subjected to shear stress generated by the orbital shaker (PSU-10i, Grand-bio) rotating at 210 rpm for 24 or 72 hours (specified in Chapter 5). Inhibitors were added to the medium 1 hour before the shear stress was applied. Cells were cultured in 2 ml medium, so that the shear stress at the edge of the wells was ~10-15 $dyn.cm^{-2}$ (Dardic et al., 2005, Warboys et al., 2014). Cells were then imaged using the Incucyte microscope. The method for analyzing the EC alignment is described in the next section.
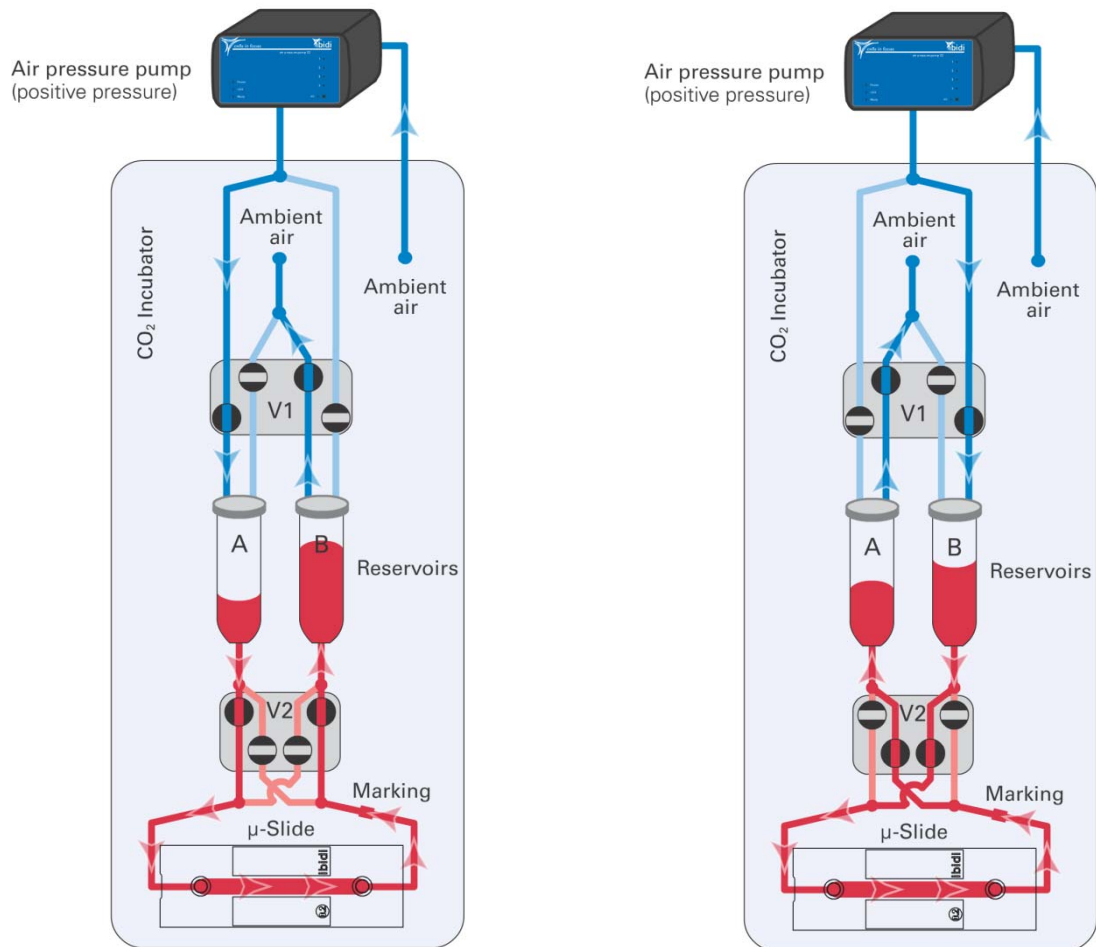
Figure 2.3. Schematic principle of flow generation using Ibidi pump system. Applying pressured air to the reservoirs generates the flow in the µ-Slide channels. In order to save medium, liquid was pumped back and forth between the two media reservoirs. In state (A), pressured air is guided to reservoir A while reservoir B is connected to the ambient air pressure. In state (B), reservoir B is subjected to air pressure. Two pinch valve sets, V1 and V2, act as a fluidic rectifier. The synchronous switching of both valves creates a continuous and unidirectional flow through the µ-Slide channels. Cited from ibidi.com with permission. Copyrights are reserved by Ibidi.

2.11. Calpain activity

Calpain activity assay was performed using a kit from Abcam as per the manufacturer's instructions. Cytosolic proteins were specifically extracted using The Extraction Buffer from the kit, which also prevented auto-activation of calpain during the extraction procedure. The fluorometric assay detected cleavage of calpain substrate Ac-LLY-AFC. Ac-LLY-AFC emitted blue light with a wavelength of 400nm, while upon cleavage by calpain, free AFC emitted fluorescence at 505nm, which was quantified using a fluorescence plate reader (Thermo Scientific™). Briefly, the protocol is as follows. HUVECs were cultured in a 6-well plate with or without shear stress (orbital shaker) for 15 min. Cells were counted, pelleted by centrifugation (1000 rpm, 4 min), and resuspended in 100 µl of extraction buffer for each well. Cells in extraction buffer were then incubated on ice for 20 min, and were tapped gently to mix during the incubation. The cell lysate was centrifuged at 10000 x g before being diluted with 85 µl of extraction buffer and transferred to wells in a 96-well plate. 5 µl of calpain substrate and 10 µl of reaction buffer (10 x) were added to each well and incubated at in dark at 37 °C for 1 hour. The measurements were made using fluorescence plate. Optical density values were in arbitrary units, and were presented after background subtraction. Calpain activity assay was performed by Dr. Jing Li.

2.12. Data analysis

Fluorescence intensity, co-localization (Rcoloc, Pearson's correlation coefficient for pixels above threshold), EC alignment, and densities of western blotting protein bands were quantified by ImageJ software. Intracellular Ca^{2+} measurement data were analyzed using OriginLab software (OriginLab Corporation, Northampton, MA, USA). Statistical analysis and data presentation were also performed using OriginLab software.

2.12.1. Co-localization analysis

The Rcoloc value (Pearson's correlation coefficient for pixels above threshold) was used as an indication for co-localization of two proteins. It was obtained using the co-localization threshold function of ImageJ software. The method for determining the threshold level for each channel was proposed by Costes, et al. (2004). 2-color image stack were split into two separate channels by Image J. The Rcoloc function returns Pearson's correlation coefficient for pixels where both channels are above their respective threshold. A Rcoloc value of 1 indicates perfect co-localization where as a value of 0 indicates no co-localization.

2.12.2. EC alignment assay

Cells subjected to shear stress (orbital shaker) to achieve alignment on a 6-well plate were imaged using the software controlled-Incucyte microscope (ESSEN BioSCIENCE). The microscope imaged cells in the same relative position in each well so that alignment induced by the same shear stress was quantified in each well of a 6-well plate. For cell alignment in microfluidic chambers, cells were fixed, stained for f-actin, and imaged using DeltaVision deconvolution system. Images were processed using Difference of Gaussians function in GSDC, a plug-in of ImageJ software, to define cell edges

(http://www.sussex.ac.uk/gdsc/intranet/microscopy/imagej/utility).   Automated quantification of cell orientation relative to the direction of flow was analyzed using   OrientationJ,   which   is   also   a   plugin   of   Image   J (http://bigwww.epfl.ch/demo/orientation/).   The   software   computes   the orientation of each pixel throughout the image and returns the frequency of pixels at each degree (Rezakhaniha et al., 2011). Frequency of the pixels at the direction of flow was used for comparison. Adam Hyman developed the method, and the protocol of which is summarized in Figure 2.4.
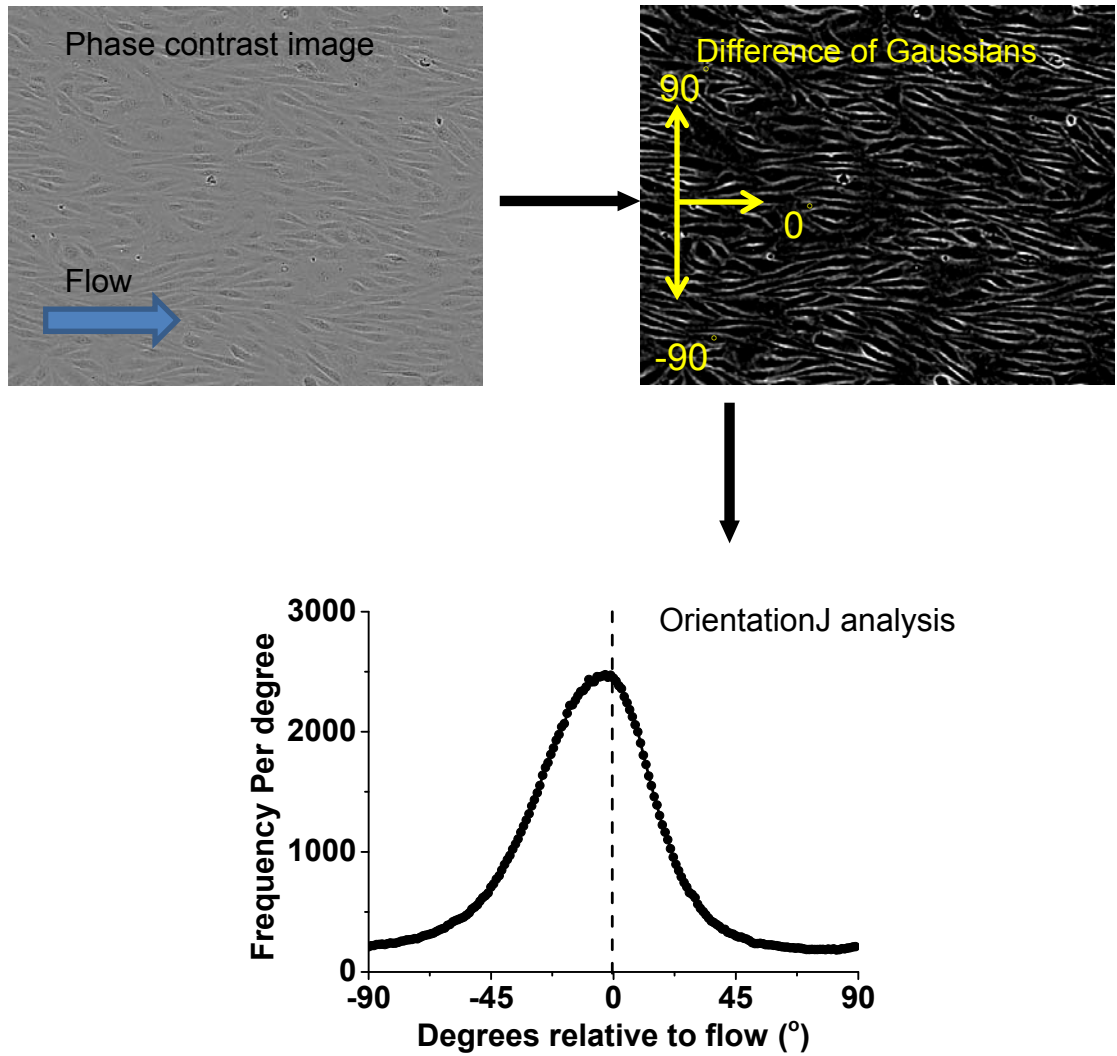
Figure 2.4. Method for cell alignment analysis. Phase-contrast image is processed using Difference of Gaussians function in ImageJ software to define the cell edge. Orientations of the HUVECs are quantified using OrientationJ software, a plugin for ImageJ. The software returns the frequency of cells at each degree. The frequency of the aligned edges in the direction of flow are used for comparison.

2.12.3. Intracellular Ca^{2+} measurement

For Ca^{2+} measurement using flexstation, the change (Δ) in intracellular Ca^{2+} concentration above baseline was indicated as the ratio of fura-2 emission intensities for 340 nm and 380 nm excitation (F ratio). The peak Δ F ratio was used for statistical analysis. For shear stress induced Ca^{2+} signal, because the Ca^{2+} signal is always oscillating with multiple peaks, a single peak value cannot reveal the real ΔF, as shown in Figure 4.3. For the statistical comparison, the integral ΔF ratio for each shear stress was divided by the time period over which the ΔF ratio was measured (F ratio.s^{-1}).

2.12.4. Statistical analysis

Data (test and control) were compared using independent Student t-tests unless specified. Data for EC alignment to shear stress (orbital shaker) were compared using paired Student t-tests. Data for experiments with one control group and multiple test groups were compared using One-way ANOVA, followed by Dunnett's test. Statistical significance was indicated by * ($P \leqslant 0.05$) and no significant difference by NS ($P > 0.05$). All intracellular Ca^{2+} measurement data were presented as n/N, where n indicates the number of independent experiments and N indicates the number of tested wells in the 96-well plates (FlexStation II[384]) or tested cells (microscope).

Chapter 3. TRPC1 segregates TRPC5 to protect calcium entry against cholesterol-evoked internalization

3.1. Introduction

TRPC1 is widely expressed in many kinds of human tissues including vascular smooth muscles, vascular endothelium, neurons, liver, platelets and salivary glands (Beech, 2005b). A feature of TRPC1 is that it can form a heterotetrameric complex with other TRPCs including TRPC4 and TRPC5, and possibly TRPC3 (Hofmann et al., 2002, Strubing et al., 2001, Strubing et al., 2003). TRPC1-TRPC5 heteromer is especially well established (Al-Shawaf et al., 2010, Beech, 2005a, Sukumar et al., 2012, Xu et al., 2006, Xu et al., 2008). TRPC5 is reported to be expressed in many kinds of vascular cells, including vascular smooth muscle cells (Beech et al., 2004, Xu et al., 2006), endothelial cells (Yoshida et al., 2006, Chaudhuri et al., 2008) and neurons (Greka et al., 2003). Many suggested roles of TRPC5 overlap with those of TRPC1, including cardiac development and vascular remodeling relevant events (Beech et al., 2004, Beech, 2013, Graham et al., 2012, Jiang et al., 2011). TRPC5 is known to form Ca^{2+}- permeable channels through assembly with TRPC1 in some of these contexts (Strubing et al., 2001, Sukumar et al., 2012, Xu et al., 2006, Xu et al., 2008).

The role of TRPC1 in heteromultimeric channels is not entirely clear. TRPC1 fails to form functional ion channels on its own and actually suppresses the conductance of channels formed by other TRPCs (Beech, 2005a, Strubing et al., 2001). This would suggest an inhibitory effect of TRPC1 on other TRPCs. These observations raise a paradox because TRPC1 expression is reported to be up-regulated under physical and metabolic injury conditions in vivo (Kumar et al., 2006, Edwards et al., 2010) and has positive effects on many cell

functions like VSMC proliferation, migration, and hypertrophy (Sweeney et al., 2002, Takahashi et al., 2007, Li et al., 2008). There are several activators of TRPC5 and TRPC1-TRPC5 containing channels, including lanthanides like Gd^{3+} and La^{3+} (Jiang et al., 2011, Jung et al., 2003, Zeng et al., 2004), and oxidized endogenous phospholipids like 1-palmitoyl-2-glutaroyl-phosphatidylcholine (PGPC, Al-Shawaf et al., 2010). Lanthanides act directly at extracellular site of the channel as facilitators of channel opening whereas PGPC acts through G protein signaling.

Cholesterol is a key constituent of membranes and one of the most important drivers of cardiovascular and other diseases (Maxfield and Tabas, 2005). Several members in the TRP family of ion channels have been shown to be regulated by cholesterol, including TRPC1, TRPC3 and TRPC6 (Beech, 2005a, Brownlow et al., 2005, Graziani et al., 2006, Huber et al., 2006).

The aim of this chapter was to investigate TRPC1 and TRPC5 in relation to cholesterol, and provide insight into the roles of TRPC1 in heteromultimeric channels.

3.2. Results

3.2.1. Cholesterol inhibits TRPC5 channel function

Methyl β-cyclodextrin (mβCD) is a 7-D-glycopyranose cyclic oligosaccharide. The size of the hydrophobic cavity of mβCD makes it highly effective to include and extract cholesterol from cell plasma membrane and, consequently, it is the most used compound to deplete cellular cholesterol, while incubation with mβCD/cholesterol complex which water-solubilise cholesterol can increase the cholesterol level in cell membrane (Zidovetzki and Levitan, 2007).To study the effect of cholesterol on TRPC5 channel activity, intracellular Ca^{2+} was measured after cholesterol-depletion using 2.78 mM mβCD or cholesterol loading using 0.5 mM water-soluble cholesterol in TRPC5 over-expressing HEK293 cells (Tet+). Cells were incubated with mβCD or cholesterol for 1 hour before Ca^{2+} measurement. Cells loaded with SBS were used as vehicle control.

Stimulation with 100 µM gadolinium (Gd^{3+}) leads to elevation of the intracellular Ca^{2+} concentration in TRPC5 over-expressing HEK293 cells (Tet+), while cells without TRPC5 expression (Tet-) did not respond to Gd^{3+} (Fig. 3.1 A). Cholesterol loading significantly blocked the Gd^{3+} activation of TRPC5 (Fig. 3.1 B, C), but did not alter the basal Ca^{2+} (Fig. 3.1 B, D). On the other hand cholesterol-depletion by mβCD significantly potentiated the Gd^{3+} -induced Ca^{2+} influx through TRPC5 (Fig. 3.1 B,C) and increased the baseline Ca^{2+} signal (Fig. 3.1 B,D). α-cyclodextrin (αCD) is similar in structure to mβCD but the smaller hydrophobic cavity makes it unable to bind cholesterol. Therefore, αCD-treated cells were used as negative control. Pre-treatment with 2.78 mM αCD did not alter Gd^{3+} -induced Ca^{2+} influx through TRPC5 compared with vehicle control (Fig. 3.1 E).

The data suggested both endogenous and exogenous cholesterol played negative roles in regulating over-expressed TRPC5 in HEK293 cells.
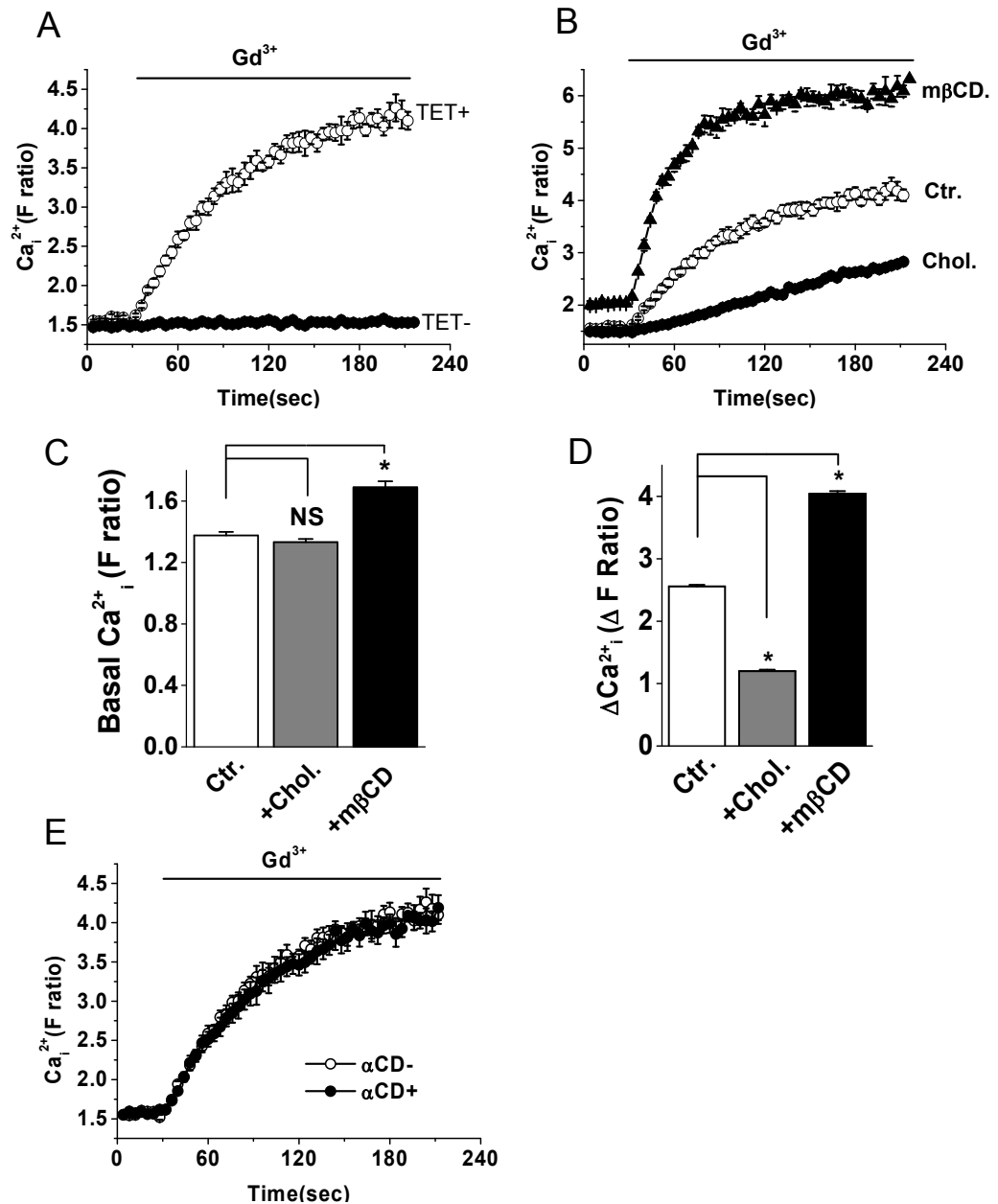
Figure 3.1. Cholesterol inhibits TRPC5 function in HEK293 cells. (**A**) Example Ca^{2+} measurement data from a single 96-well plate. Gadolinium chloride (Gd^{3+}, 100 µM) was applied to each well. Gd^{3+} induced Ca^{2+} influx only if TRPC5 was expressed (Tet+); Cells without TRPC5 expression (Tet-) did not respond to Gd^{3+}. (**B**) Example data from a single 96-well plate. Prior to recordings cells were treated with 0.5 mM cholesterol (+Chol.), 2.78 mM methyl-β-cyclodextrin alone (mβCD), or buffer alone (Ctr.). (**C**, **D**) Mean data for multiple 96-well plate recordings of the type shown in (**B**) (n/N=7/36 Ctr., 6/28 +Chol., 7/36 mβCD). (**C**) Change (Δ) in Ca^{2+} in response to Gd^{3+}. (**D**) Basal intracellular Ca^{2+} prior to application of Gd^{3+}. (**E**) Example Gd^{3+} response trace with or without αCD pre-treatment of a single experiment, from n=5.

3.2.2. Cholesterol induces internalization of surface TRPC5 in HEK293 cells

The effect of cholesterol or mβCD was tested after relatively brief pre-incubation with cholesterol or mβCD. Cholesterol or mβCD was not present when Ca^{2+} entry signals were measured. So it is possible that cholesterol or mβCD affects surface density of TRPC5. To test this hypothesis, GripTite™ 293 MSR cells were transfected with TRPC5-GFP cDNA construct tagged with the hemagglutinin (HA) at the second extracellular loop to allow the detection of plasma membrane localization of TRPC5-GFP (Naylor et al., 2011). 293 MSR cell line is a genetically engineered HEK-293 cell line that expresses the human macrophage scavenger receptor. It strongly adheres to standard tissue culture plates for dependable results in cell-staining protocols. While non-permeablized cells were incubated with anti-HA and then Dylight™ 594 conjugated secondary antibody after cholesterol loading to detect surface HA-tag only, cells incubated with anti-HA before cholesterol-loading and following permeablization and application of secondary antibodies were used to detect the HA-tag in the intracellular vesicles.

In cells pre-treated with vehicle control (Fig. 3.2 A), both intracellular and surface GFP fluorescence could be observed, partially overlapping with surface HA tag indicating membrane TRPC5. Less intense HA staining was detected in non-permeablized cell surface after cholesterol loading (Fig. 3.2 B). HA was detected in vesicles after permeablization, and co-localized with GFP (Fig. 3.2 C). Cholesterol depletion by mβCD increased surface localization of HA and GFP (Fig. 3.2 D). Surface intensity of HA staining was quantified using ImageJ software by Dr S. Tumova. Cholesterol loading decreased surface density of TRPC5 significantly compared with control (Fig. 3.2 E). While cholesterol depletion by mβCD upregulated it (Fig. 3.2 E). Consistent with Ca^{2+} measurement result, αCD did not affect surface density of TRPC5 (Fig. 3.3).To observe cholesterol-induced internalization of TRPC5 directly, live-cell imaging on TRPC5-GFP over-expressing MSR cells was performed. After 0.5 mM cholesterol treatment for 5 minutes, the formation of vesicles containing

TRPC5-GFP was observed, followed by vesicle internalization after cholesterol treatment for 15 minutes (Fig. 3.4). These data suggested that cholesterol affects TRPC5 activity by promoting the internalization of TRPC5 protein.
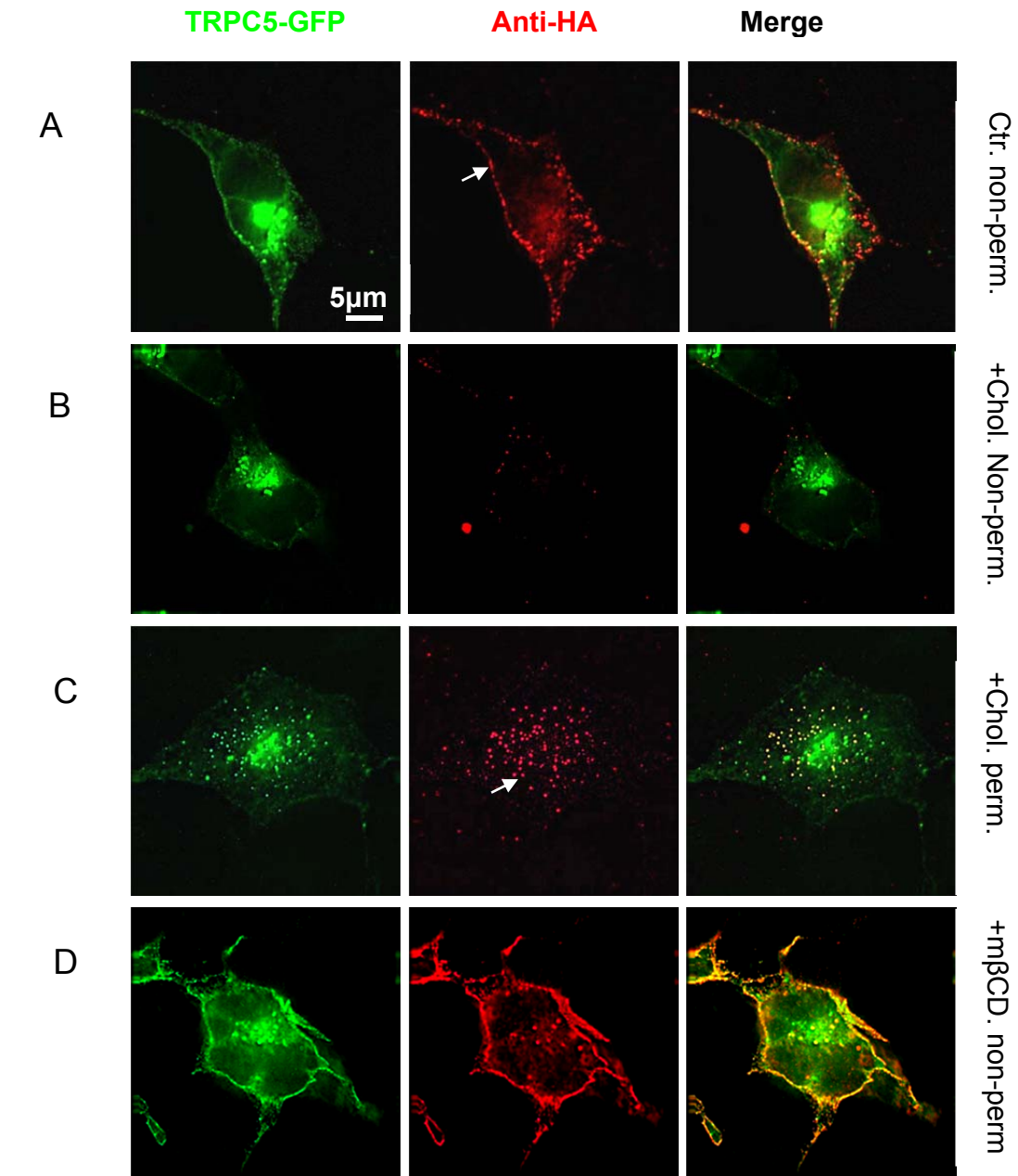
Figure 3.2. Cholesterol stimulates internalization of TRPC5. (**A-D**) Fixed-cell images of TRPC5-[HA]-GFP after labelling with anti-HA antibody. Cells were exposed to cholesterol (**B,C**) or mβCD (**D**) and permeabilized (perm.) or non-permeabilized (non-perm.) prior to labelling. The scale bar applies to all of the images. The arrow in 'Ctr. non-perm.'(**A**) points to the surface membrane, whereas in '+Chol. perm.'(**C**) it points to intracellular vesicles. (**E**) Quantification for multiple repeats of the experiment typified in (**A-D**): n/N=3/17 (Ctr.), n/N=3/20 (+Chol.), n/N=3/19 (mβCD).
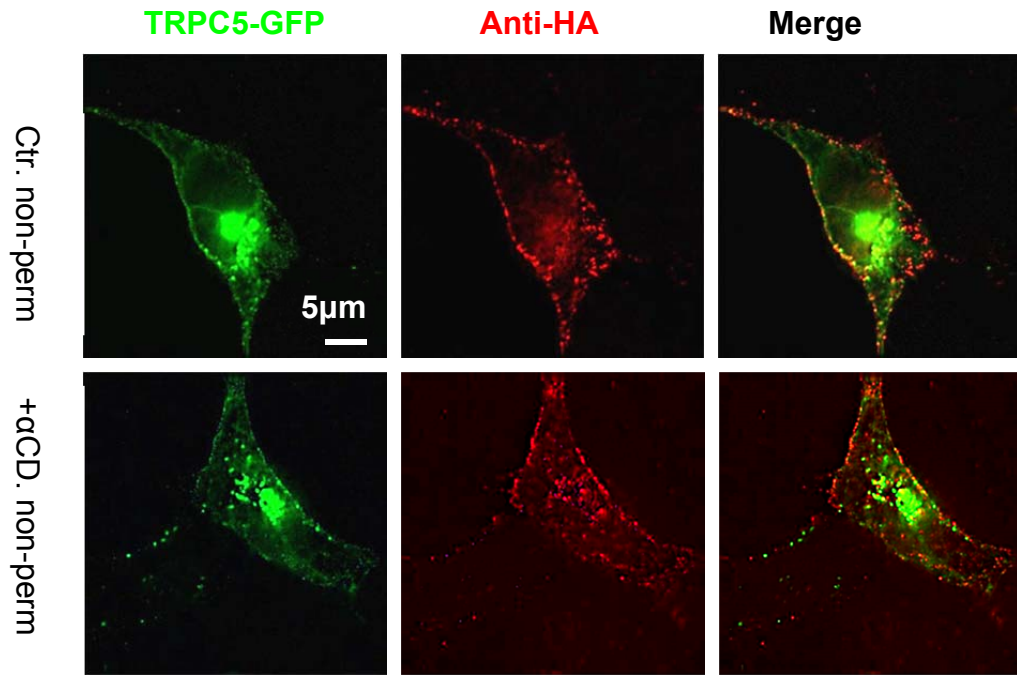
Figure 3.3. αCD did not affect surface density of TRPC5. Fixed-cell images of TRPC5-[HA]-GFP after labelling with anti-HA antibody. Cells were exposed to vehicle control or αCD prior to labelling. Representative images from 3 experiments.
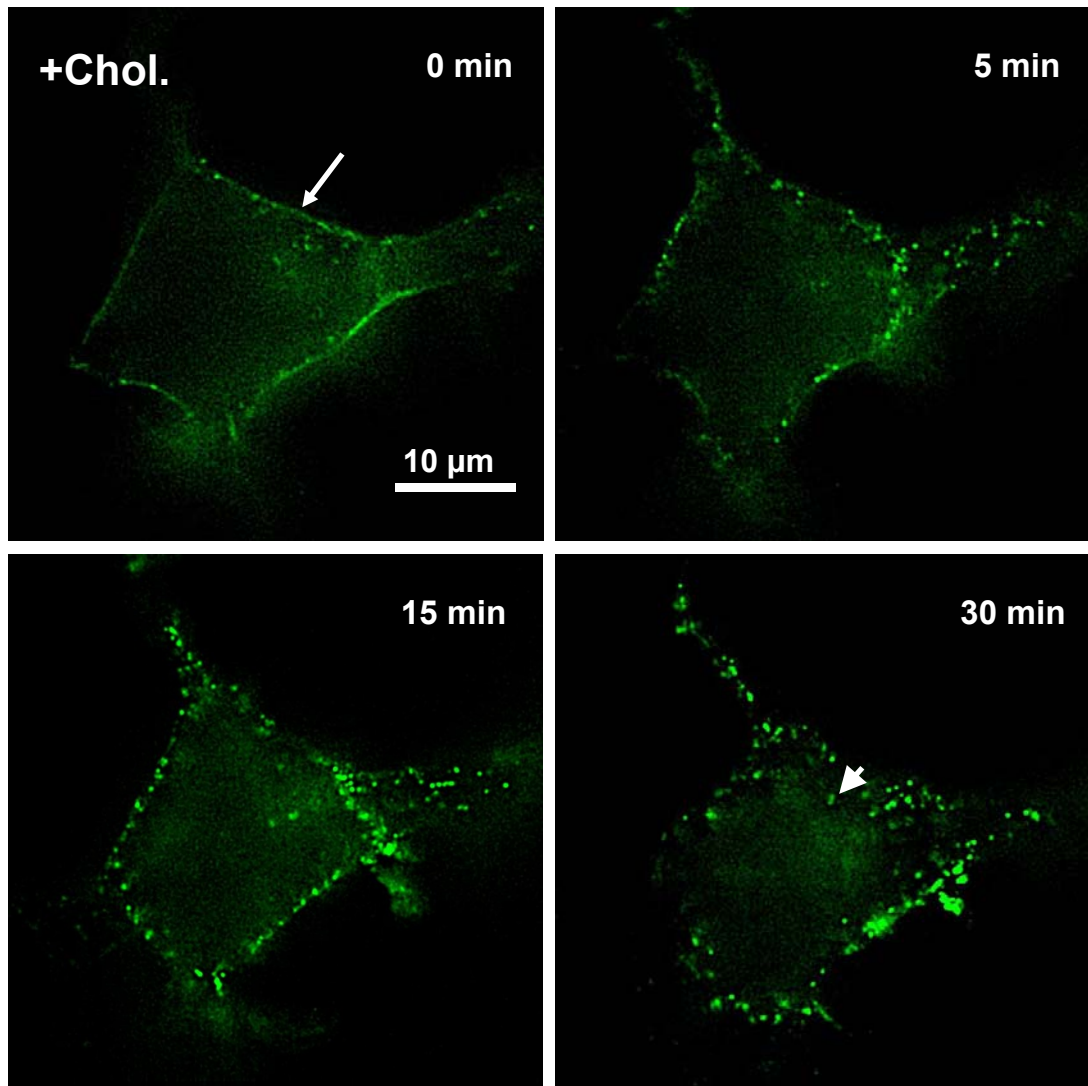
Figure 3.4. Live-cell TRPC5-GFP fluorescence at the indicated time points after application of cholesterol. The arrow at t=0 min points to the surface membrane. At t=30 min, the arrow head points to an intracellular vesicle. Representative images from 4 independent experiments.

3.2.3. Cholesterol-induced internalization of TRPC5 is caveolin-1 dependent

Lipid rafts are the microdomains rich in organized sphingolipids and cholesterol in the plasma membranes. One of the most investigated lipid rafts are the caveolae. They play an important role in signal transduction by forming a platform on which a variety of receptors, ion channels, and signalling factors accumulate (Simon and Toomre, 2000). Caveolin-1 and cholesterol are important components of caveolae. Over-expression of caveolin-1 in HEK293 cell is enough to induce formation of caveolaes (Simard et al., 2010). Caveolin-1 has been implicated in protein internalization by caveolin-1-rich membranes budding off to form intracellular vesicles (Bastiani and Parton, 2010).

To test if caveolin-1 is involved in cholesterol induced internalization of TRPC5, wild-type caveolin-1 was over-expressed in HEK-TRPC5 cells. Cells were treated with vehicle control or cholesterol before Ca^{2+} measurement was performed. Over-expressing caveolin-1 inhibited TRPC5 activity both with and without 0.25mM cholesterol treatment, compared with mock transfection control (Fig. 3.5 A-C). To test if caveolin-1 also causes internalization of TRPC5, EGFP-tagged caveolin-1 was over-expressed with TRPC5 in HEK293 cell. TRPC5 was detected using T5E3 antibodies that target the third extracellular loop of the TRPC5 protein (Xu et al., 2005). Over-expression of Cav1-EGFP down regulated surface TRPC5 density (quantification was performed by Dr. Sarka Tumova) (Fig. 3.5 D-E).
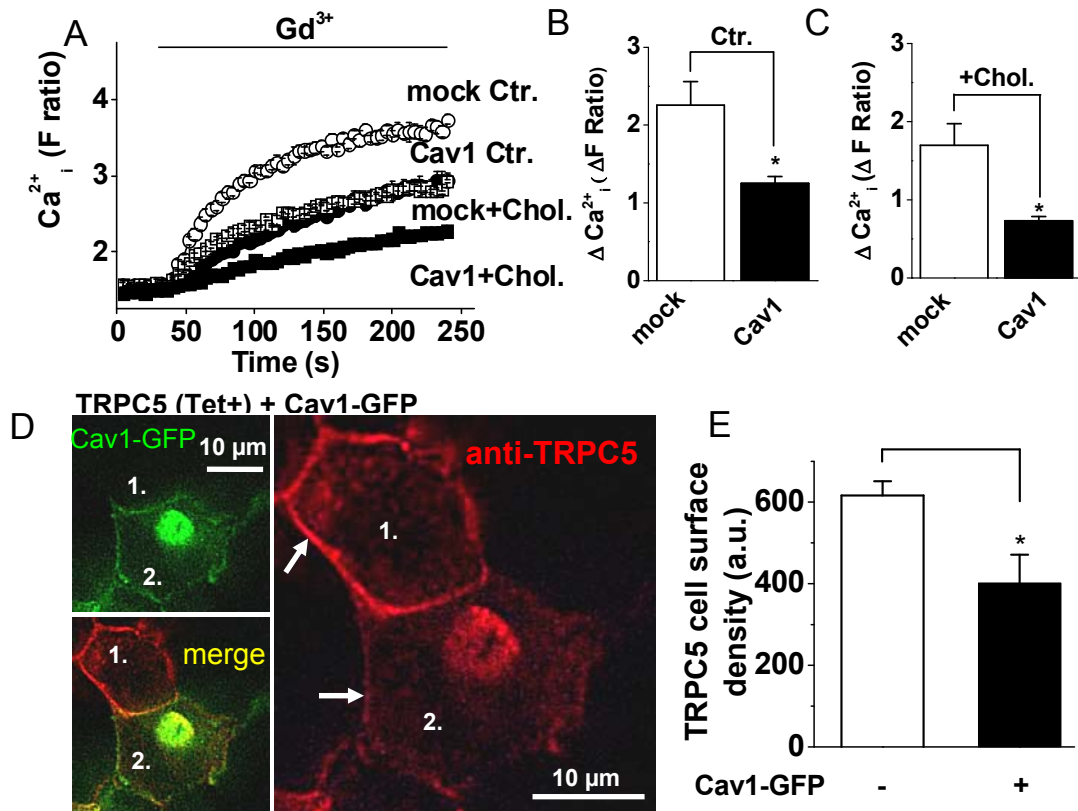
Figure 3.5. Caveolin-1 suppresses TRPC5 localization to the surface membrane and inhibits the channel activity. (**A-C**) Intracellular Ca^{2+} measurements from Tet+ cells expressing TRPC5. (**A**) Example data from single 96-well plates. Cells were mock transfected or tranfected with wild type caveolin1(Cav1). Gd^{3+} (100 µM) was applied to each well. Prior to recordings, cells were treated with 0.5 mM cholesterol (+Chol.) or buffer alone (Ctr.). (**B-C**) Mean data (n/N=3/12) for the type of experiment shown in (A) for Ctr. and +Chol. (**D**) Images of Tet+ cells expressing TRPC5, which was labelled with anti-TRPC5 antibody (T5E3, red), and transfected with Cav1-GFP (green). The images show the same two adjoining cells, one of which had no Cav1-GFP expression (1.) and the other which had Cav1-GFP expression (2.). The red image, showing only the TRPC5, contains arrows that point to the surface membrane. (**E**) Mean data (n/N=3/18) for the type of experiment shown in (**D**).

To further test the hypothesis, HEK293 cells over-expressing TRPC5 and Cav1-EGFP protein were treated with 0.5mM cholesterol for 20 minutes before stained with anti-TRPC5 antibodies (T5C3, 1:250, Xu et al., 2006). TRPC5 and Cav1-EGFP were detected co-localizing in the intracellular vesicles after cholesterol treatment (Fig. 3.6). Co-localization threshold was tested using ImageJ software. The average Rcoloc for TRPC5 and caveolin1 is 0.893 (standard error = 0.03), which confirmed the two protein were co-localized.

If cholesterol induced internalization of TRPC5 is caveolin-1 dependent, down-regulation of endogenous caveolin-1 should suppress the inhibitory effect of cholesterol on TRPC5 channel activity. To test this hypothesis, experiments similar to that typified in figure 3.5A were carried out. Knock-down of caveolin-1 expression in HEK-TRPC5 cells using siRNA had no effect on Gd^{3+} induced Ca^{2+} signal in the cells treated with vehicle control (Fig. 3.7 A,B), but significantly suppressed cholesterol inhibition of TRPC5 channel activity (Fig. 3.7 A,C). The data are consistent with the negative effect of caveolin-1 on TRPC5 via a caveolin-1-dependent retraction process.

TRPC5 (Tet+) + Cav1-GFP
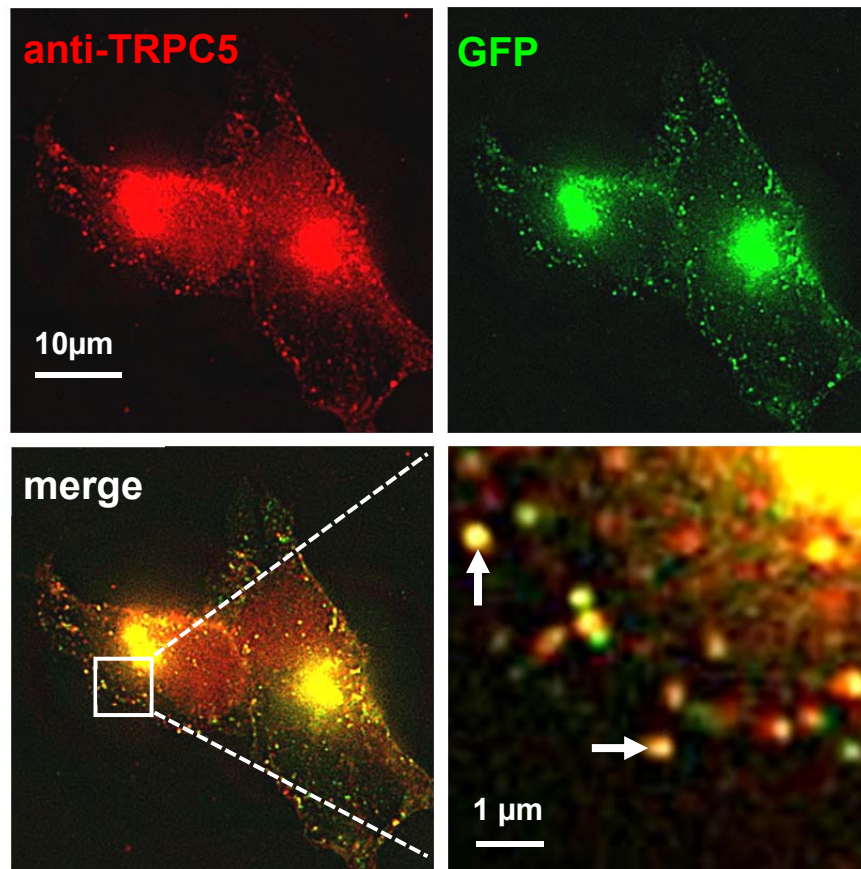
Figure 3.6. Cav1-EGFP co-localizes with TRPC5 in the intracellular vesicles after cholesterol treatment. Images of Tet+ cells expressing TRPC5 labelled with anti-TRPC5 antibody (T5E3, red), transfected with caveolin-1-EGFP (Cav1-GFP, green), and pre-treated with cholesterol for 20 min. The merger of the red and green images is also magnified (bottom right) to show more clearly the intracellular structures containing both TRPC5 and Cav1 (yellow; arrows point to two examples). Co-localization assay was performed using ImageJ software. The average Rcoloc for TRPC5 and caveolin1 is 0.893, SE=0.03 (n/N=3/15).
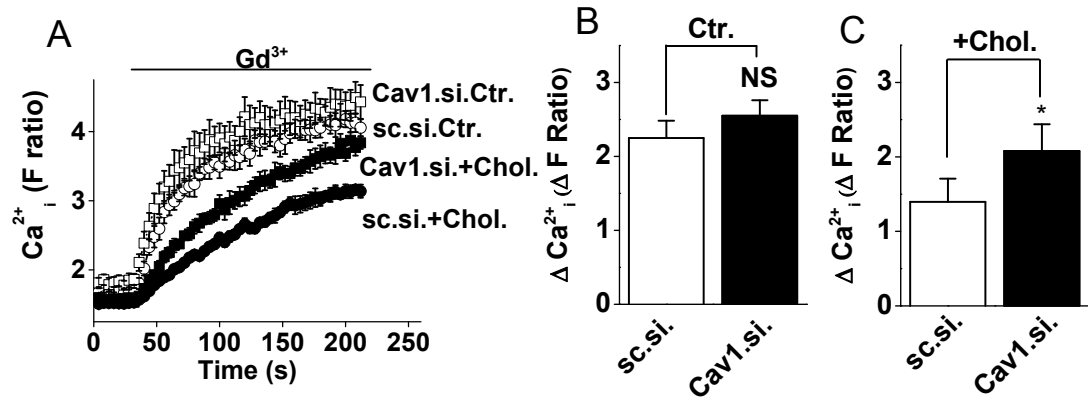
Figure 3.7. Depletion of endogenous caveolin1 suppressed the inhibitory effect of cholesterol on TRPC5 channel activity. (**A-C**) Intracellular Ca^{2+} measurements from Tet+ cells expressing TRPC5. (**A**) Example data from single 96-well plates. Cells were transfected with control siRNA (sc.si) or caveolin-1 siRNA(Cav1.si). Gd^{3+} (100 μM) was applied to each well. Prior to recordings, cells were treated with 0.5 mM cholesterol (+Chol.) or buffer alone (Ctr.). (**B-C**) Mean data (n/N=5/20) for the type of experiment shown in (**A**) for Ctr. and +Chol.

3.2.4. TRPC1 prevents cholesterol-induced internalization of TRPC5 in HEK cells

Given the involvement of TRPC1 and cholesterol in disease processes, it is important to examine the effect of cholesterol effect on TRPC1/TRPC5 heteromeric channels. As reported by Sukumar et al.(2012), when TRPC1 was over-expressed in TRPC5-HEK cells (tet+), TRPC1 and TRPC5 formed heteromultimeric channels.

To test if cholesterol affects surface localization of TRPC1/TRPC5 heteromultimer, TRPC1-Flag was over-expressed with TRPC5-GFP in MSR cells. Cholesterol-loading failed to induce internalisation of TRPC5-GFP in co-transfected cells and membrane localization of TRPC5-GFP was observed after cholesterol-loading (Fig. 3.8 A). Surface intensity of TRPC5-GFP was quantified using ImageJ software. Cholesterol significantly down-regulated surface density of TRPC5-GFP alone, while with co-expression of TRPC1, the internalizing effect of cholesterol on surface TRPC5 was abolished (Fig. 3.8 B). Co-localization of TRPC1-Flag and TRPC5-GFP on the cell surface was observed (Fig.3.8 B), Rcoloc value was 0.89043 (SE=0.0204) (n/N=3/16), consistent with widespread formation of heteromeric channels as reported previously (Hofmann et al., 2002, Shi et al., 2012, Strubing et al., 2001, Sukumar et al., 2012, Xu et al., 2006).

These data suggest TRPC1 prevents cholesterol-induced internalization of TRPC5 in HEK cells by forming heteromultimers with TRPC5.
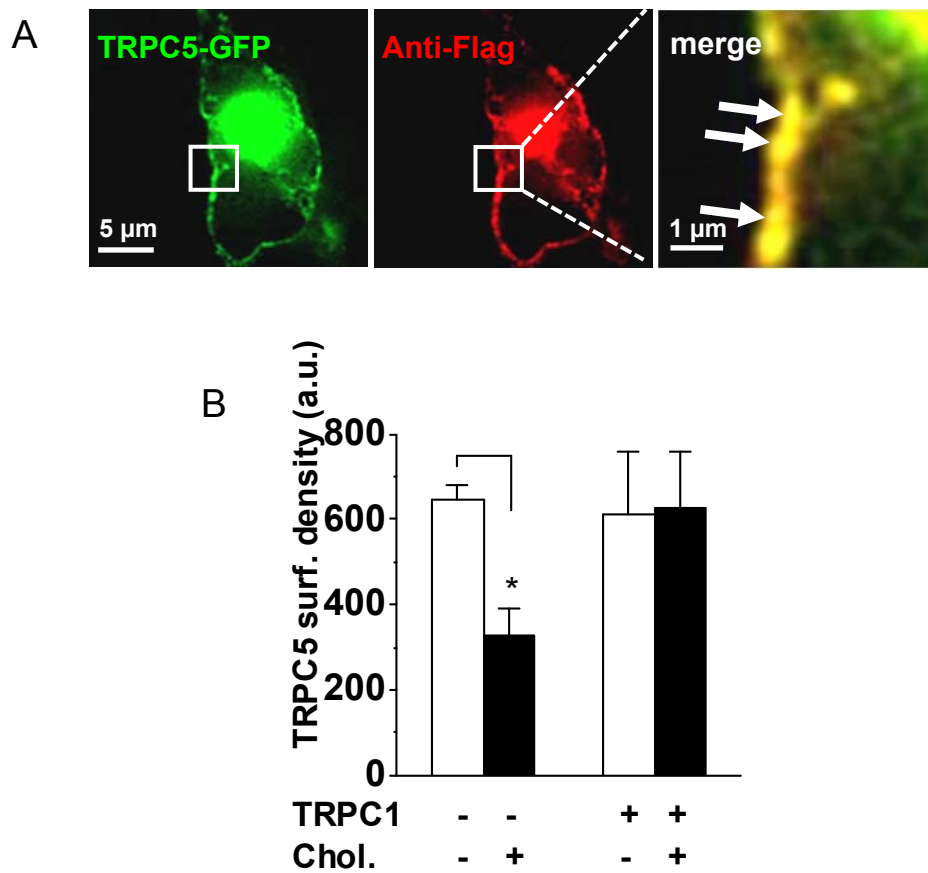
Figure 3.8. TRPC1 prevents cholesterol-induced internalization of TRPC5 in HEK cells. (**A**) Images of MSR cells co-expressing TRPC5-GFP (green) and TRPC1-Flag (labelled with anti-Flag antibody, red). Cells were pre-treated with cholesterol. The merged and magnified image contains arrows that point to co-localized (yellow) TRPC5-GFP and TRPC1-Flag at the cell surface. (**B**) Mean data for the type of experiment shown in (A) and comparing cells with (+) and without (-) cholesterol (Chol.) (n/N=3/28-29). Also shown are data for TRPC5-GFP alone (n/N=3/27-29).

3.2.5. TRPC1 decreases association of TRPC5 and caveolin-1 and regulates TRPC5 in a low-buoyancy membrane fraction

As cholesterol induced internalization of TRPC5 is caveolin-1 dependent, it is possible that TRPC1 affects the association of TRPC5 and caveolin-1, and thus protects TRPC5 against cholesterol- and caveolin-1-dependent internalization.

To test this hypothesis, GFP-trap pull-down assays were performed. GFP-tagged TRPC5 was over-expressed with wild-type caveolin1 in MSR cells with or without TRPC1. Cells were treated with 0.5mM cholesterol for 1 hour and lysed. Cell lysate was incubated with GFP-Trap agarose beads. The protein complexes were then eluted. TRPC5-GFP and caveolin-1 was detected using anti-GFP or anti-caveolin-1 antibodies respectively. Caveolin1 was pulled down with the TRPC5-GFP, and the expression level of cavelolin-1 in cell lysate was not altered by the co-expression with TRPC1-flag (Fig. 3.9 A). However, the related band density of caveolin-1 in GFP-trap was significantly decreased with the presence of TRPC1 (Fig. 3.9 A). The data supported the idea that TRPC1 protects TRPC5 from internalization by impairing the association of TRPC5 and caveolin-1.

It has been shown that TRPC1 binds to caveolin-1(Ong and Ambudkar, 2011), which seems contrast to our result (Fig. 3.9). However, cholesterol has been shown to redistribute TRPC1 residency in membrane fractions (Kannan et al., 2007), and so it was hypothesized that TRPC1 changes the lipid raft localization of TRPC5, leading to its residency in a compartment that is physically separate from caveolin-1. To test this hypothesis, distribution of TRPC5-GFP in membrane compartments was investigated using density centrifugation (Yao et al., 2009). TRPC5 was detected in the low buoyancy membrane fraction 2 and 3 (primarily fraction 2), as well as higher density, caveolar, fractions from 5 to 9 (Fig. 3.9 C, upper panel). TRPC1 co-expression remarkably decreased TRPC5 in fraction 2-3. Cholesterol treatment also led to less TRPC5 in these fractions (Fig. 3.9 C, middle panels). However, when TRPC1 is co-expressed, cholesterol

loading increased the abundance of TRPC5 in fraction 2-3 (Fig. 3.9 C, bottom panel). The data suggested that TRPC1 regulates TRPC5 in a low-buoyancy membrane fraction.
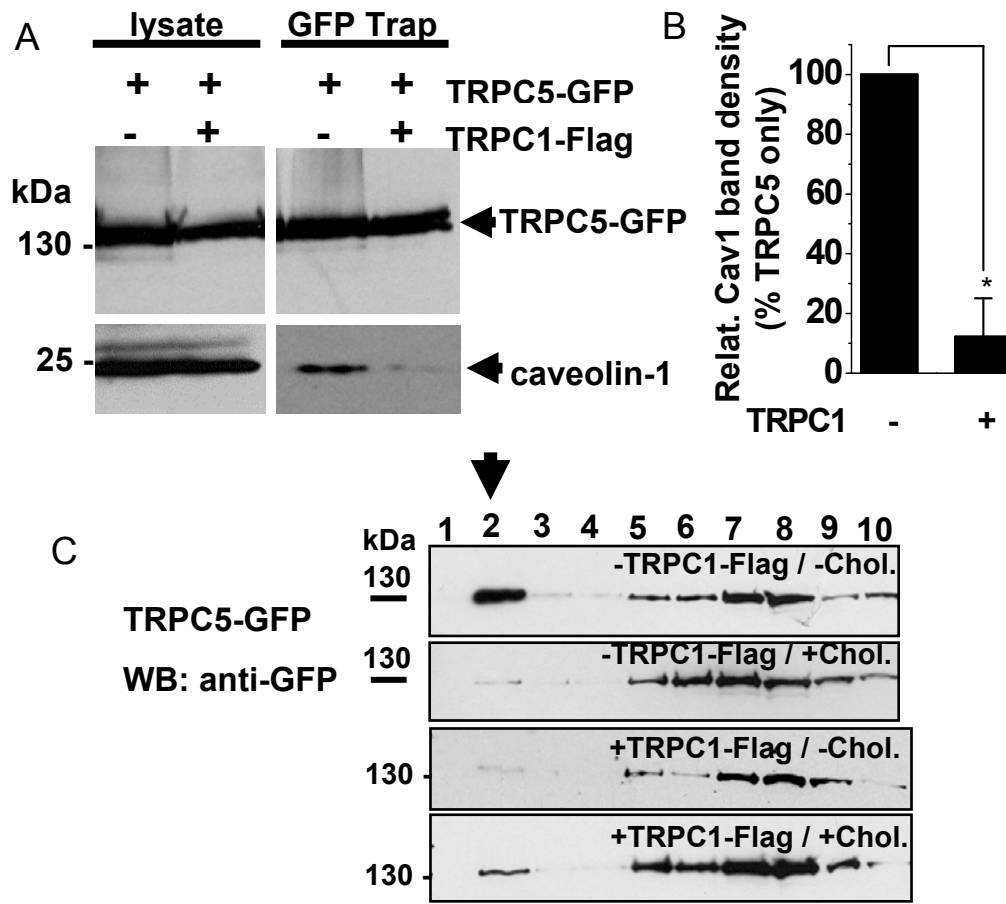
Figure 3.9. TRPC1 decreases association between TRPC5 and caveolin-1 and regulates TRPC5 in a low-buoyancy membrane fraction. (**A**) Western blotting for TRPC5-GFP (anti-GFP antibody) and caveolin-1 (anti-Cav1 antibody) co-expressed in MSR cells with or without TRPC1-Flag. Cells were treated with cholesterol prior to being lysed. Shown are the proteins in the total cell lysate (left) and retained by GFP-Trap beads (right). (**B**) Mean data for the type of experiment shown in (**A**), n=3. (**C**) Western blotting with anti-GFP antibody to detect TRPC5-GFP in MSR cell lysates fractionated (1-10) by density centrifugation. Cells were transfected with TRPC5-GFP alone (top two panels) or co-transfected with TRPC1-flag (bottom two panels), and pre-treated with buffer only (-Chol.), or 0.5mM cholesterol (+Chol.). Representative blots from n=3. All of these experiments were performed by Dr Sarka Tumova.

3.2.6. TRPC1 increases TRPC5 and GM1 co-localization after cholesterol treatment

It has been reported that fraction 2-3 contains non-caveolar lipid microdomains enriched in ganglioside GM1 (Simons and Gerl, 2010, Yao et al., 2009). GM1 is a member of the ganglio series of gangliosides. A ganglioside is a molecule composed of a glycosphingolipid with one or more sialic acids, which predominantly localized in plasma membrane. It has been reported that the cross-linking of GM1 with multivalent ligands induced TRPC5-dependent Ca^{2+} influx (Wu et al., 2007). To investigate if GM1 is implicated in the cholesterol-dependent internalization of TRPC5, MSR cells were transfected with TRPC5-GFP or co-transfected with TRPC5-GFP/TRPC1-Flag. Cells were treated with 0.5mM cholesterol. Flag tag and GM1 were then labeled using anti-flag antibody and ChtxB (cholera toxin subunit B)-Alexa 594 respectively. Without TRPC1 expression, TRPC5 internalised as expected in response to cholesterol. Little co-localization of TRPC5 and GM1 was observed in the intracellular vesicles (Figure 3.10 A). However, the co-localization of TRPC5 and GM1 was significantly higher when TRPC1 was expressed, and TRPC5 remained in the cell edge, co-localizing with TRPC1 and GM1 (Fig. 3.10 B-C).

These results suggested that TRPC1 caused TRPC5 to localize to a GM1-enriched lipid raft, reducing the association of TRPC5 and caveolin-1, and thus protecting TRPC5 from cholesterol-dependent retraction.
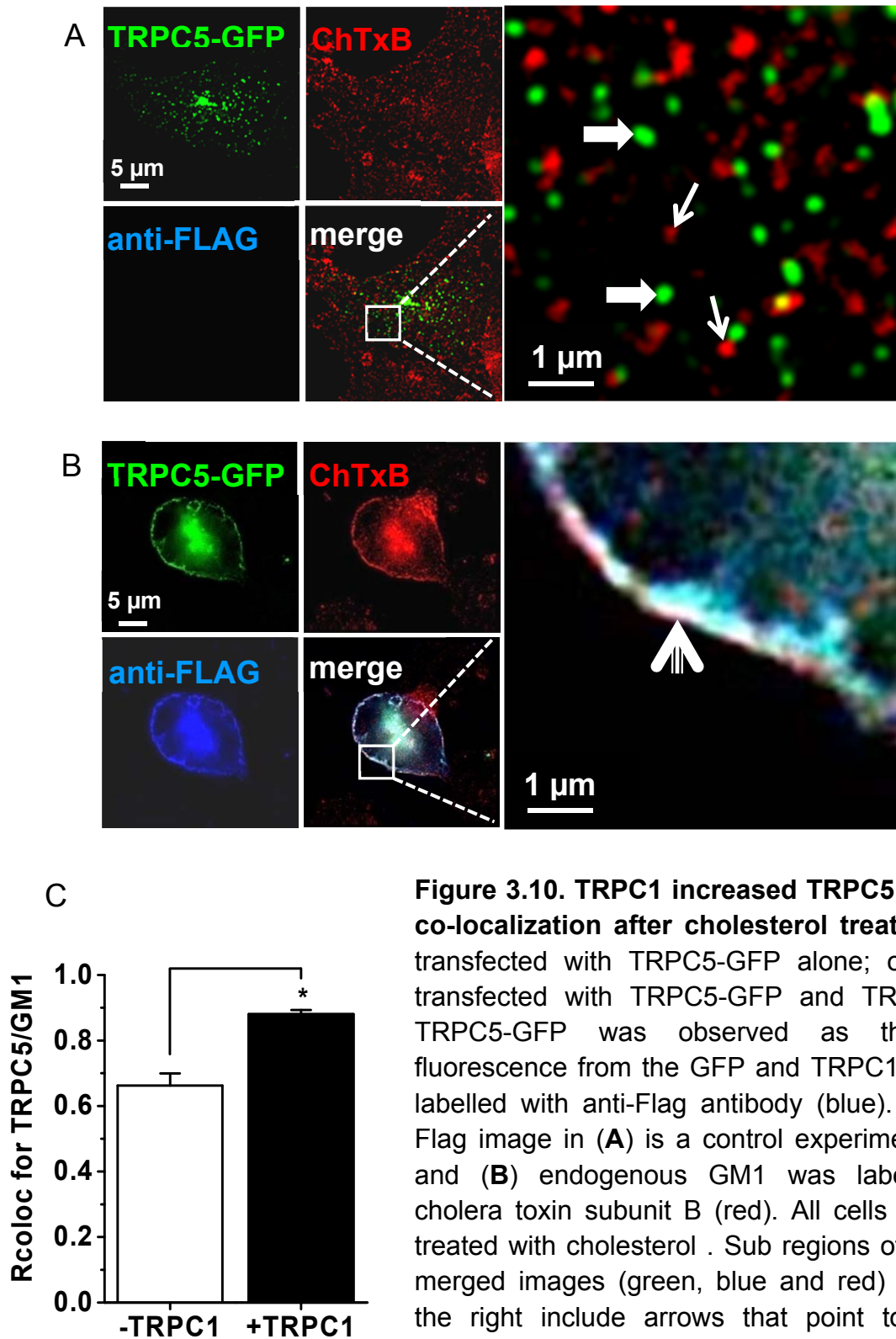
Figure 3.10. TRPC1 increased TRPC5 and GM1 co-localization after cholesterol treatment. (**A**) transfected with TRPC5-GFP alone; or (**B**) co-transfected with TRPC5-GFP and TRPC1-Flag. TRPC5-GFP was observed as the green fluorescence from the GFP and TRPC1-Flag was labelled with anti-Flag antibody (blue). The anti-Flag image in (**A**) is a control experiment. In (**A**) and (**B**) endogenous GM1 was labelled with cholera toxin subunit B (red). All cells were pre-treated with cholesterol . Sub regions of the triple merged images (green, blue and red) shown on the right include arrows that point to vesicles containing TRPC5-GFP (thick arrows) or GM1 alone (thin arrows) (**A**), or to surface membrane containing colocalized TRPC5-GFP, TRPC1-Flag and GM1 (triple arrow) (**B**).(**C**) Mean data for Rcoloc value of TRPC5 and GM1, as the experiments shown in (**A-B**). n/N=3/12-13.

3.2.7. Cholesterol did not cause internalization of TRPC5 in VSMCs, unless TRPC1 was depleted

It was demonstrated that TRPC1 inhibited cholesterol-induced retraction of TRPC5 in an over-expression system (Fig. 3.8). To test cholesterol function on endogenous TRPC5, human vascular smooth muscle cells (VSMCs) isolated from patients undergoing coronary artery bypass operations were used, as these cells exhibit endogenous up-regulation of TRPC1 (Kumar et al., 2006). Endogenous TRPC5 was labelled using TRPC5 antibody, T5E3. VSMCs were incubated with T5E3 diluted in 0.5mM cholesterol or in vehicle control before fixation and labelling with secondary antibodies. Cells were not permeablized, so that only surface TRPC5 was labelled. Cholesterol did not affect surface TRPC5 localization (Fig. 3.11 A-C).

To investigate further, VSMCs were transfected with TRPC5-GFP with the HA tag in the extracellular loop and all surface TRPC5 was detected using anti-HA in non-permeablized cells. Again, cholesterol did not cause internalization of TRPC5 (Fig. 3.12 B), compared with vehicle control (Fig. 3.12 A). To test whether TRPC1 protects TRPC5 against cholesterol-dependent retraction in VSMCs, VSMCs over-expressing TRPC5-GFP were transfected with control or TRPC1 siRNA. Cholesterol caused internalization of TRPC5 only if endogenous TRPC1 was knocked down (Fig. 3.12 C-E).

Similar experiments were done using human umbilical vein endothelial cells (HUVECs), which are vascular endothelial cells expressing TRPC1 (Li et al., 2011). Again, cholesterol only caused retraction of TRPC5 when TRPC1 was knocked down (Fig. 3.13). The data supported the conclusion that TRPC1 suppresses cholesterol-induced internalization of not only over-expressed TRPC5, but also endogenous TRPC5 in two cell types. All surface expression was quantified by Dr.Sarka Tumova.
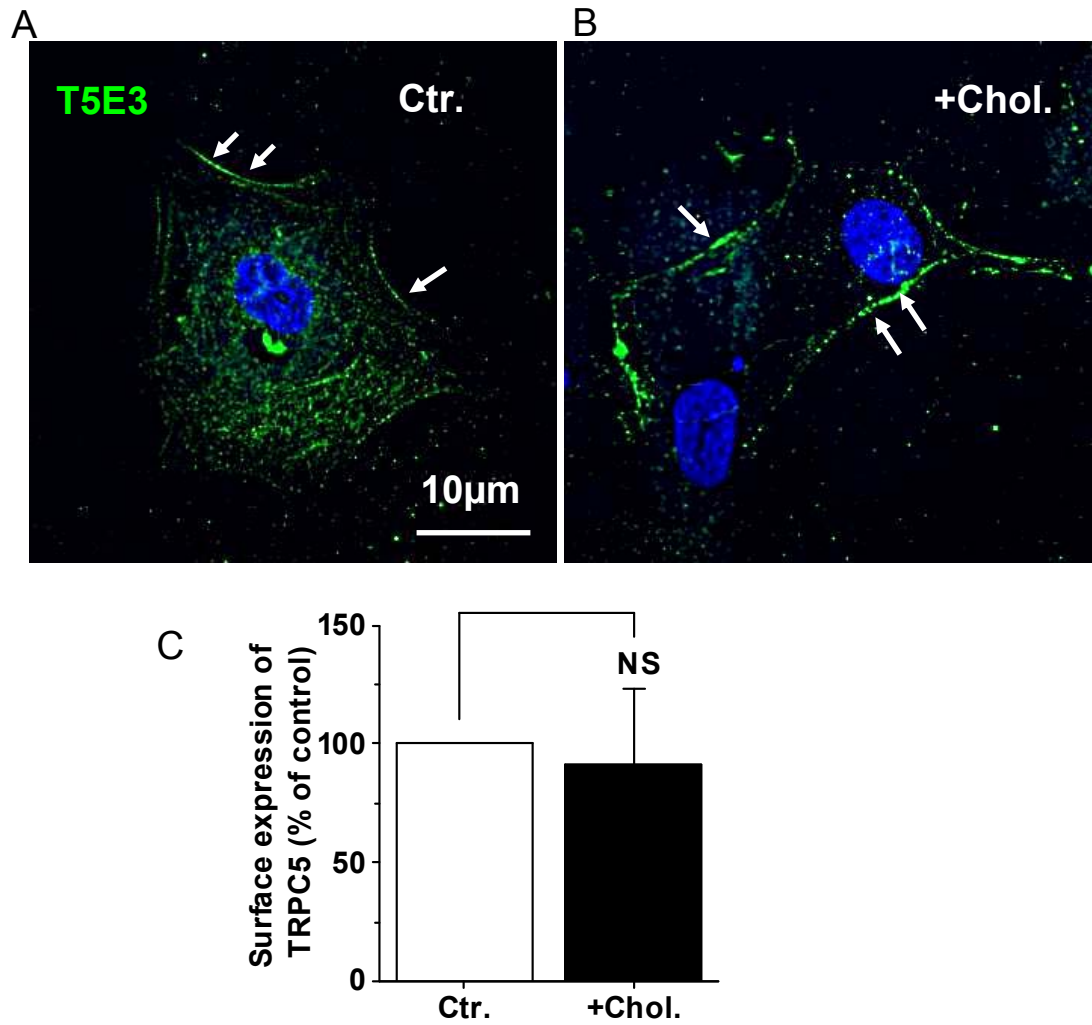
Figure 3.11. Cholesterol does not cause internalization of endogenous TRPC5 in VSMC. (**A-B**) Images of VSMC isolated from patients, labelled with TRPC5 antibodies, T5E3, with (**A**) or without (**B**) cholesterol treatment. (**C**) Mean data for the type of experiment shown in (**A-B**) and comparing cells with (+Chol.) and without (Ctr.) cholesterol (n/N=3/12-15).
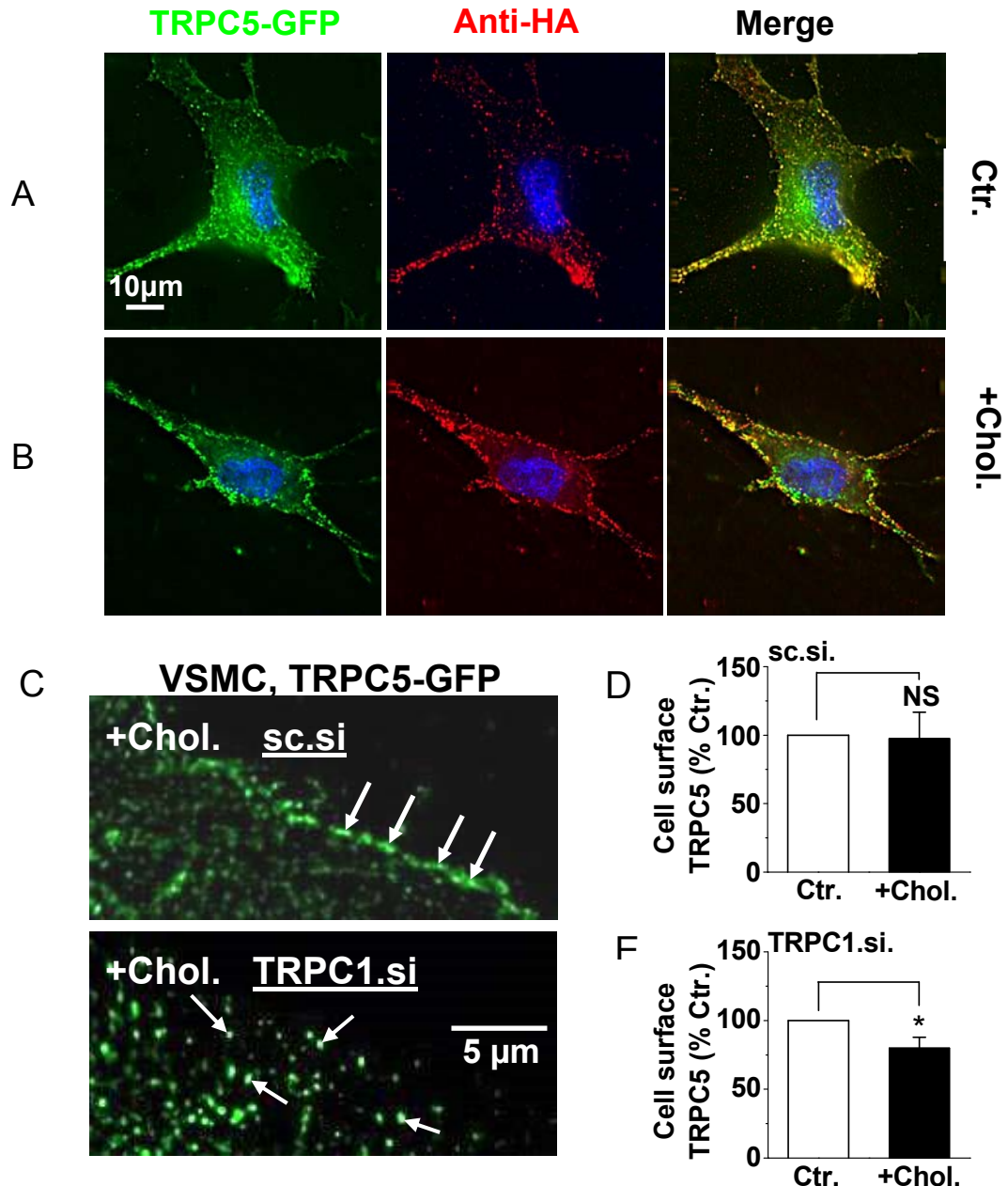
Figure 3.12. Cholesterol causes internalization of over-expressed TRPC5 in VSMCs only if TRPC1 is depleted. (**A-B**). Fixed-cell images of VSMC over-expressing TRPC5-[HA]-GFP after labelling with anti-HA antibody (red). Cells were exposed to 0.5mM cholesterol (**B**) (+Chol.) or buffer only (**A**) (Ctr.). Representative images from 3 independent experiments. (**C**) Images of the edges of VSMCs, showing the fluorescence from TRPC5-GFP transfected in the cells. Examples are shown for cells transfected with scrambled (control) siRNA (sc.si) or TRPC1 siRNA (TRPC1.si). The cells were treated with cholesterol (+Chol.). (**D,E**) Quantification of TRPC5-GFP fluorescence at the cell perimeter as exemplified by the images (**C**) (sc.si, n/N=4/22; TRPC1.si, n/N=4/20). Data are shown for paired experiments in which cells were pre-treated with cholesterol (+Chol.) or not (Ctr., control).
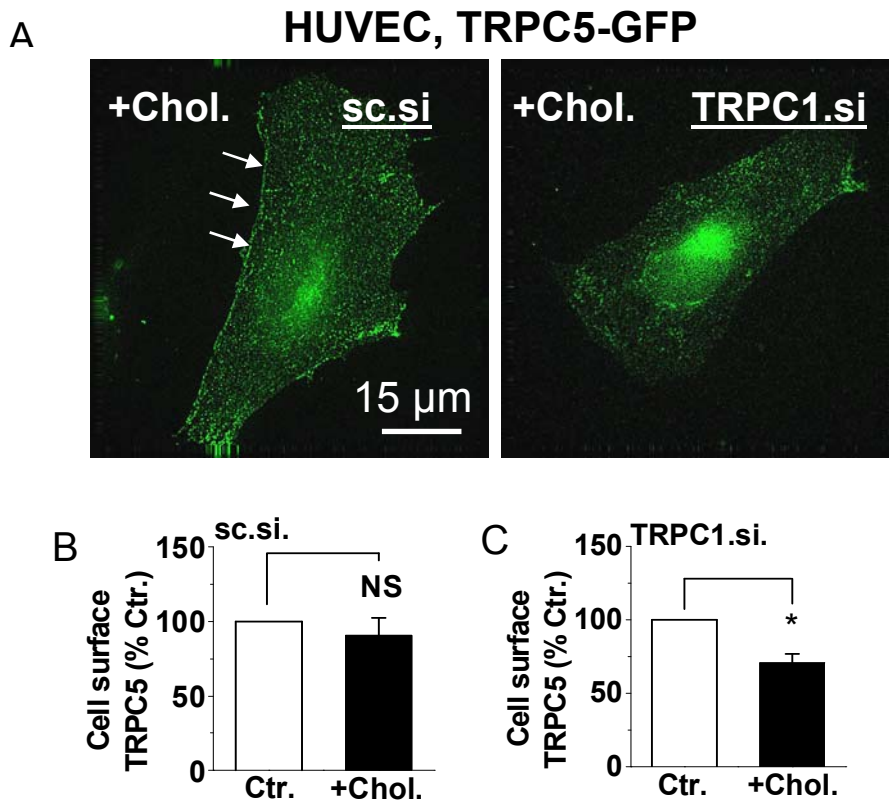
Figure 3.13. Cholesterol causes internalisation of TRPC5-GFP in HUVECs only if TRPC1 is depleted. (**A**) Images of the edges of HUVECs, showing the fluorescence from TRPC5-GFP transfected in the cells. Examples are shown for cells transfected with scrambled (control) siRNA (sc.si) or TRPC1 siRNA (TRPC1.si). The cells were treated with cholesterol (+Chol.). (**B,C**) Quantification of TRPC5-GFP fluorescence at the cell perimeter as exemplified by the images (**A**) (sc.si, ctr. n/N=3/11; +chol. n/N=3/13; TRPC1.si, ctr. n/N=3/13; +chol. n/N=3/10). Data are shown for paired experiments in which cells were pre-treated with cholesterol (+Chol.) or not (Ctr., control).

3.2.8. Cholesterol-induced enhancement of PGPC response in VSMCs is TRPC1-dependent

The oxidised phospholipid PGPC stimulates Ca^{2+} entry in VSMCs via TRPC1/5-containing channels (Al-Shawaf et al., 2010). As cholesterol failed to induce internalization of TRPC1, it would be expected not to inhibit the PGPC response. To test this hypothesis, PGPC response was investigated in VSMCs pre-incubated with 0.5mM cholesterol or vehicle control. Strikingly, cholesterol potentiated the PGPC response in VSMCs by ~2 times compared with vehicle control (Fig. 3.14 A, B). When TRPC1 was knocked-down using siRNA, cholesterol caused less potentiation of PGPC response compared with scrambled control (Fig. 3.14 A, B).

To test if PGPC response in cholesterol was through TRPC1/5-containing channels, VSMCs were pre-incubated with TRPC1 or TRPC5 blocking antibody, T1E3 or T5E3 (Li et al., 2008, Xu et al., 2006, Xu et al., 2008). Neutralized antibodies were used as controls. The antibodies significantly blocked the response compared with peptide control (Fig. 3.14 C-D). Combined with the observation that cholesterol causes TRPC5 internalization when TRPC1 is knocked-down, these data suggested that TRPC1 is important in maintaining TRPC5 heteromer channel-function after cholesterol treatment.
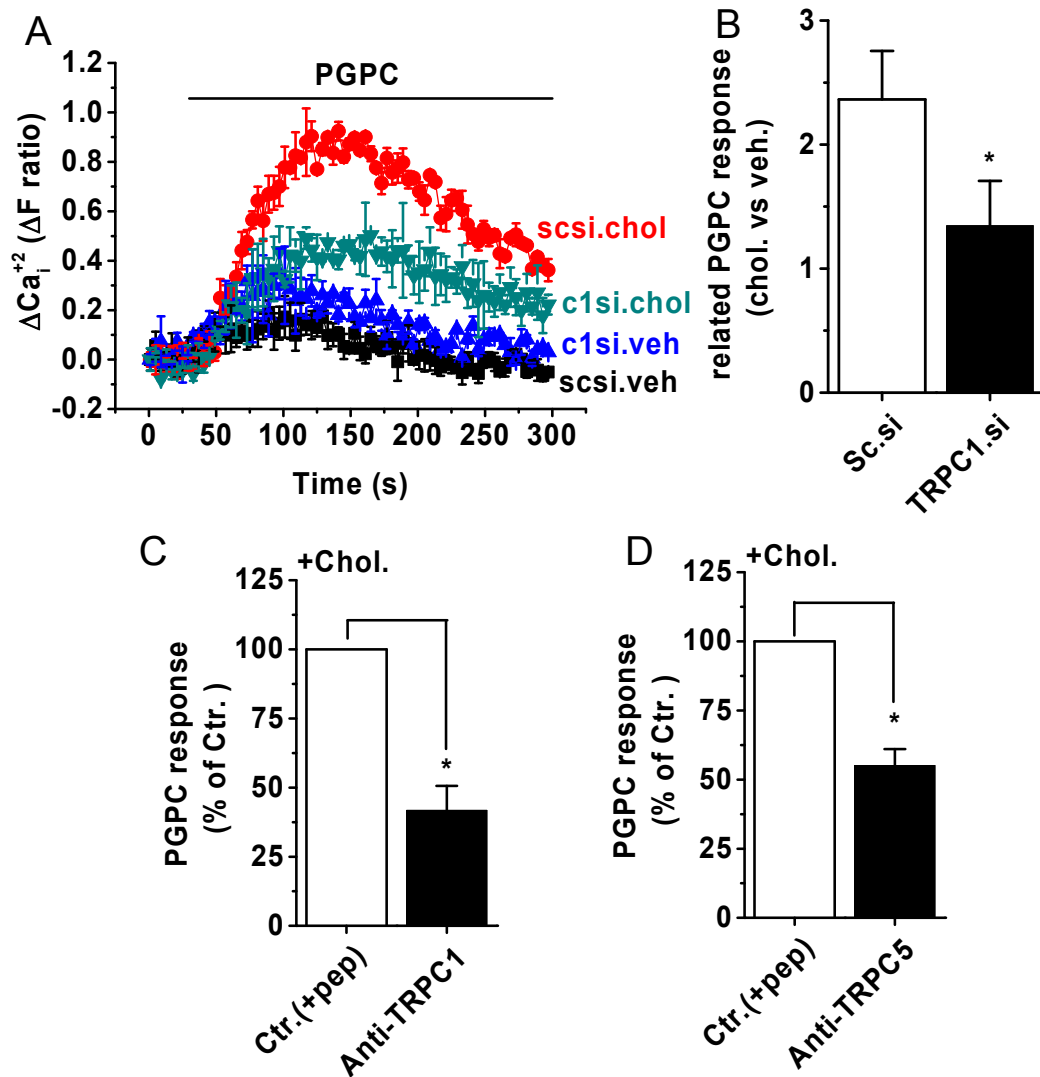
Figure 3.14. Depletion of TRPC1 in VSMC inhibited cholesterol-induced potentiation of PGPC response through TRPC1/5 channels. (**A**) Example data for a 96-well plate experiment showing responses evoked by 30 µM PGPC (1-palmitoyl-2-glutaroylphosphatidylcholine) in control (sc.si) or TRPC1 siRNA (c1.si) transfected VSMCs, after cholesterol (+Chol.) or vehicle (veh.) pre-treatment. (N=5 each). (**B**) Mean data for the type of experiment shown in (**A**) (n/N=6/30). (**C-D**) Mean normalized data for PGPC evoked responses in VSMCs pre-incubated with peptide control (Ctr.(+pep)) or anti-TRPC1 antibody (**C**) and anti-TRPC5 antibody (**D**) (n/N=3/18 for each). (**C-D**) All cells were pre-treated with cholesterol.

3.2.9. GM1 gangliosides evoke Ca^{2+} entry through endogenous cholesterol-resistant TRPC5-containing channels

The present study showed that cholesterol increased the PGPC response through TRPC1/5 channels in VSMCs (Fig. 3.14A, B). However, the surface expression of TRPC5 was not affected by cholesterol (Fig. 3.11), indicating the increased PGPC response was not due to changes in the surface density of the channels. It has been reported that the cross-linking of GM1 with multivalent ligands induced TRPC5-dependent Ca^{2+} influx (Wu et al., 2007). Cholesterol increased localization of TRPC1/5 heteromers in the GM1 enriched raft (Fig. 3.9 and Fig. 3.10), leading to enhanced lipid-protein interaction between GM1 and the channels, which might be the mechanism underlying the potentiation of the channel activity. To test this hypothesis, the effect of applying exogenous GM1 gangliosides on VSMCs was investigated. Indeed, there was transient elevation of intracellular Ca^{2+} evoked by 25µM GM1 gangliosides, which was cholesterol-resistant (Fig. 3.15 A, B). The responses were TRPC5-related because they were suppressed by anti-TRPC5 antibodies (Fig. 3.15 C, D). The data suggested that GM1 gangliosides are important not only for stabilising TRPC5 containing channels at the surface membrane but also for stimulating them.
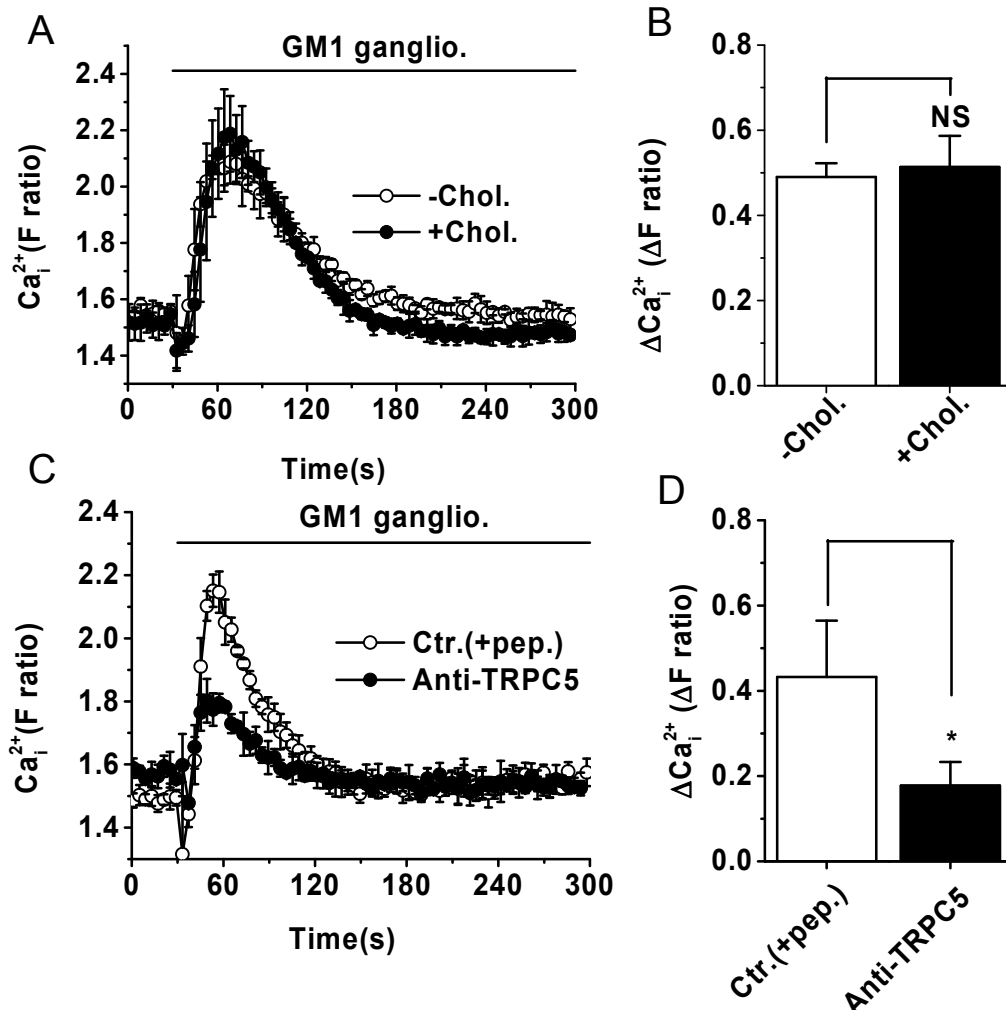
Figure 3.15. GM1 gangliosides evoke Ca^{2+} entry through endogenous cholesterol-resistant TRPC5-containing channels. (**A**) Example data for a 96-well plate experiment showing responses evoked by 25 µM GM1-rich ganglioside extract in VSMCs. Cells were pre-treated with vehicle (-Chol.) or 0.5mM Cholesterol (+Chol.). (**B**) Mean data for the type of experiment shown in (**A**). n/N= 3/14. (**C**) As for (**A**), only cells were pre-treated with anti-TRPC5 antibody T5E3 or T5E3 preadsorbed to its antigenic peptide (Ctr. +pep.). (**D**) Mean data for the type of experiment shown in (**C**). n/N=4/16.

3.3. Discussion

This study reveals cholesterol's ability to inhibit TRPC5 channel function by inducing caveolin-1 dependent internalization of the channel over-expressed in HEK293 cells. TRPC1, however, protects TRPC5 from cholesterol and caveolin-1 dependent retraction. TRPC1 decreases association of TRPC5 and caveolin-1 by segregating the channels to a GM1-rich lipid microdomain (lipid raft) that physically separates TRPC5 from caveolin-1, and thus protects TRPC5 against cholesterol dependent internalization. In addition, GM1 itself has a potentiating effect on TRPC5 activity. In VSMCs, cholesterol fails to induce internalization of both endogenous and over-expressed TRPC5, unless TRPC1 is knocked-down. Cholesterol enhances TRPC1/5 channels activity in VSMCs. The cholesterol's effect on channel activity can be also blocked by TRPC1 knock-down.

TRPC1 expression is up-regulated under physical and metabolic injury conditions in vivo (Kumar et al., 2006, Edwards et al., 2010). Furthermore, TRPC1 has positive effects on VSMC proliferation, migration and hypertrophy (Sweeney et al., 2002, Takahashi et al., 2007, Li et al., 2008). TRPC5 has been implicated in VSMC migration (Xu et al., 2006). These observations raise a paradox because TRPC1 fails to form functional ion channels on its own and actually suppresses the conductance of channels formed by other TRPCs (Beech, 2005a, Strubing et al., 2001). This study suggests a novel function of TRPC1, which segregates TRPC5 to a membrane raft by forming a heteromer with it, stabilizing the channels at the cell surface and profoundly alters the functional impact of cholesterol. Therefore, TRPC1 has positive effect on the channel activity under certain conditions (e.g. high cholesterol) which may solve the paradox. It has been reported that TRPC5 homomer and TRPC1/5 heteromer has opposite functional impact on neurite extension rate in neural cells (Kumar et al., 2012). The data in this chapter suggest that TRPC1-dependent segregation of TRPC5 may be the underlying mechanism of the opposite function.

The positive effect of TRPC1 on neurite outgrowth was fully retained by the channel-dead (CD) pore mutants of TRPC1 (CD-TRPC1), whereas the inhibitory effect of TRPC5 was attenuated by CD-TRPC5 (Heo et al., 2012). These data suggest TRPC1 is capable of regulating TRPC5 by a channel-activity independent mechanism. The data in this chapter provide evidence that TRPC1-dependent channel segregation to a specific membrane raft could be the underlying mechanism.

There are nevertheless additional reasons why TRPC1 is important. It has been shown that TRPC1/5-containing channels of mice VSMC were activated by protein kinase C, but not if the Trpc1 gene was disrupted (Shi et al., 2012). Therefore, a function of TRPC1 is to confer sensitivity to stimulation by protein kinase C (Beech, 2013). So it is supposed that the combined roles of TRPC1 in surface stability and activation by protein kinase C are important for the net positive effect of TRPC1 as a driver of cell proliferation and remodeling in events such as neointimal hyperplasia and restenosis (Ding et al., 2011, Edwards et al., 2010, Kumar et al., 2006). Pertussis toxin (PTX), which blocks G $_{i/0}$ (Al-Shawaf et al., 2010), could be used to test this hypothesis.

Lipid rafts are dynamic membrane microdomains that are comprised of tightly packed cholesterol, sphingolipids and phospholipids (Simons and Toomre, 2000, Simons and Gerl, 2010). Multiple types of lipid rafts vary considerably in size and composition (Dart, 2010). Many have reported the lipid raft regulation of ion channels (Dart, 2010), either by altering channel kinetics, affecting trafficking and surface expression of the channels, or lipid-protein interaction. (Alioua et al., 2008, Jiao et al., 2008, Epshtein et al., 2009, Dart, 2010). Studies of glycosyl-phosphatidylinositol-anchored protein in the HeLa cell-line revealed that the slow protein diffusion correlated with entry into, or interaction with, stationary non-caveolar GM1-rich microdomains (Pinaud et al., 2009). Distinct caveolae were observed in the same cells (Pinaud et al., 2009). The data in this chapter revealed the diffusion of heteromeric TRPC1/5 heteromeric channels into the GM1 enriched domains confers stability on channels and protects the channels from caveolin-1-dependent internalization. The underlying mechanism is

unclear at the moment. However, our finding is consistent with the previous report that cholesterol enrichment resulted in a redistribution of TRPC1 to raft fractions with light density (Kannan et al., 2007). GM1 has been shown localizing in these fractions (Yao et al., 2009). Cholesterol loading increased TRPC1 protein in membrane lipid raft fractions which appeared to reflect trafficking of the protein to raft fractions rather than protein synthesis (Kannan et al., 2007).

The data in this chapter support the idea that GM1 positively regulates TRPC5 channel activity, so the PGPC response is more profound when the channels are localized in the GM1 enriched microdomains. However, the gangliosides used in this study is a total ganglioside extracted from porcine brain (Figure 3.15.), which contains not only GM1 but also other types of gangliosides such as GM2, GM3, GD1a, GD1b and GT1b. It has been reported that TRPC5 activity regulates activation of murine $CD4^+$ and $CD8^+$ effector T cells, which increases GM1 and GD1a level in the cell (Wang et al., 2009). There is possibility that the response is due to other gangliosides other than GM1. Further investigation is needed to identify the effect of individual gangliosides on TRPC1/5 channels.

Cholesterol is an important structural component of the cell membrane, which is well established as a key player of membrane functions (Bastiaanse et al., 1997). Cholesterol dyshomeostasis has been implicated in a variety of cardiovascular diseases such as atherosclerosis (Ikonen, 2008, Rader and Daugherty, 2008). VSMC migration to the intima is an important stage of atherosclerotic plaque formation, and both TRPC1 and TRPC5 could be involved in the process. TRPC1 had positive effects on VSMC proliferation, migration and hypertrophy (Sweeney et al., 2002, Takahashi et al., 2007, Li et al., 2008). TRPC5 has been implicated in VSMC migration (Xu et al., 2006). Consequently, the impact of cholesterol on TRPC5 channels and the changes to this process conferred by TRPC1 reported in this chapter, are likely to have particular significance in the context of gene mutations or high fat diets that elevate plasma cholesterol and lead to potentially life-threatening disease

processes such as atherosclerosis, which suggest TRPC1/5 containing channels could be a potential drug target for the treatment of the disease.

3.4. Conclusion

TRPC1 protects TRPC5 from cholesterol and caveolin-1 dependent retraction of TRPC5 by forming heteromultimer and segregating the channels to a GM1 enriched lipid raft that physically separates TRPC5 from caveolin-1. Both the increased channel stability and GM1 enhancing effect contribute to increased function of the channels.

The findings show a novel mechanism by which TRPC1 redistributes TRPC5 and therefore positively regulates heteromeric TRPC1/5 channel function in vascular smooth muscle cells. As TRPC1 and TRPC5 are important for VSMC migration, which is an important stage of atherosclerotic plaque formation, to block TRPC1-dependent segregation process may lead to the discovery of new drug for atherosclerosis.

Chapter 4. Piezo1 is an essential component for shear-stress sensing in vascular endothelial cells

4.1. Introduction

Every cell is exposed to a range of subtle but important physical forces, which can be sensed by mechanosensitive channels. They have been found in nearly all kinds of organisms (Gillespie and Walker, 2001). These channels can be directly activated by force, and convert mechanical stimuli into electrical signals (Gillespie and Walker, 2001). However, the molecular identities of the channels remain largely elusive, particularly in mammals. A recent study by Coste et al. (2010) showed Piezo1/Fam38A protein is linked to Mechanically Activated (MA) cation channel activities. In sensory neurons or when over-expressed in the HEK293 cell-line, Piezo1 generated Ca^{2+}-permeable non-selective cationic channels that were activated rapidly and transiently by mechanical impact. Furthermore, Piezo1 was able to reconstitute an ion channel when purified and incorporated in artificial lipid bilayers (Coste et al., 2012). Drosophila Piezo mediates an ion channel that responds to noxious mechanical stimuli in vivo (Kim et al., 2012). Piezo1 has also been associated both with β1-integrin activation in epithelial cell adhesion (McHugh et al., 2010) and epithelial cell extrusion in the homeostatic regulation of tissue cell numbers (Eisenhoffer et al., 2012). Mutations in the Piezo1 gene are linked to xerocytosis, a rare hereditary haemolytic anaemia (Zarychanski et al., 2012, Bae et al., 2013, Andolfo et al., 2013). Although Piezo1 has been reported to be expressed widely (Coste et al., 2010), it has not previously been linked to shear stress or blood vessels.

A cell type that has a particularly striking ability to sense physical forces, such as frictional force caused by blood flow (shear stress), is the endothelial cell. Physiological change in shear stress regulates both acute changes in vascular diameter and adaptive, structural wall remodelling (Davies, 2009). These changes and remodelling are endothelium dependent, and disorders of the

shear stress response, are implicated in many diseases like hyperlipidemia, hypertension, diabetes and inflammatory disorders (Davies, 2009). Determination of the mechanisms by which these cells sense physical forces remains one of the major challenges in vascular biology research. Multiple molecules are implicated, including extracellular matrix proteins, adhesion molecules (e.g. CD31/PECAM-1), and membrane proteins (integrins, ion channels, receptors, caveolins etc) (Johnson et al., 2011). Several studies have suggested sensing of shear stress by endothelial cells via a Ca^{2+}-permeable non-selective cation channel (Ando and Yamamoto, 2013, Conway and Schwartz, 2012, Johnson et al., 2011), but the molecular basis of the channel has remained controversial and elusive (Ando and Yamamoto, 2013, Conway and Schwartz, 2012).

The aims of this study are to test the expression of Piezo1 in vascular endothelium cells and examine its role in shear stress sensing and related functions of the cells.

4.2. Results

4.2.1. Endogenous Piezo1 is expressed in endothelial cells from patients and other sources

Piezo1 mRNA was expressed strongly in mouse aorta, liver micro vascular endothelial cells freshly isolated from patients undergoing liver surgery, mouse lung micro vascular endothelial cells, a range of cultured arterial, venous and micro vascular human endothelial cells, and late outgrowth endothelial progenitor cells derived from healthy human volunteers (Li et al., 2014). To test Piezo1 protein expression in endothelial cells, western blotting was performed for human umbilical vein endothelial cells (HUVECs) and liver micro vascular endothelial cells freshly isolated from patients (LECs, cells were isolated by Dr. Richard Young). Anti-Piezo1 antibody was used to detect full-length Piezo1 in both cell types, which is predicted to be 286 kDa in the absence of post-translational modification. Cells were transfected with control siRNA or Piezo1 siRNA 48 hours before the western blotting. A band sized around 280 kDa was detected by the antibody in both cell types, and Piezo1 siRNA decreased the intensity of the band (Fig. 4.1 A, B). Compared with control siRNA, Piezo1 siRNA depleted the protein by 74 % in HUVECs and 70% in LECs (Fig. 4.1 C, D). There was a non-specific band at around 250 kDa, which was not affected by Piezo1 siRNA in either cell type (Fig. 4.1 A, B). The results suggest the expression of Piezo1 protein in endothelial cells.
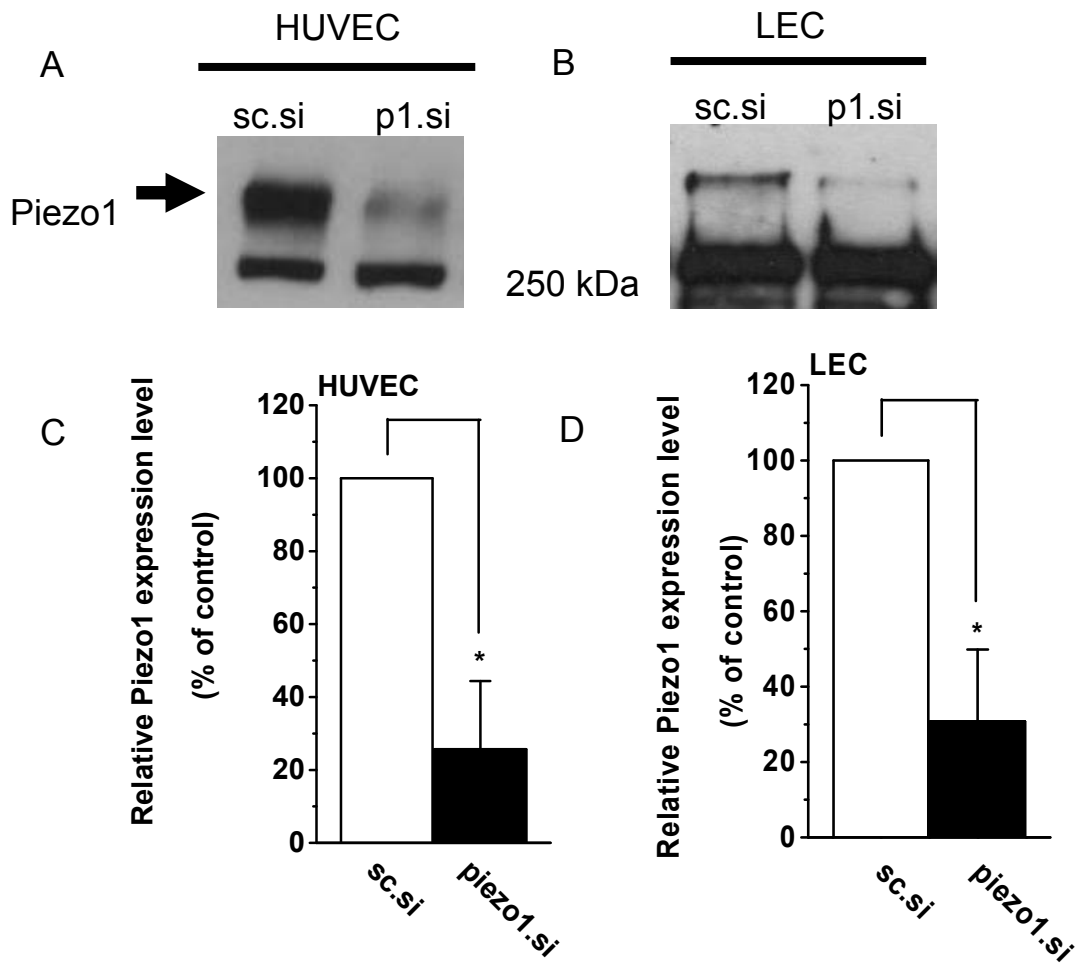
Figure 4.1. Piezo1 is expressed in endothelial cells. (**A-B**) Western blotting for HUVEC lysate (**A**) or isolated human liver endothelial cell lysate (**B**), labeled with anti-Piezo1 antibody after transfection with control siRNA (sc.si.) or Piezo1 siRNA (p1.si). The arrow points to Piezo1 protein. The other band sized 250 kDa is non-specific (Piezo1-unrelated protein). (**C-D**) Mean data for the experiments shown in (**A**) and (**B**). Total β-actin is used as a loading control. n=6 for (**C**) and n=3 for (**D**).

4.2.2. Shear stress causes elevation of intra-cellular Ca^{2+} signal in HUVECs

Shear stress has been shown to induce Ca^{2+} elevation in endothelial cells (Yamamoto et al., 2003). To confirm this and to further study shear stress sensing in endothelial cells, microfluidic chambers, Ibidi μ-Slide VI$^{0.4}$ were used to apply laminar shear stresses to HUVECs (Fig. 4.2 A). HUVECs were seeded 4 hours before loaded with Fluo-4 AM to visualize intracellular Ca^{2+}. Elevation of intracellular Ca^{2+} results in increased fluorescence excitation of Fluo-4 at 488 nm and consequently higher fluorescence signal levels. Live-cell imaging was performed to detect the change of intracellular Ca^{2+} signal. The onset of physiological shear stress (10 dyn.cm^{-2}) induced elevation, often oscillating, of intra-cellular Ca2+ signal in HUVECs (Fig. 4.2 B).
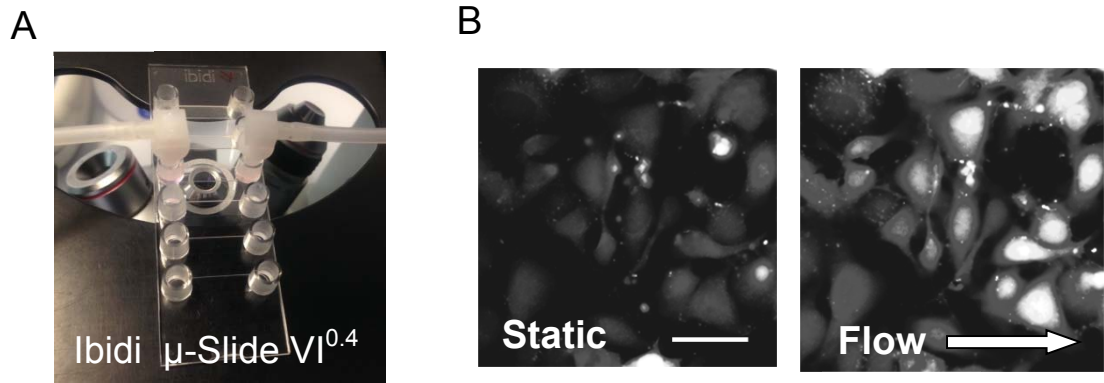
Figure 4.2. Shear stress caused elevation of intra-cellular Ca^{2+} signal in HUVECs. (**A**) Microfluidic chamber, Ibidi μ-Slide VI$^{0.4}$. HUVECs are seeded in the chamber. Shear stress is generated using Ibidi pump system. (**B**) Intracellular Ca^{2+} level of HUVEC before or after exposure to flow (10 dyn.cm^2) for 3 minutes. Cells were loaded with Ca^{2+} indicator, Fluo-4 AM. Elevation of intracellular Ca^{2+} results in increased fluorescence excitation of Fluo-4 at 488 nm and consequently higher fluorescence signal levels. Arrow indicates the direction of flow. Scale bar, 50 μm. Representative from n=3.

4.2.3. Piezo1 is important for shear stress-evoked Ca^{2+} entry in human endothelial cells

To test if Piezo1 was linked to shear stress-evoked Ca^{2+} response of endothelial cells, Piezo1 siRNA was used to deplete endogenous Piezo1 in HUVECs and isolated hepatic endothelial cells from patients undergoing surgical liver resection (LECs) prior to the Ca^{2+} signal recording. To better characterize the Ca^{2+} responses to different rates of shear stress, incrementing shear stresses were applied. Cells were loaded with Fura-2, and exposed to laminar flow at each shear stress for 250 s.

Although small in amplitude, intracellular Ca^{2+} elevations were evident in response to shear stress as low as 5 $dyn.cm^{-2}$ (Fig. 4.3-4.4). Depletion of Piezo1 significantly down-regulated Ca^{2+} signal induced by a range of shear stresses in HUVECs (Fig. 4.3 A-B) and LECs (Fig. 4.4 A-B). In HUVECs, Piezo1 siRNA decreased flow response by 68%, 78%, 86%, 84% respectively for shear stress of 5, 10, 15, 20 $dyn.cm^{-2}$. For LEC, the deduction were 70%, 57%, 66%, 61% for shear stress of 10, 15, 20, 25 $dyn.cm^{-2}$ respectively. The reductions are quantitatively similar to the loss of Piezo1 protein (Fig. 4.1). Two other siRNAs targeting different sites of Piezo1 mRNA showed similar inhibitory effect on shear stress evoked Ca^{2+} signal (Li et al., 2014). These findings suggested an important role of Piezo1 in shear stress-mediated Ca^{2+} signals.
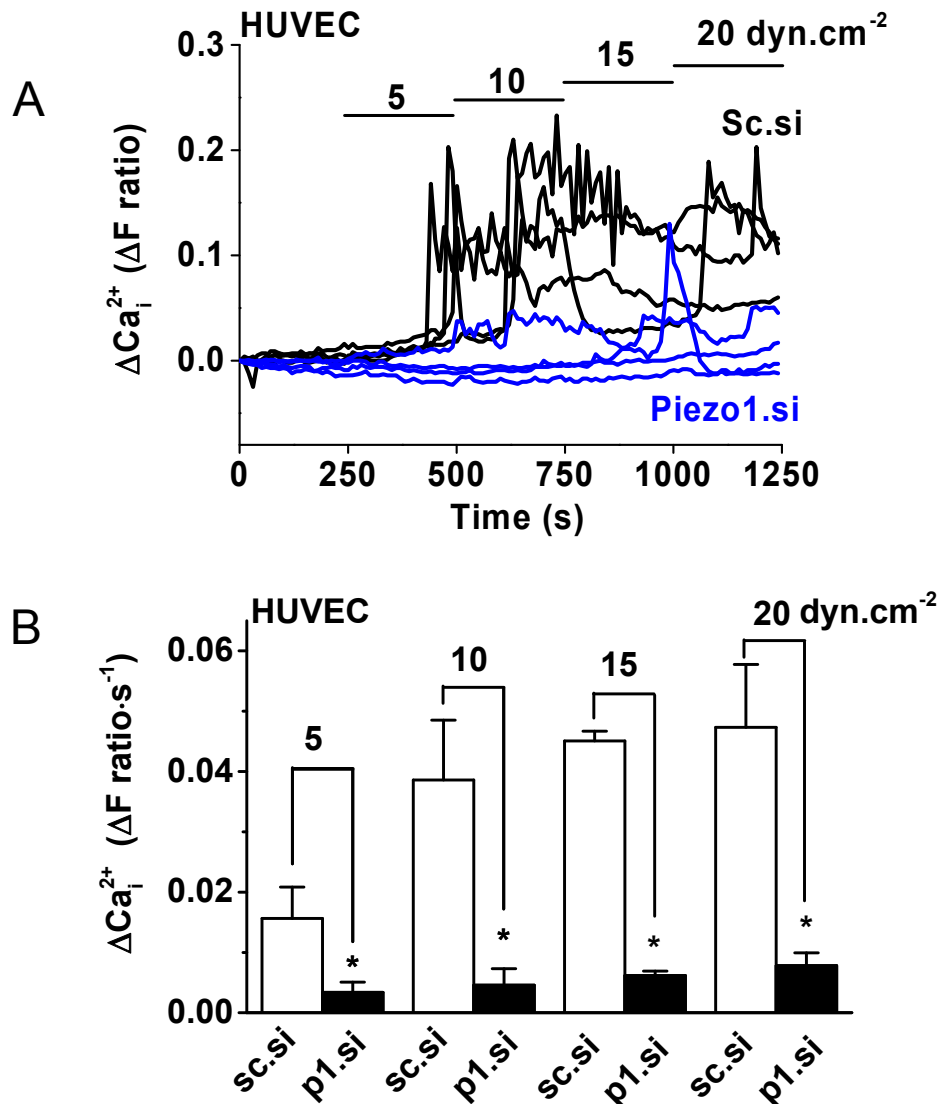
Figure 4.3. Piezo1 is important for shear stress-induced Ca²⁺ signal in HUVECs. (**A**) Example recordings of intracellular Ca²⁺ in single cells transfected with sc.si. or Piezo1.si. (P1.si) (4 cells each, n=1). Shear stress was applied as indicated. (**B**) Mean data for experiments of the type exemplified in (**A**) and expanded to paired comparisons of sc.si. and p1.si. (n/N=5/50 each).
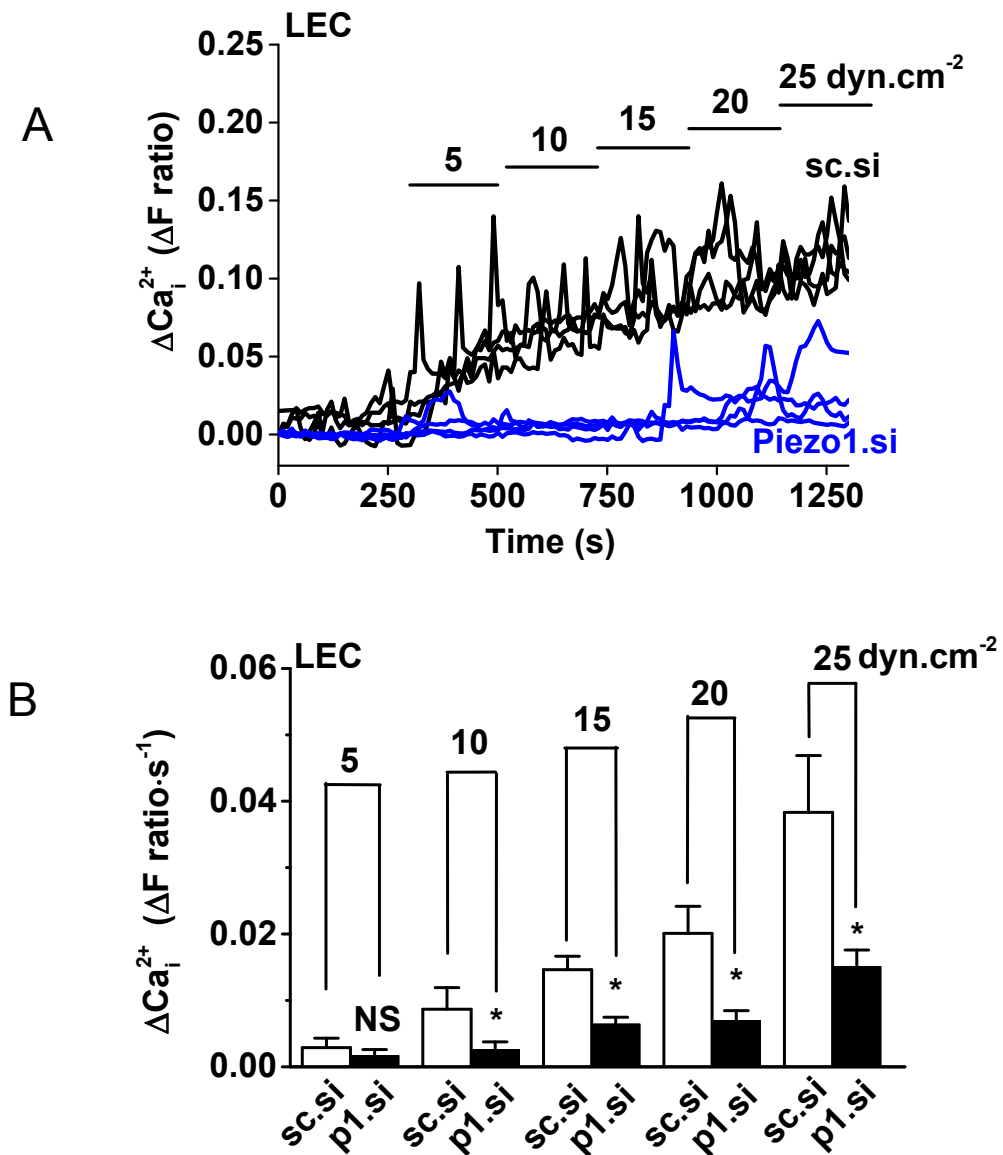
Figure 4.4. Piezo1 is important for shear stress induced Ca^{2+} signal in LECs. (**A**) Example recordings of intracellular Ca^{2+} in single cells transfected with sc.si. or Piezo1.si. (P1.si) (4 cells each, n=1). Shear stress was applied as indicated. (**B**) Mean data for experiments of the type exemplified in (**A**) and expanded to paired comparisons of sc.si. and P1.si. (n=3, 4, 10, 5 and 8 for 5, 10, 15, 20 and 25 dyn.cm^{-2}).

4.2.4. Endothelial cells from mouse embryo with disrupted endogenous Piezo1 gene show less shear-stress induced Ca^{2+} signalling

To study Piezo1 function in an animal model, Piezo1 gene disrupted mouse was generated by Dr Jing Li (Li et al., 2014). Homozygosity (-/-) was embryonic lethal. No homozygous animals were born. However several homozygous embryos were found at E9.5-11.5, which is a critical time for vascular development (Li et al., 2014, Olsson, 2006).

Endothelial cells were isolated from mouse E9.5 wild type (Piezo1 +/+) or Piezo1 -/- embryos by Dr Jing Li. The cells were cultured on microfluidic chambers for 24 hours before shear stress-evoked Ca^{2+} signal was measured. The method used to isolate endothelial cells couldn't ensure a pure population of ECs. Therefore, 30ng/ml VEGF was added into the flowing bath solution 300s before the experiments ended. VEGF has good specificity for endothelial cells. Therefore, shear stress-evoked Ca^{2+} signal was quantified only for VEGF responsive cells (Fig. 4.5 A). Significantly lower but not completely abolished shear stress-evoked Ca^{2+} response was observed in the homozygous (Piezo1-/-) condition, compared with cells from wild type (+/+) embryos (Fig. 4.5 B-C). The data suggested Piezo1 is important for shear-stress sensing in mouse embryonic endothelium around the time of the first blood flow after the heart starts at E8.5.
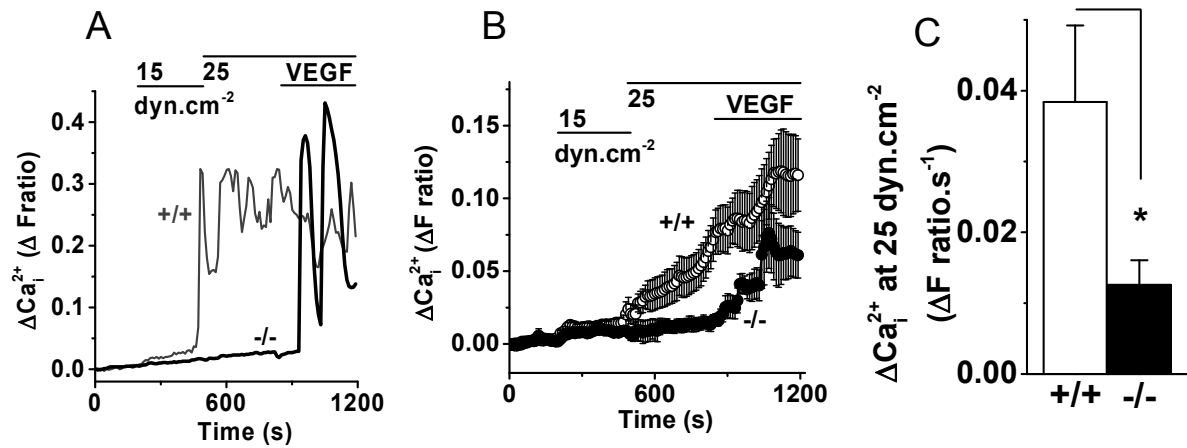
Figure 4.5. Endothelial cells from E9.5 embryo of Piezo1 knock-out mouse (-/-) show less shear stress-evoked Ca^{2+} entry compared with wild type (+/+). (A-C) Data from mouse embryonic endothelial cells. (**A**) example traces for flow-induced Ca^{2+} signal in 2 single cells: one from a Piezo1+/+ embryo and one from a Piezo1-/- embryo (both embryos were from the same mother). Shear stress was applied at 15 and 25 dyn.cm^{-2} and then 30 ng.mL^{-1} VEGF was introduced while maintaining shear stress at 25 dyn.cm^{-2}. (**B**) Mean± s.e.mean data for all VEGF responsive cells as exemplified in (**A**). n/N=6/54 for +/+, 5/42 for -/-. (**C**) Mean data for experiments of the type exemplified in (**A-B**).

4.2.5. Shear stress-evoked Ca^{2+} entry is blocked by GsMTx4

Intracellular Ca^{2+} elevations occurred promptly in response to physiological shear stress. They were complex in character, containing both sustained and oscillating features (Fig. 4.3 A, Fig. 4.4 A, and Fig. 4.6 A). To characterize shear stress-evoked Ca^{2+} signals and further investigate the link of shear-stress evoked Ca^{2+} signal to Piezo1 channel activity, the effect of inhibitors of Piezo1 channels (Coste et al., 2010, Bae et al., 2011) was tested.

HUVECs were loaded with Fura-2 in normal SBS, then washed with normal SBS, or SBS containing 2.5 µM GsMTx4 (a spider toxin blocker of Piezo1 channel and other mechanosensitve channels), or 10 µM gadolinium ion (Ca^{2+} channel blocker), or with Ca^{2+}-free SBS for 20 minutes before Ca^{2+} measurements under these test conditions. Strong suppression of shear stress-evoked Ca^{2+} signal occurred in the presence of GsMTx4 (Fig. 4.6 B, E), gadolinium ion (Fig. 4.6 C, E), or after removal of extracellular Ca^{2+} (Fig. 4.6 D, E) compared with control.

These data suggested that shear stress-evoked Ca^{2+} signals involve Ca^{2+} entry which is linked to Piezo1 channel activity.
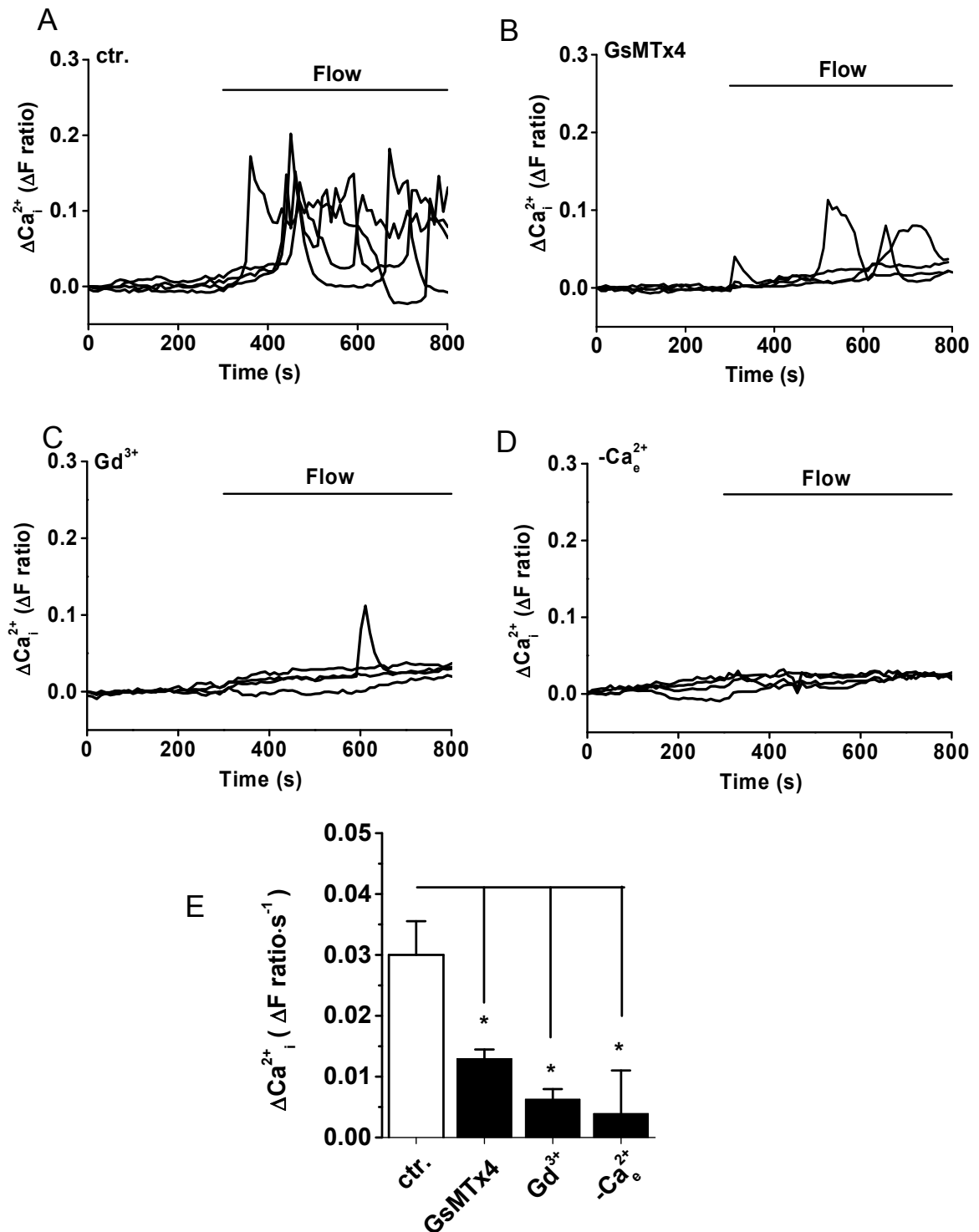
Figure 4.6. Characteristics of shear stress-evoked Ca^{2+} signal in endothelial cells. (A-D) Each panel shows 4 example recordings of intracellular Ca^{2+} from single HUVECs. Recordings were in the continuous presence 2 ng.ml^{-1} VEGF and shear stress was applied at 20 dyn.cm^{-2}. (**A**) Recordings in Standard Bath Solution (containing Ca^{2+}). n/N=8/48. (**B**) As for (**A**) except including 25 μM GsMTx4. n/N= 3/37. (**C**) As for (**A**) except including 10 μM gadolinium (Gd^{3+}). n/N=3/29. (**D**) As for (**A**) except Ca^{2+} was omitted. n/N=3/23. (**E**) Mean data for the types of experiment illustrated in (A-D) (n=3-5).

4.2.6. Exogenous Piezo1 confers shear stress-evoked Ca^{2+} entry

Based on the results shown above, it is suggested that Piezo1 is critical for sensing shear stress in endothelial cells. But is Piezo1 alone sufficient to be a direct shear stress sensor and mediate Ca^{2+} entry in response to flow? To test this, we over-expressed GFP-tagged wild type Piezo1 in HEK293 cells, which do not normally exhibit shear stress response. Previous studies suggested that Piezo1 is not expressed endogenously in HEK293 cells (Coste *et al.*, 2010).

Piezo1-GFP was successfully expressed in HEK293 cells (Fig. 4.7 A). Shear stress-evoked Ca^{2+} influx was compared between cells with mock and Piezo1-GFP transfection. HEK293 cells had little shear stress response unless Piezo1-GFP was expressed (Fig. 4.7 B-C). In Piezo1-expressing HEK293 cells, Ca^{2+} entry occurred in proportion to the amplitude of the shear stress (Fig. 4.7 B).

The data suggested that wild-type Piezo1 is sufficient to generate shear stress sensing in a cell type that does not normally exhibit it.
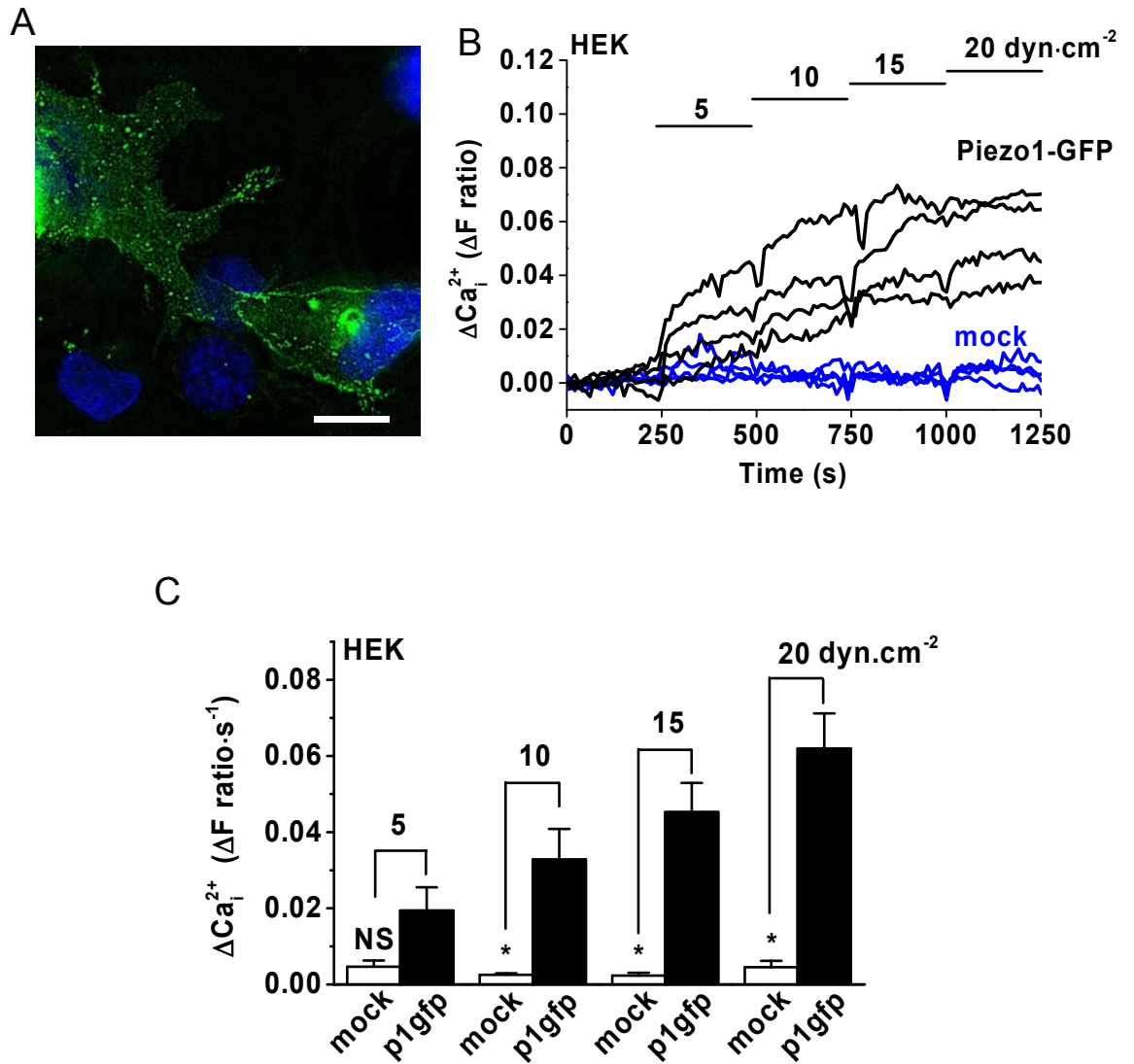
Figure 4.7. Exogenous Piezo1 confers shear stress-evoked Ca^{2+} entry. (**A**) Image of GFP fluorescence of HEK293 expressing Piezo1-GFP (p1gfp) constructs. Scale bar, 10 µm. (**B**) 4 example recordings of intracellular Ca^{2+} from single HEK293 cell transfected with Piezo1-GFP or with mock transfection (4 cells each, n=1). Shear stress was applied as indicated. (**C**) Mean data for experiments of the type exemplified in (**B**), n/N=4/40.

4.2.7. Piezo1 is important for alignment of HUVECs in the direction of shear stress

Alignment of endothelial cells in the direction of shear stress is one of the defining characteristics of endothelial cells and occurs both physiologically in blood vessels in the direction of blood flow, and in vitro when there is culture under flow (Chiu and Chien, 2011, Langille and Adamson, 1981, Tzima et al., 2005). As Piezo1 is important for shear stress sensing in endothelial cells, it was reasoned that Piezo1 might also be important for endothelial cell alignment along the direction of flow.

To test this hypothesis, HUVECs were cultured in microfluidic chambers. Shear stress of 15 dyn·cm^{-2} was applied to the cells for 15 hours. Cells were then fixed and labeled with Rhodamine phalloidin for f-actin (Fig. 4.8A). Orientation of the cells was analyzed using OrientationJ plug-in of ImageJ software (Rezakhaniha et al., 2012). Knock-down of Piezo1 strongly affected the alignment of endothelial cells to shear stress (Fig. 4.8 A, C, D), significantly decreasing the frequency of cells aligned to the direction of flow (mode, Fig. 4.8 C-D).

To further investigate the effect, another method was used to apply flow to endothelial cells. HUVECs were cultured under circulating flow provided by orbital shaker for 24 hours as described in Chapter 2. Cells were imaged using the Incucyte microscope. Again, shear stress caused alignment of the cells, which was suppressed by Piezo1 siRNA (Fig. 4.8 B, E).

Similar results were also observed using endothelial cells isolated from wild type and Piezo1 knock-out mouse E9.5 embryos. Cells were not passaged and were exposed to shear stress of 15 dyn·cm^{-2} in microfluidic chambers within 24 hours after isolation. Mouse endothelial cells need longer time to achieve alignment then HUVECs. Clear alignment of the cells from +/+ mouse was observed after 60 hours exposure to shear stress and it was significantly

decreased in the cells of Piezo1-/- genotype (Fig. 4.9 A, B). It has also been shown endogenous Piezo1 is important for EC orientation in cerebral arteries in adult mice (Li et al., 2014).

The data are consistent with Piezo1 acting as a shear stress sensor that promotes endothelial cell organization and alignment in the response to shear stress.
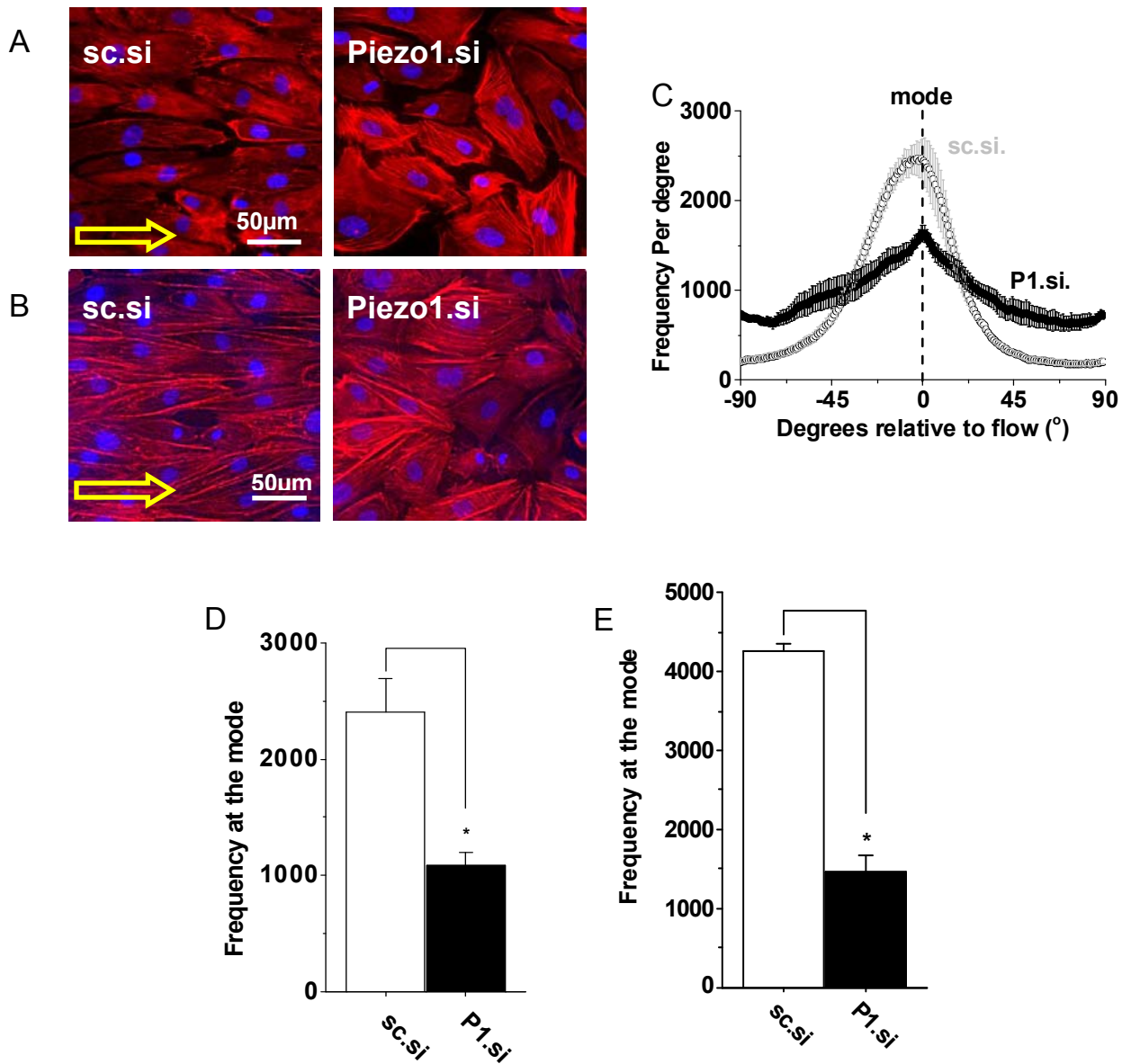
Figure 4.8. Importance of Piezo1 in HUVEC alignment to shear stress. (**A**) HUVECs under 15 dyn.cm^{-2} shear stress for 15 hr in a microfluidic chamber. Rhodamine phalloidin labelled F-actin (red) and DAPI labelled cell nuclei (blue). A paired comparison was made of cells transfected with control siRNA (sc.si) or Piezo1 siRNA (P1.si). The direction of flow is indicated by open arrows. Scale bar, 50 µm. (**B**) As for (**A**) except under shear stress on the orbital shaker in a 6-well dish for 24 hours. (**C**) Example orientation analysis for a pair of images of the type shown in (**A**). (**D**) As for (**C**) but mean data for the frequency (number of angles) at the mode (n/N=3/9 for each). (**E**) As for (**D**) but mean data for the type of experiment exemplified in (**B**) (n/N=3/8 for each). Adam Hyman contributed to the analysis.
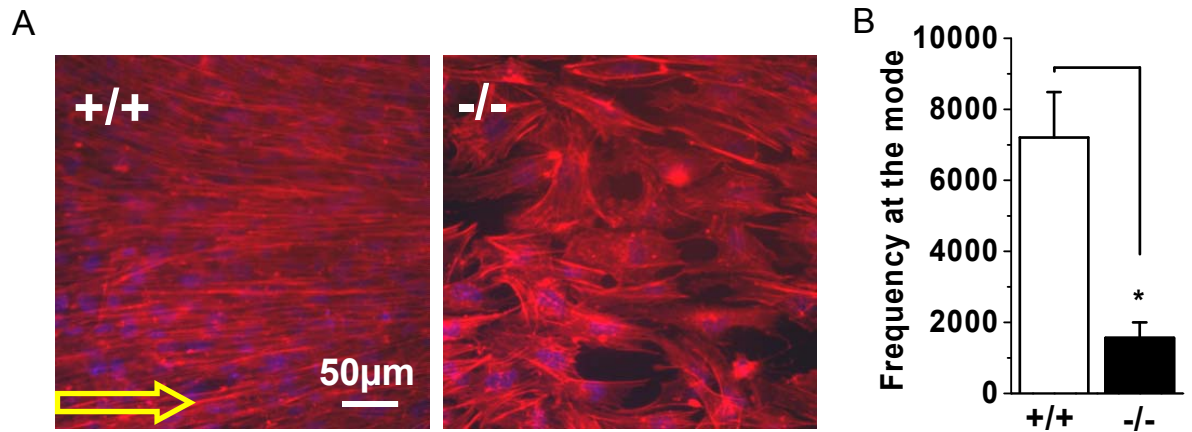
Figure 4.9. Endothelial cells from E9.5 embryo of Piezo1 knock-out mouse (-/-) show less shear stress-evoked Ca^{2+} entry compared with wild type (+/+). (A-B) Data from mouse embryos. (**A**) Example images from endothelial cells isolated from E9.5 Piezo1+/+ and Piezo1-/- embryos and after 15 dyn.cm^{-2} shear stress for 60 hr. Cells were labeled for F-actin and nucleus. Scale bar, 50 μm. (**B**) Mean data for experiments of the type exemplified in (f) (n=4 +/+, n=5 -/-).

4.2.8. Piezo1 channel activity is important for shear-stress induced alignment of HUVECs

As shown above, shear stress-evoked Ca^{2+} entry is linked with Piezo1 channel activity. To test if Ca^{2+} and Piezo1 channel activity are also important for HUVEC alignment to shear stress, the effect of removal of extracellular Ca^{2+} or treatment with GsMTx4 was tested. Cells were cultured under shear stress provided by the orbital shaker for 72 hours before the alignment was quantified.

To test whether shear stress-induced alignment of HUVECs is a Ca^{2+} dependent event, cells cultured in Ca^{2+}-free Krebs solution were compared with cells under control condition (normal Krebs solution, 1.2mM Ca^{2+}). Shear stress induced less alignment in cells cultured in Ca^{2+}-free Krebs solution, compared with cells under control condition (Fig.4.10 A).GsMTx4 was used to inhibit Piezo1 channel activity. To reduce the non-specific binding of the toxin with the peptide in the serum, and maximize the effect of the toxin, HUVECs were cultured in serum-free EGM-2 medium with 2.5 µM GsMTx4 or vehicle control. GsMTx4 also suppressed shear stress-evoked alignment of HUVECs (Fig.4.10 A).

Since removal of extracellular Ca^{2+} or addition of GsMTx4 also blocked shear-stress evoked Ca^{2+} entry in HUVECs (Fig.4.6), the combined data suggest Piezo1 channel activity is important for shear-stress induced alignment of HUVECs.
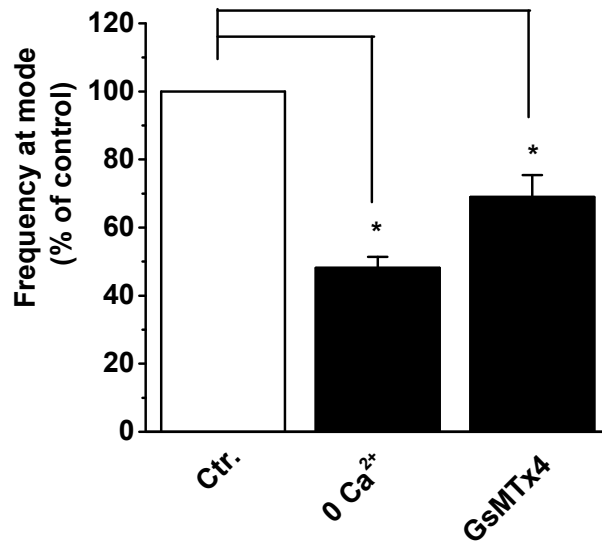
Figure 4.10. Importance of Piezo1 channel activity in HUVEC alignment to shear stress. (**A**) As for Fig.4.10(D), but normalized mean data for the frequency (number of angles) at the mode in experiments comparing cells cultured in Normal (1.2mM Ca^{2+}) and Ca^{2+}-free Krebs solution (n=3 each), or the cells in the presence of 2.5 µM GsMTx4 with its vehicle control (n=4 each).

4.2.9. Piezo1-GFP moves to the cell apex in response to shear stress

To test if Piezo1 might adapt its subcellular localization in response to shear stress to optimize the sensing process in the direction of applied force, cDNA encoding Piezo1 with C-terminal tagged with GFP (Piezo1-GFP) was used to track Piezo1 in live cells by fluorescence microscopy. Piezo1-GFP is the same construct that functionally reconstitutes shear stress sensitivity (Fig. 4.7 A-C).

There is a possibility that GFP tag might affect the subcellular localization of Piezo1. To exclude the possibility, another cDNA construct encoding Piezo1 N-terminally-tagged with HaloTag® protein (Halo-Piezo1) was co-expressed with Piezo1-GFP in HUVECs (Fig. 4.11). If neither GFP nor Halo tag affects Piezo1 localization, Piezo1-GFP and Halo-Piezo1 are expected to co-localize in the cells. Halo-Piezo1 was labeled with anti-Halo antibody. Piezo1-GFP and Halo-Piezo1 showed the same subcellular localization with a Rcoloc of 0.83 (SE= 0.029, Fig. 4.11), suggesting that their localization is determined by Piezo1 protein and not the GFP or Halo tags.

Piezo1-GFP was broadly distributed in HUVECs under static conditions but accumulated at the leading edge of the cell in response to shear stress (Fig. 4.12 A-B, Fig. 4.13 B). Piezo1-GFP density in the leading edge and the trailing edge of the cell (defined in Fig. 4.13 A) was analyzed (Fig. 4.13 B). Shear stress increased Piezo1-GFP density at the cell leading edge, and the values were significantly different than those for the trailing edge of the cell after applying flow (Fig. 4.13 B).

The data suggest a reserve pool of Piezo1 that supplements an active pool at an apex optimized for sensing and responding to the direction of shear stress. The data are consistent with the proposed role of Piezo1 as a shear stress sensor that promotes downstream endothelial cell alignment to the direction of stress.
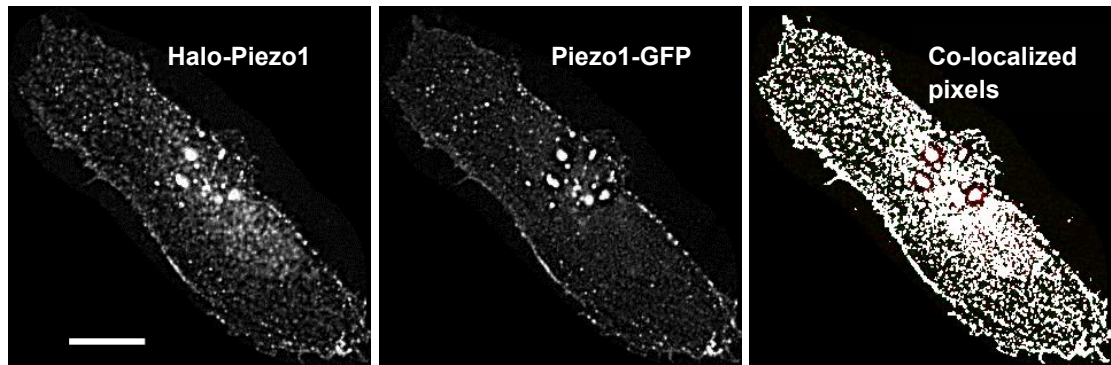
Figure 4.11. Comparison of the sub cellular localizations of Piezo1-GFP and Halo-Piezo1. Example images are of the same HUVEC after co-transfection with cDNAs encoding Piezo1 N-terminally-tagged with HaloTag® protein (Piezo1-Halo, left panel) or Piezo1 C-terminally tagged with GFP (Piezo1-GFP, middle panel). Co-localized pixels of the two images are highlighted in white by imageJ software in the right panel. Scale bar, 20 μm. Rcoloc=0.83, SE=0.029, n/N=3/8.
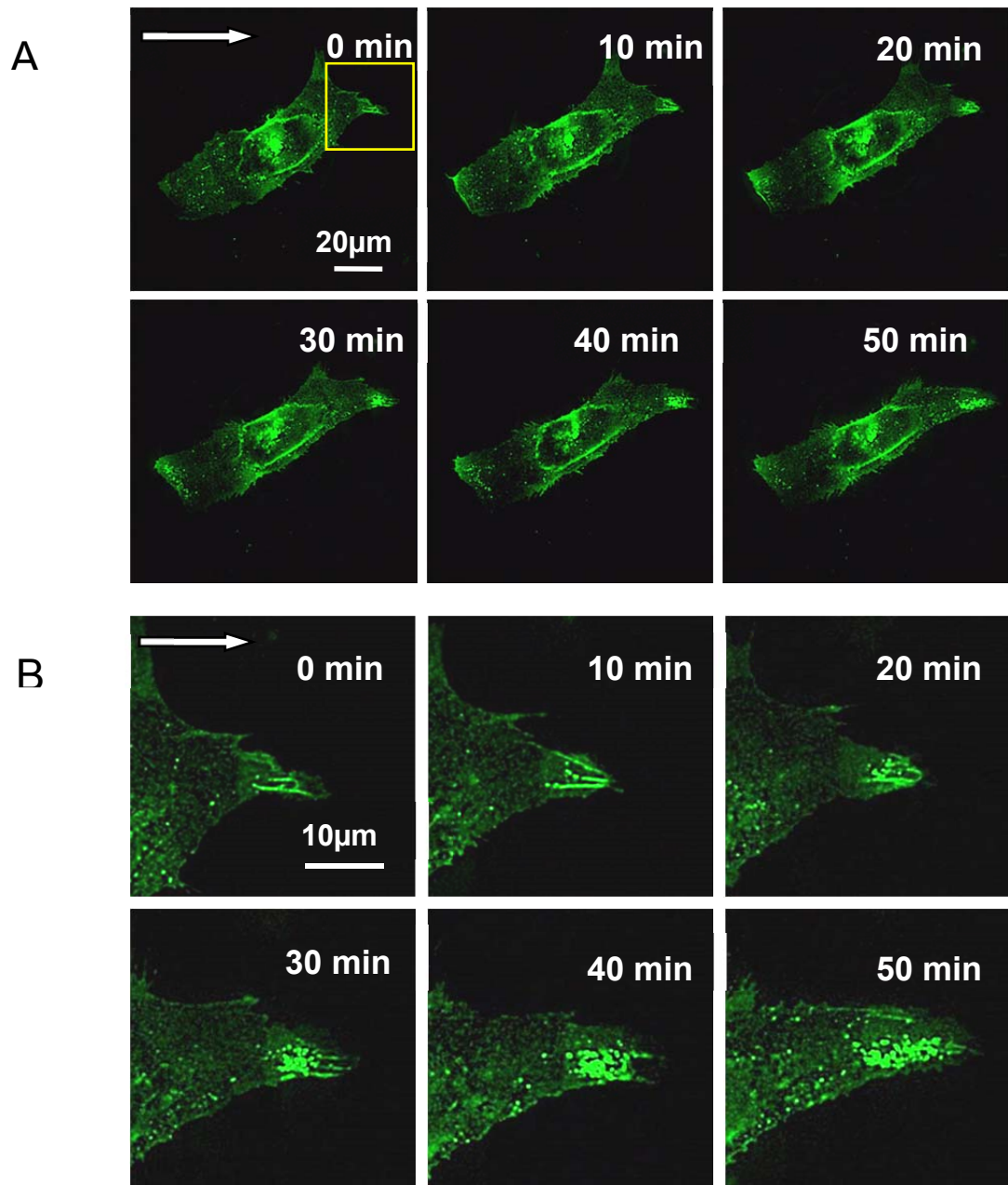
Figure 4.12. Piezo1-GFP moves to the cell apex in response to shear stress.
All data are from HUVECs and shear stress was applied from left to right as
indicated by the arrows. (**A**) Fluorescent images of Piezo1-GFP in a single cell
sampled every 10 min after the onset of 15 dyn.cm^{-2} shear stress. Selected area
indicates the part of the cell that became leading after application of shear stress.
Representative of n=8. (**B**) For the same cell as (A) but magnified to show the
leading edge at 0 and 50 min.

A

B
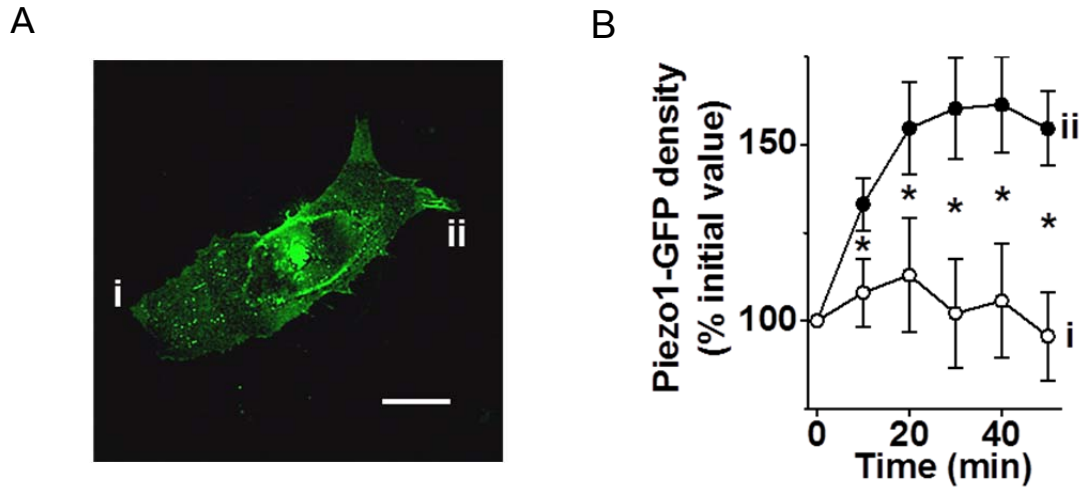
Figure 4.13. Analysis of experiments of the type shown in Fig. 4.12. Piezo1-GFP density values were measured for (i) the part of the cell that became trailing after application of shear stress and (ii) the part that became leading. i and ii are defined in (**A**), Scale bar, 10 µm. (**B**) Analysis of experiments of the type shown in **Fig. 4.12** (n= 8 per data point except for n=7 at 50 min).

4.3. Discussion

This chapter reveals a novel role of Piezo1 as a critical shear stress sensor in endothelial cells. Depletion/disruption of endogenous Piezo1 or applying Piezo1 blockers reduces shear stress-evoked Ca^{2+} signal, while over-expression of wild-type Piezo1 is sufficient to generate shear stress sensing in a cell type that does not normally exhibit it (i.e. HEK293 cells). Consistent with the role as a shear stress sensor, Piezo1 promotes downstream endothelial cell alignment to the direction of physiological shear stress. Disruption of Piezo1 affects endothelial cell alignment. Shear stress drives Piezo1 to the advancing apex of endothelial cells, suggesting a mechanism in which a reserve pool of Piezo1 supplements an active pool at an apex optimized for sensing and responding to the direction of shear stress.

Piezo1 has been reported to be activated by mechanical impact generated by the movement of a glass probe (Coste *et al.*, 2010 & 2012). However, this kind of stimuli has unclear relevance to *in vivo* physiology. Little is known about how Piezo1 responds to physiological mechano-stimuli, such as shear stress generated by blood flow. The present study is the first to link Piezo1 with the vascular system and physiological force (shear stress). The findings may be relevant to the other cell types that experience fluid flow, such as erythrocytes and renal tubular epithelial cells, which also express Piezo1 (Zarychanski *et al.*, 2012, Peyronnet *et al.*, 2013) and respond to shear stress (Platt *et al.*, 1981, Nauli *et al.*, 2003, Praetorius and Spring, 2003).

In this study, several novel experimental tools were used for investigating shear stress responses of ECs, such as ibidi pump system and Incucyte imaging system. Ibidi pump system provides a long-term, accurate, computer controllable, laminar flow over the cells, which nicely reflects the natural environment of cells under flow conditions. Orbital shaker is a widely used tool to generate shear stress, and to investigate shear stress-evoked EC alignment. The orbital shaker generates a tangential shear stress, and cells located at

different positions of the culture plate are exposed to different shear stress. Random imaging and manual quantification could cause errors of the results. Therefore, the Incucyte imaging system was used to image cells in the same relative position in each well of a 6-well plate, so that quantification of alignment induced by the same shear stress was ensured. The automated quantification for cell orientation is done by the software which reduced subjectivity.

This study shows that Piezo1 plays an important role in shear-stress evoked Ca^{2+} signal in ECs. The Ca^{2+} signal is actually induced by onset or change of the flow. However, endothelial alignment is induced by a long-term, stable flow. Although Piezo1 contributes to both processes, the Piezo1 channel activity might be different under each condition. The Ca^{2+} signal induced by a long-term flow, and shear stress-evoked Ca^{2+} signal in ECs that are already aligned need to be further investigated to test this hypothesis.

Another cell type that is exposed to shear stress in vivo are erythrocyte. Mutations in the Piezo1 gene in erythrocytes are linked to xerocytosis, a rare hereditary haemolytic anaemia (Zarychanski et al., 2012, Bae et al., 2013, Andolfo et al., 2013). It has also been suggested that xerocytosis is associated with defective shear stress sensing (Platt et al 1981). It is therefore hypothesized that Piezo1 M2225R mutant identified in studies of xerocytosis might have lower or even absent shear stress sensitization. The hypothesis is confirmed by the fact that Piezo1 M2225R mutant failed to generate shear stress sensing in HEK293 cells (Li et al., 2014). The data further link xerocytosis with defective shear stress response, and confirm the importance of Piezo1 in shear stress sensing. Nevertheless, the Piezo1 M2225R mutant shows higher pressure-activated currents that inactivate more slowly than wild-type currents in cell-attached patches (Albuisson et al., 2013). This suggests that the shear stress-dependent electrophysiological properties of the channel might be different from that induced by pressure. The shear stress-activated current need to be further investigated for Piezo1 M2225R mutant.

The alignment of cells in the direction of shear stress is specific to endothelial cells (Levesque and Nerem, 1985). In regions in laminar shear stress in arteries, vascular endothelial cells elongate along the direction of flow and atherosclerosis is suppressed (Davis, 1995). In contrast, cells are polygonal and atherosclerosis develops in the regions in disturbed flow (Girard and Nerem, 1995). Cell alignment is considered to be an adaptive mechanism to decrease local mechanical load (Tzima *et al.*, 2001). In the present study, Piezo1 was found to be linked with shear-stress induced alignment of endothelial cells not only in vitro, but also in vivo (Li et al., 2014), suggesting the physiological importance of Piezo1 in vascular system.

The data in this chapter show endothelial cells isolated from Piezo1 gene-disrupted mouse embryos (-/-) has less shear stress-induced Ca^{2+} entry compared with those from +/+ embryos. Furthermore, the vasculature in the yolk sac of the homozygote was less prominent compared with +/+ embryos at E9.5-11.5 (Li et al., 2014), which is a critical time for vascular development (Olsson, 2006). Heart beating in the mouse starts at E9.5, which provides blood flow over vascular endothelial cells. Therefore, there is a possible link between Piezo1-dependent mechanical sensation and vascular architecture, which could be tested in future by an *in vitro* angiogenesis assay under shear stress.

While the data provide evidence that Piezo1 acts as a sensor of shear stress in endothelial cells, they do not exclude other proteins as additional shear stress sensors. Many theories have been proposed to answer how an endothelial cell senses shear stress. These include adhesive protein activation, tyrosine kinase activation, activation of multiple ion channels, or regulation of Ca^{2+} by caveoli, etc. (Johnson, 2011). Given the fact that ECs experience a large breadth of shear stress magnitude with different rate or direction, it is expected these mechano-sensory proteins could work independently or as integrated complex in shear stress sensing under different conditions. They may also work as back-up mechanisms, regulators or amplifiers in shear stress sensing. Polycystin-2, which was reported to be a shear stress sensor in kidney cells (Nauli *et al.*, 2003 & 2008), is reported to be a negative regulator of Piezo1 (Peyronnet et al.,

2013). It suggests that Piezo1 could interact and be regulated by another shear-stress sensing protein. However, the mechanism of shear stress sensing in renal epithelial cells might be different from that in ECs. The relationships of Piezo1 to other proteins remain largely undetermined and need to be further investigated.

It has been demonstrated in this chapter that a spider toxin, GsMTx4 inhibits flow-induced Ca^{2+} response and alignment of ECs. GsMTx4 is a peptide known to block stretch-activated cation channels (SACs) including Piezo1 (Bae et al., 2011). GsMTx4 has high specificity for SACs without having any known effect on voltage-gated channels (Bowman et al., 2007). GsMTx4 binds to the lipid bilayer, affects membrane mechanics around SACs, and modifies the gating of the channels, which were considered to be the key mechanism of its effect (Bowman et al., 2007). Therefore, GsMTx4 is not specific to Piezo1 but has possible effect on other shear stress-sensitive ion channels. A specific channel blocker of Piezo1 needs to be developed to further investigate the specific role of endogenous Piezo1 channel activities.

Piezo1 is also shown to be responsible for shear stress-evoked Ca^{2+} signal in LECs. LECs were isolated from patients undergoing liver resection for colorectal metastases. The cells were from mixed types of blood vessels from a section of normal liver (Li et al., 2014). ECs in different types of blood vessels are exposed to different levels of shear stress, ranged from 1 in small veins to 70 dyn.cm^{-2} in some arteries and capillaries (Chiu and Chien, 2011). To better investigate Piezo1 function in LECs isolated from different source vessels, incrementing shear stresses (5-25 dyn.cm^{-2}) were applied to induce Ca^{2+} signal. However, shear stress over 30 dyn.cm^{-2} caused detachment of the cells from the microfluidic chamber and therefore, to further determine Piezo1 function under higher shear stress, a fibronectin-coated chamber needs to be used. Given the importance of Piezo1 and shear stress sensing in angiogenesis, comparison of Piezo1-dependent shear stress response between normal LECs and LECs isolated from tumor tissue may lead to new therapeutic strategies for cancer.

Tzima *et al.* (2005) reported a shear-stress sensory complex in endothelial cells, which is comprised of PECAM-1 (which is suggested to directly transmit mechanical force), vascular endothelial cell cadherin (which functions as an adaptor) and VEGFR2 (which activates phosphatidylinositol-3-OH kinase). The activation of this complex by shear stress is upstream of integrin activation. Piezo1 was reported to be necessary for integrin activation in epithelial cells (McHugh *et al.*, 2010). The relationship between Piezo1 and the mechano-sensory complex in shear stress sensing, and downstream pathways would be further discussed in the next chapter.

4.4. Conclusion

This chapter reveals a novel role of Piezo1 as a critical shear stress sensor in endothelial cells. Depletion or inhibition of Piezo1 impairs flow-induced Ca^{2+} signal and downstream endothelial cell alignment and endothelium function, while exogeneous Piezo1 expression is sufficient to generate shear stress sensing in cells that do not normally exhibit it. The Piezo1 sensing function is dependent on its channel activity and may be supported by shear stress-triggered Piezo1 translocation to the leading edge of the cells. These findings suggest Piezo1 could be a potential drug target for shear stress-related diseases like atherosclerosis and cancer.

Chapter 5. Piezo1 cross-talks with CD31, promoting calpain-dependent alignment of ECs to shear stress

5.1. Introduction

Shear stress generated by blood flow plays a key role in the cardiovascular system in both normal physiology and in diseases such as cancer and atherosclerosis (Davies, 2009). A better understanding of the mechanisms underlying mechanotransduction in the vascular system could greatly help development of new therapeutic approaches. The mechanisms by which vascular cells sense shear-stress remains incompletely understood. However, multiple molecules are implicated, including extracellular matrix proteins, adhesion molecules (e.g. CD31/PECAM-1), and membrane proteins (integrins, ion channels, receptors, caveolins etc) (Johnson et al., 2011).

It has been reported that CD31 (or PECAM-1, platelet endothelial cell adhesion molecule 1), VE-cadherin (vascular endothelial cell cadherin) and VEGFR2 (vascular endothelial growth factor receptor 2) comprise a shear-stress sensory complex in endothelial cells (Tzima et al., 2005). In this model, CD31 directly transmits mechanical force; VE-Cadherin works as an adaptor; and VEGFR2 activates phosphatidylinositol-3-OH kinase (Tzima et al., 2005). It has been suggested the activation of CD31 by shear stress results in activation of a src family kinase, probably Fyn (Chiu et al., 2008). VEGFR2 is then brought into this complex in the presence of VE-Cadherin, and is activated by Fyn in a ligand-independent manner (Conway and Schwartz, 2012). It subsequently mediates downstream pathways including activation of phosphatidylinositol-3-OH kinase and production of nitric oxide (Tzima et al., 2005).

Data presented in the previous chapter show that Piezo1 functions as a direct shear stress sensor in endothelial cells, and promotes shear-stress dependent alignment of the cells. The aims of the study in this chapter are to investigate the relationship between Piezo1 and proteins of the known shear-stress sensing complex, including CD31 and VEGFR2, and to elucidate the downstream pathways of Piezo1.

5.2. Results

5.2.1. Piezo1 over-expressing HEK293 cell don't align to shear stress

Piezo1 is shown to be a shear stress sensor in the Chapter 4, enabling endothelial cells to align along the direction of shear stress. Shear stress evoked Ca^{2+} entry in HEK293 cells over-expressing Piezo1 (Fig.4.7). However, it is still unclear whether Piezo1 itself is sufficient to reconstitute shear stress-mediated alignment in HEK cells, or if other components are needed. To test this, Piezo1-GFP was transfected into HEK293 cells 2 days before experiments. Cells were cultured on poly-D-lysine coated plate under shear stress generated by an orbital shaker for 24 hours. Cells were then imaged using the Incucyte microscope. While phase contrast imaging was used to visualize all the cells, cells expressing Piezo1-GFP were detected using fluorescence imaging (Fig.5.1A). There is no indication that the HEK293 cells align to the shear stress with or without Piezo1-GFP (Fig.5.1 A).

HEK293 cells over-expressing Piezo1-GFP were exposed to flow generated also by microfluidic chambers. Cells were cultured under $15 dyn/cm^2$ shear stress for 24 hours before fixation and labeled with rhodamine phalloidin for f-actin. Again, HEK293 cells with Piezo1-GFP expression showed little alignment in the direction of flow, suggesting Piezo1 itself is not sufficient for this process (Fig.5.1 B), and other components are required.
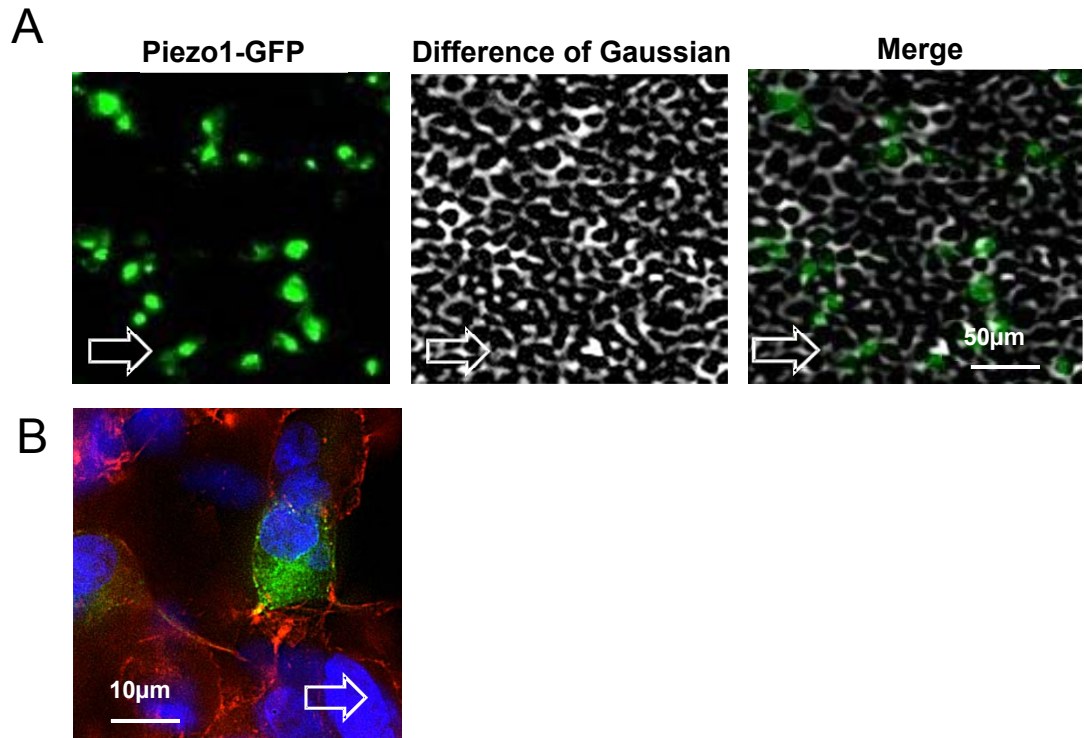
Figure 5.1. Piezo1 over-expressing HEK293 cells do not align to shear stress. (**A**) Images of HEK293 cells transfected with Piezo1-GFP after culturing under shear stress generated by the orbital shaker for 24 hours. Left panel, image for GFP fluorescence from HEK293 cells expressing Piezo1-GFP. Middle panel, highlighted cell edges for all the cells in the same area as shown in the left panel. Right panel, merged image. n=3. Scale bar, 50 μm. The direction of flow is indicated by open arrows. (**B**) Fluorescent image for HEK293 cells over-expressing Piezo1-GFP (green) after cultured under 15 dyn.cm^{-2} shear stress in a microfluidic chamber for 24 hours. Nuclei are labelled blue with DAPI. F-actin is labelled red. n=2. Scale bar, 10 μm.

5.2.2. Piezo1 co-localises and interacts with CD31

CD31/VE-Cadherin/VEGFR2 mechanosensory complex has been suggested to be important for shear stress-evoked alignment of endothelial cells, similar to Piezo1 in this study. These proteins are sufficient to confer mechanosensitive behavior in HEK293 cells (Tzima et al., 2005). As there is no commercially available Piezo1 antibody suitable for immunofluorescence staining, to study if Piezo1 cross-talks with the mechanosensory complex, HUVECs over-expressing GFP-tagged Piezo1 (Piezo1-GFP) were labelled with anti-CD31 antibodies. Piezo1-GFP was strikingly co-localized with CD31, especially at cell-cell junctions (Fig.5.2 A). Co-localization (Rcoloc) between Piezo1-GFP and CD31 was 0.757(Fig.5.2 B).

To determine whether the two molecules interact, HaloTag® Mammalian Pull-Down System was used. The system enables isolation and identification of intracellular protein complexes containing Halo-tagged protein. HaloTag binds to Halo-resin and protein complexes containing Halo-tagged protein can be pulled-down and isolated. Proteins within the complexes can be then identified using western blotting. Halo-pull down assay was performed by Dr. S.Tumova. Plasmids encoding HaloTag protein tagged human Piezo1 (HPiezo1) and wild type human CD31 were co-transfected into HEK-MSR cells. HaloTag protein alone (Halo) overexpressing with CD31 was used as a control. HPiezo1 was pulled-down using a standard promega Halo-pull-down protocol. Cell lysate was incubated with Halo-resin for 1 hour so that proteins with HaloTag bound to the resin. The proteins were then eluted by boiling in loading buffer, and analyzed by western blotting. HPiezo1 was detected by anti-Piezo1 antibody. It was found in both lysate and pull-down eluate of HPiezo1 transfected cells (Fig.5.2 C). However, in lysate and pull-down from HaloTag transfected cells, no HPiezo1 was detected. CD31 was also detected by anti-CD31 antibody both in pull-down and lysate from HPiezo1 transfected cells, but not Halo transfected cells (Fig. 5.2 C). CD31 was pulled-down with HPiezo1, suggesting that Piezo1 not only co-localizes with endogenous CD31, but also physically interacts with it when over-expressed together.
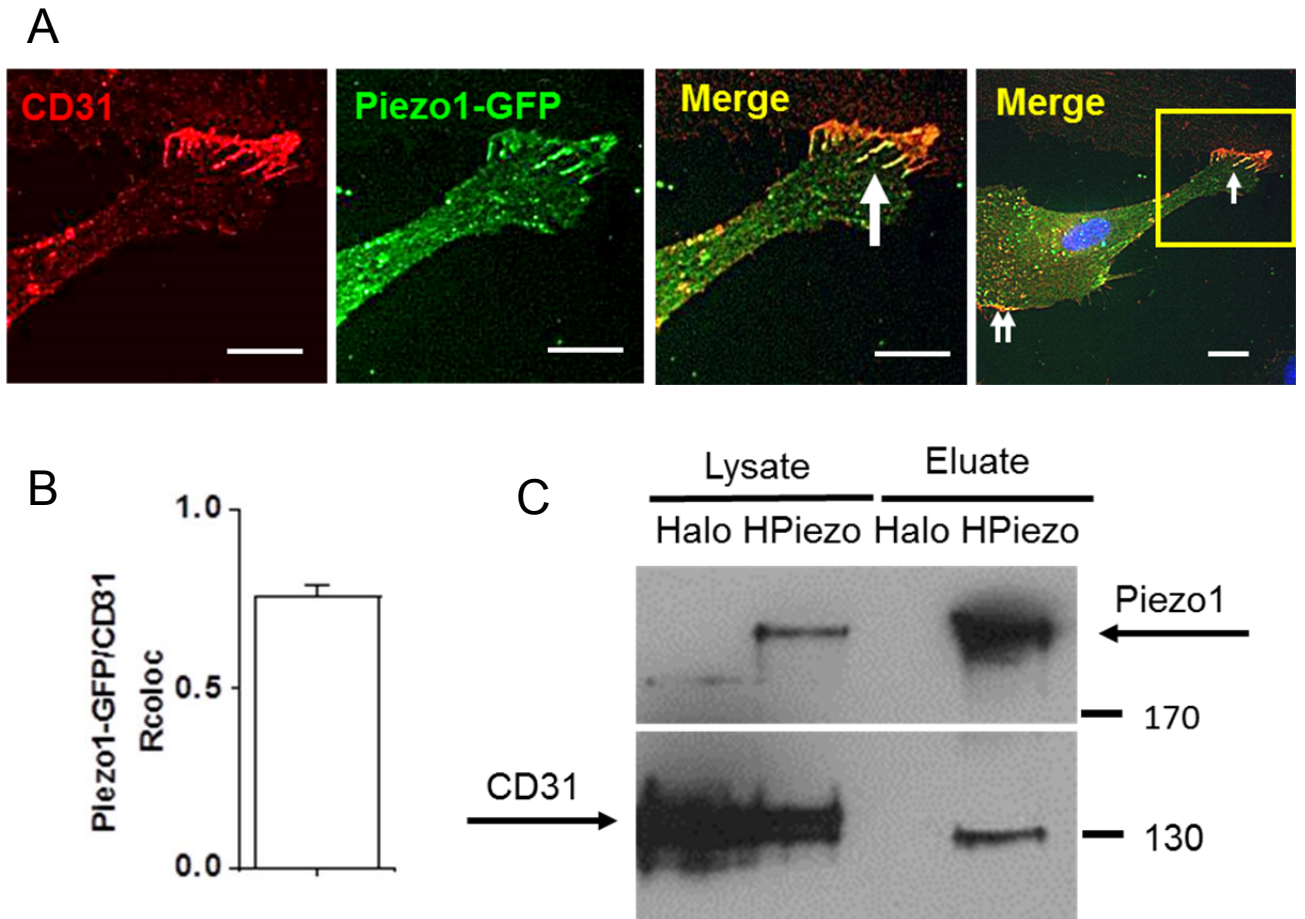
Figure 5.2. Piezo1 co-localises and interacts with CD31. (**A**) Fluorescent images of HUVECs expressing Piezo1-GFP and labelled with anti-CD31 antibodies. Nucleus is labelled blue with DAPI. Left and two middle panels show the expanded area selected in the right panel. Arrows point to co-localised Piezo1-GFP and CD31. Scale bar is 20µm. (**B**) Rcoloc of Piezo1-GFP and CD31 for the type of experiments shown in (**A**), n/N=5/17. (**C**) Western blot for Piezo1 (anti-Piezo1 antibody) and CD31 (anti-CD31 antibody) in HEK-MSR cells over-expressing CD31 and Halo-Piezo1 (HPiezo) or Halo alone. Shown are the proteins in the total cell lysate (left) and retained by Halo-pull-down beads (right, Eluate). Representative of n=3. By Dr. Sarka Tumova.

5.2.3. Piezo1 and CD31 have mutually dependent expression

To further investigate the relationship between Piezo1 and CD31, the protein expression levels were detected using western blotting and immunostaining. HUVECs were transfected with scrambled siRNA, or siRNAs targeting human Piezo1 or CD31 two days before western blotting. Piezo1 and CD31 protein were detected using anti-Piezo1 and anti-CD31 antibody respectively. Piezo1 siRNA suppressed the expression of Piezo1 as expected. western blotting result showed HUVECs transfected with Piezo1 siRNA also had decreased band intensity of CD31 protein compared with control, which suggested knock-down of Piezo1 negatively regulated the expression of CD31 (Fig.5.3 A-C). Likewise, CD31 siRNA suppressed expression of both Piezo1 and CD31 protein (Fig.5.3 A-C), suggesting a mutual dependency of their expression.

VEGFR2 is a component of the mechanosensory complex, and is suggested to be downstream of CD31 activation (Tzima et al., 2005). Therefore, it was hypothesized Piezo1 might also regulate the expression of VEGFR2. To test this hypothesis, expression of VEGFR2 was also studied using western blot. HUVECs were transfected with scrambled siRNA, or siRNAs targeting human Piezo1 or VEGFR2 two days before western blotting. Piezo1 knock-down also negatively regulated VEGFR2 protein abundance (Fig.5.3 D-E). However, VEGFR2 siRNA had no effect on Piezo1 protein expression (Fig. 5.3 F). These data suggest Piezo1 and CD31 have mutually dependent expression, and VEGFR2 was down-stream of Piezo1/CD31, and its expression was regulated by Piezo1, but not vice versa.
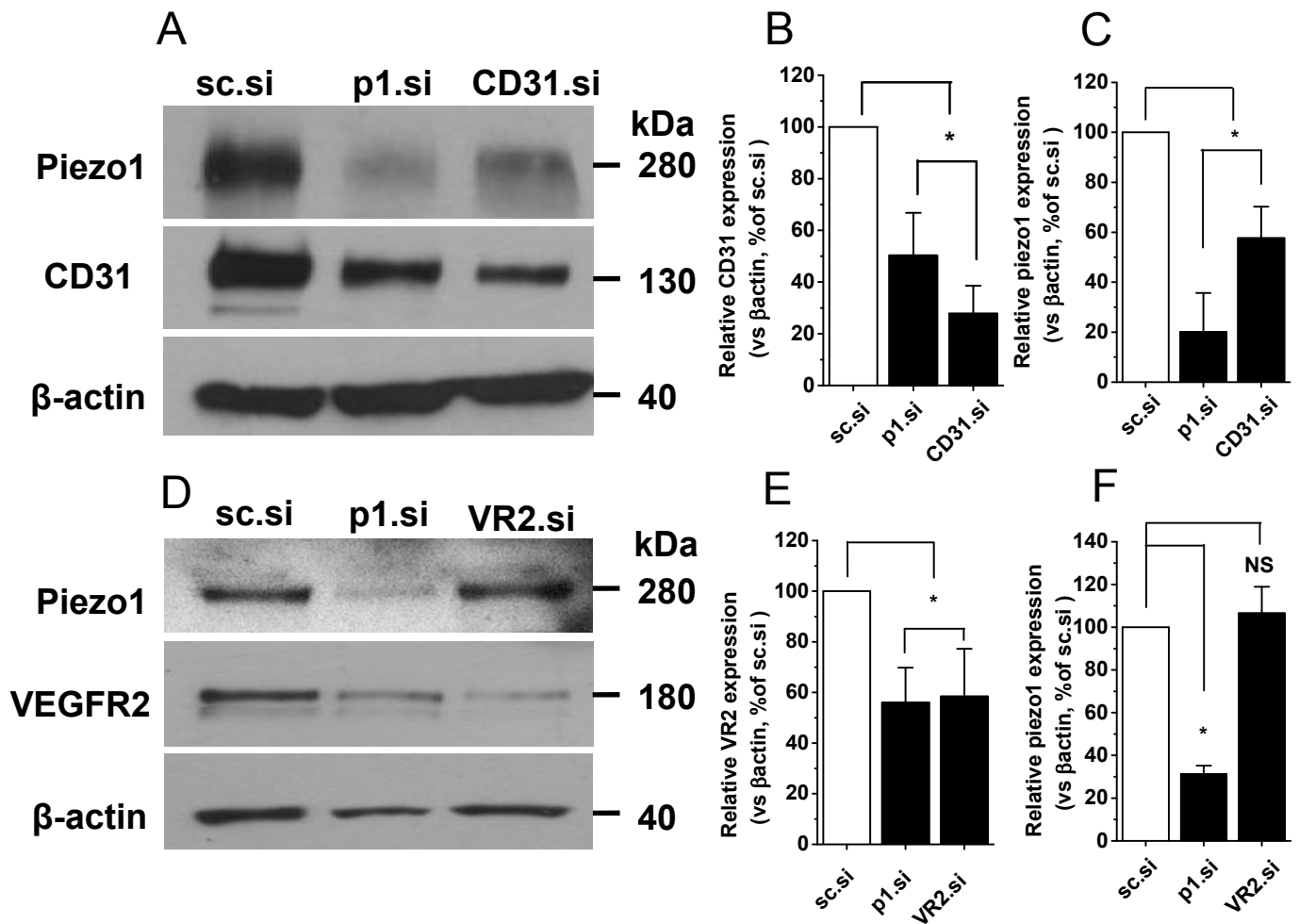
Figure 5.3. Piezo1 and CD31 have mutually dependent expression. (**A-F**) Data from HUVECs. (**A**) Example western blots for Piezo1 (anti-Piezo1 antibody), CD31 (anti-CD31 antibody) and β-actin (anti-β-actin antibody) expressed in HUVECs transfected with control siRNA (sc.si), Piezo1 siRNA (p1.si) or CD31 siRNA (CD31.si). (**B-C**) Mean data for the protein expression levels for the type of experiments shown in (**A**). Total β-actin is used as a loading control. Mean data are normalized to the sc.si control. (**B**) showing CD31; (**C**) showing Piezo1. n=3. (**D**) As (**A**), only the cells were transfected with sc.si, p1.si or VEGFR2 siRNA (VR2.si). (**E-F**) Mean data for the type of experiments shown in (**D**). Total β-actin is used as a loading control. (**E**) showing VEGFR2; (**F**) showing Piezo1. n=3.

5.2.4. Piezo1, CD31 and VEGFR2 have similar functional impact on shear-stress sensing

As suggested in the previous chapter, Piezo1 is important for shear-stress induced Ca^{2+} influx and alignment of endothelial cells. Also knock-down of Piezo1 negatively regulates the expression of CD31 and VEGFR2 expression in HUVECs (Fig. 5.3). Therefore, if Piezo1 cross-talks with the mechanosensory complex and shares the same downstream pathway, knock-down of CD31 or VEGFR2 would have similar impact on shear-stress sensing of endothelial cells as Piezo1 knock-down. To test this hypothesis, Ca^{2+} imaging experiments were carried out in cells exposed to shear stress (as shown in Fig 4.3 and Fig 4.10). HUVECs were transfected with scrambled siRNA, or siRNAs targeting Piezo1, CD31, or VEGFR2 48 hours before seeding onto microfluidic chambers. Incrementing shear stresses were applied on the cells to induce Ca^{2+} signals. HUVECs transfected with siRNAs targeting CD31 or VEGFR2 showed less shear stress-induced Ca^{2+} signal compared with cells transfected with scrambled siRNA, as did the cells lacking Piezo1 (Fig.5.4 A-E). Therefore, knock-down of CD31 or VEGFR2 had the similar inhibiting effect on shear-stress evoked Ca^{2+} signal as Piezo1 knock-down.

Because of the result that flow-induced alignment of endothelial cells is a downstream function of Piezo1 (Chapter 4), the involvement of CD31 and VEGFR2 in shear stress-evoked alignment of HUVECs was also investigated. HUVECs transfected with scrambled siRNA, or siRNAs targeting Piezo1, CD31, or VEGFR2 were cultured under shear stress provided by the orbital shaker. Consistent with Ca^{2+} measurement results, all three siRNAs showed similar inhibitory effects on shear-stress induced endothelial cell alignment (Fig.5.5 A-E). Compared with controls, the inhibition of frequency of cells at the mode was 66%, 50%, and 46% respectively for Piezo1, CD31 and VEGFR2 siRNA (Fig.5.5 A-E).

These data suggested that Piezo1, CD31 and VEGFR2 have similar effect on shear-stress response of endothelial cells, and the proteins might share the same or partially overlapping downstream pathways in shear-stress sensing.
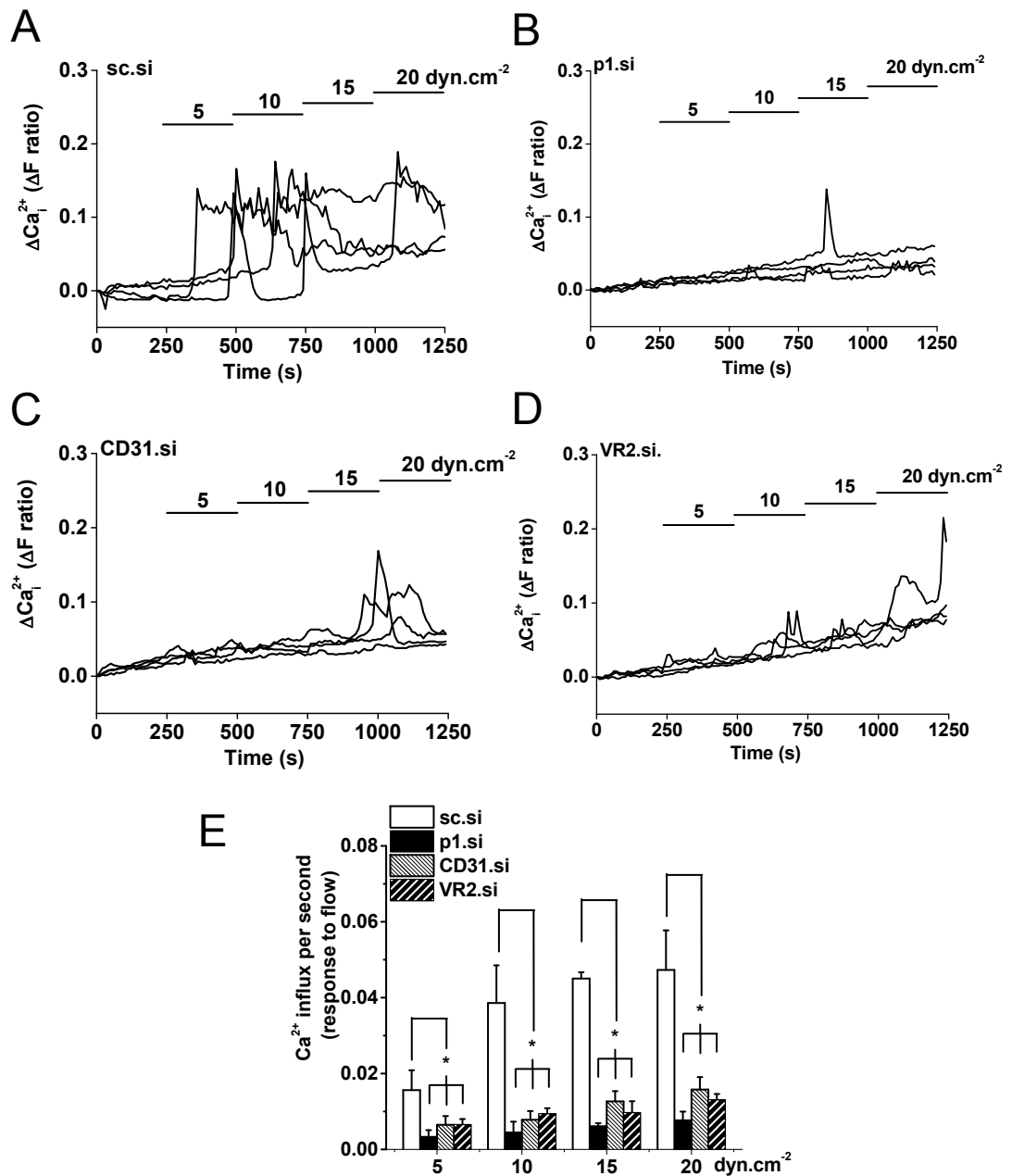
Figure 5.4. Knock-down of Piezo1/CD31/VEGFR2 suppresses shear-stress induced Ca^{2+} entry. (A-E) Data from HUVECs. (**A-D**) Each panel showes 4 example recordings of intracellular Ca^{2+} evoked by shear stress in single cells in the same microfluidic chamber. Cells were transfected with sc.si, Piezo1.si (p1.si), CD31.si or VEGFR2.si (VR2.si). (**E**) Mean data for the type of experiments shown in (**A-D**). n/N=3/30 each.
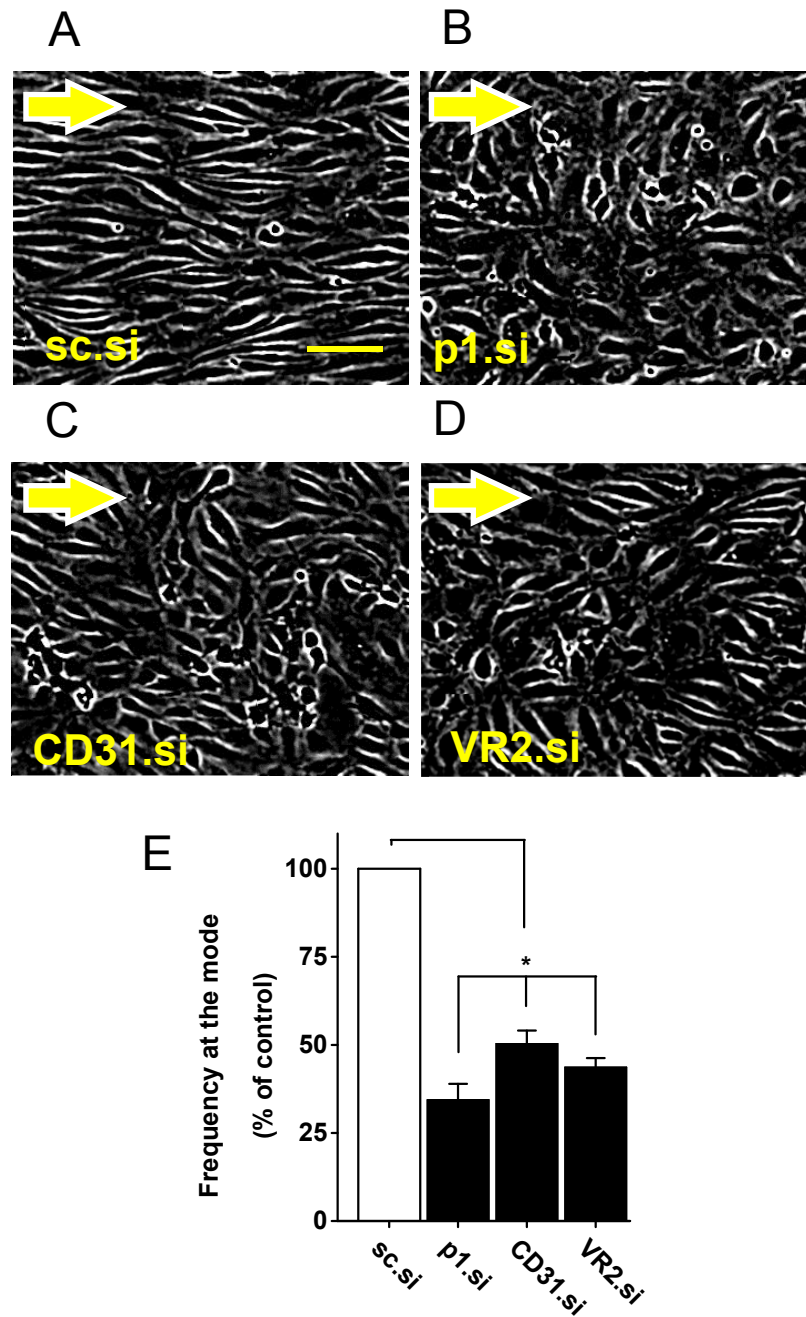
Figure 5.5. Knock-down of Piezo1/CD31/VEGFR2 suppresses shear-stress induced alignment of HUVECs. (**A-D**) Example images of HUVECs transfected with sc.si (**A**), p1.si (**B**), CD31.si(**C**) or VR2.si (**D**). Cells were cultured under shear stress generated by the orbital shaker for 24h. Shown are highlighted cell edges by Difference of Gaussian. The direction of flow is indicated by arrows. Scale bar is 50μm. (**E**) Normalized mean data for the type of experiment exemplified in (**A-E**). Data are normalized to the sc.si. n=3 each.

5.2.5. Endothelial nitric oxide synthase is not involved in shear-stress induced alignment

VEGFR2 was reported to be activated after CD31 sensing shear-stress, and lead to the activation of Akt and production of nitric oxide (Tzima et al., 2005). However, multiple downstream pathways can be activated following the activation of VEGFR2 (Fig.5.6 A). It remains unclear which of these are responsible for shear-stress induced alignment of endothelial cells. Although there is no direct evidence that VEGFR2 is downstream of Piezo1, the data shown above suggests they may have overlapping downstream pathways in shear-stress sensing. As little is known about the downstream pathways of Piezo1, study of downstream pathways of VEGFR2 may help to understand the mechanism of Piezo1. Therefore, the functions of different siRNAs or inhibitors targeting different downstream pathways of VEGFR2 were tested.

Activation of VEGFR2 by VEGF or shear-stress promotes phosphorylation of endothelial nitric oxide synthase (eNOS) and production of NO, which is important for normal endothelial functions (Dimmeler and Andreas, 1999). eNOS activation was shown to be important for Piezo1 dependent cell migration under static condition (Li et al., 2014). HUVECs transfected with eNOS siRNA were cultured under flow generated by the orbital shaker. eNOS siRNA did not show any effect on shear-stress induced alignment of HUVECs compared with scrambled control after cultured under shear stress for 72 hours (Fig.5.6 B). As an independent method for detecting the function of eNOS, HUVECs cultured under flow with or without the presence of non-selective inhibitors of NOS isoforms, L-N^G-monomethyl Arginine citrate (L-NMMA) or L-N^G-Nitroarginine methyl ester (L-NAME), were studied (Chang et al., 1997, De et al., 2000). Cells were incubated with vehicle control, 0.3 mM L-NMMA or 0.1 mM L-NAME in serum free medium for 1 hour before cultured under flow for 72 hours. Like eNOS siRNA, neither L-NMMA nor L-NAME exhibits any effect on shear-stress induced alignment of endothelial cells compared with vehicle controls (Fig.5.6 B). These data suggested eNOS is not involved in endothelial cell alignment induced by shear-stress.

5.2.6. P38 MAPK is not involved in shear-stress induced alignment

It has been reported that p38 MAPK (P38 mitogen-activated protein kinase) is activated by shear stress and/or VEGFR2 and is essential for shear stress-induced angiogenesis (Gee et al., 2010). To test if p38 MAPK is the downstream mechanism of Piezo1, a specific blocker of p38 MAPK pathway, 10 µM SB203580 was used (Barančík et al., 2001). The concentration was recommended by the manufacturer's instruction, which has been show to completely blocked p38 MAPK activation in cardiac fibroblasts (Mir et al., 2012). HUVECs were incubated with vehicle control or 10 µM SB203580 in serum-free medium statically for 1 hour before cultured under flow generated by the orbital shaker for 72h. SB203580 lacked any effect on shear-stress induced alignment compared with the vehicle control (Fig. 5.6 B). The data suggested p38 MAPK is also not a mechanism of endothelial cell alignment to shear-stress.

A
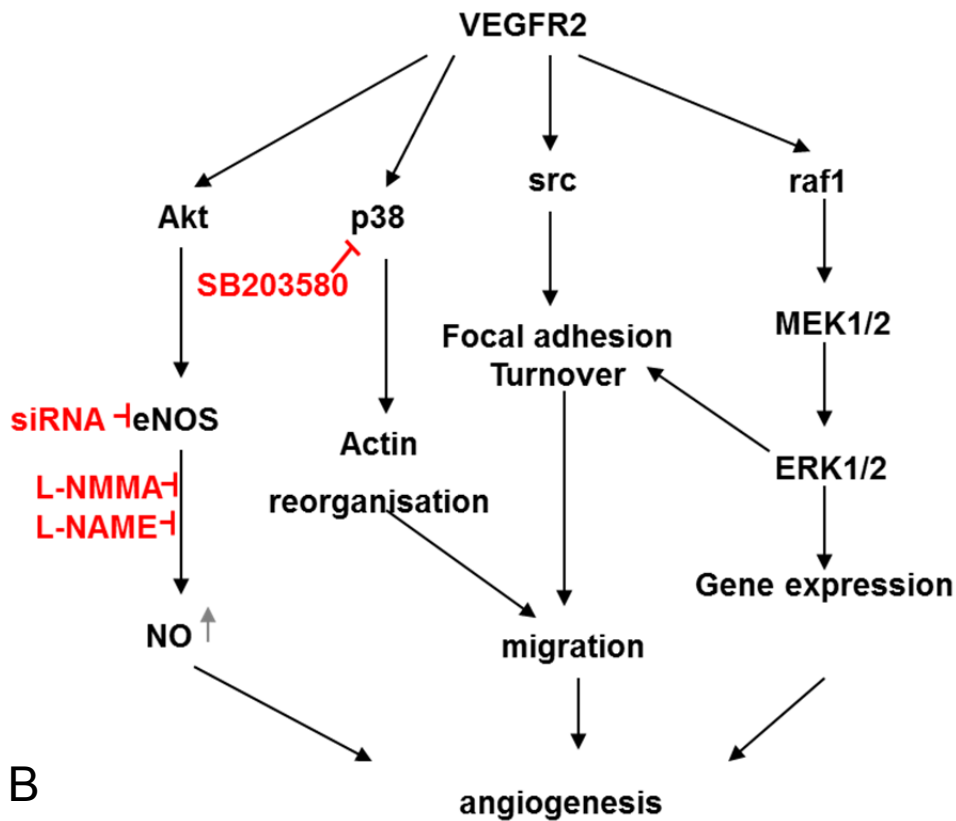
B
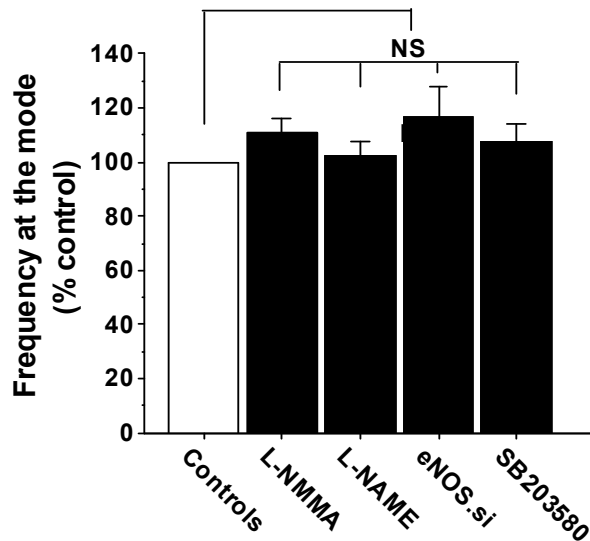
Figure 5.6. Nitric oxide synthase or MAPK/p38 is not a downstream mechanism of shear stress-induced alignment. (**A**) Simplified VEGFR2 signal transduction and targeting site of the inhibitors. Src, Proto-oncogene tyrosine-protein kinase Src; p38, P38 mitogen-activated protein kinases; raf1, proto-oncogene serine/threonine-protein kinase; eNOS, endothelial nitric oxide synthase; MEK1/2, ERK1/2 kinase. (**B**) Frequency of HUVEC alignment induced on the orbital shaker. Data for each test condition were normalized to their own control. Test conditions were 0.3 mM L-NMMA (n=3), 0.1 mM L-NAME (n=3), transfection with eNOS siRNA (eNOS.si, n=4, by Adam Hyman) or 10 µM SB203580 (n=3).

5.2.7. Inhibition of focal adhesion turnover suppresses shear-stress-induced alignment

As shown in the previous section, eNOS and p38 MAPK are not downstream mechanisms of EC alignment to shear stress. Therefore, the involvement of other downstream pathways initiated by VEGFR2 was tested (Fig.5.7 A). The focal adhesion (FA) is one of the downstream pathways of VEGFR2 (Olsson et al., 2006). The FAs are attachment sites comprised of large, dynamic protein complexes between cell and extracellular matrix (ECM) or neighboring cells. Assembly and disassembly of FAs are dynamically regulated and plays key roles during cell migration. Many proteins are implicated in the process, including paxillin, focal adhesion kinase (FAK), Src family kinases, Calpain-2 (Carragher and Frame, 2004). FAK has been reported to be activated by shear stress in endothelial cells (Li et al., 1997), and shear stress induces remodeling FAs for directional migration (Li et al., 2002). Also the activation of VEGFR2 by shear stress was suggested to be Src-dependent (Tzima et al., 2005). Thus, it is hypothesized that FA turnover is the mechanism of endothelial cells alignment to shear stress. To test this hypothesis, HUVECs were treated with inhibitors against focal adhesion turnover or vehicle control for 1 h statically, followed by 72 h-treatment under shear stress generated by the orbital shaker (Fig.5.7 A). All tested inhibitors, including 1 µM PP2 (Src-family kinases inhibitor, Hanke et al., 1996), 1 µM UO126 (MEK inhibitor, Hotokezaka et al., 2002) and 3 µM PD150606 (calpain inhibitor, Wang et al., 1996) suppressed shear stress-induced alignment of HUVECs after 72 h exposure to shear stress (Fig.5.7 B), suggesting focal adhesion turnover is a mechanism of shear stress-induced alignment.
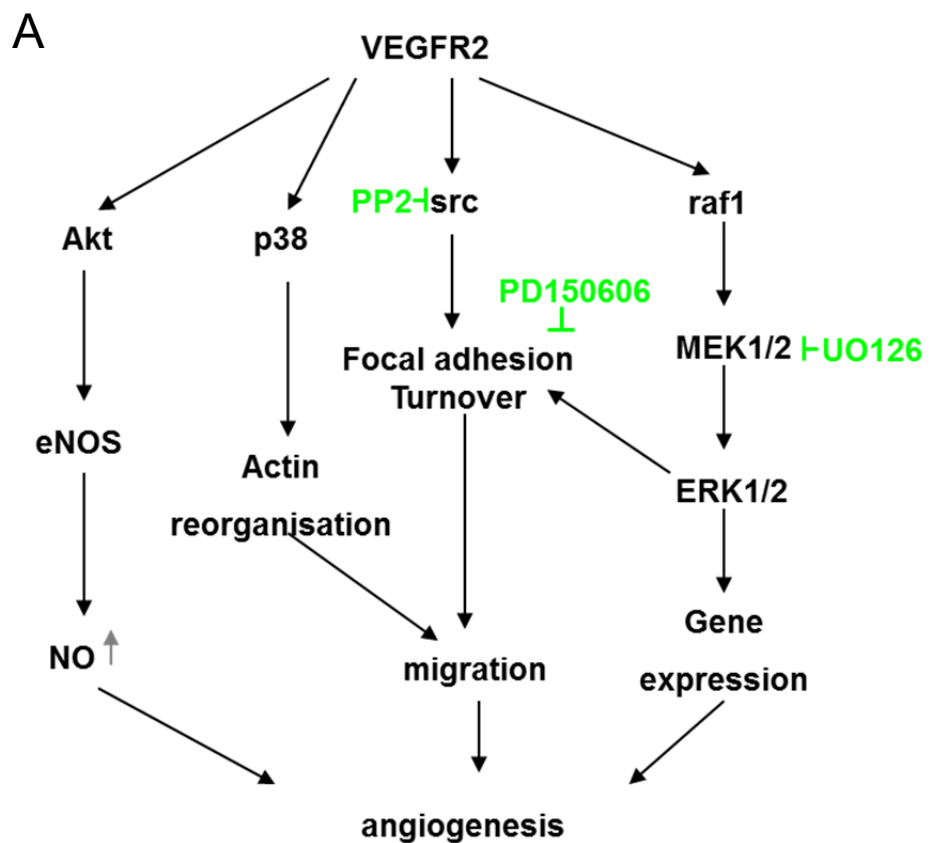
Figure 5.7. Inhibition of Focal adhesion turnover suppresses shear stress-induced alignment. (**A**) Simplified VEGFR2 signal transduction and targeting site of the inhibitors. (**B**) As in Fig.5.6 (**B**), except the test conditions are 1 µM PP2, 1 µM UO126 or 3 µM PD150606, compared with vehicle controls. n=3 each.

5.2.8. Calpain is a downstream mechanism of Piezo1

Piezo1 cross-talks with CD31 and senses shear stress. And its Ca^{2+} channel activity regulates alignment of ECs to flow. The data shown above reveal that blockade of calpain, a Ca^{2+}-activated proteolytic enzyme, suppresses flow-induced alignment of ECs (Fig.5.7B). Unbiased phosphoproteomic study in mouse suggests that Piezo1 depletion causes decrease of the protein abundance of calpain-2 and 11 of its known substrates (Li et al., 2014). Calpain-2 has been reported to be important for focal adhesion turn-over (Lebart and Benyamin, 2006). So it was hypothesized that calpain is a downstream mechanism of Piezo1.

To test this hypothesis, the function of another calpain inhibitor, PD151746, was tested. As calpains are Ca^{2+} activated, the impact of removing extracellular Ca^{2+} was also studied (Wang et al., 1996). Unlike PD150606 used in Fig.5.6, which has equally high selectivity for both calpain-1 and calpain-2 (K_i= 0.21 and 0.37 µM respectively), PD151746 exhibits 20-fold greater selectivity over calpain-1 compared to calpain-2 (K_i=0.26 and 5.33 µM respectively, Wang et al., 1996). Therefore, a higher concentration of PD151746 (20 µM) was used to ensure the inhibition of calpain-2, a concentration that has been showed to completely block oxLDL-induced calpain activity (Porn-Ares et al., 2002). PD145305 is an ineffective analogue of PD151746, and is used as a negative control for PD151746 (Wang et al., 1996). HUVECs were incubated with 3 µM PD150606, 20 µM PD151746, 20 µM PD145305, or vehicle control for 1 hour in serum free medium under static condition. Cells were then cultured under shear stress for 72 hours. To test the function of Ca^{2+}, cells cultured in Ca^{2+}-free Krebs solution were compared with cells under control condition (normal Krebs solution, 1.2mM Ca^{2+}) after 72h exposure to shear stress. The blockade of endothelial cell alignment to shear stress by calpain inhibitors, PD150606, PD151746, or removing extracellular Ca^{2+}, further confirmed the hypothesis that calpain is a mechanism of EC alignment in response to shear stress (Fig.5.8A). In contrary, PD145305 showed little effect on EC alignment (Fig. 5.8A).

Ca^{2+}/calmodulin-dependent protein kinase II is a serine/threonine-specific protein kinase that is regulated by the Ca^{2+}/calmodulin complex. It has been shown to be required for oscillatory shear stress-induced upregulation of endothelial NO production (Cai et al., 2004). Calcineurin is a calcium-dependent serine/threonine phosphatase, and has been reported to be activated by shear stress (Sabine et al., 2012). To test whether the inhibition of EC alignment by Ca^{2+} removal is through these two alternative Ca^{2+}-activated mechanisms, inhibitors of calcineurin (6 µM CN585, Erdmann et al., 2010) and CaMKII (25 µM CK59, Karls and Mynlieff, 2013) were used to treat HUVECs. Compared with vehicle control, these inhibitors had no effect on EC alignment after 72h treatment under flow (Fig. 5.8).

To link calpain activity with Piezo1 channel, Piezo1 channel blocker GsMTx4 was used (Bae et al., 2011). Calpain activity was measured by detection of cleavage of calpain substrate Ac-LLY-AFC. Calpain activity in HUVECs without or with shear stress (orbital shaker) for 15 min was tested. Shear stress significantly increased Calpain activity 3 fold (Li et al., 2014). However, presence of 2.5µM GsMTx4 during the experiment strongly blocked shear stress-evoked calpain activity, bringing it back to that of static conditions (Li et al., 2014). These data suggest calpain is a downstream mechanism of Piezo1 under shear stress.
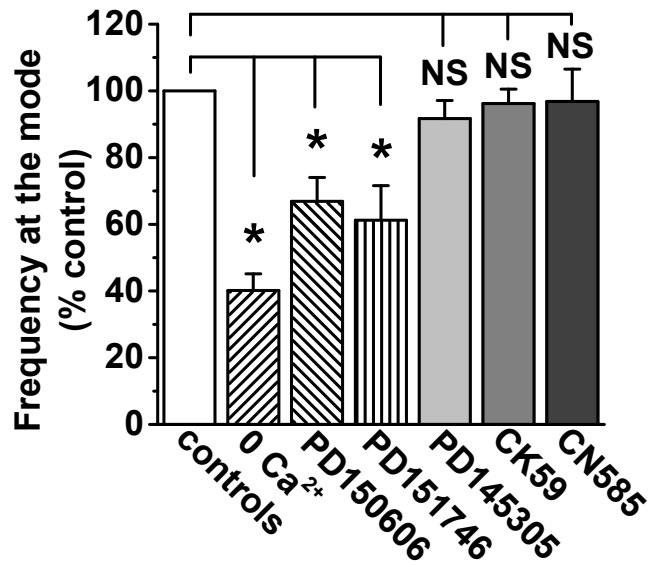
Figure 5.8. Calpain is a downstream mechanism of Piezo1. Frequency of HUVEC alignment (frequency of the cell at the mode) induced on the orbital shaker. Data for each test condition were normalized to their own control. Tested conditions were removal of the extracellular Ca^{2+} (0 Ca^{2+}), 3 μM PD150606, 20 μM PD151746, 20 μM PD145305, 25 μM CK59, 6 μM CN585. Data for PD150606 is the same as that shown in Fig.5.6. n=3 each.

5.2.9. Piezo1 is implicated in focal adhesion turnover

As shown above, calpain is a downstream mechanism of Piezo1 under shear stress. Piezo1 regulates protein abundance of calpain-2 and its substrates (Li et al., 2014). Calpains have been shown to play a key role in focal adhesion assembly and disassembly (Chan et al., 2010, Cortesio et al., 2011, Franco et al., 2004). Therefore, it was hypothesized that Piezo1 is also involved in FAs. Paxillin is a signal transduction adaptor protein targeted to focal adhesions, binding to a diverse range of proteins including structural proteins, regulators of actin organization, or protein tyrosine kinases, such as Src and focal adhesion kinase (FAK) (Turner, 1998). To test the hypothesis, HUVECs over-expressing Piezo1-GFP were labeled with anti-paxillin antibody. Antibody staining revealed puncta-like distribution of endogenous paxillin, which was overlapping with Piezo1-GFP in these puncta (Fig.5.9 A). The Rcoloc was 0.699 for paxilin and Piezo1-GFP (Fig. 5.9 B), suggesting the localizing of Piezo1 to focal adhesions. Focal adhesion assembly and disassembly have been reported to be important for adjustment of ECs to achieve alignment under shear stress (Li et al., 2002). It is shown shear stress caused accumulation of Piezo1-GFP at the leading apical lamellipodia of the cell (Fig.4.13, Fig.5.10). Real-time imaging of the trailing edges of ECs revealed that Piezo1-GFP had a focal adhesion-like localization, which dissolved as shear stress was applied (Fig. 5.10). However, the total abundance of Piezo1-GFP at the trailing edge of the cell did not change on average (Fig.4.13). The data suggest the involvement of Piezo1 in focal adhesion dynamics under shear stress.
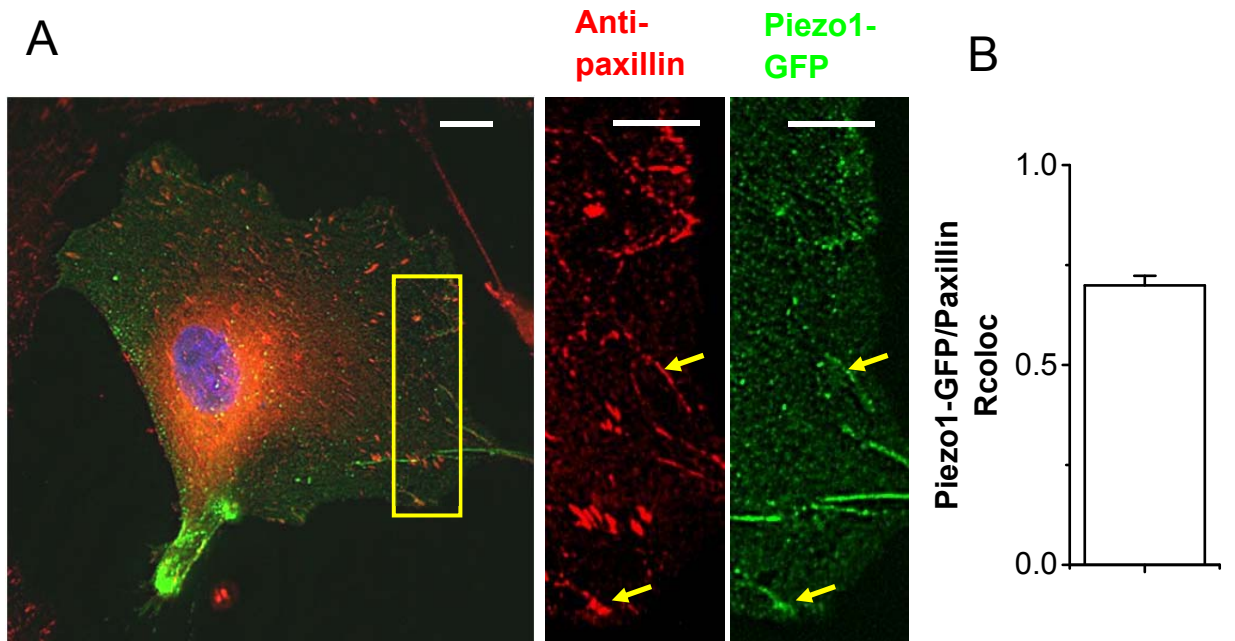
Figure 5.9. Piezo1 co-localizes with paxillin. (**A**) Fluorescent images of HUVECs expressing Piezo1-GFP and labelled with anti-paxillin antibody. Nuclei are labelled blue with DAPI. The selected area is expanded in the middle and right panels. Arrows point to the co-localization of paxillin and Piezo1-GFP. Scale bars are 10 µm. (**B**) Rcoloc of Piezo1-GFP and paxillin for the type of experiments shown in (**A**), n/N=3/12

A
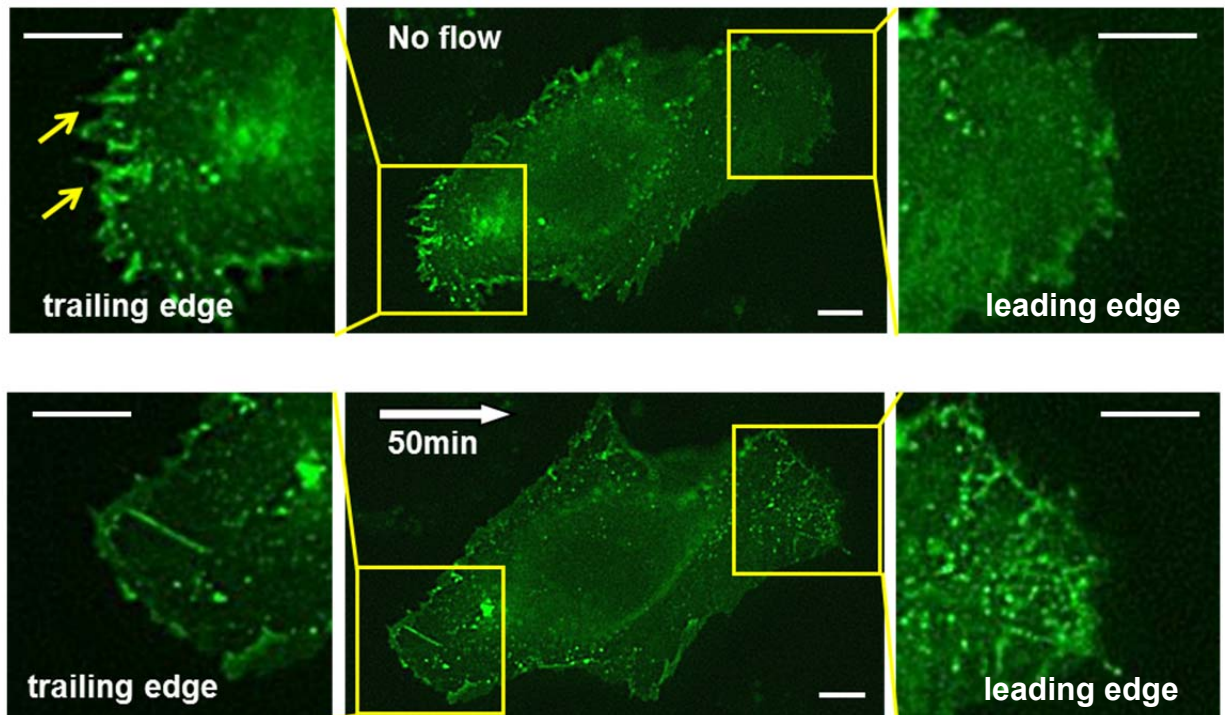
Figure 5.10. Focal adhesion-like localization of Piezo1-GFP dissolves at the trailing edge of the cell as shear stress was applied. Fluorescence images of Piezo1-GFP in HUVEC before (upper image) and after (lower image) applying 15 dyn.cm^{-2} shear stress for 50 min. Selected areas are expanded to show the trailing edge and the leading edge of the cell. The small yellow arrows in the upper image point to focal adhesion structures containing Piezo1-GFP. Large white arrow indicates the direction of the flow. Scale bar, 10 µm. Representative of n=4 out of 8.

5.3. Discussion

The data presented in this chapter suggest cross-talk between Piezo1 and CD31, with focal adhesion as a down-stream mechanism of CD31/VEGFR2/VE-Cadherin complex. Piezo1 participates in this pathway by regulating calpain activity, and enables endothelial cells to align to shear stress.

Piezo1 is suggested to be a direct shear stress sensor in Chapter 4, enabling endothelial cells to align along the direction of shear stress. However, it alone is not sufficient to induce alignment of HEK293 cells to shear stress when over-expressed (Fig.5.1). This suggests Piezo1 might cross-talk with other components in the endothelial cell to achieve alignment. Tzima et al (2005) showed that CD31/VEGFR2/VE-Cadherin was a shear-stress sensory complex at cell-cell junction, which is important for shear stress induced alignment of endothelial cells, similar to Piezo1 in this study. These proteins are not normally expressed in COS-7 cells, but are sufficient to confer mechanosensitive behavior in those cells (Tzima et al., 2005). CD31 was suggested to directly transmit mechanical force (Tzima et al., 2005). The shown co-localization and co-regulation of expression of Piezo1 and CD31 suggest that CD31 may be the cross-talking protein with Piezo1. Furthermore, knock-down of CD31 or VEGFR2 has the similar functional impact on shear-stress response as Piezo1 knock-down, which suggests possible cooperation between Piezo1 and the CD31/VEGFR2/VE-Cadherin complex in shear stress sensing. The effect of co-expression of Piezo1 and these proteins in HEK293 cells need to be further investigated to determine if there is a functional cooperation.

Acute onset of flow triggers the activation of a number of signal transduction pathways, including MAPK/ERK (extracellular signal-regulated kinase), c-JNK(c-Jun N-terminal kinases), PI3-Kinase, Akt, FAK (focal adhesion kinase), Rho Family GTPases, NF-κB (nuclear factor-κB), and protein kinase C (Johnson et al., 2011). Although shear stress-induced activation of Akt and NO production are CD31/VEGFR2/VE-Cadherin complex-dependent (Tzima et al.,

2005, Anto and Yamamoto, 2009), the data in this chapter showed eNOS is not involved in EC alignment to shear stress.

By using inhibitors or siRNAs, several signal transduction pathways were identified to be important for shear stress-evoked alignment of ECs to shear stress, including Src, MEK/ERK, and calpain, all of which have been implicated in regulating focal adhesions (Carragher and Frame, 2004), suggesting focal adhesion may be a mechanism of EC alignment to shear stress. This is consistent with the activation of FAK by shear stress (Li et al., 1997, Zebda et al., 2012). Co-localization of Piezo1 and paxillin, and the focal adhesion-like localization of Piezo1 suggest the involvement of Piezo1 in focal adhesions.

In light of a proteomics study we found that Piezo1 deletion in -/- mouse embryos caused significant down regulation of calpain-2 and 11 of its known substrates (Li et al., 2014). Calpains have been shown to play a key role in focal adhesion assembly and disassembly (Chan et al., 2010, Cortesio et al., 2011, Franco et al., 2004), and to be activated by shear stress (Kang et al., 2011). Calpains are Ca^{2+}-activated proteolytic enzymes, and calpain-2 has been associated with Piezo1 (McHugh et al., 2010). The data in this chapter suggest calpain activity is dependent on Piezo1 activity, and is important for shear stress-evoked alignment of ECs, revealing a novel Piezo1-calpain-FAs-alignment mechanism of shear stress, as summarised in Fig.5.11. It is consistent with the suggested role of calpains in EC alignment to shear stress (Miyazaki et al., 2007). Moreover, an important regulatory protein of calpain-2 (calpain small subunit 1) has been reported to be critical in regulating vascular development in the yolk sac at E10.5 (Arthur et al., 2000), suggesting calpain may be also involved in Piezo1-dependent vessel formation (Li et al., 2014). As Piezo1 cross-talks with CD31, further studies are needed to determine whether calpain activity is CD31/VEGFR2 dependent or not. Calpain inhibitors used in this study are not specific for calpain-2, but also inhibit calpain-1. Furthermore, both calpain-1 and calpain-2 contribute to the calpain activity tested in this study. However, it has been reported that calpain-1 and calpain2 play different roles in focal adhesion turnover (Cortesio et al., 2011). Therefore, it needs to be further

investigated whether or not calpain-1 and calpain-2 play different roles in Piezo1-mediated EC alignment.
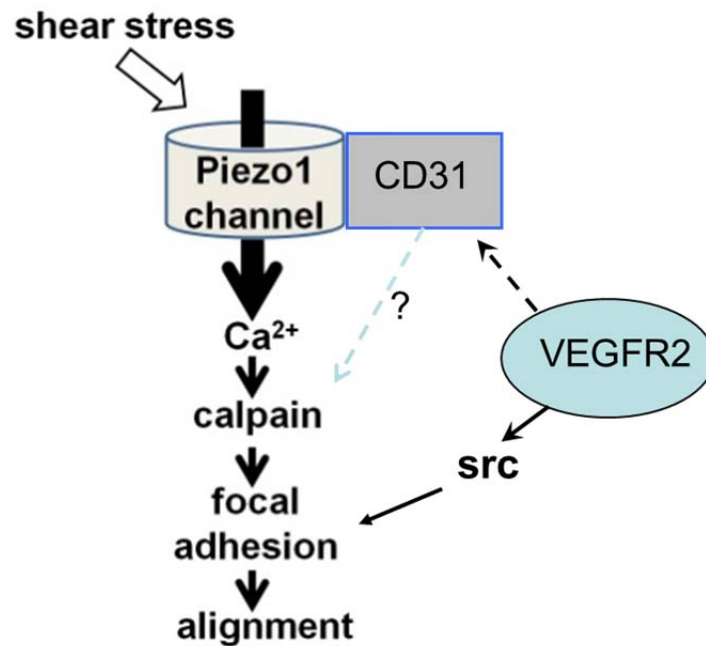
Figure 5.11. Data Interpretation

It has been shown that flow induces ATP release and triggers Ca^{2+} waves at caveolae by activating a shear stress-sensitive ion channel, P2X4 (Yamamoto et al., 2000 & 2011). It is not clear whether flow-evoked Ca^{2+} elevation in HEK293 cells over-expressing Piezo1 is ATP dependent or not. Nevertheless, we performed alignment assay and found apyrase (ATP-diphosphatase) had no effect on endothelial cell alignment, while it abolished the ATP release evoked by shear stress (data not shown, by Adam Hyman and Dr. Melanie Ludlow). The results suggest ATP release is not a mechanism of EC alignment, which is shown to be a major end point of Piezo1 channel activity in the present study.

However, further studies are needed to determine if there is a relationship between Piezo1 and P2X4.

P38/MAPK can be activated by shear stress independently of CD31 in ECs (Sumpio et al., 2005). It was also reported to be activated by FAK in PC12 cells (Wang et al., 2012). However, inhibition of p38/MAPK by a specific blocker, SB203580 has no effect on flow-evoked alignment of ECs (Fig.5.5B). Although the concentration of SB203580 used for this study (10 μM) has been reported to be enough to complete block p38/MAPK activity (Mir et al., 2012), it was still unknown how good the inhibition of p38/MAPK activity was in the present study, which needs to be further investigated. Subconfluent endothelial cells do not align to shear stress, but still show flow-dependent morphology adaption, and migrate selectively in the direction of flow (Masuda and Fujiwara, 1993). As p38/MAPK pathway has been shown to be critical for endothelial cell actin reorganization and migration (Rousseau et al., 1997 & 2000), p38/MAPK might be a mechanism of flow-triggered morphological changes and oriented migration of ECs. This hypothesis and any involvement of Piezo1 remain to be confirmed by experiments.

It has been found that there is also low frequency activity of Piezo1 channels under static condition which has functional implications for endothelial nitric oxide synthase and migration (Li et al., 2014). Furthermore, Piezo1 co-localizes with Paxillin without flow (Fig. 5.10). These data suggest that even in the absence of shear stress, Piezo1 could still be a sensor of mechanical forces as the cells change in morphology and integrate with their physical environment. Although eNOS is not a mechanism of Piezo1-dependent alignment of ECs to shear stress (Fig.5.6), it has been reported to be important for Piezo1-dependent migration of ECs (Li et al., 2014). NO production plays a key role in EC migration and vasodilatation (Li et al., 2014, Ross, 1999). Low NO bioavailability can increase the expression of vascular cell adhesion molecule-1 (VCAM-1), which binds to monocytes and T lymphocytes, initiating invasion of inflammatory cells into the vessel wall in atherogenesis (Khan et al., 1996, Libby et al., 2010). It has been suggested nuclear-localized focal adhesion kinase (FAK) negatively regulates inflammatory VCAM-1 expression (Lim et al., 2012).

Therefore, the functions of Piezo1 under static condition might be atheroprotective.

5.4. Conclusion

The findings of this study suggest cross-talk between Piezo1 and CD31/VE-cadherin/VEGFR2 mechanosensory complex in sensing shear stress, and show calpain protease activity, which regulates focal adhesion turnover, as a downstream mechanism that leads to spatial organization of endothelial cells to the polarity of the applied shear stress.

The findings show a novel mechanism by which vascular endothelial cells could sense shear stress caused by blood flow. Shear stress is a key determinator for vascular function both under physiological and pathological conditions. Therefore, the findings have important implications for understanding vascular physiology and could contribute to developing new therapeutic strategies for calpain- or shear stress-related diseases like sickle cell anaemia, atherosclerosis and cancer.

Chapter 6. Final summary and future work

The overall objective of this thesis was to gain deeper insight into molecular mechanisms of Ca^{2+} regulation in vascular cells. This was achieved using a wide range of biological techniques, such as western blotting, immunostaining, Ca^{2+} measurement, and cell function assays.

High-fat diet and hypercholesterolemia are risk factors for atherosclerosis. In Chapter 3, cholesterol regulation of TRPC homo- and heteromeric channels was investigated. The data suggested that with the presence of TRPC1, cholesterol redistributed TRPC1-TRPC5 heteromeric channels to a GM1-enriched domain and increased the channel activity in response to PGPC. While when TRPC1 was depleted, cholesterol inhibited TRPC5 channel activity by causing caveolin-1-dependent internalization of the channel. PGPC induces a TRPC5-dependent migration of VSMCs (AL-Shawaf et al., 2010). Migrating VSMCs are one of the key contributors to the plaque formation in atherosclerosis. It is also reported VSMC contributes to cholesterol accumulation and macrophage-like cells formation in human atherosclerosis (Allahverdian et al., 2014). Therefore, under high-cholesterol condition, increased TRPC1-TRPC5 heteromeric channel activity might lead to upregulated VSMC migration and atherogenesis, which needs to be confirmed by experiments. However, when TRPC1 was depleted, cholesterol inhibited TRPC5 homomeric channel, which is hypothesized to inhibit VSMC migration and be atheroprotective. Therefore TRPC1 has the ability to protect TRPC5 from cholesterol and caveolin-1 dependent retraction and cause unwanted Ca^{2+} influx. The future challenges are to understand the mechanism by which TRPC1 redistribute the channel to a GM1-enriched fraction, and to block this process, which may lead to the discovery of new drug targets for atherosclerosis (Fig. 6.1).
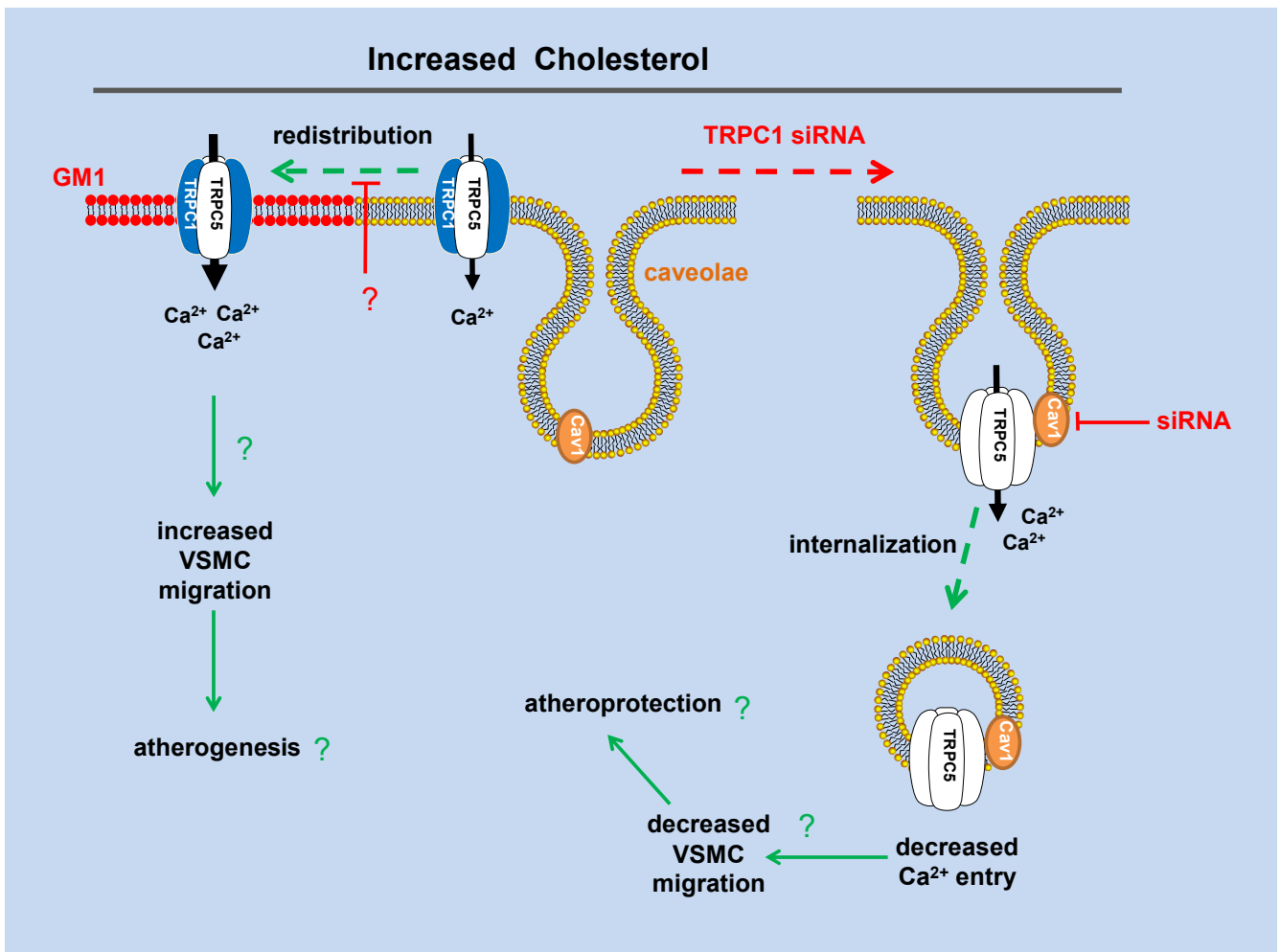
Figure 6.1. Cartoon summarising the data in Chapter 3 and new hypothesis based on the data. Cholesterol causes redistribution of TRPC1-TRPC5 heteromeric channel to a GM1-enriched domain, where the channel function is enhanced. Elevated Ca^{2+} entry thus increases VSMC migration and leads to atherogenesis. Further investigation is needed to generate methods to block the redistribution process, which may lead to the finding of new drug targets for atherosclerosis. When TRPC1 is depleted, cholesterol cholesterol inhibits TRPC5 homomeric channel function by inducing caveolin-1 dependent internalization, which is hypothesized to inhibit VSMC migration and be atheroprotective. The relevance between cholesterol-regulated Ca^{2+} entry and VSMC migration need to be further confirmed by experiments.

Chapter 4 revealed a novel role of Piezo1 as a critical shear stress sensor in endothelial cells. Depletion/disruption of endogenous Piezo1 or applying Piezo1 inhibitors abolished shear stress-evoked Ca^{2+} entry. Consistent with the role as a shear stress sensor, Piezo1 promoted downstream endothelial cell alignment to the direction of physiological shear stress. Shear stress drove Piezo1 to the advancing apex of endothelial cells, suggesting a mechanism in which a reserve pool of Piezo1 supplements an active pool at an apex optimized for sensing and responding to the direction of shear stress. While these data provide evidence that Piezo1 acts as a sensor of shear stress in endothelial cells, they do not exclude other proteins as additional shear stress sensors. A known candidate for shear stress sensing, PC2 (TRPP2) has been reported to be a negative regulator of Piezo1 activity in response to stretch (Peyronnet *et al.,* 2013). Whether Piezo1 cooperated with other ion channels in shear stress sensing requires further study. Under laminar shear stress, which is atheroprotective, Piezo1 promotes downstream endothelial cell alignment to the direction of flow. Piezo1 is therefore hypothesized to maintain the physiological function of ECs under laminar flow and be atheroprotective. As mentioned above, high-cholesterol condition is an important risk factor for atherosclerosis. Disturbed shear stress promotes endothelial dysfunction, induce expression of inflammatory proteins, and create an atheroprone environment (Firasat et al., 2014, Heo et al., 2014). Finding out whether cholesterol and disturbed flow affect Piezo1-dependent shear stress response could greatly help the understanding of the role of Piezo1 in atherosclerosis, which needs to be further investigated.

Chapter 5 revealed the cross-talk between Piezo1 and CD31, with focal adhesion as a down-stream mechanism of CD31/VEGFR2/VE-Cadherin complex. Piezo1 participated in this pathway by regulating calpain activity, and enabled endothelial cells to align to shear stress. It has been reported that there is also low frequency activity of Piezo1 channels under static condition which has functional implications for endothelial nitric oxide synthase and migration (Li et al., 2014). Whether CD31 is involved in these downstream mechanisms, eNOS and calpain, needs to be further studied. As shown in Chapter 5, Piezo1

co-localises with paxillin, an important candidate of focal adhesions. More investigation is required to determine if Piezo1 activity under static condition directly contributes to FAs. The data from Chapter 4 and 5 are summarised in Figure 6.2.

In summary, this research has generated new knowledge and hypotheses about molecular mechanism of Ca^{2+} entry and mechanosensing of vascular cells under physiological and pathological conditions, which may help generate new strategies to treat cardiovascular diseases such as atherosclerosis.
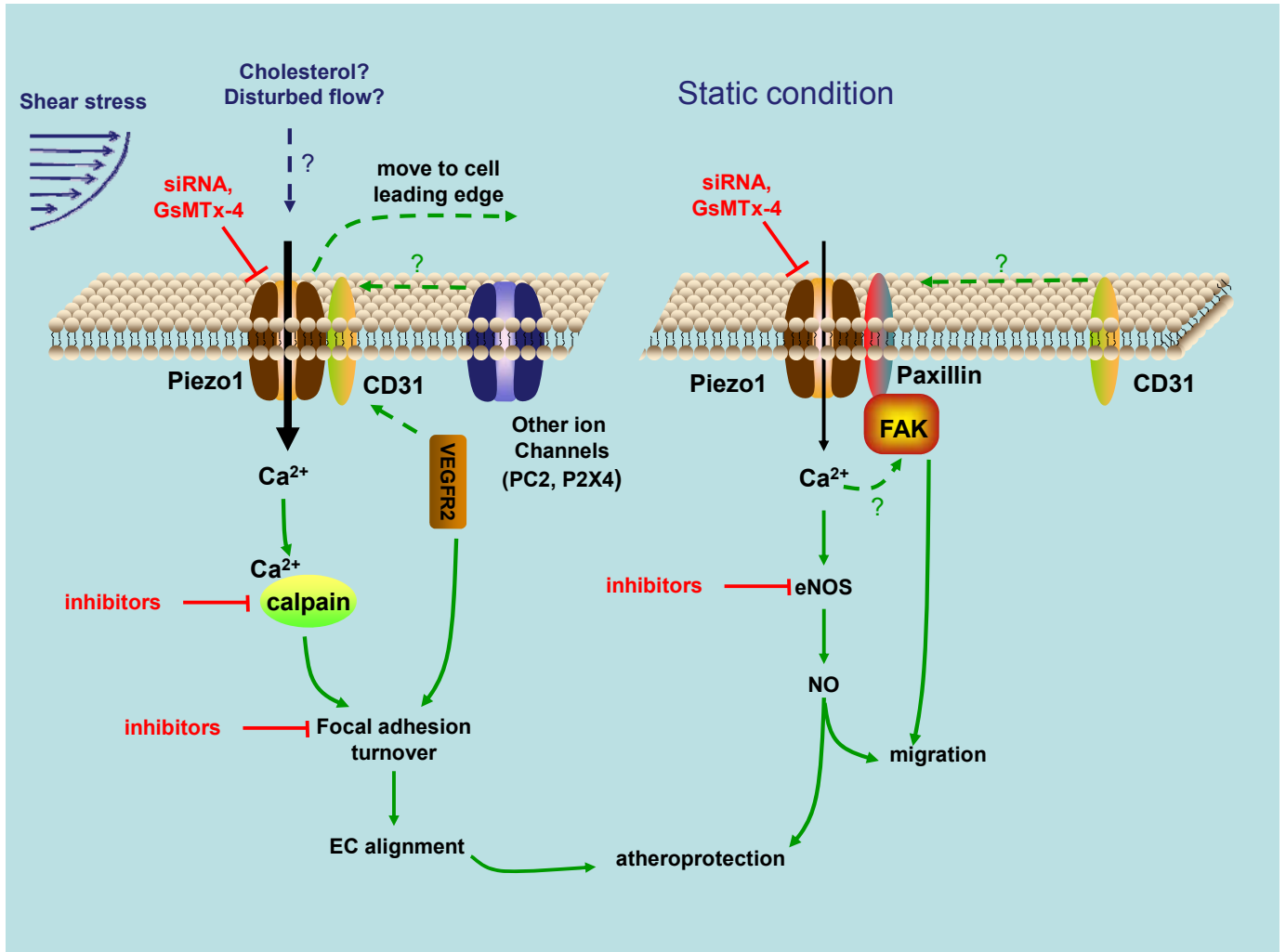
Figure 6.2. Cartoon summarising the data in Chapter 4 and 5, and new hypothesis based on the data. Laminar flow induces Piezo1-dependent Ca^{2+} entry, activates calpain and leads to the EC alignment to shear stress. Under static condition, Piezo1 colocalises with paxillin. Piezo1 activity has functional implications for endothelial nitric oxide synthase and migration. As Piezo1 crosstalks with CD31, the role of CD31 in these processes needs to be further investigated. Also further investigation is needed to understand whether cholesterol and disturbed flow affect Piezo1, and whether Piezo1 has a role in diseases such as atherosclerosis.

References

AbouAlaiwi, W.A., M. Takahashi, B.R. Mell, T.J. Jones, S. Ratnam, R.J. Kolb, and S.M. Nauli. 2009. Ciliary polycystin-2 is a mechanosensitive calcium channel involved in nitric oxide signaling cascades. *Circulation research*. 104:860-869.

Abramowitz, J., A. Aydemir-Koksoy, T. Helgason, S. Jemelka, T. Odebunmi, C.L. Seidel, and J.C. Allen. 2000. Expression of plasma membrane calcium ATPases in phenotypically distinct canine vascular smooth muscle cells. *Journal of molecular and cellular cardiology*. 32:777-789.

Ahmmed, G.U., D. Mehta, S. Vogel, M. Holinstat, B.C. Paria, C. Tiruppathi, and A.B. Malik. 2004. Protein kinase Calpha phosphorylates the TRPC1 channel and regulates store-operated Ca2+ entry in endothelial cells. *The Journal of biological chemistry*. 279:20941-20949.

Al-Shawaf, E., J. Naylor, H. Taylor, K. Riches, C.J. Milligan, D. O'Regan, K.E. Porter, J. Li, and D.J. Beech. 2010. Short-term stimulation of calcium-permeable transient receptor potential canonical 5-containing channels by oxidized phospholipids. *Arteriosclerosis, thrombosis, and vascular biology*. 30:1453-1459.

Albuisson, J., S.E. Murthy, M. Bandell, B. Coste, H. Louis-Dit-Picard, J. Mathur, M. Feneant-Thibault, G. Tertian, J.P. de Jaureguiberry, P.Y. Syfuss, S. Cahalan, L. Garcon, F. Toutain, P. Simon Rohrlich, J. Delaunay, V. Picard, X. Jeunemaitre, and A. Patapoutian. 2013. Dehydrated hereditary stomatocytosis linked to gain-of-function mutations in mechanically activated PIEZO1 ion channels. *Nature communications*. 4:1884.

Alioua, A., R. Lu, Y. Kumar, M. Eghbali, P. Kundu, L. Toro, and E. Stefani. 2008. Slo1 caveolin-binding motif, a mechanism of caveolin-1-Slo1 interaction regulating Slo1 surface expression. *Journal of Biological Chemistry*. 283:4808-4817.

Allahverdian, S., A.C. Chehroudi, B.M. McManus, T. Abraham, and G.A. Francis. 2014. Contribution of intimal smooth muscle cells to cholesterol accumulation and macrophage-like cells in human atherosclerosis. *Circulation*. 129:1551-1559.

Ando, J., and K. Yamamoto. 2009. Vascular mechanobiology: endothelial cell responses to fluid shear stress. *Circulation journal: official journal of the Japanese Circulation Society*. 73:1983-1992.

Ando, J., and K. Yamamoto. 2013. Flow detection and calcium signalling in vascular endothelial cells. *Cardiovascular research*. 99:260-268.

Andolfo, I., S.L. Alper, L. De Franceschi, C. Auriemma, R. Russo, L. De Falco, F. Vallefuoco, M.R. Esposito, D.H. Vandorpe, and B.E. Shmukler. 2013. Multiple clinical forms of dehydrated hereditary stomatocytosis arise from mutations in PIEZO1. *Blood*. 121:3925-3935.

Arthur, J.S.C., J.S. Elce, C. Hegadorn, K. Williams, and P.A. Greer. 2000. Disruption of the murine calpain small subunit gene, Capn4: calpain is essential for embryonic development but not for cell growth and division. *Molecular and cellular biology*. 20:4474-4481.

Bae, C., R. Gnanasambandam, C. Nicolai, F. Sachs, and P.A. Gottlieb. 2013. Xerocytosis is caused by mutations that alter the kinetics of the mechanosensitive channel PIEZO1. *Proceedings of the National Academy of Sciences*. 110:E1162-E1168.

Bae, C., F. Sachs, and P.A. Gottlieb. 2011. The mechanosensitive ion channel Piezo1 is inhibited by the peptide GsMTx4. *Biochemistry*. 50:6295-6300.

Balligand, J.L., O. Feron, and C. Dessy. 2009. eNOS activation by physical forces: from short-term regulation of contraction to chronic remodeling of cardiovascular tissues. *Physiological reviews*. 89:481-534.

Barakat, A.I., E.V. Leaver, P.A. Pappone, and P.F. Davies. 1999. A Flow-Activated Chloride-Selective Membrane Current in Vascular Endothelial Cells. *Circulation research*. 85:820-828.

Barančík, M., V. Boháčová, J. Kvačkajová, S. Hudecová, O.g. Križanová, and A. Breier. 2001. SB203580, a specific inhibitor of p38-MAPK pathway, is a new reversal agent of P-glycoprotein-mediated multidrug resistance. *European Journal of Pharmaceutical Sciences*. 14:29-36.

Barbee, K.A., P.F. Davies, and R. Lal. 1994. Shear stress-induced reorganization of the surface topography of living endothelial cells imaged by atomic force microscopy. *Circulation research*. 74:163-171.

Bastiaanse, E.L., K.M. Höld, and A. Van der Laarse. 1997. The effect of membrane cholesterol content on ion transport processes in plasma membranes. *Cardiovascular research*. 33:272-283.

Bastiani, M., and R.G. Parton. 2010. Caveolae at a glance. *Journal of cell science*. 123:3831-3836.

Beech, D.J. 2005a. Emerging functions of 10 types of TRP cationic channel in vascular smooth muscle. *Clinical and experimental pharmacology & physiology*. 32:597-603.

Beech, D.J. 2005b. TRPC1: store-operated channel and more. *Pflugers Archiv : European journal of physiology*. 451:53-60.

Beech, D.J. 2012. Integration of transient receptor potential canonical channels with lipids. *Acta physiologica*. 204:227-237.

Beech, D.J. 2013. Characteristics of Transient Receptor Potential Canonical Calcium-Permeable Channels and Their Relevance to Vascular Physiology and Disease. *Circulation Journal*. 77:570-579.

Beech, D.J., Y.M. Bahnasi, A.M. Dedman, and E. Al-Shawaf. 2009. TRPC channel lipid specificity and mechanisms of lipid regulation. *Cell calcium*. 45:583-588.

Beech, D.J., K. Muraki, and R. Flemming. 2004. Non-selective cationic channels of smooth muscle and the mammalian homologues of Drosophila TRP. *The Journal of physiology*. 559:685-706.

Bergdahl, A., M.F. Gomez, K. Dreja, S.Z. Xu, M. Adner, D.J. Beech, J. Broman, P. Hellstrand, and K. Sward. 2003. Cholesterol depletion impairs vascular reactivity to endothelin-1 by reducing store-operated Ca2+ entry dependent on TRPC1. *Circulation research*. 93:839-847.

Berridge, M. 1995. Capacitative calcium entry. *Biochem. j*. 312:1-11.

Berridge, M.J. 2002. The endoplasmic reticulum: a multifunctional signaling organelle. *Cell calcium*. 32:235-249.

Berridge, M.J., M.D. Bootman, and H.L. Roderick. 2003. Calcium signalling: dynamics, homeostasis and remodelling. *Nature reviews. Molecular cell biology*. 4:517-529.

Bezzerides, V.J., I.S. Ramsey, S. Kotecha, A. Greka, and D.E. Clapham. 2004. Rapid vesicular translocation and insertion of TRP channels. *Nature cell biology*. 6:709-720.

Birnbaumer, L. 2009. The TRPC Class of ion channels: A critical review of their roles in slow, sustained increases in intracellular Ca2+ concentrations*. *Annual review of pharmacology and toxicology*. 49:395-426.

Blankenberg, S., S. Barbaux, and L. Tiret. 2003. Adhesion molecules and atherosclerosis. *Atherosclerosis*. 170:191-203.

Bobryshev, Y.V. 2006. Monocyte recruitment and foam cell formation in atherosclerosis. *Micron*. 37:208-222.

Bossu, J.L., A. Elhamdani, and A. Feltz. 1992a. Voltage-dependent calcium entry in confluent bovine capillary endothelial cells. *FEBS letters*. 299:239-242.

Bossu, J.L., A. Elhamdani, A. Feltz, F. Tanzi, D. Aunis, and D. Thierse. 1992b. Voltage-gated Ca entry in isolated bovine capillary endothelial cells: evidence of a new type of BAY K 8644-sensitive channel. *Pflugers Archiv : European journal of physiology*. 420:200-207.

Bowman, C.L., P.A. Gottlieb, T.M. Suchyna, Y.K. Murphy, and F. Sachs. 2007. Mechanosensitive ion channels and the peptide inhibitor GsMTx-4: history, properties, mechanisms and pharmacology. *Toxicon*. 49:249-270.

Brailoiu, E., D. Churamani, X. Cai, M.G. Schrlau, G.C. Brailoiu, X. Gao, R. Hooper, M.J. Boulware, N.J. Dun, J.S. Marchant, and S. Patel. 2009. Essential requirement for two-pore channel 1 in NAADP-mediated calcium signaling. *The Journal of cell biology*. 186:201-209.

Brownlow, S.L., A.G. Harper, M.T. Harper, and S.O. Sage. 2004. A role for hTRPC1 and lipid raft domains in store-mediated calcium entry in human platelets. *Cell calcium*. 35:107-113.

Buffelli, M., R.W. Burgess, G. Feng, C.G. Lobe, J.W. Lichtman, and J.R. Sanes. 2003. Genetic evidence that relative synaptic efficacy biases the outcome of synaptic competition. *Nature*. 424:430-434.

Burnstock, G., and V. Ralevic. 2014. Purinergic signaling and blood vessels in health and disease. *Pharmacological reviews*. 66:102-192.

Cahalan, M.D. 2009. STIMulating store-operated Ca(2+) entry. *Nature cell biology*. 11:669-677.

Cai, H., J.S. McNally, M. Weber, and D.G. Harrison. 2004. Oscillatory shear stress upregulation of endothelial nitric oxide synthase requires intracellular hydrogen peroxide and CaMKII. *Journal of molecular and cellular cardiology*. 37:121-125.

Carmeliet, P., M.G. Lampugnani, L. Moons, F. Breviario, V. Compernolle, F. Bono, G. Balconi, R. Spagnuolo, B. Oosthuyse, M. Dewerchin, A. Zanetti, A. Angellilo, V. Mattot, D. Nuyens, E. Lutgens, F. Clotman, M.C. de Ruiter, A. Gittenberger-de Groot, R. Poelmann, F. Lupu, J.M. Herbert, D. Collen, and E. Dejana. 1999. Targeted deficiency or cytosolic truncation of the VE-cadherin gene in mice impairs VEGF-mediated endothelial survival and angiogenesis. *Cell*. 98:147-157.

Carragher, N.O., and M.C. Frame. 2004. Focal adhesion and actin dynamics: a place where kinases and proteases meet to promote invasion. *Trends in cell biology*. 14:241-249.

Catterall, W.A. 2011. Voltage-gated calcium channels. *Cold Spring Harbor perspectives in biology*. 3:a003947.

Chachisvilis, M., Y.L. Zhang, and J.A. Frangos. 2006. G protein-coupled receptors sense fluid shear stress in endothelial cells. *Proceedings of the National Academy of Sciences of the United States of America*. 103:15463-15468.

Chan, K.T., D.A. Bennin, and A. Huttenlocher. 2010. Regulation of adhesion dynamics by calpain-mediated proteolysis of focal adhesion kinase (FAK). *The Journal of biological chemistry*. 285:11418-11426.

Chang, H.Y., C.W. Chen, and T.R. Hsiue. 1997. Comparative effects of l‑NOARG and l‑NAME on basal blood flow and ACh‑induced vasodilatation in rat diaphragmatic microcirculation. *British journal of pharmacology*. 120:326-332.

Chaudhuri, P., S.M. Colles, M. Bhat, D.R. Van Wagoner, L. Birnbaumer, and L.M. Graham. 2008. Elucidation of a TRPC6-TRPC5 channel cascade that restricts endothelial cell movement. *Molecular biology of the cell*. 19:3203-3211.

Chen, K.D., Y.S. Li, M. Kim, S. Li, S. Yuan, S. Chien, and J.Y.J. Shyy. 1999. Mechanotransduction in Response to Shear Stress: ROLES OF RECEPTOR TYROSINE KINASES, INTEGRINS, AND Shc. *Journal of Biological Chemistry*. 274:18393-18400.

Cheng, K.T., X. Liu, H.L. Ong, W. Swaim, and I.S. Ambudkar. 2011. Local Ca(2)+ entry via Orai1 regulates plasma membrane recruitment of TRPC1 and controls cytosolic Ca(2)+ signals required for specific cell functions. *PLoS biology*. 9:e1001025.

Cheng, K.T., H.L. Ong, X. Liu, and I.S. Ambudkar. 2013. Contribution and regulation of TRPC channels in store-operated Ca2+ entry. *Current topics in membranes*. 71:149-179.

Chien, S. 2008. Effects of disturbed flow on endothelial cells. *Ann Biomed Eng*. 36:554-562.

Chiu, J.J., and S. Chien. 2011. Effects of disturbed flow on vascular endothelium: pathophysiological basis and clinical perspectives. *Physiological reviews*. 91:327-387.

Chiu, Y.J., E. McBeath, and K. Fujiwara. 2008. Mechanotransduction in an extracted cell model: Fyn drives stretch- and flow-elicited PECAM-1 phosphorylation. *The Journal of cell biology*. 182:753-763.

Clapham, D.E. 2007. Calcium signaling. *Cell*. 131:1047-1058.

Conway, D., and M.A. Schwartz. 2012. Lessons from the endothelial junctional mechanosensory complex. *F1000 biology reports*. 4:1.

Cortesio, C.L., L.R. Boateng, T.M. Piazza, D.A. Bennin, and A. Huttenlocher. 2011. Calpain-mediated proteolysis of paxillin negatively regulates focal adhesion dynamics and cell migration. *The Journal of biological chemistry*. 286:9998-10006.

Coste, B., J. Mathur, M. Schmidt, T.J. Earley, S. Ranade, M.J. Petrus, A.E. Dubin, and A. Patapoutian. 2010. Piezo1 and Piezo2 are essential components of distinct mechanically activated cation channels. *Science*. 330:55-60.

Coste, B., B. Xiao, J.S. Santos, R. Syeda, J. Grandl, K.S. Spencer, S.E. Kim, M. Schmidt, J. Mathur, and A.E. Dubin. 2012. Piezo proteins are pore-forming subunits of mechanically activated channels. *Nature*. 483:176-181.

Costes, S.V., D. Daelemans, E.H. Cho, Z. Dobbin, G. Pavlakis, and S. Lockett. 2004. Automatic and quantitative measurement of protein-protein colocalization in live cells. *Biophysical journal*. 86:3993-4003.

Dardik, A., L. Chen, J. Frattini, H. Asada, F. Aziz, F.A. Kudo, and B.E. Sumpio. 2005. Differential effects of orbital and laminar shear stress on endothelial cells. *Journal of vascular surgery*. 41:869-880.

Dart, C. 2010. Lipid microdomains and the regulation of ion channel function. *The Journal of physiology*. 588:3169-3178.

Davies, P.F. 1995. Flow-mediated endothelial mechanotransduction. *Physiological reviews*. 75:519-560.

Davies, P.F. 2009. Hemodynamic shear stress and the endothelium in cardiovascular pathophysiology. *Nature clinical practice. Cardiovascular medicine*. 6:16-26.

De, A., L. Pisera, B. Duvilanski, V. Rettori, M. Lasaga, and A. Seilicovich. 2000. Neurokinin A inhibits oxytocin and GABA release from the posterior pituitary by stimulating nitric oxide synthase. *Brain research bulletin*. 53:325-330.

De Villiers, W., and E.J. Smart. 1999. Macrophage scavenger receptors and foam cell formation. *Journal of leukocyte biology*. 66:740-746.

Deanfield, J.E., J.P. Halcox, and T.J. Rabelink. 2007. Endothelial function and dysfunction: testing and clinical relevance. *Circulation*. 115:1285-1295.

dela Paz, N.G., T.E. Walshe, L.L. Leach, M. Saint-Geniez, and P.A. D'Amore. 2012. Role of shear-stress-induced VEGF expression in endothelial cell survival. *Journal of cell science*. 125:831-843.

DeLisser, H.M., M. Christofidou-Solomidou, R.M. Strieter, M.D. Burdick, C.S. Robinson, R.S. Wexler, J.S. Kerr, C. Garlanda, J.R. Merwin, J.A. Madri, and S.M. Albelda. 1997. Involvement of endothelial PECAM-1/CD31 in angiogenesis. *The American journal of pathology*. 151:671-677.

Delmas, P., H. Nomura, X. Li, M. Lakkis, Y. Luo, Y. Segal, J.M. Fernandez-Fernandez, P. Harris, A.M. Frischauf, D.A. Brown, and J. Zhou. 2002. Constitutive activation of G-proteins by polycystin-1 is antagonized by polycystin-2. *The Journal of biological chemistry*. 277:11276-11283.

Deramaudt, T.B., D. Dujardin, A. Hamadi, F. Noulet, K. Kolli, J. De Mey, K. Takeda, and P. Ronde. 2011. FAK phosphorylation at Tyr-925 regulates cross-talk between focal adhesion turnover and cell protrusion. *Molecular biology of the cell*. 22:964-975.

Dickson, E.J., J.G. Duman, M.W. Moody, L. Chen, and B. Hille. 2012. Orai-STIM-mediated Ca2+ release from secretory granules revealed by a targeted Ca2+ and pH probe. *Proceedings of the National Academy of Sciences of the United States of America*. 109:E3539-3548.

Dimmeler, S., I. Fleming, B. Fisslthaler, C. Hermann, R. Busse, and A.M. Zeiher. 1999. Activation of nitric oxide synthase in endothelial cells by Akt-dependent phosphorylation. *Nature*. 399:601-605.

Dimmeler, S., and A.M. Zeiher. 1999. Nitric oxide-an endothelial cell survival factor. *Cell death and differentiation*. 6:964-968.

Ding, R.Q., J. Tsao, H. Chai, D. Mochly-Rosen, and W. Zhou. 2010. Therapeutic potential for protein kinase C inhibitor in vascular restenosis. *Journal of cardiovascular pharmacology and therapeutics*:1074248410382106.

Dragoni, S., U. Laforenza, E. Bonetti, M. Reforgiato, V. Poletto, F. Lodola, C. Bottino, D. Guido, A. Rappa, S. Pareek, M. Tomasello, M.R. Guarrera, M.P. Cinelli, A. Aronica, G. Guerra, G. Barosi, F. Tanzi, V. Rosti, and F. Moccia. 2014. Enhanced expression of Stim, Orai, and TRPC transcripts and proteins in endothelial progenitor cells isolated from patients with primary myelofibrosis. *PloS one*. 9:e91099.

Du, J., X. Ma, B. Shen, Y. Huang, L. Birnbaumer, and X. Yao. 2014. TRPV4, TRPC1, and TRPP2 assemble to form a flow-sensitive heteromeric channel. *FASEB journal : official publication of the Federation of American Societies for Experimental Biology*.

Earley, S., B.J. Waldron, and J.E. Brayden. 2004. Critical role for transient receptor potential channel TRPM4 in myogenic constriction of cerebral arteries. *Circulation research*. 95:922-929.

Eder, P., and K. Groschner. 2008. TRPC3/6/7: Topical aspects of biophysics and pathophysiology. *Channels (Austin, Tex.)*. 2:94-99.

Edwards, J.M., Z.P. Neeb, M.A. Alloosh, X. Long, I.N. Bratz, C.R. Peller, J.P. Byrd, S. Kumar, A.G. Obukhov, and M. Sturek. 2010. Exercise training decreases store-operated Ca2+entry associated with metabolic syndrome and coronary atherosclerosis. *Cardiovascular research*. 85:631-640.

Egginton, S. 2011. In vivo shear stress response. *Biochemical Society transactions*. 39:1633-1638.

Eisenhoffer, G.T., and J. Rosenblatt. 2013. Bringing balance by force: live cell extrusion controls epithelial cell numbers. *Trends in cell biology*. 23:185-192.

Endemann, D.H., and E.L. Schiffrin. 2004. Endothelial dysfunction. *Journal of the American Society of Nephrology : JASN*. 15:1983-1992.

Epshtein, Y., A.P. Chopra, A. Rosenhouse-Dantsker, G.B. Kowalsky, D.E. Logothetis, and I. Levitan. 2009. Identification of a C-terminus domain critical for the sensitivity of Kir2. 1 to cholesterol. *Proceedings of the National Academy of Sciences*. 106:8055-8060.

Erdmann, F., M. Weiwad, S. Kilka, M. Karanik, M. Patzel, R. Baumgrass, J. Liebscher, and G. Fischer. 2010. The novel calcineurin inhibitor CN585 has potent immunosuppressive properties in stimulated human T cells. *The Journal of biological chemistry*. 285:1888-1898.

Ertel, E.A., K.P. Campbell, M.M. Harpold, F. Hofmann, Y. Mori, E. Perez-Reyes, A. Schwartz, T.P. Snutch, T. Tanabe, L. Birnbaumer, R.W. Tsien, and W.A. Catterall. 2000. Nomenclature of voltage-gated calcium channels. *Neuron*. 25:533-535.

Falk, E. 2000. Multiple culprits in acute coronary syndromes: systemic disease calling for systemic treatment. *Italian heart journal : official journal of the Italian Federation of Cardiology*. 1:835-838.

Falk, E. 2006. Pathogenesis of atherosclerosis. *Journal of the American College of Cardiology*. 47:C7-12.

Faxon, D.P., V. Fuster, P. Libby, J.A. Beckman, W.R. Hiatt, R.W. Thompson, J.N. Topper, B.H. Annex, J.H. Rundback, R.P. Fabunmi, R.M. Robertson, J. Loscalzo, and A. American Heart. 2004. Atherosclerotic Vascular Disease Conference: Writing Group III: pathophysiology. *Circulation*. 109:2617-2625.

Fellner, S.K., and W.J. Arendshorst. 2000. Ryanodine receptor and capacitative Ca2+ entry in fresh preglomerular vascular smooth muscle cells. *Kidney international*. 58:1686-1694.

Fernandez, R.A., P. Sundivakkam, K.A. Smith, A.S. Zeifman, A.R. Drennan, and J.X. Yuan. 2012. Pathogenic role of store-operated and receptor-operated ca(2+) channels in pulmonary arterial hypertension. *Journal of signal transduction*. 2012:951497.

Feske, S., Y. Gwack, M. Prakriya, S. Srikanth, S.H. Puppel, B. Tanasa, P.G. Hogan, R.S. Lewis, M. Daly, and A. Rao. 2006. A mutation in Orai1 causes immune deficiency by abrogating CRAC channel function. *Nature*. 441:179-185.

Firasat, S., M. Hecker, L. Binder, and A.R. Asif. 2014. Advances in endothelial shear stress proteomics. *Expert review of proteomics*:1-9.

Florian, J.A., J.R. Kosky, K. Ainslie, Z. Pang, R.O. Dull, and J.M. Tarbell. 2003. Heparan sulfate proteoglycan is a mechanosensor on endothelial cells. *Circulation research*. 93:e136-142.

Fountain, S.J. 2013. Primitive ATP-activated P2X receptors: discovery, function and pharmacology. *Frontiers in cellular neuroscience*. 7:247.

Franco, S.J., M.A. Rodgers, B.J. Perrin, J. Han, D.A. Bennin, D.R. Critchley, and A. Huttenlocher. 2004. Calpain-mediated proteolysis of talin regulates adhesion dynamics. *Nature cell biology*. 6:977-983.

Galkina, E., and K. Ley. 2009. Immune and inflammatory mechanisms of atherosclerosis (*). *Annual review of immunology*. 27:165-197.

Gao, X., L. Wu, and R.G. O'Neil. 2003. Temperature-modulated diversity of TRPV4 channel gating: activation by physical stresses and phorbol ester derivatives through protein kinase C-dependent and -independent pathways. *The Journal of biological chemistry*. 278:27129-27137.

Gee, E., M. Milkiewicz, and T.L. Haas. 2010. p38 MAPK activity is stimulated by vascular endothelial growth factor receptor 2 activation and is essential for shear stress-induced angiogenesis. *Journal of cellular physiology*. 222:120-126.

Gees, M., B. Colsoul, and B. Nilius. 2010. The role of transient receptor potential cation channels in Ca2+ signaling. *Cold Spring Harbor perspectives in biology*. 2:a003962.

Gerthoffer, W.T. 2007. Mechanisms of vascular smooth muscle cell migration. *Circulation research*. 100:607-621.

Gilbert, G., T. Ducret, R. Marthan, J.P. Savineau, and J.F. Quignard. 2014. Stretch-induced Ca2+ signalling in vascular smooth muscle cells depends on Ca2+ store segregation. *Cardiovascular research*. 103:313-323.

Gillespie, P.G., and R.G. Walker. 2001. Molecular basis of mechanosensory transduction. *Nature*. 413:194-202.

Girard, P.R., and R.M. Nerem. 1995. Shear stress modulates endothelial cell morphology and F‑actin organization through the regulation of focal adhesion‑associated proteins. *Journal of cellular physiology*. 163:179-193.

Gomis, A., S. Soriano, C. Belmonte, and F. Viana. 2008. Hypoosmotic- and pressure-induced membrane stretch activate TRPC5 channels. *The Journal of physiology*. 586:5633-5649.

Gonzalez-Perrett, S., K. Kim, C. Ibarra, A.E. Damiano, E. Zotta, M. Batelli, P.C. Harris, I.L. Reisin, M.A. Arnaout, and H.F. Cantiello. 2001. Polycystin-2, the protein mutated in autosomal dominant polycystic kidney disease (ADPKD), is a Ca2+-permeable nonselective cation channel. *Proceedings of the National Academy of Sciences of the United States of America*. 98:1182-1187.

Graham, S., J.P. Yuan, and R. Ma. 2012. Canonical transient receptor potential channels in diabetes. *Experimental biology and medicine*. 237:111-118.

Graziani, A., C. Rosker, S.D. Kohlwein, M.X. Zhu, C. Romanin, W. Sattler, K. Groschner, and M. Poteser. 2006. Cellular cholesterol controls TRPC3 function: evidence from a novel dominant-negative knockdown strategy. *The Biochemical journal*. 396:147-155.

Greka, A., B. Navarro, E. Oancea, A. Duggan, and D.E. Clapham. 2003. TRPC5 is a regulator of hippocampal neurite length and growth cone morphology. *Nature neuroscience.* 6:837-845.

Grynkiewicz, G., M. Poenie, and R.Y. Tsien. 1985. A new generation of Ca2+ indicators with greatly improved fluorescence properties. *The Journal of biological chemistry.* 260:3440-3450.

Guan, J.L. 1997. Role of focal adhesion kinase in integrin signaling. *The international journal of biochemistry & cell biology.* 29:1085-1096.

Gudi, S., I. Huvar, C.R. White, N.L. McKnight, N. Dusserre, G.R. Boss, and J.A. Frangos. 2003. Rapid activation of Ras by fluid flow is mediated by Galpha(q) and Gbetagamma subunits of heterotrimeric G proteins in human endothelial cells. *Arteriosclerosis, thrombosis, and vascular biology.* 23:994-1000.

Gudi, S., J.P. Nolan, and J.A. Frangos. 1998. Modulation of GTPase activity of G proteins by fluid shear stress and phospholipid composition. *Proceedings of the National Academy of Sciences of the United States of America.* 95:2515-2519.

Gudi, S.R.P., C.B. Clark, and J.A. Frangos. 1996. Fluid Flow Rapidly Activates G Proteins in Human Endothelial Cells: Involvement of G Proteins in Mechanochemical Signal Transduction. *Circulation research.* 79:834-839.

Guharay, F., and F. Sachs. 1984. Stretch-activated single ion channel currents in tissue-cultured embryonic chick skeletal muscle. *The Journal of physiology.* 352:685-701.

Guler, A.D., H. Lee, T. Iida, I. Shimizu, M. Tominaga, and M. Caterina. 2002. Heat-evoked activation of the ion channel, TRPV4. *The Journal of neuroscience : the official journal of the Society for Neuroscience.* 22:6408-6414.

Hamilton, S.L., and Serysheva, II. 2009. Ryanodine receptor structure: progress and challenges. *The Journal of biological chemistry.* 284:4047-4051.

Hanke, J.H., J.P. Gardner, R.L. Dow, P.S. Changelian, W.H. Brissette, E.J. Weringer, B.A. Pollok, and P.A. Connelly. 1996. Discovery of a Novel, Potent, and Src Family-selective Tyrosine Kinase Inhibitor: STUDY OF Lck- AND FynT-DEPENDENT T CELL ACTIVATION. *Journal of Biological Chemistry.* 271:695-701.

Hansen, P.B., C.B. Poulsen, S. Walter, N. Marcussen, L.L. Cribbs, O. Skott, and B.L. Jensen. 2011. Functional importance of L- and P/Q-type voltage-gated calcium channels in human renal vasculature. *Hypertension.* 58:464-470.

Hansson, G.K., and A. Hermansson. 2011. The immune system in atherosclerosis. *Nature immunology.* 12:204-212.

Harraz, O.F., and C. Altier. 2014. STIM1-mediated bidirectional regulation of Ca2+ entry through Voltage-Gated Calcium Channels (VGCC) and Calcium-Release Activated Channels (CRAC). *Frontiers in cellular neuroscience.* 8.

Harrington, L.S., R.J. Evans, J. Wray, L. Norling, K.E. Swales, C. Vial, F. Ali, M.J. Carrier, and J.A. Mitchell. 2007. Purinergic 2X1 receptors mediate

endothelial dependent vasodilation to ATP. *Molecular pharmacology*. 72:1132-1136.

Hartmannsgruber, V., W.T. Heyken, M. Kacik, A. Kaistha, I. Grgic, C. Harteneck, W. Liedtke, J. Hoyer, and R. Kohler. 2007. Arterial response to shear stress critically depends on endothelial TRPV4 expression. *PloS one*. 2:e827.

Helmke, B.P., and P.F. Davies. 2002. The Cytoskeleton Under External Fluid Mechanical Forces: Hemodynamic Forces Acting on the Endothelium. *Annals of Biomedical Engineering*. 30:284-296.

Henrion, D., F. Terzi, K. Matrougui, M. Duriez, C.M. Boulanger, E. Colucci-Guyon, C. Babinet, P. Briand, G. Friedlander, P. Poitevin, and B.I. Levy. 1997. Impaired flow-induced dilation in mesenteric resistance arteries from mice lacking vimentin. *The Journal of clinical investigation*. 100:2909-2914.

Heo, D.K., W.Y. Chung, H.W. Park, J.P. Yuan, M.G. Lee, and J.Y. Kim. 2012. Opposite regulatory effects of TRPC1 and TRPC5 on neurite outgrowth in PC12 cells. *Cellular signalling*. 24:899-906.

Heo, K.S., K. Fujiwara, and J. Abe. 2014. Shear stress and atherosclerosis. *Molecules and cells*. 37:435-440.

Hofmann, T., M. Schaefer, G. Schultz, and T. Gudermann. 2002. Subunit composition of mammalian transient receptor potential channels in living cells. *Proceedings of the National Academy of Sciences of the United States of America*. 99:7461-7466.

Hotokezaka, H., E. Sakai, K. Kanaoka, K. Saito, K. Matsuo, H. Kitaura, N. Yoshida, and K. Nakayama. 2002. U0126 and PD98059, specific inhibitors of MEK, accelerate differentiation of RAW264.7 cells into osteoclast-like cells. *The Journal of biological chemistry*. 277:47366-47372.

Hou, X.Y., G.Y. Zhang, J.Z. Yan, M. Chen, and Y. Liu. 2002. Activation of NMDA receptors and L-type voltage-gated calcium channels mediates enhanced formation of Fyn-PSD95-NR2A complex after transient brain ischemia. *Brain research*. 955:123-132.

Huber, T.B., B. Schermer, R.U. Müller, M. Höhne, M. Bartram, A. Calixto, H. Hagmann, C. Reinhardt, F. Koos, and K. Kunzelmann. 2006. Podocin and MEC-2 bind cholesterol to regulate the activity of associated ion channels. *Proceedings of the National Academy of Sciences*. 103:17079-17086.

Huttenlocher, A., S.P. Palecek, Q. Lu, W. Zhang, R.L. Mellgren, D.A. Lauffenburger, M.H. Ginsberg, and A.F. Horwitz. 1997. Regulation of Cell Migration by the Calcium-dependent Protease Calpain. *Journal of Biological Chemistry*. 272:32719-32722.

Ikonen, E. 2008. Cellular cholesterol trafficking and compartmentalization. *Nature Reviews Molecular Cell Biology*. 9:125-138.

Imberti, B., M. Morigi, C. Zoja, S. Angioletti, M. Abbate, A. Remuzzi, and G. Remuzzi. 2000. Shear stress-induced cytoskeleton rearrangement

mediates NF-kappaB-dependent endothelial expression of ICAM-1. *Microvascular research.* 60:182-188.

Jeong, W., J. Kim, F.W. Bazer, and G. Song. 2014. Stimulatory Effect of Vascular Endothelial Growth Factor on Proliferation and Migration of Porcine Trophectoderm Cells and Their Regulation by the Phosphatidylinositol-3-Kinase-AKT and Mitogen-Activated Protein Kinase Cell Signaling Pathways. *Biology of reproduction.* 90:50.

Jernigan, N.L., L.M. Herbert, B.R. Walker, and T.C. Resta. 2012. Chronic hypoxia upregulates pulmonary arterial ASIC1: a novel mechanism of enhanced store-operated Ca2+ entry and receptor-dependent vasoconstriction. *American journal of physiology. Cell physiology.* 302:C931-940.

Jernigan, N.L., and T.C. Resta. 2014. Calcium homeostasis and sensitization in pulmonary arterial smooth muscle. *Microcirculation.* 21:259-271.

Jiang, L.H., N. Gamper, and D.J. Beech. 2011. Properties and therapeutic potential of transient receptor potential channels with putative roles in adversity: focus on TRPC5, TRPM2 and TRPA1. *Current drug targets.* 12:724-736.

Jiao, J., V. Garg, B. Yang, T.S. Elton, and K. Hu. 2008. Protein kinase C-epsilon induces caveolin-dependent internalization of vascular adenosine 5'-triphosphate-sensitive K+ channels. *Hypertension.* 52:499-506.

Jo, H., K. Sipos, Y.M. Go, R. Law, J. Rong, and J.M. McDonald. 1997. Differential Effect of Shear Stress on Extracellular Signal-regulated Kinase and N-terminal Jun Kinase in Endothelial Cells: Gi2- AND G / -DEPENDENT SIGNALING PATHWAYS. *Journal of Biological Chemistry.* 272:1395-1401.

Johnson, B.D., K.J. Mather, and J.P. Wallace. 2011. Mechanotransduction of shear in the endothelium: basic studies and clinical implications. *Vascular medicine.* 16:365-377.

Jung, S., A. Muhle, M. Schaefer, R. Strotmann, G. Schultz, and T.D. Plant. 2003. Lanthanides potentiate TRPC5 currents by an action at extracellular sites close to the pore mouth. *The Journal of biological chemistry.* 278:3562-3571.

Kalapesi, F.B., J.C. Tan, and M.T. Coroneo. 2005. Stretch-activated channels: a mini-review. Are stretch-activated channels an ocular barometer? *Clinical & experimental ophthalmology.* 33:210-217.

Kang, H., H.I. Kwak, R. Kaunas, and K.J. Bayless. 2011. Fluid shear stress and sphingosine 1-phosphate activate calpain to promote membrane type 1 matrix metalloproteinase (MT1-MMP) membrane translocation and endothelial invasion into three-dimensional collagen matrices. *The Journal of biological chemistry.* 286:42017-42026.

Kanki, H., M. Kinoshita, A. Akaike, M. Satoh, Y. Mori, and S. Kaneko. 2001. Activation of inositol 1,4,5-trisphosphate receptor is essential for the opening of mouse TRP5 channels. *Molecular pharmacology.* 60:989-998.

Kannan, K.B., D. Barlos, and C.J. Hauser. 2007. Free cholesterol alters lipid raft structure and function regulating neutrophil Ca2+ entry and respiratory

burst: correlations with calcium channel raft trafficking. *The Journal of Immunology*. 178:5253-5261.

Karls, A.S., and M. Mynlieff. 2013. Nonspecific, reversible inhibition of voltage-gated calcium channels by CaMKII inhibitor CK59. *Cellular and molecular neurobiology*. 33:723-729.

Kelly, R.F., and H.M. Snow. 2007. Characteristics of the response of the iliac artery to wall shear stress in the anaesthetized pig. *The Journal of physiology*. 582:731-743.

Khan, B.V., D.G. Harrison, M.T. Olbrych, R.W. Alexander, and R.M. Medford. 1996. Nitric oxide regulates vascular cell adhesion molecule 1 gene expression and redox-sensitive transcriptional events in human vascular endothelial cells. *Proceedings of the National Academy of Sciences of the United States of America*. 93:9114-9119.

Khazaei, M., F. Moien-Afshari, and I. Laher. 2008. Vascular endothelial function in health and diseases. *Pathophysiology : the official journal of the International Society for Pathophysiology / ISP*. 15:49-67.

Kim, S.E., B. Coste, A. Chadha, B. Cook, and A. Patapoutian. 2012. The role of Drosophila Piezo in mechanical nociception. *Nature*. 483:209-212.

Knudsen, H.L., and J.A. Frangos. 1997. Role of cytoskeleton in shear stress-induced endothelial nitric oxide production. H347-H355 pp.

Kohler, R., W.T. Heyken, P. Heinau, R. Schubert, H. Si, M. Kacik, C. Busch, I. Grgic, T. Maier, and J. Hoyer. 2006. Evidence for a functional role of endothelial transient receptor potential V4 in shear stress-induced vasodilatation. *Arteriosclerosis, thrombosis, and vascular biology*. 26:1495-1502.

Kumar, B., K. Dreja, S.S. Shah, A. Cheong, S.Z. Xu, P. Sukumar, J. Naylor, A. Forte, M. Cipollaro, D. McHugh, P.A. Kingston, A.M. Heagerty, C.M. Munsch, A. Bergdahl, A. Hultgardh-Nilsson, M.F. Gomez, K.E. Porter, P. Hellstrand, and D.J. Beech. 2006. Upregulated TRPC1 channel in vascular injury in vivo and its role in human neointimal hyperplasia. *Circulation research*. 98:557-563.

Kumar, S., S. Chakraborty, C. Barbosa, T. Brustovetsky, N. Brustovetsky, and A.G. Obukhov. 2012. Mechanisms controlling neurite outgrowth in a pheochromocytoma cell line: the role of TRPC channels. *Journal of cellular physiology*. 227:1408-1419.

Kwon, H.S., M.-J. Kim, H.J. Jeong, M.S. Yang, K.H. Park, T.-S. Jeong, and W.S. Lee. 2008. Low-density lipoprotein (LDL)-antioxidant lignans from< i> Myristica fragrans</i> seeds. *Bioorganic & medicinal chemistry letters*. 18:194-198.

Lamalice, L., F. Houle, and J. Huot. 2006. Phosphorylation of Tyr1214 within VEGFR-2 triggers the recruitment of Nck and activation of Fyn leading to SAPK2/p38 activation and endothelial cell migration in response to VEGF. *The Journal of biological chemistry*. 281:34009-34020.

Langille, B.L., and S.L. Adamson. 1981. Relationship between blood flow direction and endothelial cell orientation at arterial branch sites in rabbits and mice. *Circulation research*. 48:481-488.

Le Boeuf, F., F. Houle, and J. Huot. 2004. Regulation of vascular endothelial growth factor receptor 2-mediated phosphorylation of focal adhesion kinase by heat shock protein 90 and Src kinase activities. *The Journal of biological chemistry*. 279:39175-39185.

le Duc, Q., Q. Shi, I. Blonk, A. Sonnenberg, N. Wang, D. Leckband, and J. de Rooij. 2010. Vinculin potentiates E-cadherin mechanosensing and is recruited to actin-anchored sites within adherens junctions in a myosin II–dependent manner. *The Journal of cell biology*. 189:1107-1115.

Lebart, M.C., and Y. Benyamin. 2006. Calpain involvement in the remodeling of cytoskeletal anchorage complexes. *The FEBS journal*. 273:3415-3426.

Lee, S.Y., and R. MacKinnon. 2004. A membrane-access mechanism of ion channel inhibition by voltage sensor toxins from spider venom. *Nature*. 430:232-235.

Levesque, M., and R. Nerem. 1985. The elongation and orientation of cultured endothelial cells in response to shear stress. *Journal of biomechanical engineering*. 107:341-347.

Levitan, I., Y. Fang, A. Rosenhouse-Dantsker, and V. Romanenko. 2010. Cholesterol and ion channels. *Sub-cellular biochemistry*. 51:509-549.

Lewis, R.S. 2011. Store-operated calcium channels: new perspectives on mechanism and function. *Cold Spring Harbor perspectives in biology*. 3.

Li, J., R.M. Cubbon, L.A. Wilson, M.S. Amer, L. McKeown, B. Hou, Y. Majeed, S. Tumova, V.A. Seymour, H. Taylor, M. Stacey, D. O'Regan, R. Foster, K.E. Porter, M.T. Kearney, and D.J. Beech. 2011. Orai1 and CRAC channel dependence of VEGF-activated Ca2+ entry and endothelial tube formation. *Circulation research*. 108:1190-1198.

Li, J., B. Hou, S. Tumova, K. Muraki, A. Bruns, M.J. Ludlow, A. Sedo, A.J. Hyman, L. McKeown, R.S. Young, N.Y. Yuldasheva, Y. Majeed, L.A. Wilson, B. Rode, M.A. Bailey, H.R. Kim, Z. Fu, D.A. Carter, J. Bilton, H. Imrie, P. Ajuh, T.N. Dear, R.M. Cubbon, M.T. Kearney, R.K. Prasad, P.C. Evans, J.F. Ainscough, and D.J. Beech. 2014. Piezo1 integration of vascular architecture with physiological force. *Nature*.

Li, J., P. Sukumar, C.J. Milligan, B. Kumar, Z.Y. Ma, C.M. Munsch, L.H. Jiang, K.E. Porter, and D.J. Beech. 2008. Interactions, functions, and independence of plasma membrane STIM1 and TRPC1 in vascular smooth muscle cells. *Circulation research*. 103:e97-104.

Li, S., P. Butler, Y. Wang, Y. Hu, D.C. Han, S. Usami, J.L. Guan, and S. Chien. 2002. The role of the dynamics of focal adhesion kinase in the mechanotaxis of endothelial cells. *Proceedings of the National Academy of Sciences of the United States of America*. 99:3546-3551.

Li, S., M. Kim, Y.L. Hu, S. Jalali, D.D. Schlaepfer, T. Hunter, S. Chien, and J.Y.J. Shyy. 1997. Fluid Shear Stress Activation of Focal Adhesion Kinase: LINKING TO MITOGEN-ACTIVATED PROTEIN KINASES. *Journal of Biological Chemistry*. 272:30455-30462.

Libby, P., Y. Okamoto, V.Z. Rocha, and E. Folco. 2010. Inflammation in Atherosclerosis. *Circulation Journal*. 74:213-220.

Lim, S.T., N.L. Miller, X.L. Chen, I. Tancioni, C.T. Walsh, C. Lawson, S. Uryu, S.M. Weis, D.A. Cheresh, and D.D. Schlaepfer. 2012. Nuclear-localized focal adhesion kinase regulates inflammatory VCAM-1 expression. *The Journal of cell biology*. 197:907-919.

Lin, M.J., G.P. Leung, W.M. Zhang, X.R. Yang, K.P. Yip, C.M. Tse, and J.S. Sham. 2004. Chronic hypoxia-induced upregulation of store-operated and receptor-operated Ca2+ channels in pulmonary arterial smooth muscle cells: a novel mechanism of hypoxic pulmonary hypertension. *Circulation research*. 95:496-505.

Lin, S. 2000. Sustained Endothelial Nitric-oxide Synthase Activation Requires Capacitative Ca2+ Entry. *Journal of Biological Chemistry*. 275:17979-17985.

Liou, J., M.L. Kim, W.D. Heo, J.T. Jones, J.W. Myers, J.E. Ferrell, Jr., and T. Meyer. 2005. STIM is a Ca2+ sensor essential for Ca2+-store-depletion-triggered Ca2+ influx. *Current biology : CB*. 15:1235-1241.

Liu, C.L., Y. Huang, C.Y. Ngai, Y.K. Leung, and X.Q. Yao. 2006. TRPC3 is involved in flow- and bradykinin-induced vasodilation in rat small mesenteric arteries. *Acta pharmacologica Sinica*. 27:981-990.

Liu, X., B.B. Singh, and I.S. Ambudkar. 2003. TRPC1 is required for functional store-operated Ca2+ channels. Role of acidic amino acid residues in the S5-S6 region. *The Journal of biological chemistry*. 278:11337-11343.

Loukotova, J., J. Kunes, and J. Zicha. 1998. Cytosolic free calcium response to angiotensin II in aortic VSMC isolated from male and female SHR. *Physiological research / Academia Scientiarum Bohemoslovaca*. 47:507-510.

Lundy, A., N. Lutfi, and C. Beckey. 2009. Review of nifedipine GITS in the treatment of high risk patients with coronary artery disease and hypertension. *Vascular health and risk management*. 5:429-440.

Lusis, A.J. 2000. Atherosclerosis. *Nature*. 407:233-241.

Majeed, Y., Y. Bahnasi, V.A. Seymour, L.A. Wilson, C.J. Milligan, A.K. Agarwal, P. Sukumar, J. Naylor, and D.J. Beech. 2011. Rapid and contrasting effects of rosiglitazone on transient receptor potential TRPM3 and TRPC5 channels. *Molecular pharmacology*. 79:1023-1030.

Marin, J., A. Encabo, A. Briones, E.C. Garcia-Cohen, and M.J. Alonso. 1999. Mechanisms involved in the cellular calcium homeostasis in vascular smooth muscle: calcium pumps. *Life sciences*. 64:279-303.

Maroto, R., A. Raso, T.G. Wood, A. Kurosky, B. Martinac, and O.P. Hamill. 2005. TRPC1 forms the stretch-activated cation channel in vertebrate cells. *Nature cell biology*. 7:179-185.

Masuda, M., and K. Fujiwara. 1993. Morphological responses of single endothelial cells exposed to physiological levels of fluid shear stress. *Frontiers of medical and biological engineering : the international journal of the Japan Society of Medical Electronics and Biological Engineering*. 5:79-87.

Mathers, C.D., and D. Loncar. 2006. Projections of global mortality and burden of disease from 2002 to 2030. *PLoS medicine*. 3:e442.

Maxfield, F.R., and I. Tabas. 2005. Role of cholesterol and lipid organization in disease. *Nature*. 438:612-621.

McFadzean, I., and A. Gibson. 2002. The developing relationship between receptor-operated and store-operated calcium channels in smooth muscle. *British journal of pharmacology*. 135:1-13.

McHugh, B.J., R. Buttery, Y. Lad, S. Banks, C. Haslett, and T. Sethi. 2010. Integrin activation by Fam38A uses a novel mechanism of R-Ras targeting to the endoplasmic reticulum. *Journal of cell science*. 123:51-61.

Mestas, J., and K. Ley. 2008. Monocyte-endothelial cell interactions in the development of atherosclerosis. *Trends in cardiovascular medicine*. 18:228-232.

Mir, S.A., A. Chatterjee, A. Mitra, K. Pathak, S.K. Mahata, and S. Sarkar. 2012. Inhibition of signal transducer and activator of transcription 3 (STAT3) attenuates interleukin-6 (IL-6)-induced collagen synthesis and resultant hypertrophy in rat heart. *The Journal of biological chemistry*. 287:2666-2677.

Miyamoto, T., T. Mochizuki, H. Nakagomi, S. Kira, M. Watanabe, Y. Takayama, Y. Suzuki, S. Koizumi, M. Takeda, and M. Tominaga. 2014. Functional role for Piezo1 in stretch-evoked Ca(2)(+) influx and ATP release in urothelial cell cultures. *The Journal of biological chemistry*. 289:16565-16575.

Miyazaki, T., K. Honda, and H. Ohata. 2007. Requirement of Ca2+ influx- and phosphatidylinositol 3-kinase-mediated m-calpain activity for shear stress-induced endothelial cell polarity. *American journal of physiology. Cell physiology*. 293:C1216-1225.

Moccia, F., R. Berra-Romani, and F. Tanzi. 2012. Update on vascular endothelial Ca(2+) signalling: A tale of ion channels, pumps and transporters. *World journal of biological chemistry*. 3:127-158.

Montell, C., L. Birnbaumer, and V. Flockerzi. 2002. The TRP channels, a remarkably functional family. *Cell*. 108:595-598.

Montell, C., and G.M. Rubin. 1989. Molecular characterization of the Drosophila trp locus: a putative integral membrane protein required for phototransduction. *Neuron*. 2:1313-1323.

Moore, K.J., and I. Tabas. 2011. Macrophages in the pathogenesis of atherosclerosis. *Cell*. 145:341-355.

Morello, F., A. Perino, and E. Hirsch. 2009. Phosphoinositide 3-kinase signalling in the vascular system. *Cardiovascular research*. 82:261-271.

Muller, J.M., W.M. Chilian, and M.J. Davis. 1997. Integrin Signaling Transduces Shear Stress-Dependent Vasodilation of Coronary Arterioles. *Circulation research*. 80:320-326.

Munzel, T., C. Sinning, F. Post, A. Warnholtz, and E. Schulz. 2008. Pathophysiology, diagnosis and prognostic implications of endothelial dysfunction. *Annals of medicine*. 40:180-196.

Muraki, K., Y. Iwata, Y. Katanosaka, T. Ito, S. Ohya, M. Shigekawa, and Y. Imaizumi. 2003. TRPV2 is a component of osmotically sensitive cation channels in murine aortic myocytes. *Circulation research*. 93:829-838.

Muramatsu, M., R.C. Tyler, D.M. Rodman, and I.F. McMurtry. 1997. Possible role of T-type Ca2+ channels in L-NNA vasoconstriction of hypertensive rat lungs. *The American journal of physiology*. 272:H2616-2621.

Nakache, M., and H.E. Gaub. 1988. Hydrodynamic hyperpolarization of endothelial cells. *Proceedings of the National Academy of Sciences of the United States of America*. 85:1841-1843.

Nauli, S.M., F.J. Alenghat, Y. Luo, E. Williams, P. Vassilev, X. Li, A.E. Elia, W. Lu, E.M. Brown, S.J. Quinn, D.E. Ingber, and J. Zhou. 2003. Polycystins 1 and 2 mediate mechanosensation in the primary cilium of kidney cells. *Nature genetics*. 33:129-137.

Nauli, S.M., Y. Kawanabe, J.J. Kaminski, W.J. Pearce, D.E. Ingber, and J. Zhou. 2008. Endothelial cilia are fluid shear sensors that regulate calcium signaling and nitric oxide production through polycystin-1. *Circulation*. 117:1161-1171.

Navar, L.G., E.W. Inscho, S.A. Majid, J.D. Imig, L.M. Harrison-Bernard, and K.D. Mitchell. 1996. Paracrine regulation of the renal microcirculation. *Physiological reviews*. 76:425-536.

Naylor, J., E. Al-Shawaf, L. McKeown, P.T. Manna, K.E. Porter, D. O'Regan, K. Muraki, and D.J. Beech. 2010. TRPC5 Channel Sensitivities to Antioxidants and Hydroxylated Stilbenes. *Journal of Biological Chemistry*. 286:5078-5086.

Newby, A.C. 2007. Metalloproteinases and vulnerable atherosclerotic plaques. *Trends in cardiovascular medicine*. 17:253-258.

Newby, L.J., A.J. Streets, Y. Zhao, P.C. Harris, C.J. Ward, and A.C. Ong. 2002. Identification, characterization, and localization of a novel kidney polycystin-1-polycystin-2 complex. *The Journal of biological chemistry*. 277:20763-20773.

Ngai, C., and X. Yao. 2010. Vascular responses to shear stress: the involvement of mechanosensors in endothelial cells. *Open Circ Vasc J*. 3:85-94.

Nissen, S.E. 2005. Effect of intensive lipid lowering on progression of coronary atherosclerosis: evidence for an early benefit from the Reversal of Atherosclerosis with Aggressive Lipid Lowering (REVERSAL) trial. *The American journal of cardiology*. 96:61F-68F.

Noria, S., D.B. Cowan, A.I. Gotlieb, and B.L. Langille. 1999. Transient and Steady-State Effects of Shear Stress on Endothelial Cell Adherens Junctions. *Circulation research*. 85:504-514.

Oancea, E., J.T. Wolfe, and D.E. Clapham. 2006. Functional TRPM7 channels accumulate at the plasma membrane in response to fluid flow. *Circulation research*. 98:245-253.

Olesen, S.-P., D. Claphamt, and P. Davies. 1988. Haemodynamic shear stress activates a K+ current in vascular endothelial cells. *Nature*. 331:168-170.

Olsson, A.K., A. Dimberg, J. Kreuger, and L. Claesson-Welsh. 2006. VEGF receptor signalling - in control of vascular function. *Nature reviews. Molecular cell biology*. 7:359-371.

Ong, A.C., and P.C. Harris. 2005. Molecular pathogenesis of ADPKD: the polycystin complex gets complex. *Kidney international*. 67:1234-1247.

Ong, H.L., and I.S. Ambudkar. 2011. The dynamic complexity of the TRPC1 channelosome. *Channels*. 5:424.

Osawa, M., M. Masuda, K. Kusano, and K. Fujiwara. 2002. Evidence for a role of platelet endothelial cell adhesion molecule-1 in endothelial cell mechanosignal transduction: is it a mechanoresponsive molecule? *The Journal of cell biology*. 158:773-785.

Owsianik, G., K. Talavera, T. Voets, and B. Nilius. 2006. Permeation and selectivity of TRP channels. *Annu. Rev. Physiol.* 68:685-717.

Pani, B., and B.B. Singh. 2009. Lipid rafts/caveolae as microdomains of calcium signaling. *Cell calcium*. 45:625-633.

Parekh, A.B., and J.W. Putney, Jr. 2005. Store-operated calcium channels. *Physiological reviews*. 85:757-810.

Park, H., Y.M. Go, P.L.S. John, M.C. Maland, M.P. Lisanti, D.R. Abrahamson, and H. Jo. 1998. Plasma Membrane Cholesterol Is a Key Molecule in Shear Stress-dependent Activation of Extracellular Signal-regulated Kinase. *Journal of Biological Chemistry*. 273:32304-32311.

Patel, S., and R. Docampo. 2010. Acidic calcium stores open for business: expanding the potential for intracellular Ca2+ signaling. *Trends in cell biology*. 20:277-286.

Pedersen, S.F., G. Owsianik, and B. Nilius. 2005. TRP channels: an overview. *Cell calcium*. 38:233-252.

Peyronnet, R., J.R. Martins, F. Duprat, S. Demolombe, M. Arhatte, M. Jodar, M. Tauc, C. Duranton, M. Paulais, J. Teulon, E. Honore, and A. Patel. 2013. Piezo1-dependent stretch-activated channels are inhibited by Polycystin-2 in renal tubular epithelial cells. *EMBO reports*. 14:1143-1148.

Pinaud, F., X. Michalet, G. Iyer, E. Margeat, H.P. Moore, and S. Weiss. 2009. Dynamic Partitioning of a Glycosyl‐Phosphatidylinositol‐Anchored Protein in Glycosphingolipid‐Rich Microdomains Imaged by Single‐Quantum Dot Tracking. *Traffic*. 10:691-712.

Platt, O., S. Lux, and D. Nathan. 1981. Exercise-induced hemolysis in xerocytosis. Erythrocyte dehydration and shear sensitivity. *Journal of Clinical Investigation*. 68:631.

Porn-Ares, M.I., T.C. Saido, T. Andersson, and M.P. Ares. 2003. Oxidized low-density lipoprotein induces calpain-dependent cell death and ubiquitination of caspase 3 in HMEC-1 endothelial cells. *The Biochemical journal*. 374:403-411.

Praetorius, H.A., and K.R. Spring. 2001. Bending the MDCK cell primary cilium increases intracellular calcium. *The Journal of membrane biology*. 184:71-79.

Putney Jr, J.W. 1986. A model for receptor-regulated calcium entry. *Cell calcium*. 7:1-12.

Rader, D.J., and A. Daugherty. 2008. Translating molecular discoveries into new therapies for atherosclerosis. *Nature*. 451:904-913.

Ray, K.K., and C.P. Cannon. 2005. The potential relevance of the multiple lipid-independent (pleiotropic) effects of statins in the management of acute coronary syndromes. *Journal of the American College of Cardiology*. 46:1425-1433.

Resnick, N., H. Yahav, A. Shay-Salit, M. Shushy, S. Schubert, L.C.M. Zilberman, and E. Wofovitz. 2003. Fluid shear stress and the vascular endothelium: for better and for worse. *Progress in Biophysics and Molecular Biology*. 81:177-199.

Rezakhaniha, R., A. Agianniotis, J.T. Schrauwen, A. Griffa, D. Sage, C.V. Bouten, F.N. van de Vosse, M. Unser, and N. Stergiopulos. 2012. Experimental investigation of collagen waviness and orientation in the arterial adventitia using confocal laser scanning microscopy. *Biomechanics and modeling in mechanobiology*. 11:461-473.

Rizzo, V., A. Sung, P. Oh, and J.E. Schnitzer. 1998. Rapid Mechanotransduction in Situ at the Luminal Cell Surface of Vascular Endothelium and Its Caveolae. *Journal of Biological Chemistry*. 273:26323-26329.

Rizzuto, R., Marchi,S., Bonora,M., Aguiari,P., Bononi,A., De Stefani.,D Giorgi,C., Leo,S., Rimessi,A., Siviero,R., Zecchini,E., Pinton, P.,Ca2+ transfer from the ER to mitochondria: When, how and why, *Biochimica et Biophysica Acta (BBA) - Bioenergetics*, 1787 :1342-1351.

Rodman, D.M., K. Reese, J. Harral, B. Fouty, S. Wu, J. West, M. Hoedt-Miller, Y. Tada, K.X. Li, C. Cool, K. Fagan, and L. Cribbs. 2005. Low-voltage-activated (T-type) calcium channels control proliferation of human pulmonary artery myocytes. *Circulation research*. 96:864-872.

Roos, J., P.J. DiGregorio, A.V. Yeromin, K. Ohlsen, M. Lioudyno, S. Zhang, O. Safrina, J.A. Kozak, S.L. Wagner, M.D. Cahalan, G. Velicelebi, and K.A. Stauderman. 2005. STIM1, an essential and conserved component of store-operated Ca2+ channel function. *The Journal of cell biology*. 169:435-445.

Ross, R. 1999. Atherosclerosis--an inflammatory disease. *The New England journal of medicine*. 340:115-126.

Rousseau, S., F. Houle, H. Kotanides, L. Witte, J. Waltenberger, J. Landry, and J. Huot. 2000. Vascular endothelial growth factor (VEGF)-driven actin-based motility is mediated by VEGFR2 and requires concerted activation of stress-activated protein kinase 2 (SAPK2/p38) and geldanamycin-sensitive phosphorylation of focal adhesion kinase. *Journal of Biological Chemistry*. 275:10661-10672.

Rousseau, S., F. Houle, J. Landry, and J. Huot. 1997. p38 MAP kinase activation by vascular endothelial growth factor mediates actin reorganization and cell migration in human endothelial cells. *Oncogene*. 15:2169-2177.

Rudijanto, A. 2007. The role of vascular smooth muscle cells on the pathogenesis of atherosclerosis. *Acta medica Indonesiana*. 39:86-93.

Sabine, A., Y. Agalarov, H. Maby-El Hajjami, M. Jaquet, R. Hagerling, C. Pollmann, D. Bebber, A. Pfenniger, N. Miura, O. Dormond, J.M. Calmes, R.H. Adams, T. Makinen, F. Kiefer, B.R. Kwak, and T.V. Petrova. 2012. Mechanotransduction, PROX1, and FOXC2 cooperate to control connexin37 and calcineurin during lymphatic-valve formation. *Developmental cell*. 22:430-445.

Sagara, Y., and G. Inesi. 1991. Inhibition of the sarcoplasmic reticulum Ca2+ transport ATPase by thapsigargin at subnanomolar concentrations. *Journal of Biological Chemistry*. 266:13503-13506.

Sancak, Y., A.L. Markhard, T. Kitami, E. Kovacs-Bogdan, K.J. Kamer, N.D. Udeshi, S.A. Carr, D. Chaudhuri, D.E. Clapham, A.A. Li, S.E. Calvo, O. Goldberger, and V.K. Mootha. 2013. EMRE is an essential component of the mitochondrial calcium uniporter complex. *Science*. 342:1379-1382.

Satir, P., L.B. Pedersen, and S.T. Christensen. 2010. The primary cilium at a glance. *Journal of cell science*. 123:499-503.

Schaefer, M., T.D. Plant, A.G. Obukhov, T. Hofmann, T. Gudermann, and G. Schultz. 2000. Receptor-mediated regulation of the nonselective cation channels TRPC4 and TRPC5. *Journal of Biological Chemistry*. 275:17517-17526.

Scull, C.M., and I. Tabas. 2011. Mechanisms of ER stress-induced apoptosis in atherosclerosis. *Arteriosclerosis, thrombosis, and vascular biology*. 31:2792-2797.

Shaul, P.W. 2003. Endothelial nitric oxide synthase, caveolae and the development of atherosclerosis. *The Journal of physiology*. 547:21-33.

Shi, J., M. Ju, J. Abramowitz, W.A. Large, L. Birnbaumer, and A.P. Albert. 2012. TRPC1 proteins confer PKC and phosphoinositol activation on native heteromeric TRPC1/C5 channels in vascular smooth muscle: comparative study of wild-type and TRPC1-/- mice. *FASEB journal : official publication of the Federation of American Societies for Experimental Biology*. 26:409-419.

Shipley, J.M., R.L. Wesselschmidt, D.K. Kobayashi, T.J. Ley, and S.D. Shapiro. 1996. Metalloelastase is required for macrophage-mediated proteolysis and matrix invasion in mice. *Proceedings of the National Academy of Sciences*. 93:3942-3946.

Shirahata, M., and R.S. Fitzgerald. 1991. Dependency of hypoxic chemotransduction in cat carotid body on voltage-gated calcium channels. *Journal of applied physiology (Bethesda, Md. : 1985)*. 71:1062-1069.

Simard, J.R., T. Meshulam, B.K. Pillai, M.T. Kirber, K. Brunaldi, S. Xu, P.F. Pilch, and J.A. Hamilton. 2010. Caveolins sequester FA on the cytoplasmic leaflet of the plasma membrane, augment triglyceride formation, and protect cells from lipotoxicity. *Journal of lipid research*. 51:914-922.

Simons, K., and M.J. Gerl. 2010. Revitalizing membrane rafts: new tools and insights. *Nature reviews Molecular cell biology*. 11:688-699.

Simons, K., and D. Toomre. 2000. Lipid rafts and signal transduction. *Nature reviews Molecular cell biology*. 1:31-39.

Sipahi, I., E.M. Tuzcu, K.E. Wolski, S.J. Nicholls, P. Schoenhagen, B. Hu, C. Balog, M. Shishehbor, W.A. Magyar, and T.D. Crowe. 2007. β-Blockers and progression of coronary atherosclerosis: pooled analysis of 4 intravascular ultrasonography trials. *Annals of internal medicine*. 147:10-18.

Spassova, M.A., T. Hewavitharana, W. Xu, J. Soboloff, and D.L. Gill. 2006. A common mechanism underlies stretch activation and receptor activation of TRPC6 channels. *Proceedings of the National Academy of Sciences of the United States of America*. 103:16586-16591.

Steinberg, D., C.K. Glass, and J.L. Witztum. 2008. Evidence mandating earlier and more aggressive treatment of hypercholesterolemia. *Circulation*. 118:672-677.

Streets, A.J., B.E. Wagner, P.C. Harris, C.J. Ward, and A.C.M. Ong. 2009. Homophilic and heterophilic polycystin 1 interactions regulate E-cadherin recruitment and junction assembly in MDCK cells. *Journal of cell science*. 122:1410-1417.

Strotmann, R., C. Harteneck, K. Nunnenmacher, G. Schultz, and T.D. Plant. 2000. OTRPC4, a nonselective cation channel that confers sensitivity to extracellular osmolarity. *Nature cell biology*. 2:695-702.

Strubing, C., G. Krapivinsky, L. Krapivinsky, and D.E. Clapham. 2003. Formation of Novel TRPC Channels by Complex Subunit Interactions in Embryonic Brain. *Journal of Biological Chemistry*. 278:39014-39019.

Strübing, C., G. Krapivinsky, L. Krapivinsky, and D.E. Clapham. 2001. TRPC1 and TRPC5 form a novel cation channel in mammalian brain. *Neuron*. 29:645-655.

Suchyna, T.M., J.H. Johnson, K. Hamer, J.F. Leykam, D.A. Gage, H.F. Clemo, C.M. Baumgarten, and F. Sachs. 2000. Identification of a peptide toxin from Grammostola spatulata spider venom that blocks cation-selective stretch-activated channels. *The Journal of general physiology*. 115:583-598.

Sukumar, P., and D.J. Beech. 2010. Stimulation of TRPC5 cationic channels by low micromolar concentrations of lead ions (Pb< sup> 2+</sup>). *Biochemical and biophysical research communications*. 393:50-54.

Sukumar, P., A. Sedo, J. Li, L.A. Wilson, D. O'Regan, J.D. Lippiat, K.E. Porter, M.T. Kearney, J.F. Ainscough, and D.J. Beech. 2012. Constitutively active TRPC channels of adipocytes confer a mechanism for sensing dietary fatty acids and regulating adiponectin. *Circulation research*. 111:191-200.

Sumpio, B.E., S. Yun, A.C. Cordova, M. Haga, J. Zhang, Y. Koh, and J.A. Madri. 2005. MAPKs (ERK1/2, p38) and AKT can be phosphorylated by shear stress independently of platelet endothelial cell adhesion molecule-1

(CD31) in vascular endothelial cells. *The Journal of biological chemistry*. 280:11185-11191.

Suzuki, M., A. Mizuno, K. Kodaira, and M. Imai. 2003. Impaired pressure sensation in mice lacking TRPV4. *The Journal of biological chemistry*. 278:22664-22668.

Sweeney, M., Y. Yu, O. Platoshyn, S. Zhang, S.S. McDaniel, and J.X.-J. Yuan. 2002. Inhibition of endogenous TRP1 decreases capacitative Ca2+ entry and attenuates pulmonary artery smooth muscle cell proliferation. *American Journal of Physiology-Lung Cellular and Molecular Physiology*. 283:L144-L155.

Szewczyk, M.M., K.A. Davis, S.E. Samson, F. Simpson, P.K. Rangachari, and A.K. Grover. 2007. Ca2+-pumps and Na2+-Ca2+-exchangers in coronary artery endothelium versus smooth muscle. *Journal of cellular and molecular medicine*. 11:129-138.

Takahashi, Y., H. Watanabe, M. Murakami, T. Ohba, M. Radovanovic, K. Ono, T. Iijima, and H. Ito. 2007. Involvement of transient receptor potential canonical 1 (TRPC1) in angiotensin II-induced vascular smooth muscle cell hypertrophy. *Atherosclerosis*. 195:287-296.

Tamminen, M., G. Mottino, J.H. Qiao, J.L. Breslow, and J.S. Frank. 1999. Ultrastructure of Early Lipid Accumulation in ApoE-Deficient Mice. *Arteriosclerosis, thrombosis, and vascular biology*. 19:847-853.

Tijssen, J., and P. Hugenholtz. 1996. Critical appraisal of recent studies on nifedipine and other calcium channel blockers in coronary artery disease and hypertension. *European heart journal*. 17:1152-1157.

Tran, Q.-K., K. Ohashi, and H. Watanabe. 2000. Calcium signalling in endothelial cells. *Cardiovascular research*. 48:13-22.

Trebak, M., L. Lemonnier, W.I. DeHaven, B.J. Wedel, G.S. Bird, and J.W. Putney, Jr. 2009. Complex functions of phosphatidylinositol 4,5-bisphosphate in regulation of TRPC5 cation channels. *Pflugers Archiv : European journal of physiology*. 457:757-769.

Turner, C.E. 1998. Molecules in focus Paxillin. *The international journal of biochemistry & cell biology*. 30:955-959.

Tzima, E., M.A. del Pozo, S.J. Shattil, S. Chien, and M.A. Schwartz. 2001. Activation of integrins in endothelial cells by fluid shear stress mediates Rho‑dependent cytoskeletal alignment. *The EMBO journal*. 20:4639-4647.

Tzima, E., M. Irani-Tehrani, W.B. Kiosses, E. Dejana, D.A. Schultz, B. Engelhardt, G. Cao, H. DeLisser, and M.A. Schwartz. 2005. A mechanosensory complex that mediates the endothelial cell response to fluid shear stress. *Nature*. 437:426-431.

Uematsu, M., Y. Ohara, J.P. Navas, K. Nishida, T. Murphy, R.W. Alexander, R.M. Nerem, and D.G. Harrison. 1995. Regulation of endothelial cell nitric oxide synthase mRNA expression by shear stress. *American Journal of Physiology-Cell Physiology*. 38:C1371.

Vazquez, G., B.J. Wedel, M. Trebak, G.S.J. Bird, and J.W. Putney. 2003. Expression level of the canonical transient receptor potential 3 (TRPC3)

channel determines its mechanism of activation. *Journal of Biological Chemistry.* 278:21649-21654.

Verdaguer, E., D. Alvira, A. Jimenez, V. Rimbau, A. Camins, and M. Pallas. 2005. Inhibition of the cdk5/MEF2 pathway is involved in the antiapoptotic properties of calpain inhibitors in cerebellar neurons. *British journal of pharmacology.* 145:1103-1111.

Vig, M., C. Peinelt, A. Beck, D.L. Koomoa, D. Rabah, M. Koblan-Huberson, S. Kraft, H. Turner, A. Fleig, R. Penner, and J.P. Kinet. 2006. CRACM1 is a plasma membrane protein essential for store-operated Ca2+ entry. *Science.* 312:1220-1223.

Wallentin, L., R.C. Becker, A. Budaj, C.P. Cannon, H. Emanuelsson, C. Held, J. Horrow, S. Husted, S. James, and H. Katus. 2009. Ticagrelor versus clopidogrel in patients with acute coronary syndromes. *New England Journal of Medicine.* 361:1045-1057.

Wang, J., Z.H. Lu, H.J. Gabius, C. Rohowsky-Kochan, R.W. Ledeen, and G. Wu. 2009. Cross-linking of GM1 ganglioside by galectin-1 mediates regulatory T cell activity involving TRPC5 channel activation: possible role in suppressing experimental autoimmune encephalomyelitis. *Journal of immunology.* 182:4036-4045.

Wang, K., R. Nath, A. Posner, K.J. Raser, M. Buroker-Kilgore, I. Hajimohammadreza, F.W. Marcoux, Q. Ye, E. Takano, and M. Hatanaka. 1996. An alpha-mercaptoacrylic acid derivative is a selective nonpeptide cell-permeable calpain inhibitor and is neuroprotective. *Proceedings of the National Academy of Sciences.* 93:6687-6692.

Wang, X., Q. Chen, and D. Xing. 2012. Focal adhesion kinase activates NF-kappaB via the ERK1/2 and p38MAPK Pathways in amyloid-beta25-35-induced apoptosis in PC12 cells. *Journal of Alzheimer's disease : JAD.* 32:77-94.

Warboys, C.M., A. de Luca, N. Amini, L. Luong, H. Duckles, S. Hsiao, A. White, S. Biswas, R. Khamis, and C.K. Chong. 2014. Disturbed Flow Promotes Endothelial Senescence via a p53-Dependent Pathway. *Arteriosclerosis, thrombosis, and vascular biology.* 34:985-995.

Watanabe, H., J. Vriens, J. Prenen, G. Droogmans, T. Voets, and B. Nilius. 2003. Anandamide and arachidonic acid use epoxyeicosatrienoic acids to activate TRPV4 channels. *Nature.* 424:434-438.

Weber, C., and H. Noels. 2011. Atherosclerosis: current pathogenesis and therapeutic options. *Nature medicine.* 17:1410-1422.

Wes, P.D., J. Chevesich, A. Jeromin, C. Rosenberg, G. Stetten, and C. Montell. 1995. TRPC1, a human homolog of a Drosophila store-operated channel. *Proceedings of the National Academy of Sciences.* 92:9652-9656.

Wu, G., Z.H. Lu, A.G. Obukhov, M.C. Nowycky, and R.W. Ledeen. 2007. Induction of calcium influx through TRPC5 channels by cross-linking of GM1 ganglioside associated with alpha5beta1 integrin initiates neurite outgrowth. *The Journal of neuroscience : the official journal of the Society for Neuroscience.* 27:7447-7458.

Xiao, R., and X. Xu. 2010. Mechanosensitive channels: in touch with Piezo. *Current Biology*. 20:R936-R938.

Xu, S.-Z., P. Sukumar, F. Zeng, J. Li, A. Jairaman, A. English, J. Naylor, C. Ciurtin, Y. Majeed, and C.J. Milligan. 2008. TRPC channel activation by extracellular thioredoxin. *Nature*. 451:69-72.

Xu, S.Z., K. Muraki, F. Zeng, J. Li, P. Sukumar, S. Shah, A.M. Dedman, P.K. Flemming, D. McHugh, J. Naylor, A. Cheong, A.N. Bateson, C.M. Munsch, K.E. Porter, and D.J. Beech. 2006. A sphingosine-1-phosphate-activated calcium channel controlling vascular smooth muscle cell motility. *Circulation research*. 98:1381-1389.

Xu, S.Z., F. Zeng, M. Lei, J. Li, B. Gao, C. Xiong, A. Sivaprasadarao, and D.J. Beech. 2005. Generation of functional ion-channel tools by E3 targeting. *Nature biotechnology*. 23:1289-1293.

Yamamoto, K., K. Furuya, M. Nakamura, E. Kobatake, M. Sokabe, and J. Ando. 2011. Visualization of flow-induced ATP release and triggering of Ca2+ waves at caveolae in vascular endothelial cells. *Journal of cell science*. 124:3477-3483.

Yamamoto, K., R. Korenaga, A. Kamiya, and J. Ando. 2000. Fluid Shear Stress Activates Ca2+ Influx Into Human Endothelial Cells via P2X4 Purinoceptors. *Circulation research*. 87:385-391.

Yamamoto, K., T. Sokabe, T. Matsumoto, K. Yoshimura, M. Shibata, N. Ohura, T. Fukuda, T. Sato, K. Sekine, S. Kato, M. Isshiki, T. Fujita, M. Kobayashi, K. Kawamura, H. Masuda, A. Kamiya, and J. Ando. 2006. Impaired flow-dependent control of vascular tone and remodeling in P2X4-deficient mice. *Nature medicine*. 12:133-137.

Yamamoto, K., T. Sokabe, N. Ohura, H. Nakatsuka, A. Kamiya, and J. Ando. 2003. Endogenously released ATP mediates shear stress-induced Ca2+ influx into pulmonary artery endothelial cells. *American Journal of Physiology-Heart and Circulatory Physiology*. 285:H793-H803.

Yang, X.-R., A.H. Lin, J.M. Hughes, N.A. Flavahan, Y.-N. Cao, W. Liedtke, and J.S. Sham. 2012. Upregulation of osmo-mechanosensitive TRPV4 channel facilitates chronic hypoxia-induced myogenic tone and pulmonary hypertension. *American Journal of Physiology-Lung Cellular and Molecular Physiology*. 302:L555-L568.

Yao, X., and C.J. Garland. 2005. Recent developments in vascular endothelial cell transient receptor potential channels. *Circulation research*. 97:853-863.

Yao, Y., S. Hong, H. Zhou, T. Yuan, R. Zeng, and K. Liao. 2009. The differential protein and lipid compositions of noncaveolar lipid microdomains and caveolae. *Cell research*. 19:497-506.

Yao, Y., A. Rabodzey, and C.F. Dewey Jr. 2007. Glycocalyx modulates the motility and proliferative response of vascular endothelium to fluid shear stress. *American Journal of Physiology-Heart and Circulatory Physiology*. 293:H1023-H1030.

Yoshida, T., R. Inoue, T. Morii, N. Takahashi, S. Yamamoto, Y. Hara, M. Tominaga, S. Shimizu, Y. Sato, and Y. Mori. 2006. Nitric oxide activates

TRP channels by cysteine S-nitrosylation. *Nature chemical biology*. 2:596-607.

Yoshimura, K., and M. Sokabe. 2010. Mechanosensitivity of ion channels based on protein–lipid interactions. *Journal of The Royal Society Interface*:rsif20100095.

Yu, J., S. Bergaya, T. Murata, I.F. Alp, M.P. Bauer, M.I. Lin, M. Drab, T.V. Kurzchalia, R.V. Stan, and W.C. Sessa. 2006. Direct evidence for the role of caveolin-1 and caveolae in mechanotransduction and remodeling of blood vessels. *The Journal of clinical investigation*. 116:1284-1291.

Zarychanski, R., V.P. Schulz, B.L. Houston, Y. Maksimova, D.S. Houston, B. Smith, J. Rinehart, and P.G. Gallagher. 2012. Mutations in the mechanotransduction protein PIEZO1 are associated with hereditary xerocytosis. *Blood*. 120:1908-1915.

Zebda, N., O. Dubrovskyi, and K.G. Birukov. 2012. Focal adhesion kinase regulation of mechanotransduction and its impact on endothelial cell functions. *Microvascular research*. 83:71-81.

Zeng, F., S.Z. Xu, P.K. Jackson, D. McHugh, B. Kumar, S.J. Fountain, and D.J. Beech. 2004. Human TRPC5 channel activated by a multiplicity of signals in a single cell. *The Journal of physiology*. 559:739-750.

Zernecke, A., and C. Weber. 2010. Chemokines in the vascular inflammatory response of atherosclerosis. *Cardiovascular research*. 86:192-201.

Zhang, S.L., Y. Yu, J. Roos, J.A. Kozak, T.J. Deerinck, M.H. Ellisman, K.A. Stauderman, and M.D. Cahalan. 2005. STIM1 is a Ca2+ sensor that activates CRAC channels and migrates from the Ca2+ store to the plasma membrane. *Nature*. 437:902-905.

Zhou, C., H. Chen, J.A. King, H. Sellak, W.M. Kuebler, J. Yin, M.I. Townsley, H.-S. Shin, and S. Wu. 2010. α1G T-type calcium channel selectively regulates P-selectin surface expression in pulmonary capillary endothelium. *American Journal of Physiology-Lung Cellular and Molecular Physiology*. 299:L86-L97.

Zhou, C., H. Chen, F. Lu, H. Sellak, J.A. Daigle, M.F. Alexeyev, Y. Xi, J. Ju, J.A. van Mourik, and S. Wu. 2007. Cav3.1 (alpha1G) controls von Willebrand factor secretion in rat pulmonary microvascular endothelial cells. *American journal of physiology. Lung cellular and molecular physiology*. 292:L833-844.

Zhou, C., and S. Wu. 2006. T-type calcium channels in pulmonary vascular endothelium. *Microcirculation*. 13:645-656.

Zidovetzki, R., and I. Levitan. 2007. Use of cyclodextrins to manipulate plasma membrane cholesterol content: evidence, misconceptions and control strategies. *Biochimica et Biophysica Acta (BBA)-Biomembranes*. 1768:1311-1324.